IRRADIANCE WITHIN MONTANE TREE CANOPIES, CRAIGIEBURN RANGE, NEW ZEALAND

A thesis

submitted in partial fulfilment

of the requirements for the Degree

of

Master of Science in Geography

in the

University of Canterbury

by

S.M. Turton

University of Canterbury

1982

THESIS

FRONTISPIECE

Mount Wall (ca. 1800 m a.s.l.), Craigieburn Range, New Zealand. The monospecific forest species in the region, mountain beech (*Nothofagus solandri* var. *cliffortioides*) forms a distinct timberline at around 1350 m a.s.l.

ACKNOWLEDGEMENTS

Over the past year many people have given me help and encouragement towards the culmination of this thesis.

I would like to thank my Supervisor, Dr. Andy Sturman for his considerable interest in my fieldwork and careful and constructive criticism of my written work.

I am indebted to many F.R.I. members of staff, at both Ilam and Rangiora. In particular, I would like to thank Mr. Alan Nordmeyer and Dr. Udo Benecke for showing interest and providing expert advice on many of the aspects covered in this thesis. Gratitude is also extended to Dr. David Whitehea (F.R.I., Rotorua) for answering questions put to him by correspondence and for taking time to see me when in Christchu

Thanks are extended to Dr. Peter Holland (now, Head of Geography Department, University of Otago) for showing interes in my work and discussing problems, earlier this year.

Thanks also to the following technical staff for their help over the year: G. Rogers, J. Cruden, and S. Brailsford (F.R.I., Ilam), and A. Brown, and R. Begg (Geography Departmen

The F.R.I. (Ecology and Revegetation Section) kindly loaned equipment that was used in the field, and provided transport to and from, and accommodation at Craigieburn. The Air Pollution Section of the National Radiation Laboratory (Christchurch) provided access to the use of a reflectometer.

Many thanks to Mrs. Brenda Carter for the careful attention to detail given in the typing of this thesis.

And finally, I would like to express sincere gratitude to my wife, Wendy, who supported and helped me with many aspec of this thesis.

CONTENTS

LIST OF TABLES

LIST OF FIGURES

FIGURE PAGE

LIST OF PLATES

GLOSSARY

ROMAN CAPITALS		UNITS
CL	Crown length (H-HLC)	(metres)
H	Mean height of stand	(———)
HLC	Height to base of living crown	(———)
K	Extinction coefficient in canopy	
L	Projected leaf area index (one-side only)	(m^2 leaf area/m^2 ground area)
L_t	Total surface leaf area index	(———————)
P	Net rate of photosynthesis for a tree (net units of photosynthate produced or CO_2 uptake/ground area/ time)	($\mu mol\ m^{-2}s^{-1}$)
P_{max}	Total rate of photosynthesis for a leaf fully lit at the optimum light intensity (total units of photosynthate produced or total CO_2 uptake/leaf area/time)	(———————)
Q	Total irradiance incident on a surface ($Q_s + Q_d$)	(MJm^{-2}, Einsteins m^{-2}, Wm^{-2}, $\mu Em^{-2}s^{-1}$ or μmol photons $m^{-2}s^{-1}$)
Q_c	The compensation point, the light intensity at which photo-synthesis just balances respiration (P = 0)	(μmol photons $m^{-2}s^{-1}$)
Q_d	Diffuse/sky solar radiation	(MJm^{-2}, Einsteins m^{-2}, Wm^{-2}, $\mu Em^{-2}s^{-1}$ or μmol photons $m^{-2}s^{-1}$)
Q_o	Total irradiance (Q) incident above the canopy	(———————)
Q_s	Direct beam solar radiation	(———————)
Q_{sat}	Saturation point, the light intensity at which photo-synthesis reaches its maximum rate ($P = P_{max}$)	(μmol photons $m^{-2}s^{-1}$)

ROMAN CAPITALS		UNITS
R	Rate of respiration for a leaf (units of photosynthate used or CO_2 evolved/leaf area/time)	(μmol $m^{-2}s^{-1}$)
T	Temperature	K, ^{o}C

GREEK ALPHABET		
α	Absorption coefficient	
β	Solar elevation	(degrees)
γ	The angle between the parallel beam of irradiation and a line normal to the surface	(————)
λ	Wavelength	(μm, nm)
ρ	Reflection coefficient	
σ	Stefan-Boltzmann constant	($=5.67 \times 10^{-8} Wm^{-2} K^{-4}$)
τ	Transmission coefficient	
ω	Scattering coefficient ($= \rho+\tau$)	

ABSTRACT

A photo-chemical technique was used to measure incident and reflected irradiance over weekly periods, above and at four levels within the crown of four forest stands growing at montane altitude on the eastern side of the Craigieburn Range from February-June, 1982. All the stands were in the steepest part of their sigmoid growth pattern, and were therefore at or near canopy closure.

Differences and similarities in the light climate of the four stands have been shown to be related to their architecture. Differences occurred in total surface leaf area (L_t) and its distribution (L_t : *Larix decidua* 12.5, *Nothofagus solandri* 17.8, *Pseudotsuga menziesii* 33.3, *Pinus contorta* 35.7). Stem-branch geometry and foliage structure and orientation were other factors affecting the absorbance of light in the crown. Horizontal receiving surfaces (*P. menziesii, N. solandri*) tended to prevent strong illumination from reaching the lower crown, while more vertical receiving surfaces (*P. contorta*) allowed higher levels of irradiance to reach the lower crown. Seasonal variations in the light climate of the four stands occurred because of changes in earth-sun geometry and forest structure.

A simple model of canopy photosynthesis is presented, using light absorbance and ecophysiological characterisitcs of the four stands. The *P. contorta* canopy was estimated to have the highest photosynthetic rate and *L. decidua* the lowest. Extinction coefficients (K) for the four stands varied because of differences in their leaf area.

CHAPTER ONE

INTRODUCTION

1.1 SOLAR ENERGY

1.1.1 Background

(a) Radiant energy and irradiance

Radiant energy (radiation) is the continuous emission of waves of electromagnetic energy and high-speed particles directly from the sun's disc into space. This radiation reaches the earth some eight minutes after the emission process.

The sun has an estimated brightness of 3.85×10^{26} W (6.33×10^{7} Wm^{-2}), but the earth only intercepts two thousand millionths of this energy (1.1×10^{7} W). In turn, the earth reflects an estimated 3.52×10^{6} W back into space.

The electromagnetic spectrum contains wavelengths ranging from $10^{-4}\mu m$ to $10^{5}m$ (figure 1.1). It is assumed that the sun and earth behave as "black bodies". Such bodies absorb all energy falling on them and, in turn, radiate energy at a rate directly proportional to the fourth power of their absolute temperature. The radiant energy of a black body is emitted at a rate, Q

$$Q = \sigma T^{4} (Wm^{-2}\ {}^{o}K^{-4}) \qquad (1.0)$$

where, σ = Stefan-Boltzmann constant, and

T = absolute temperature (^{o}K).

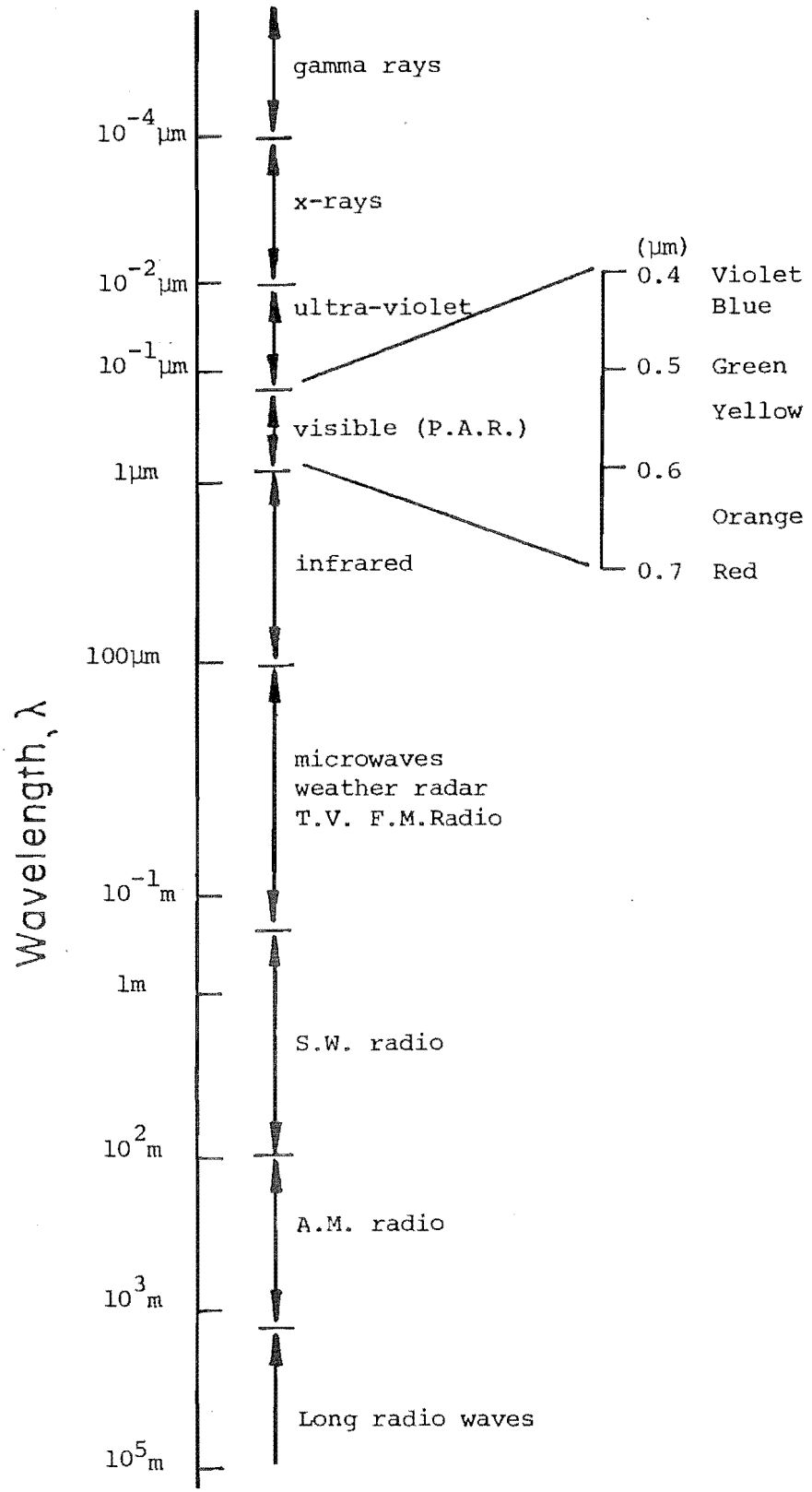

Figure 1.1: The Electromagnetic Spectrum

The surface temperature of the sun is estimated to be $6000^{o}K$ and its emission spectrum is largely contained within the 0.15-4.0μm band, with a peak at 0.5μm. The earth's surface behaves approximately as a radiator at about $300^{o}K$, and its emission spectrum is largely contained within the 4.0-100μm band, with a peak at 10μm. Hence short wave solar and long wave terrestrial radiation can be treated as effectively separate.

Irradiation is an emission of radiant flux, which is incident on the surface of some body. *Irradiance* (Q) is the irradiation of unit surface area of a body (Wm^{-2}). For a flat surface the irradiance decreases with the cosine of the angle of incidence because rays which are not normal to the surface are only incident on the projection on the surface. (Kubin, 1971.) (See section 1.1.1, e.)

(b) Astronomical effects

The annual revolution of the earth around the sun is elliptical and because of this, there is a seven percent variation in the amount of solar radiation received at the top of the atmosphere between perihelion (closest to the sun, January 3) and aphelion (farthest from the sun, July 4). The southern hemisphere therefore, has slightly more insolation during its summer. The overall effect is very small however.

Apart from the eccentricity of the elliptic, the obliquity of the ecliptic causes the earth to experience seasons as insolation varies throughout the year. Seasons

result from the considerable deviation of the plane of the earth's equator from the plane of its orbit ($23^{o}27'$) and the parallelism of the movement of the earth's axis in space as the earth moves around the sun (W.M.O., 1981).

Radiation received at the surface varies depending on the time of year. The solstices (22 June, 22 December) and the equinoxes (21 March, 23 September) are terms used to define seasonal changes in earth-sun geometry. At northern solstice (22 June), the sun's apparent path is displaced farthest north of the equator, and at southern solstice (22 December), the displacement is farthest south. During the equinoxes, the sun passes directly over the earth's equator.

The obliquity of the ecliptic therefore, causes different parts of the earth's surface to receive different amounts of solar radiation. Time of year effects day length and hence radiation totals.

Latitude is also important. At higher latitudes, the distance travelled through the atmosphere by the oblique rays from the sun will be greater than at lower latitudes where the angle of incidence is more perpendicular to the surface. Radiation received at the ground in higher latitudes will therefore be less intense than at lower latitudes because of the greater absorptive effects of the atmosphere.

(c) Atmospheric effects

The *solar constant* (1370 ± 6 Wm^{-2}) is the name given to the quantity of the sun's radiant energy which falls in a unit of time (one second) on a unit area (one square metre) perpendicular to the sun's rays at a point beyond the atmosphere at a distance from the sun equal to the average radius of the earth's orbit (W.M.O. 1981).

Upon entering the atmosphere, this radiant energy is scattered and absorbed as it passes through the successive layers (figure 1.2). All the atmospheric components contribute to a greater or lesser degree to the attenuation of direct solar radiation on its path to the earth's surface (W.M.O. 1981).

In the upper atmosphere there is absorption of the x-ray and ultraviolet regions (figure 1.1) (less than 0.3μm) due to the presence of oxygen, ozone, and nitrogen oxides. Scattering occurs in the violet and blue ranges (Rayleigh Scattering), causing the blue sky effect.

As a result of the absorption of wavelengths shorter than 0.3μm in the upper atmosphere, the remaining wavelengths (0.3-4.0μm) reach the lower atmosphere. The lower atmosphere absorbs in several narrow bands between 0.9μm to 2.1μm due to the presence of water vapour, carbon dioxide and other minor components (figure 1.2).

As figure 1.2 illustrates, about 30 percent of incoming

Figure 1.2: The balance of the atmospheric energy budget (after, Barry and Chorley, 1976)

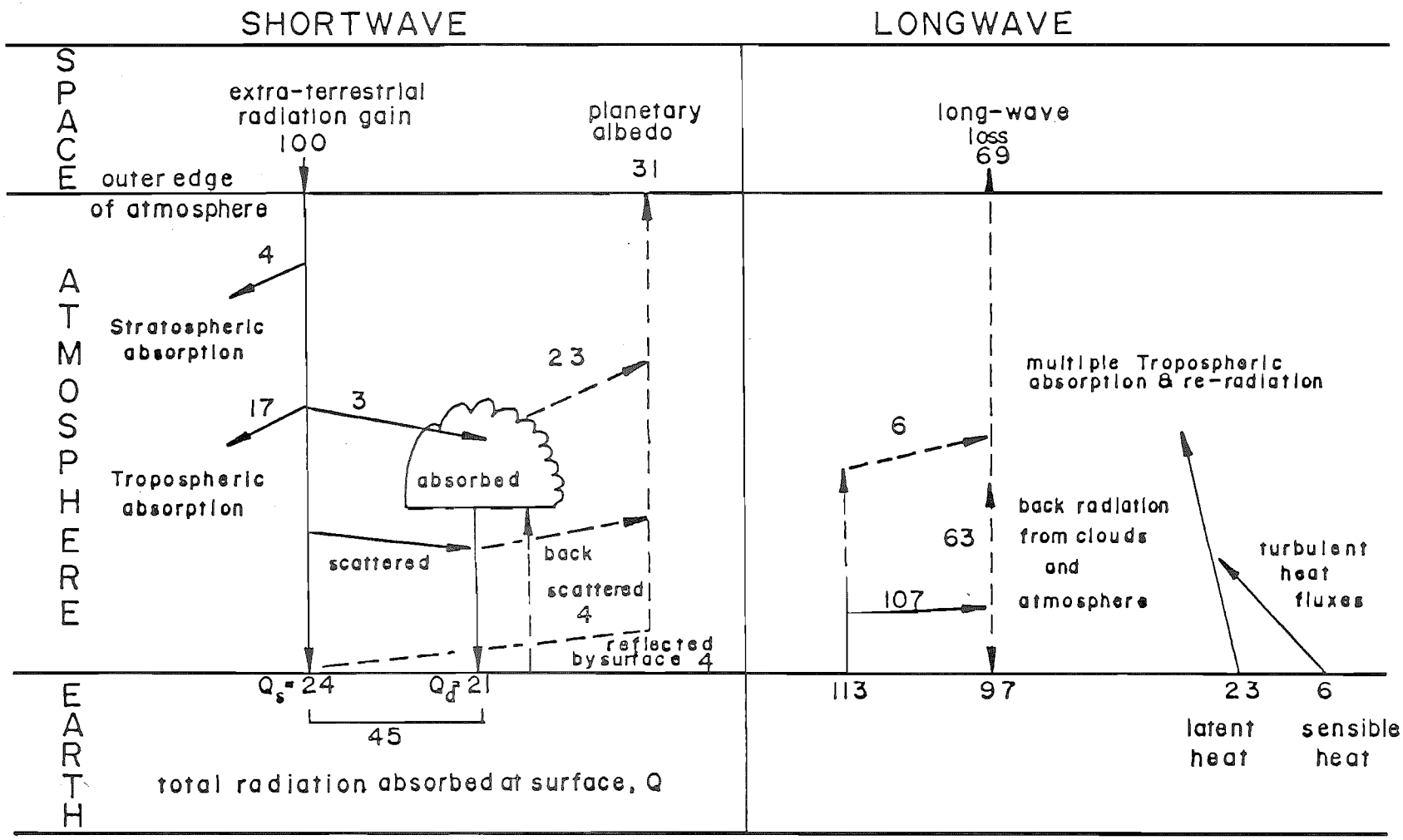

solar radiation is reflected back into space from the atmosphere, clouds and the earth's surface, leaving approximately 70 percent to heat the earth and the atmosphere. The surface absorbs 45 percent of the incoming energy available at the top of the atmosphere and re-radiates it outwards as long waves of greater than 4.0μm. Much of this energy is absorbed by water vapour, carbon dioxide, and ozone in the atmosphere, the rest escaping through 'atmospheric windows' into space.

(d) Irradiance of the ground surface

Total irradiance at the ground surface (Q) is divided into *direct* solar radiation (Q_s) and *diffuse* solar radiation (Q_d) (Coulson, 1975).

Q_s is energy directly from the sun's disc, the transmission of which decreases as the optical path of the rays increases, and particularly when the atmospheric transparency decreases.

Q_d is energy from the entire celestial dome, blue sky and clouds, excluding the energy directly from the sun's disc, but including energy reflected from the ground (diffuse reflected global radiation).

Q_s and Q_d are affected by altitude. At higher altitudes where the mass of air above is less, more Q_s is received under clear skies than at lower altitudes. However, Q_d decreases with altitude.

(e) Angle of incidence

Altitude and aspect of a site will effectively control the amount of radiation received. Some slopes are more exposed to the sun than others. The angle of the slope will also affect the amount of irradiance incident upon it.

Lambert's cosine law states "the radiant intensity (flux per unit solid angle) emitted in any direction from a unit radiating surface varies as the cosine of the angle between the normal to the surface and the direction of radiation." This radiant input is composed of direct and diffuse solar radiation and long wave radiation, of which only the direct beam receipt (Q_s) is dependent upon the angle at which it strikes the receiving surface.

Figure 1.3 illustrates Lambert's law applied to a horizontal receiving surface. Let γ be the angle between the parallel beam of irradiation and a line normal to the surface. If $Q_s(n)$ is the intensity of the beam on a perpendicular surface unit $S(n)$ and Q_s is the flux density of the surface being considered S, then by Lambert's law

$$\frac{Q_s}{Q_s(n)} = \cos \gamma \qquad (1.1)$$

where γ is drawn at the zenith distance.

The angle β (solar elevation) is the angular elevation of the sun above the horizon. For parallel solar radiation from solar elevation β impinging on a horizontal surface,

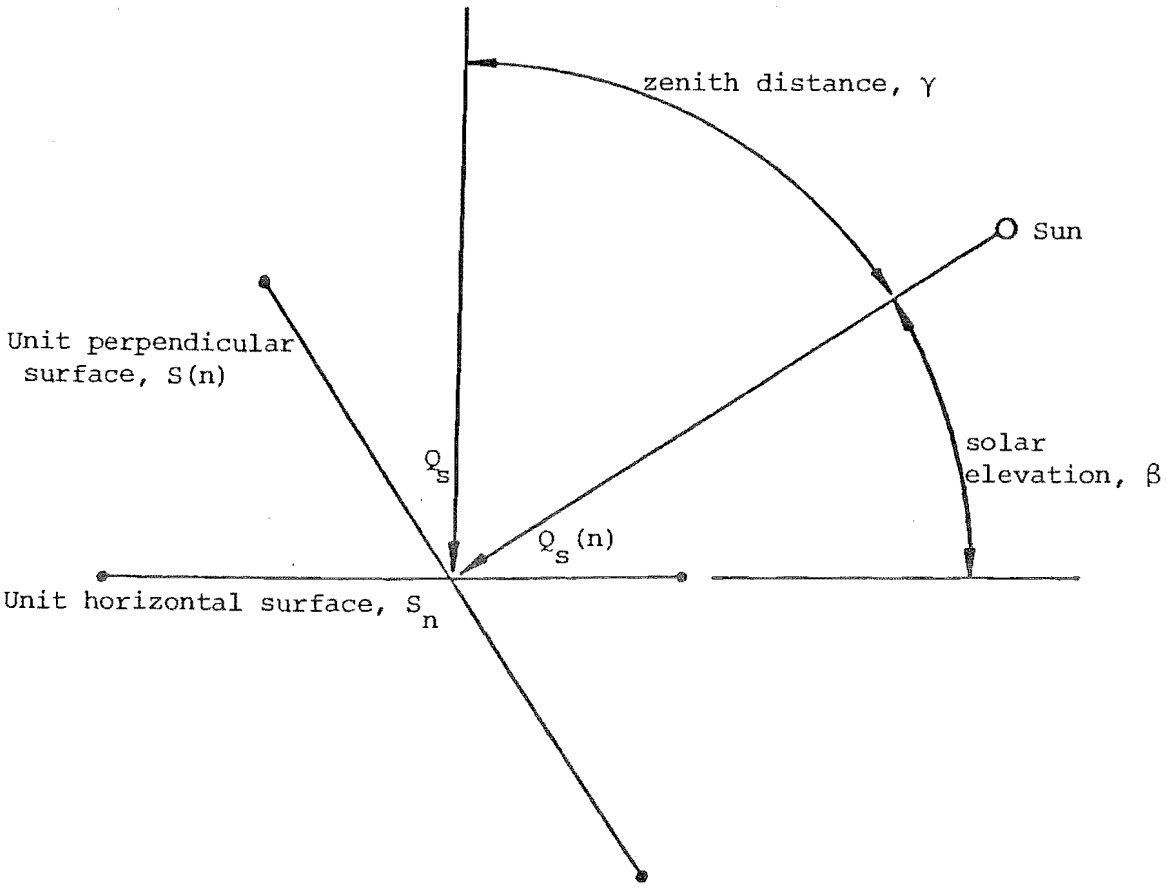

Figure 1.3: Illustration of Lambert's Cosine Law

the following expressed is derived.

$$\frac{Q_s}{Q_s(n)} = \sin \beta \qquad (1.2)$$

Lambert's cosine law provides the basis of most methods for calculating irradiance on horizontal and inclined surfaces (for example, Kondrat'yev 1965, 1977, Garnier and Omhura 1968, Omhura 1968, Hay 1978).

1.2 VEGETATION AND IRRADIANCE

1.2.1 General Characteristics

Of the radiant energy reaching the surface, some 98 percent occurs in the 0.3-4.0μm range (figure 1.1). This energy is the driving force for essentially all processes occurring within ecosystems, as green plants are capable of converting part of this waveband (0.4-0.7μm) into cellular material through the process of photosynthesis (see section 1.2.3(a)). In this way, plants are capable of storing energy in a form that is usable in other parts of the food chain.

In green plants, irradiance acts as the source of energy for photochemical reactions and as a stimulus regulating development (photomorphogenesis). Table 1.1 illustrates the wavebands (as shown by figure 1.1) and their significance for plant life.

Quite clearly, *photosynthetically active radiation* (P.A.R., 0.4-0.7μm) has significant effects on plant life for the

three factors listed. *Near infrared radiation* (N.I.R., 0.71-4.0μm) has important thermal and photomorphogenic effects (e.g. timing of germination, flowering, leaf abscission, etc), while *long wave radiation* is of purely thermal importance.

Table 1.1: Radiation wavebands and their significance for plant life. (after Ross, 1975)

type of radiation	spectral region (μm)	percent of solar energy	effect on plant life		
			thermal	Photosynthetic	Photomorphogenic
ultra-violet	0.29-0.4	0-4	insignif	signif	moderate
photosynthetically active radiation (P.A.R.)	0.4-0.7	21-46	signif	signif	signif
near infra-red (N.I.R.)	0.71-4.0	50-79	signif	insignif	signif
long wave radiation	3.0-100.0	-	signif	insignif	insignif

In terms of the effects on plant life, only absorbed irradiance can be effective. The degree of absorption, reflection and transmission in leaves depends on the wave length of the irradiation. The processes depend essentially on the optical properties of the vegetation and the ground surface, the conditions of the incident radiation, and most importantly, on the architecture of the plant community (Ross, 1970).

1.2.2 Irradiative Transfer Theory in Plant Communities

Irradiative transfer theory is the interaction of irradiance (incident, reflected and scattered) with a given medium (in this case, a plant community). A plant community

can range in size from a small mono-layered community (such as a clover crop) to a multi-layered community (such as a rainforest). The interaction of irradiance with a plant community is affected by many factors. The following discussion will focus on the most important of these.

(a) Conditions of incident irradiation

As was discussed in section 1.1.1 d, incident solar radiation consists of two components: direct solar radiation (Q_s) and diffuse sky radiation (Q_d). It was determined, that the intensity of Q_s depended on the effects of its traverse through the atmosphere, and Q_d depended on the presence of constituents in the atmosphere. Q_s increases with the increase of solar elevation β, and the transparency of the atmosphere. The irradiance of Q_s on a horizontal surface at the upper level of the plant community is of great significance in terms of its interaction with the community as the rays move through the canopy.

The exact theoretical calculation of Q_d is complicated but the flux of Q_d is strongly influenced by cloud type and amount. For example, maximum values are often observed below *altocumulus*, and *altostratus*, and minimum values below *nimbostratus* and *stratus*. The irradiance Q on a horizontal surface is derived by summing Q_s and Q_d.

The spectral distribution of Q_s and Q_d are different, the maximum value of Q_s per unit wavelength being in the green-yellow spectral region, whereas the maximum for Q_d below

a cloudless sky is in the blue region (Kondrat'yev, 1969).

In bioclimatic studies most attention is paid to photosynthetically active radiation P.A.R. (400-700 nm), but measurement of long wave radiation is seen as important also.

(b) Optical properties of vegetation

Table 1.2 and figure 1.4 illustrate some of the optical properties of average green leaves.

Table 1.2: Reflection, transmission, scattering and absorption coefficients of average green leaves in P.A.R., N.I.R., short wave, and long wave radiation wavebands. (modified after Ross, 1975) (0.1μm = 100 nm)

	P.A.R. (0.4-0.7μm)	N.I.R. (0.71-4.0μm)	S.W. (0.35-3.0μm)	L.W. (3.0-100.0μm)
reflection (ρ)	0.09	0.51	0.30	0.05
transmission (τ)	0.06	0.34	0.20	0.00
absorption (α)	0.85	0.15	0.50	0.95
scattering (ω)	0.15	0.75	0.50	-

From table 1.2, the *absorption coefficient* (α) is derived by using ρ and τ in the following expression

$$\alpha = 1-(\rho+\tau) \qquad (1.3)$$

The *coefficient of scattering* (ω) is also derived from ρ and τ

$$\omega = \rho+\tau \qquad (1.4)$$

As table 1.2 and figure 1.4 show, absorption is large for P.A.R. and long wave, the former being associated with

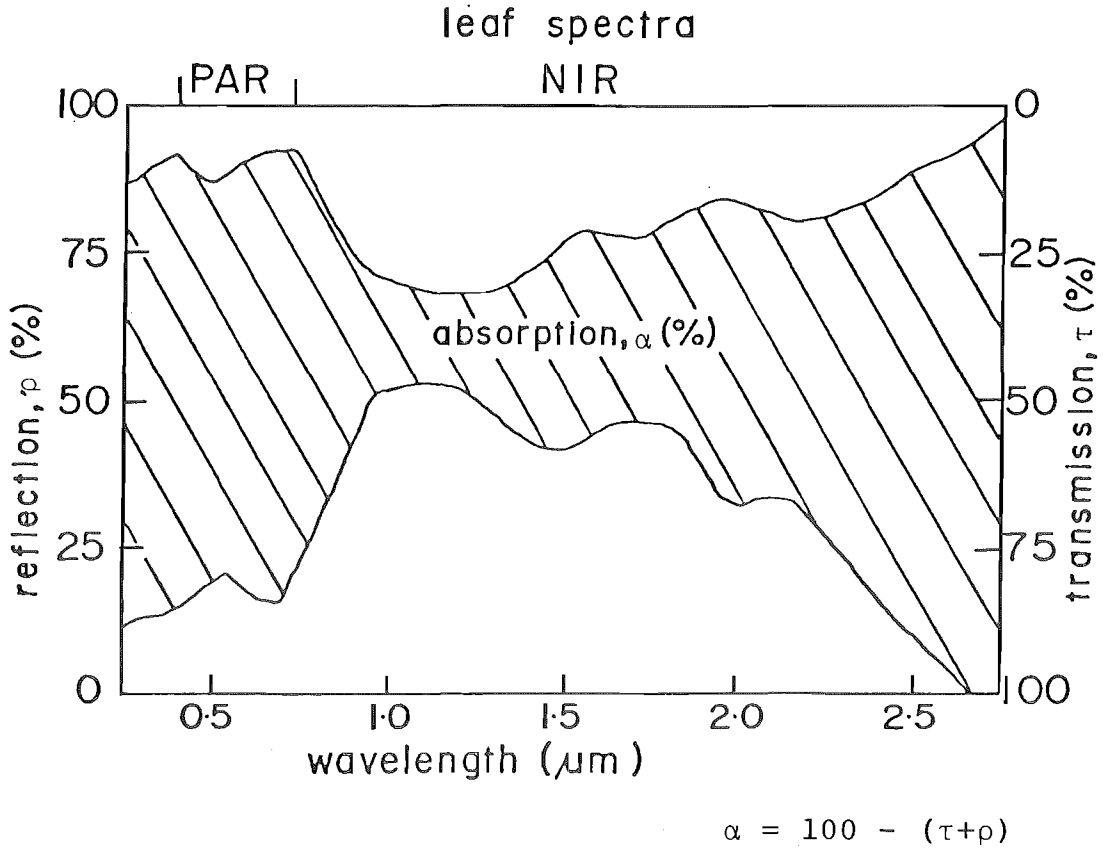

Figure 1.4: Optical properties of an 'average' green leaf (after Monteith, 1973)

photosynthesis and the latter with heating. For N.I.R., absorption is small and transmission and reflection are large.

Optical properties of leaves vary due to specific differences, leaf structure and age, adaptation, and so on. The spectral properties of leaves change during the growing season (Brandt and Tageyeva, 1967). Studies have shown that young leaves which have a bright green colour, tend to have a relatively large transmission and reflection and a small absorption. Fully mature leaves, which display dark green leaves tend to have a large absorption, and a small reflection and transmission, and old leaves which are often yellow or brown show a large reflection and a small absorption.

The work of Moldau (1965) has shown that the angular distribution of scattered radiation is affected by the nature of the leaf surface. For example, scattering of matt leaves tends to be more uniform in all directions, whereas glossy leaves are more dependent on the angle of the incident irradiation.

Gates *et al* (1965) have shown that the highest degree of absorption is possessed by the needles of coniferous plants - 97 percent in P.A.R. This relates primarily to their structure and orientation and this fact is expanded upon in chapter four of this thesis.

Absorption increases with increasing leaf thickness (Schulgin, 1963). In plant communities, the thickest leaves

are usually associated with *sun-crown* foliage, as *shade-crown* leaves tend to be much thinner (that is, have a lower weight per unit area ratio). Leaf thickness appears therefore, to be directly related to irradiation loading. Shade leaves have to be thinner, so as to operate efficiently under low light levels. Sun foliage is prone to overheating, and thicker leaves seems to be an adaptation to overcome this problem.

(c) Optical properties of the ground surface

The optical properties of the ground surface below a stand are directly related to the amount of irradiance reflected upwards (*albedo*). In situations where a substantial forest floor flora is present, the reflected levels of irradiance could be quite high; if snow is present, then the albedo could be as high as 95 percent. The albedo of a surface is directly related to the intensity of the incident irradiance. Below dense stands, where incident irradiance levels are low one would expect reflected irradiance from the ground to be correspondingly low (perhaps less than one percent of the total incident above the stand Q_o).

(d) Stand architecture

This is the most important factor determining many features of the radiation regime in a plant community. The penetration of radiation through a plant stand depends on such factors as the amount of leaves and other plant parts obstructing the beam, on the spatial distribution and the mutual shading of leaves, on their size and orientation (Ross, 1975).

Describing the architecture of a plant community is complicated by the heterogeneity of their horizontal and vertical structure, especially in the case of forests. Many authors (e.g. Monsi and Saeki 1953, Saeki and Kuroiwa 1959, Saeki 1960, Kuroiwa and Monsi 1963, Anderson 1964c, 1966b, 1970, 1971, 1981, Cowan 1968, Ross 1970, Kuroiwa 1970, Niilisk *et al* 1970, Norman and Jarvis 1975, OKer-Blom and Kellomäki 1981, 1982) have attempted to model the penetration of radiation into plant stands. Many theoretical models have assumed that a stand is horizontally uniform and that irradiance and stand architecture are only affected by height. This approach led to the classification of the *leaf-area-index* (L) a dimensionless quantity expressed as m^2 leaf area per m^2 ground area. Most work has concerned the use of the projected leaf area index rather than the total surface area leaf index, and as will be demonstrated in chapters four and six, use of the former technique has limitations with respect to calculation of total photosynthetic leaf surface (especially in conifers).

Stand architecture is also characterised by *stand height* (H *canopy depth* (CL), and a *foliage area density function* (a(z)), which determines the foliage area in unit space volume at a height z (m^2 foliage area/m^3 stand volume).

Indirect estimates of stand architecture have been derived from hemispherical (*fish eye lens*) photography (e.g. Evans and Coombe 1959, Anderson 1964a,c, 1971, 1981). In most cases leaf area index is estimated. Recently Jupp *et al*

(1980) have developed a more complex scanning program to give estimates of leaf area index, leaf angle and azimuth.

Direct measurement of foliage inclination and orientation is described in Anderson (1971). A technique developed by Wilson (1959, 1960, 1963, 1965) for non destructive sampling of foliage area index and inclination using *inclined point quadrats*, illustrates a method that has great potential for work in field crops and herbaceous plant communities.

Niilisk *et al* (1970) have divided irradiance in a stand into three components: (a) direct solar radiation (Q_s) as a beam of rays penetrating through the gaps in the foliage without appreciable spectral alteration and observed in the form of bright *sunflecks*; (b) diffuse solar radiation (Q_d) penetrating through the gaps without interacting with foliage; and (c) *complementary* radiation due to the scattering (transmission and reflection) of direct and diffuse radiation on the foliage and on the ground surface. The upward part of this radiation is defined as reflected radiation, the downward complementary radiation. The direct measurement of these three components is not always possible because of difficulties in separating complementary radiation from unobstructed radiation.

In several works (Ross and Nilson 1965, Cowan 1968, Wilson 1965, 1967, 1971, Anderson 1966b, 1970, 1971, Kuroiwa 1970, Jarvis *et al* 1976), *extinction coefficients* K for the passage of direct solar radiation (Q_s) are defined for various types of

stand. K is defined in equation 1.5

$$K = \frac{G(n_s)}{\sin\beta} \qquad (1.5)$$

where $G(n_s)$ = projected area of unit foliage in the direction n_s, and

β = solar elevation

For *horizontal* leaves K = 1, for *vertical* leaves $K = (2/\pi)\cot\beta$, and if the leaf area distribution is uniform then $K = \frac{1}{2}\sin\beta$. When leaf orientation is constant, K changes with solar elevation. Applying K theoretically assumes a random spatial distribution of leaves, and this assumption is not always valid, especially in the case of forest communities.

The penetration of direct solar radiation into a stand therefore, depends strongly on the stand architecture but the mathematical modelling of the penetration involves several complications and more work is required. The penetration of diffuse radiation into a stand holds similar problems. In general, the penetration of total radiation is greatest for a stand with vertical leaves and least for a stand with horizontal leaves (Ross, 1975).

The determination of the penetration of unobstructed direct and diffuse irradiance is a purely geometrical problem and thus requires no knowledge of the optical properties of the vegetation. In contrast, complementary direct and diffuse irradiance are strongly influenced by the optical properties of the vegetation (see section 1.2.2 b).

Since the calculation of downward irradiance in detail is complicated, usually only simplified empirical or semi-empirical formulae have been used for total irradiance. Perhaps the most famous of these is the Monsi and Saeki (1953) simple exponential formula

$$Q = Q_o \exp.^{-KL} \qquad (1.6)$$

where Q_o = irradiance above the plant community,

Q = irradiance below the canopy layer,

K = extinction coefficient, and

L = leaf area index.

From equation 1.6 K, which is a function of wavelength and solar elevation, is defined by

$$K = \frac{Ln(Q_o/Q)}{L} = \frac{Ln(1/\tau)}{L} \qquad (1.7)$$

where $\tau = Q_o/Q$ is the mean transmissivity of the canopy, and

Ln = natural logarithm

K is an empirical extinction coefficient constant which is related to a particular species and most often ranges between 0.2 and 1.5. The higher values of K correspond to large horizontal leaves (e.g. cotton, clover) and the lower values to vertical ones (e.g. ryegrass). In chapter six of this thesis, K values are calculated for the four tree species studied (see chapter two).

The upward radiation reflected from a stand is composed of reflection and multiple scattering by plant organs and by

the ground surface. The reflection coefficient of a stand ρ plays a fairly important role in the energy balance of a plant community. Reflected radiation is the upward part of complementary radiation which depends on the absorption coefficient and scattering function of leaves, on their orientation, on the architecture and the depth of the stand, on the reflection coefficient of the ground surface, and on the geometry and spectral distribution of incident radiation (Ross, 1970).

Work has shown, that reflected radiation decreases motonically with the depth of the stand and differs from the downward profile of complementary radiation. The influence of leaf orientation on reflected radiation is mostly in the uppermost layer of the stand.

The reflection coefficient(ρ) of a stand usually ranges between 0.02 and 0.05 for P.A.R., between 0.20 and 0.35 for short-wave radiation and between 0.40 and 0.60 for N.I.R. This being a function of the optical properties of the leaves and wavelength (see section 1.2.2 b).

Irradiance intensity and quality are intimately linked to the process of photosynthesis. The ability of a stand to absorb irradiance is a function of its architecture and at best, only about a quarter of the photosynthetically active radiation is converted into chemical energy by photosynthesis after absorption by the stand (Anderson, 1971).

1.2.3 Carbon Metabolism and Exchange in Plants

(a) Photosynthesis and respiration

Photosynthesis (P) is concerned with the photochemical and biochemical reactions whereby electromagnetic energy is absorbed and transformed into chemical energy of a form usable for cellular metabolic reactions (San Pietro, 1967). P is measured as units of photosynthate produced or net carbon dioxide uptake/ground area/time. In most plants, only the leaves can photosynthesise and in all plants the process is restricted to the daylight period.

Respiration (R) is measured as units of photosynthate used or carbon dioxide evolved/leaf area/time. All plant parts (stem, branches, leaves) respire and the process occurs by day and night.

Equation 1.8 illustrates green plant photosynthesis.

$$2H_2O+CO_2 \xrightarrow{P.A.R.} O_2+(CH_2O)+H_2O \qquad (1.8)$$

The result of photosynthesis in green plants is the *evolution* of oxygen and the *assimilation* of CO_2 into *cellular material* (CH_2O) at the expense of photosynthetically active radiation (400-700 nm). Details of the photochemical and biochemical reactions involved in photosynthesis are numerous (e.g. Vernon 1967, Kok 1967, San Pietro 1967, Larcher 1975).

The yield of the photochemical reaction in photosynthesis depends upon the amount of energy supplied, and the duration of irradiation. Chlorophyll content of leaves is also

important; differences in content are hardly detectable if irradiance is strong, but they become evident under insufficient light. If there is a distinct lack of chlorophyll then photosynthetic efficiency declines. Chlorophyll content is often associated with the light climate. Leaves that have developed in the lower levels of the plant canopy show morphological and physiological adaption to the prevailing low light conditions. Shade leaves show adaptation to prevailing low light conditions.

(b) Carbon dioxide exchange in plants

Carbon metabolism in the plant cell is linked to the external environment by *gas exchange*. In photosynthesis the chloroplasts use up carbon dioxide, of which a supply must be maintained, and liberate oxygen (Larcher, 1975). At the same time, by both day and night, the cells take up oxygen for respiration and give off carbon dioxide. In assimilating leaves, one or the other of these two opposed processes can predominate at a given time.

During the day the rate of CO_2 uptake per unit of plant mass required for photosynthesis is greater, as a rule, than the rate at which CO_2 is freed by the total respiration in light, so there is a net uptake of CO_2 into the leaf (net photosynthesis). If the rate of photosynthesis is the same as the respiration rate then the *compensation point* ($P = R$) is reached. If the rate of photosynthesis declines still further, respiration may predominate ($P < R$), and in the dark, respiratory release of CO_2 alone prevails.

Gas exchange is regulated by the stomata. The *stomatal diffusion resistance* (r_s) depends upon both the environment and the interior of the plant. The most important external factors are irradiance, temperature, humidity and water supply; the internal factors include the CO_2 partial pressure in the intercellular system, the content of water and ions in the tissues, and presence of phytohormones.

Under optimal conditions, that is, strong illumination, good water supply, favourable temperature, and air in which the CO_2 concentration is 0.3-1 percent by volume, herbaceous plants are capable of taking up as much as 150 mg CO_2 per dm^2 leaf surface per hour (photosynthetic capacity, usually only reached under laboratory conditions).

Photosynthetic capacity varies among species and is of ecological significance, but its greatest importance is as a basis for the selective breeding and cultivation of plants valuable in agriculture, gardening and forestry.

Photosynthetic capacity and respiratory activity are characteristics of a plant species, but they are not constants. Within a given plant, gas-exchange behaviour changes in the course of development and with seasonal and even diurnal fluctations in activity (Larcher, 1975). For example, younger plants respire more rapidly than older plants, and very young leaves are not able to fix CO_2 efficiently, especially in conifers.

When a canopy is exposed to increasing intensities of irradiance, the CO_2 uptake increases at first in proportion to light intensity and then more slowly to a maximum value. The relationship between rate of photosynthesis and the intensity of light is represented by a saturating curve (figure 1.5). At Q_{sat}, *irradiance saturation point* is reached. At this point, even if all the ingredients are in ample concentrations (i.e. CO_2, water and minerals), photosynthesis still reaches a maximum rate. At Q_c, *irradiance compensation point* is reached. At this point photosynthesis fixes exactly as much CO_2 as is set free by respiration ($P = 0$).

In general, the Q_c within canopies lies at 2-3 percent of full sunlight, and Q_{sat} occurs at around 20 percent of full sunlight (Horn, 1971).

The effect of temperature upon the processes of photosynthesis and respiration is exerted through the temperature dependence of the various enzymes involved. The fixation and reduction of CO_2 occurs with increasing speed as the ambient temperature rises, until an optimum temperature is reached. With very high temperatures the rate of photosynthesis falls off sharply and respiration increases. The temperature limits for net photosynthesis, given saturating light conditions, vary widely with different plant species. In the temperate zone plants assimilate CO_2 at temperatures as low as $0^{\circ}C$. Plants adapt to temperature change during the seasons by adjusting their photosynthetic and respiratory rates.

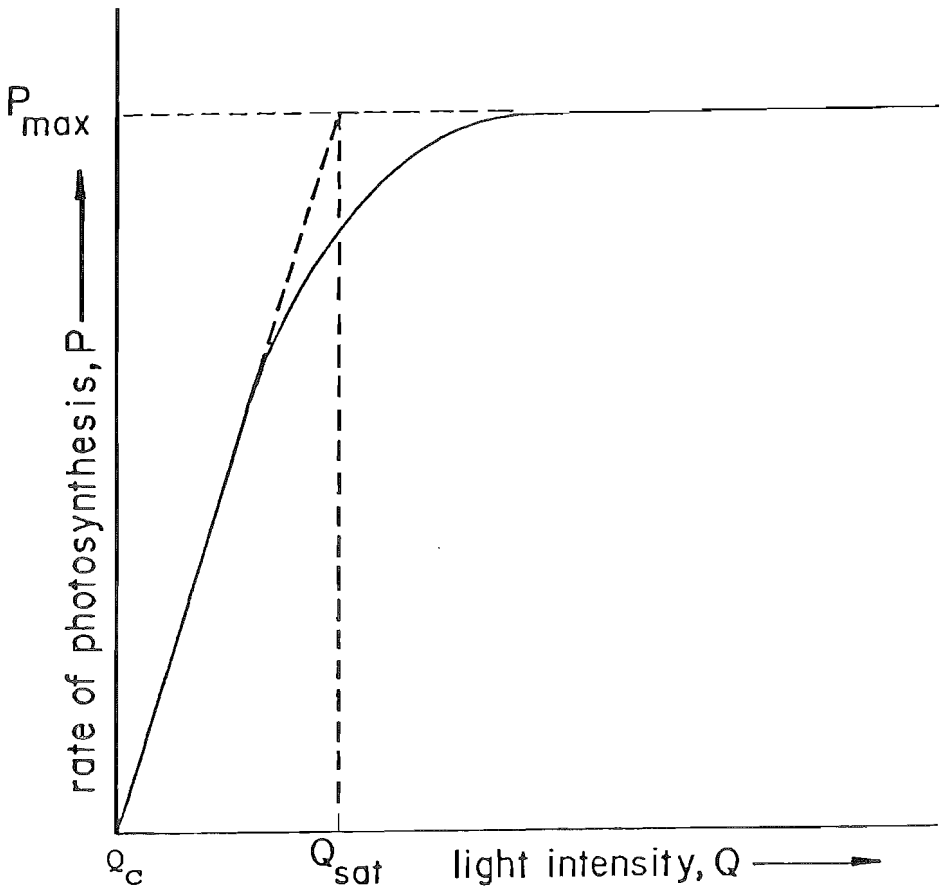

Figure 1.5: Schematic diagram illustrating the typical effect of light on the rate of photosynthesis.

Water also plays an important role in the photosynthetic process, mainly by maintaining a high turgidity in the protoplasm. In this way, CO_2 exchange through the stomata is turgor-regulated. If there is a water deficiency in a plant, the stomata narrow and CO_2 exchange slows down. If the deficiency continues, photosynthetic capacity declines as the protoplasm becomes increasingly desiccated. At this stage, appreciable CO_2 uptake is no longer possible. The sensitivities of CO_2 exchange to lack of water, are to a large extent characteristics of a plant species, but they are also adaptable (Larcher, 1975).

Photosynthesis and respiration are influenced by the ground temperature, by the mobility of water and the air content of the soil, and by mineral nutrients. Soil temperature, soil oxygen concentration, and water content of the soil affect mainly respiration in the roots, their growth, and their absorptive activity. In soils not seriously deficient in particular nutrients, the availability of minerals is less critical than the environmental factors. Mineral nutrients affect gas exchange by influencing the behaviour of the stomata, and by their effect on other properties of the leaves such as their anotomic structure, size, life span, and above all their number (Larcher, 1975).

In summary, the gas exchange rate of plants is an expression of the interplay of many internal and external environmental factors. Of these factors, one is usually rate limiting at any given time.

(c) Plant productivity

When concerned with *plant productivity* it is necessary to consider the average yield of CO_2 uptake. Plants consist not only of green (photosynthetically productive tissues), but also of others (branches, twigs, roots) that respire and must therefore be nourished by the leaves. These factors must be considered when determining an overall CO_2 budget for a plant (or plant community).

Assimilated carbon not lost by respiration increases the dry matter of a plant and can be used for growth and for laying down reserves. To measure the amount of accumulated carbon, gathered and dried plants are weighed and the increase in weight is an indication of the amount assimilated.

The quantity of organic dry matter formed per unit time by the vegetation covering a given area is the measure of the productivity of a stand of plants (commonly expressed as tonnes of organic dry matter per hectare per year). From Larcher (1975), the production Pr of a plant community is greater, the higher the assimilation rates (N.A.R.) of the species composing the community, the more completely the available light is captured by the assimilation surfaces (the leaf area index, L), and the longer the time in which the plants can maintain a positive gas-exchange balance (duration, t) of the production period. That is,

$$Pr = N.A.R. \cdot L \cdot t \qquad (1.9)$$

The extent and arrangement of the *assimilation surfaces* is taken into account by the total surface leaf area index (see section 1.2.2 this chapter). The extent to which the layers of foliage are orientated is important for production if the photosynthetically active radiation (P.A.R.) is absorbed as completely as possible during its passage through the canopy of leaves (Larcher, 1975). The canopy architecture, more especially the spatial distribution of foliage within the canopy are key factors with respect to determining productivity (seen as the ability of a plant community to utilize P.A.R. to the greatest possible extent over the greatest possible leaf area).

In chapter six of this thesis, estimates of stand productivity in terms of these factors are made on the basis of empirical light and stand architecture measurements.

1.3 MEASUREMENT OF IRRADIANCE IN FOREST COMMUNITIES

1.3.1 Introduction

While an enormous literature exists on the theory and measurement of irradiance in crop and herbaceous canopies, there has in contrast been comparatively little work carried out in forests.

Comprehensive reviews of irradiance in forest communities have been published (e.g. Anderson 1964c, 1966a, 1970, 1971, Reifsnyder and Lull 1965, Evans 1966, Reifsnyder 1967, Ross, 1975, Jarvis *et al* 1976, Rauner 1976, Allen and Lemon 1976).

In an attempt to cover some of the literature, the following section will provide a summary of the approaches and problems in the measurement of irradiance in forest communities.

1.3.2 Approaches and Problems in the Measurement of Irradiance in Forest Communities

The penetration of direct beam irradiance into a forest depends upon the intensity of the solar beam incident upon the stand and upon the number, size, and space distribution of canopy openings (Anderson 1964c, Horn 1971, Reifsnyder *et al* 1971). Whereas, the penetration of diffuse irradiance depends upon the distribution and amount of sky brightness, the number, the size, and the space distribution of canopy openings, and the geometry, space distribution, and optical characteristics of the forest biomass (Anderson 1964b, c, Horn 1971, Reifsnyder *et al* 1971, Ross 1975).

Changes in earth-sun geometry and variations in canopy openings affect the penetration of direct beam irradiance, making it highly variable in time and space. In contrast, the factors governing the penetration of diffuse radiation within a forest are not highly variable, therefore diffuse radiation within a forest is more uniform in space and time.

The main obstacle to the measurement of irradiance in forests therefore, is adequate sampling. Most workers are aware of the *spatial* and *temporal* variability of irradiance in

forests - more especially in direct beam irradiance, and have therefore tended to measure the direct and diffuse radiation components separately (see Anderson 1964c).

Ross (1975) divides the time frequency spectrum of fluctuations of irradiance in forests into four intervals: (a) fluctuations with a period of about a second due to leaf flutter in wind; (b) fluctuations with a period of about 10 minutes caused by the movement of the sun's disc or broken clouds and occurring as an alternation of sunflecks and shaded areas; (c) the diurnal change of radiation; and (d) the annual change of radiation.

(a) Measurement of irradiance beneath forest canopies

Most work in forests has tended to focus on either, the *short-term variability* in irradiance (e.g. Evans 1956, Vézina 1961, Vézina and Péch 1964, Reifsnyder 1967, Gay *et al* 1971, Reifsnyder *et al* 1971) or the *long-term variability* in irradiance (e.g. Anderson 1964a, b, Coombe 1966, Eber 1971, Young and Whitehead 1981) on the forest floor.

A number of ingenious techniques have been proposed to permit adequate short-term sampling on the forest floor, but none has proved especially successful. However, Gay *et al* (1971), and Reifsnyder *et al* (1971) have achieved a substantial reduction in sampling deviations by averaging several readings in space. There are still substantial problems with the measurement and adequate sampling of penetrating direct beam irradiance and because of this, a large number of readings

are needed to sample with a reasonable degree of precision, especially for *instantaneous values* or short-period averages (Reifsnyder *et al*, 1971). It is the enormous expense of photo-electrical measuring equipment that frequently restricts the multiple sampling of irradiance beneath canopies.

Young and Whitehead (1981) propose a simple, inexpensive technique for the long-term measurement of irradiance on the forest floor using photosensitive paper booklets contained in plastic petri dishes (after Friend, 1961). The advantages of the technique are firstly, its cheapness and simplicity, and secondly, because of the multiple replication of sensors *integration* of irradiance over time and space is possible (details concerning this technique are extensively covered in chapter three of this thesis).

The seasonal variation in the light climate beneath a forest stand has been studied by several workers (e.g. Anderson 1964a, b, Coombe 1966, Hutchison and Matt 1977). Anderson's studies (1964a, b) were all made in a deciduous forest and show great *diurnal* and *seasonal* variations in direct beam irradiance as compared with diffuse irradiance. The variations in direct beam irradiance were shown to be functions of diurnal and seasonal changes in solar elevation, and seasonal variations of leaf mass. She calculated transmission percentages (monthly averages) for direct and diffuse irradiance through the course of the seasons. Anderson's data and careful analysis deserve close study by anyone interested with the problem of irradiance beneath forest stands.

Federer and Tanner (1966a) measured the *spectral distribution* of light under a variety of canopy types, including broadleaves and conifers, using a portable spectrophotometer. Direct beam irradiance was excluded in their study because this form of irradiance can pass through a canopy without impinging on plants and is therefore spectrally similar to irradiance in the open.

From the work of Coombe (1957), Federer and Tanner (1966a), and Freyman (1968), it appears that tree canopies lead to a depletion of the blue region of the spectrum (400-450 nm) and an enrichment of the red and near infrared (650-750 nm). The light on the floor is therefore photosynthetically less active and taken in combination with the reduced magnitude of radiation this tends to limit the variety and productivity of plants growing on the floor (Oke, 1978).

Evans and Coombe (1959) discuss the use of hemispherical and woodland canopy photography as a technique for estimating the light climate of the forest floor. The hemispherical image is obtained by using a *fish eye* lens which has a 180^{o} angle of acceptance. They point out the utility of these photographs by superimposing a solar track diagram on the image.

Anderson (1964a, c, 1971, 1981) attempted to apply architectural techniques to hemispherical photographs in a variety of plant communities. By comparison with some three years records of daily totals of radiation at several sites

under a forest canopy, she showed that fish eye photographs can be used to predict the mean percentage transmission of diffuse and direct radiation. This is done by superimposing grids and estimating the amount of obstruction (for details, see Anderson 1964a).

This method does not take into account the contribution of scattered radiation, but gives a good estimate of the average transmission of photosynthetically active radiation, which is little scattered (Anderson, 1971).

Studies of the light climate beneath forest canopies neglect most often to consider the light climate of the canopies' themselves. Jarvis *et al* (1976) rightfully point out, that whilst these analyses are of considerable relevance to the production of the ground flora, they provide only limited information on the influence of canopy structure on radiation penetration, and on the variability of radiation for processes within the canopy.

(b) Measurement of irradiance within forest canopies

Despite the importance of the canopy radiation climate with respect to processes such as photosynthesis, respiration, and transpiration very little empirical research in forest canopies has been made.

Hutchison and Matt (1977) have made a comprehensive study of solar radiation within a deciduous forest over a two year period. Their study illustrates rather well, the

diurnal changes in the forest radiation regime due to the earth's rotation, and seasonal variations due to earth-sun geometry and phenological changes in forest structure. Measurements were made using elevated solarimeters at three levels within the forest. Diffuse and direct radiation were sampled separately.

The results of their study are comparable with those of Anderson (1964b). Of the two radiative components, direct beam radiation suffers the greatest attenuation by the *forest biomass* - especially in the overstorey canopy. The diffuse component, on the other hand, is less attenuated by the forest biomass and its attenuation is more uniform in the three-canopy strata of the leaf-less forest than that of the direct beam component (Hutchison and Matt, 1977). However, in the fully leafed forest, the greatest amount of attenuation of diffuse radiation occurs in the overstorey canopy as well. This study deserves close examination because the effects of horizontal and vertical heterogeneity in forest structure are quantified through replication of measurements of forest radiation in horizontal and vertical space.

Description of the radiation regime within evergreen, in particular, coniferous forests are especially limited. A study by Norman and Jarvis (1974) of canopy structure and interception of radiation in Sitka Spruce (*Picea sitchensis*) is a good example of a highly specialised method. The objective of their study was to predict photosynthesis of leaves at certain positions in the canopy by measuring the radiation at different levels.

The average transmittance and transmittance distributions of visible and near-infrared radiation were measured at four levels under various conditions of sun inclination angle, and diffuse/direct irradiance. A sensor was used to scan 14 m transects through the foliage-bearing portion of the canopy at each of four levels. A data logger was used for recording and the sensor scanning speed was set at 1.8 cms^{-1}, allowing irradiance to be measured every 7 mm along the transect. The distributions of transmitted radiation were strongly influenced by leaf area index, sun inclination and fraction of diffuse/direct radiation (Norman and Jarvis, 1974).

A study by Mayer (1981) illustrates the vertical distribution of irradiance within a Spruce forest in summer. For that purpose three stationary radiation measuring systems were set up at 2 m above the forest floor, within the canopy, and at the tree top level. Horizontal variations in irradiance were not considered in this study.

From the preceding discussion it seems, that the problems of sampling irradiance within forest canopies are undoubtedly severe. A satisfactory solution to overcome the spatial variability in irradiance in canopies, seems to be to traverse sensors along transects at a number of levels under different sky conditions as was illustrated by Norman and Jarvis (1974).

Spatial variability of irradiance within canopies is especially difficult to overcome. The prohibitive costs of photo-electric sensors and data logging equipment being the main problem. The technique described by Young and Whitehead (1981) using photosensitive paper booklets contained in petri dishes is perhaps one method where both the spatial and temporal variability of irradiance in canopies can be adequately sampled. Multiple replication of the sensors is quick and inexpensive, and integration of irradiance over a period of one week under all sky conditions is possible.

1.4 OBJECTIVES

Solar radiation is the driving force for essentially all processes occurring within ecosystems. The success of a plant species at a particular site is best determined by its carbon uptake. Different ecosystems have evolved different strategies in utilising solar radiation to fix carbon and in distributing this to best advantage (Benecke and Nordmeyer, 1982).

By virtue of the architecture of forest ecosystems, the canopy of photosynthetic tissue largely governs both *abiotic* and *biotic* energy flows within these ecosystems. The canopy controls abiotic energy flow through the combined effects of its architecture and optical characteristics. Knowledge of leaf area and its spatial distribution is essential for estimating photosynthesis, tranpiration, respiration, canopy interception, and energy transmission to the ground. Since

forest canopies shade the ground beneath, the bulk of photosynthetic production occurs in the upper crown, which suggests that the biotic energy flow within the system is closely controlled as well.

The main aim of this thesis is to achieve a better understanding of the radiative component of the abiotic and biotic energy flow strategies in different forest ecosystems.

The specific objectives are as follows:

1. To develop adequate sampling techniques which allow for measurement of spatial and temporal variability of irradiance within forests.
2. To select several tree species (in stand form) with different architecture but as similar as possible site and growth-stage characteristics.

For each of the selected forest stands:

3. To determine the effects of horizontal and vertical heterogeneity in stand structure by measuring incident and reflected irradiance above and in a horizontal plane at three levels within the canopy, and at one level in the trunk-space.
4. To illustrate the effects of seasonality, site characteristics, and phenological changes in canopy structure on the stand radiation regime.
5. To make tentative estimates of carbon uptake in different parts of the canopy on the basis of its architecture and ability to absorb irradiance.

CHAPTER TWO

THE STUDY AREA

2.1 THE PHYSICAL SETTING

2.1.1 Location and Topography

The study area is located 20 kilometres east of the Main Divide on the eastern slopes of the Craigieburn Range ($43^{o}09'S$, $171^{o}43'E$) - the east and west coasts of the South Island being more or less equidistant at about 100 kilometres. (figure 2.1).

The Craigieburn Range rises from an altitude of 800 m to 1900 m and is orientated north-south, swinging to the north-east at the northern end. To the east lie, Castle Hill Basin (a small intermontane basin at 700-800 m altitude), the Torlesse Range, and the Canterbury Plains.

2.1.2 Geology, Hydrology and Soils

Geologically, the Craigieburn Range is fairly typical of the eroded mountain land east of the Main Divide from North Otago in the south to Cook Strait in the north.

Substrata on the field sites consists almost exclusively of thick beds of strongly undulated greywacke and argillite of Triassic/Jurassic age. The substrata and surface strata tend to be unstable and easily weathered. The Castle Hill Basin to the east is geologically different having Tertiary sedimentary deposits.

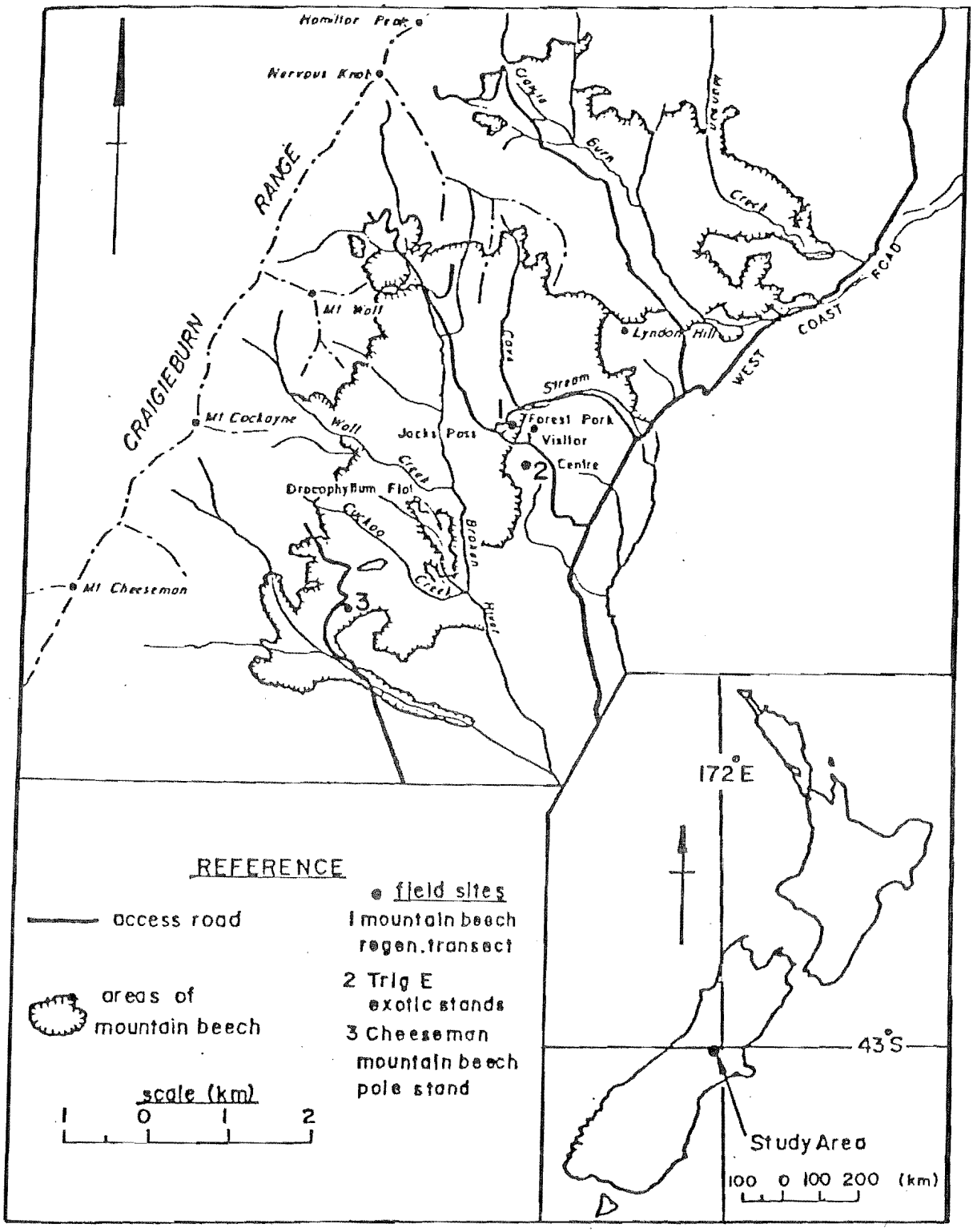

Figure 2.1: The Study Area

The Craigieburn Range is flanked by several streams, the most notable of these being Broken River which drains the eastern face of the range. This upper level catchment forms part of the watershed between the Waimakariri and Rakaia catchments (figure 2.1).

Soils in the study area are High-Country yellow-brown earths and related steepland soils, known specifically as the Tekoa-Bealey Soils. These soils have developed on greywacke materials under forest on steep and very steep slopes between 600-1200 m where the rainfall is 1000-1600 mm. Profiles have brown or greyish brown granular or crumb topsoils and yellowish brown very friable crumb to nutty or blocky subsoils (Raeside *et al*, 1968).

These soils are subject to frequent frost action in areas where the vegetation cover has been removed, resulting in widespread erosion. In some sites erosion has removed the topsoil completely exposing subsoil surfaces. In more severe cases, the subsoil has been eroded forming extensive screes. These soils have low fertility, and the implications for plant growth have been studied (e.g. Kellard 1978, Nordmeyer 1978a, b, and Davis 1978, 1981). More recently, Harrison (1982) has made a comprehensive study of their erosion cycles.

2.1.3 Climate

Details of the climate of the study area have been published (Morris 1965, McCracken 1980). According to

Coutler (1973), who has provided a classification of New Zealand mountain climates, there are three main categories. The Craigieburn Range falls into category three, having annual precipitation of 1500-2500 mm, less fog and cloud than the other two, periods of strong drying conditions at times, and mild temperatures. The climate of the study area is comparable with that experienced in the inland ranges of Marlborough and the Kaweka Range in the North Island.

Climate data have been collected daily at two sites in the study area, Craigieburn Forest (914 m) since January 1964, and Ski Basin (1550 m) since July 1966. Details of the instrumentation at these sites is given in McCracken (1980).

Table 2.1 illustrates average mean monthly climate data for the Craigieburn Forest site (plate 3.4). The altitude of the station (914 m) is similar to the field sites chosen for this study.

Annual mean temperatures are mild (7.9^{o}C) with a summer period of four months (monthly mean temperature 10^{o}C or more). February is the warmest month (mean 13.8^{o}C) and July is the coolest month (mean 2.0^{o}C). Annual mean soil temperatures at a depth of 10 cm (10.4^{o}C) are mild also, February being the warmest month (mean 18.2^{o}C) and July the coolest month (mean 2.1^{o}C).

Table 2.1: Average mean monthly climate data at Craigieburn Forest (914 m a.s.l.) (1964-79, except where stated) (data after McCracken 1980, and Cruden 1981)

	J	F	M	A	M	J	J	A	S	O	N	D	annual mean or total
Temperature (^{o}C)													
absolute maximum	31.5	32.9	28.0	23.4	18.1	16.5	13.5	16.2	24.3	25.2	26.4	29.5	
mean maximum	19.2	20.5	18.0	14.3	9.7	6.9	6.3	8.1	10.6	13.2	15.3	17.9	13.3
mean (1964-80)	13.2	13.8	12.1	8.9	5.2	2.4	2.0	3.4	5.5	7.5	9.6	11.9	7.9
mean minimum	7.1	7.2	6.5	3.7	0.4	-2.1	-2.5	-1.3	0.3	1.7	3.6	5.7	2.5
absolute minimum	-0.9	-1.1	-2.6	-6.7	-6.8	-9.0	-8.6	-9.6	-7.1	-6.7	-6.5	-2.6	
grass minimum (1965-79)	5.3	5.2	4.6	1.0	-2.1	-4.7	-5.1	-3.1	-1.3	-0.2	1.7	4.0	0.4
mean soil 10 cm (1966-79)	17.9	18.2	15.5	10.6	6.1	2.8	2.1	4.0	7.2	10.3	13.4	16.3	10.4
days ground frost	1	1	3	10	20	25	27	24	17	13	7	2	150 (total)
days screen frost	0	0	1	5	15	23	25	22	14	10	5	1	121 (total)
Rainfall (mm)													
mean total (1964-80)	118.3	70.7	80.8	126.3	132.3	94.7	110.3	143.1	152.8	174.8	148.8	117.2	1461.6 (total)
Windspeed ($m.s^{-1}$)													
mean daily (1966-80)	1.4	1.1	1.2	1.1	0.9	0.7	0.7	0.9	1.3	1.3	1.4	1.4	1.1
Radiation (MJm^{-2})													
mean daily (1965-80)	20.7	18.6	13.3	9.5	6.0	4.7	5.1	7.7	11.6	16.7	19.5	20.8	13.0
													4745 (total)

The occurrence of ground frost is common (150 days on average per year) with no month of the year ground frost-free. The average number of screen frosts per year (121 days) is also high with only January and February being free of screen frosts.

Rainfall is reasonably well distributed throughout the year but dry periods can occur, especially in the late summer months of February and March - this is shown by the mean rainfall totals for these months, 70.7 mm and 80.8 mm respectively. October (mean 174.8 mm) and November (mean 148.8 mm) are the wettest months - associated with an increase in rain-bearing westerlies at this time of the year. Precipitation at the Craigieburn Forest site is largely in the form of rain, and snow contributes to a small extent as well, but is more important above 1000 m (McCracken, 1980).

Windspeeds are on the average low (1.1 $m.s^{-1}$). This is because the meteorological site is situated on the eastern side of the Craigieburn Range which affords some protection from prevailing westerly winds. However, the study area is subject to frequent, strong and often dry north-west (*föhn*) winds. Together with low humidities these conditions can lead to plant moisture deficits even after only short periods without rain (Benecke *et al*, 1978). June and July are the least windy months (both, mean 0.7 $m.s^{-1}$), and can be explained by the more frequent occurrence of anticyclones over New Zealand in the winter months. The spring and summer months (September-February) are more windy, largely because of increased westerly wind systems over the warmer months.

The mean annual radiation total for Craigieburn Forest (4745 MJm^{-2}) is quite high compared with the New Zealand annual average (4200-5000 MJm^{-2}), especially considering the reduction of potential radiation caused by horizon obstruction. McCracken (1980) has estimated that horizon obstruction accounts for a 3% reduction in mid-summer and a 12% reduction in mid-winter of the clear-day potential radiation. Figure 2.2 illustrates the horizon effects at the site. Extra-atmospheric radiation at $43^{o}S$ ranges from 42 $MJm^{-2}dy^{-1}$ in December to 11 $MJm^{-2}dy^{-1}$ in June. Daily radiation totals at the ground in the study area have been measured as high as 80% of the extra-atmospheric total.

2.1.4 Vegetation

The native vegetation of the study area is typical of the South Island high country east of the main divide. The lower slopes of the Craigieburn Range support monospecific forests of mountain beech (*Nothofagus solandri* (var.) *cliffortioides*) up to 1350 m a.s.l. Snow tussock (*Chionochloa flavscens*) is dominant above timberline.

As a result of burning practices over the last 1000 years and browsing by animals in the last 150 years the forest cover is far from continuous today (Molloy, 1969). Coupled with the fact, that mountain beech is poorly adapted to surviving fire and regenerating on exposed sites (Wardle 1970, 1980), it seems unlikely that the original forest cover will ever return.

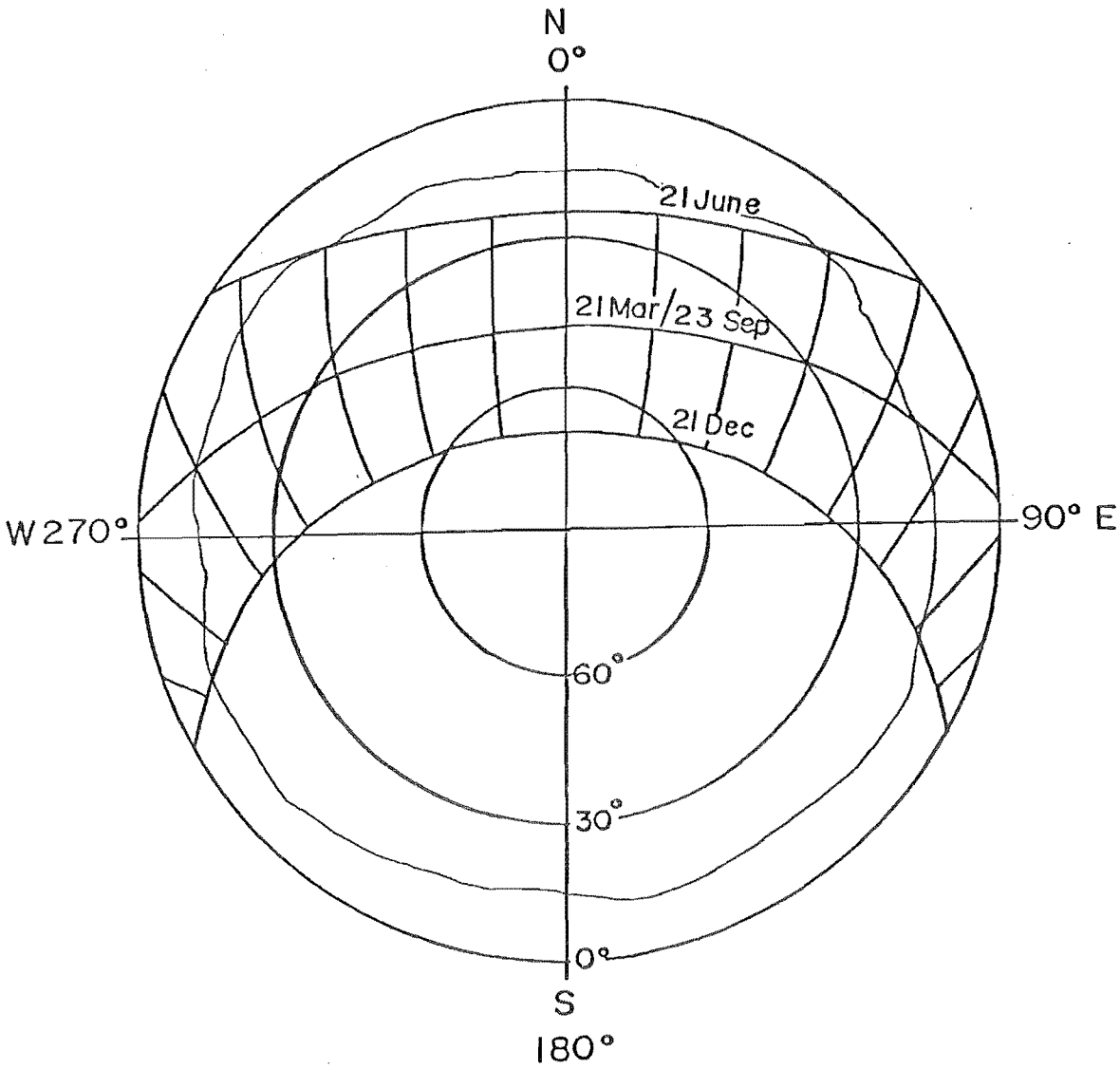

Figure 2.2: Horizon at Craigieburn Forest meteorological site (Craigieburn Range). Solar paths for solstices and equinoxes shown for 43°S.

After burning, previously forested sites have been colonised by tall snow grasses (predominantly *Chionochloa macra*) at higher elevations, and by fescue grasslands (dominated by *Festuca* tussocks) at lower elevations (Evans, 1980).

In more recent times, destruction of tussocks by fires and browsing animals has led to widespread erosion accompanied by the development of screes in some areas. Exotic conifers and more especially those of the *Pinus* spp. have proved to be much more successful for erosion control and reforestation of depleted grasslands in the Craigieburn Range, and elsewhere (Nordmeyer, 1980a).

2.2 THE HUMAN SETTING

2.2.1 History of Settlement

Early polynesian peoples travelled through this area and were responsible for causing numerous fires. Evidence of past fire activity is best illustrated by charcoal remains (Molloy, 1969). Natural fires also affected the vegetation in the area.

The biggest impact of the landscape came with the arrival of the first Europeans. Significant areas of forest were burned and domestic grazing animals were introduced. Later introductions of game animals such as rabbits and deer combined with burning and domestic browsing led to severe erosion problem in some areas.

Flock Hill Station to the north and Castle Hill Station to the south are the two major high country sheep/cattle stations in the region. The large inland basins of Castle Hill and Cass are primarily used for agriculture. A lime quarry is situated in the Castle Hill basin, associated with the Tertiary sedimentary deposits.

The Craigieburn Range offers much in the way of recreation (e.g. skiing, skating, and tramping). The Craigieburn Forest Park contains numerous bush walks which are easily accessed from the main road. The park is especially popular in the summer with day trippers from Christchurch and elsewhere.

2.2.2 Research in the Study Area

In 1959 the New Zealand Forest Service set up a field station in the Craigieburn Range to further watershed-management studies in mountain lands. Since then, the Forest Research Institute has carried out numerous trials in the area, with agricultural legumes, grasses and forest species (see Orwin, J. (Ed), 1978 for further details).

From 1956 to 1962 several hundred different plant species, both native and exotic, were planted at altitudes from 800 to 1500 m on sites varying from grassed slopes to steep running screes.

In 1963, intensive testing was begun for a number of forest species to identify the provenances best adapted for vigorous growth in New Zealand mountain climates, as typified

by the Craigieburn Range (see Benecke and Morris 1978, Ledgard 1980). It was found that many species, including native plants, failed completely on the exposed subsoils or screes. In many species, those provenances from a latitude similar to ours have grown well, but the best results are obtained with seed from New Zealand grown plants.

The study of the mountain climates has also received considerable attention because of its importance to the survival and growth of plants, and its effect on edaphic processes. Work has been conducted at the regional and micro-climatic scales. Information is used in an attempt to define the conditions that limit plant establishment, growth and succession.

Much slope stabilisation work has been done over the 20 years since revegetation research was initiated in the high country. Revegetation work on screes and protection of capital works, such as roadsides, are examples of projects.

Other research has focused on: (a) tree growth and primary production (Nordmeyer 1980a, Benecke and Havranek 1980a), and (b) ecophysiology of montane and subalpine trees (Benecke and Havranek, 1980b). The latter has involved the use of a mobile laboratory, where the gas-exchange processes are measured in the field. More recently, first attempts to integrate (a) and (b) have been made, by comparing native and exotic forest species (Benecke and Nordmeyer, 1982).

2.3 THE FIELD SITES

Forest stands were chosen at montane altitudes (800-1000 m a.s.l.) close to the Craigieburn Forest meteorological site (914 m a.s.l.). Exactly comparable site characteristics were not possible because the exotic tree species were artificially planted on deforested slopes while the only native species is natural on old well developed soils. However, the forest stands chosen for this study were in the steepest part of their sigmoid growth pattern. Therefore, biomass productivity and canopy closure were at or close to maximum. Stand characteristics are discussed in detail in chapter four.

2.3.1 Exotic Forest Stands

The exotic forest species chosen for this study were: lodgepole pine (*Pinus contorta* Douglas ex. Loudon ssp. *contorta*), Douglas fir (*Pseudotsuga menziesii* (Mirbel) Franco), and European larch (*Larix decidua* Mill). These species are all conifers and, with the exception of *Larix decidua*, evergreen.

The stands are all located on Trig E (figure 2.1, plate 2.1). Stand characteristics are shown in table 2.2, and figure 2.3 illustrates the horizon at the site. Because of the northerly aspect, the angle of slope, and limited horizon effects the site receives adequate insolation throughout the year.

According to Ledgard (1980), from 200 exotic species tested in the Craigieburn Range, less than 10% have proved

Plate 2.1: The exotic forest stands situated on Trig E (1050 m a.s.l.) on a 30° north facing slope.

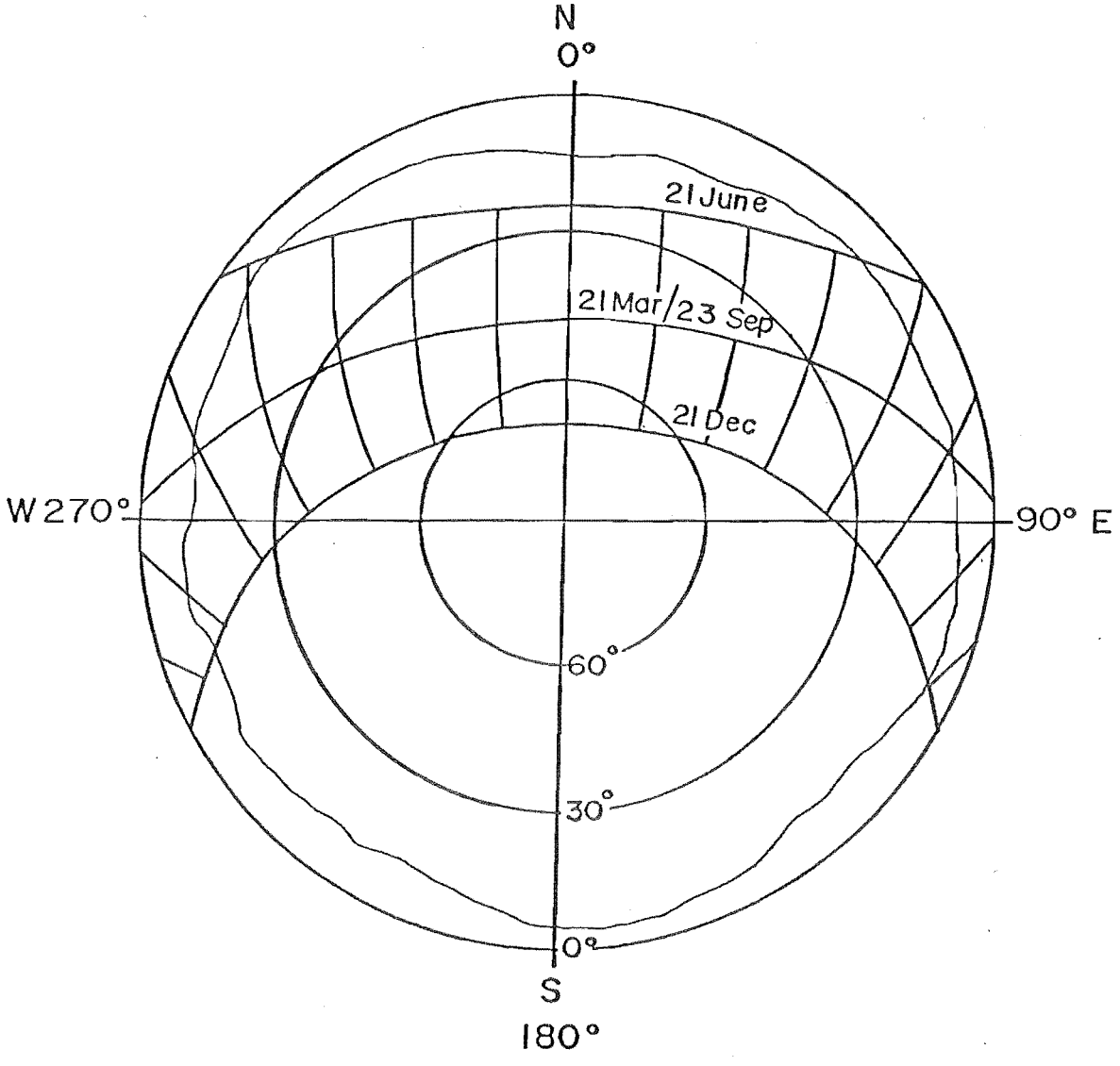

Figure 2.3: Horizon at Trig E site (Craigieburn Range). Solar paths for solstices and equinoxes shown for 43°S.

Table 2.2: Stand characteristics of *Pinus contorta*, *Pseudotsuga menziesii*, *Larix decidua*, and *Nothofagus solandri* used in this study. (data after, Benecke and Nordmeyer, 1982, and Ledgard 1980, unpublished)

	exotic species			native species
Characteristics	*Pinus contorta*	**Pseudotsuga menziesii*	**Larix decidua*	*Nothofagus solandri*
Altitude (m.a.s.l)	1050	1050	1050	1000
Slope (degrees)	30	30	30	25
Aspect	north	north	north	east
Age (years)	20	15	15	52
Stocking (stems ha^{-1})	4430	2700	2400	19000
Mean height (m)	9.0	7.5	7.0	6.5
Dominant height (m)	10.4	8.4	8.7	8.6
Basal area (b.h.o.b $m^2 ha^{-1}$)	74.6	38.6	20.4	94.0
Total stem vol. (o.b $m^3 ha^{-1}$)	373	165	107.4	410
Stem M.A.I.(o.b $m^3 ha^{-1} a^{-1}$)	18.7	11.0	7.2	7.9

*1980 data

b.h.o.b = breast height over bark

M.A.I. = mean annual increment

suitable for reforestation work above 900 m. The exotic tree species chosen for this study are amongst the 10% listed as successful.

Of the exotic tree species, *Pinus contorta* has proved the fastest growing on virtually all sites up to timberline (Benecke *et al*, 1978; Benecke and Morris, 1978). *Pseudotsuga menziesii* has proved more successful on stable topsoil and subsoil sites, preferably with a northerly aspect up to 1000 m (Ledgard, 1980). *Larix decidua* has proved the most successful of the larch group, but is susceptible to wind, summer frosts (Benecke and Havranek, 1980a), and opossum browsing.

2.3.2 Native Forest Stands

The monospecific forest species in the study area is mountain beech (*Nothofagus solandri* var. *cliffortioides* (Hooke.f.) Poole), a broad-leaved evergreen (hereafter referred to as *Nothofagus solandri*). Wardle (1970) has made a detailed study of this species.

The stand of *Nothofagus solandri* used in this study is located at Cheeseman (figure 2.1). The stand is of uniform age and of pole form, corresponding to the steepest part of its sigmoid growth pattern. Details of the stand characteristics are given in table 2.2, and figure 2.4 illustrates the horizon at the site. Unlike the Trig E site, the aspect is easterly and horizon effects are more marked.

A less detailed study of the light environment beneath

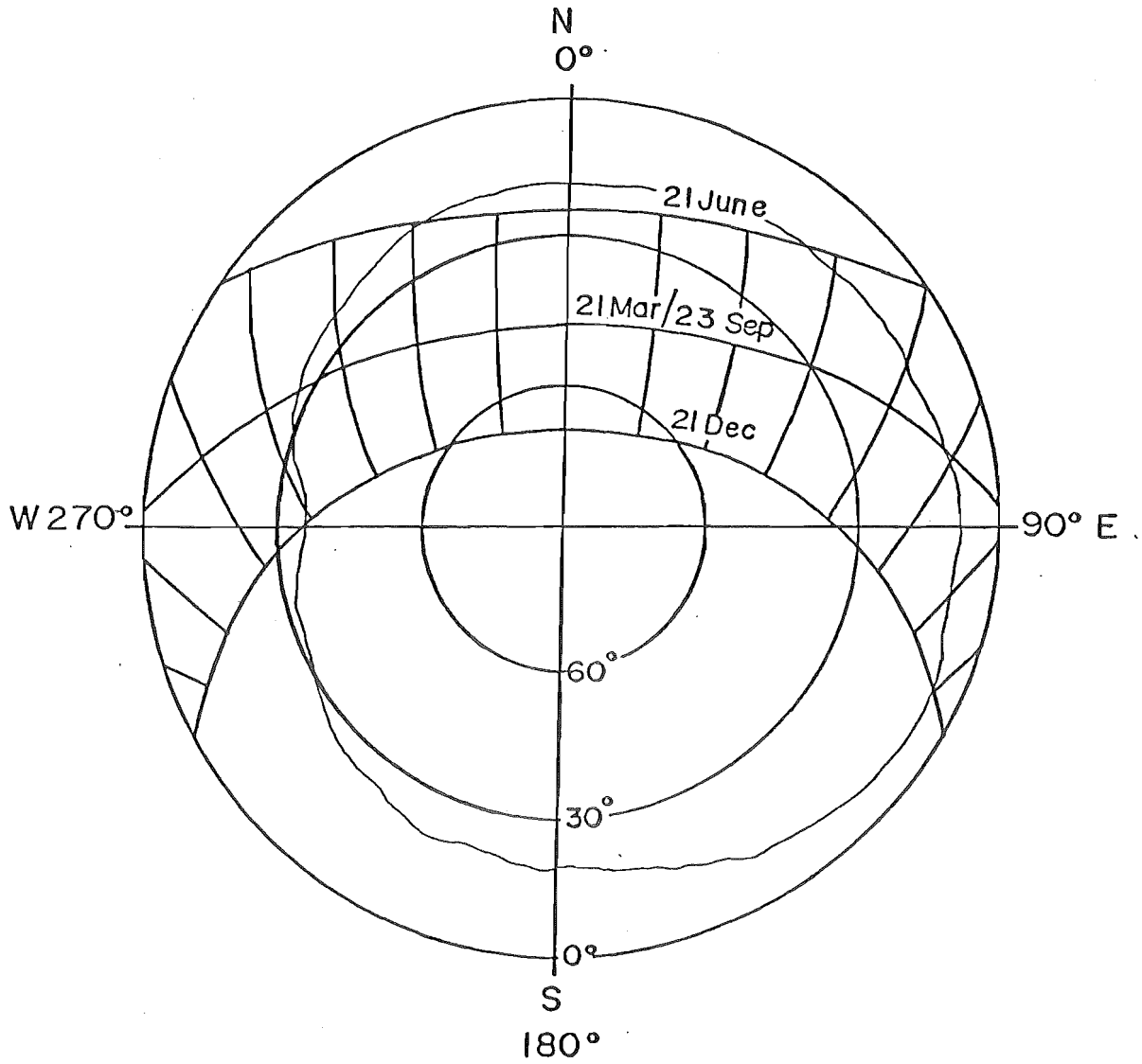

Figure 2.4: Horizon at Cheeseman site (Craigieburn Range). Solar paths for solstices and equinoxes shown for 43°S.

a canopy opening in a post-mature *Nothofagus solandri* forest was made near Jack's Pass (figure 2.1). Measurements were made along a transect, sensors being set up to correspond with the height of the regenerating beech seedlings (see chapter three, section 3.1.2, h(ii)). Horizon effects at this site are similar to those at the Craigieburn Forest meteorological site (figure 2.2).

CHAPTER THREE

METHODS AND MATERIALS

3.1 PHOTO-CHEMICAL MEASUREMENT OF IRRADIANCE

3.1.1 Photo-Chemical Techniques

A recently published review (Agnew and Causton, 1982) covers the photo-chemical techniques for the measurement of irradiance. Advantages and disadvantages of the various techniques are assessed. The following discussion will review the various techniques and will be followed by a detailed account of the ammonia diazo paper technique (Friend, 1961) which was used in the field.

(a) Anthracene

Dore (1958, p.151) proposes a simple inexpensive technique for measuring irradiance. The technique uses anthracene ($C_{14}H_{10}$) in benzene solution which polymerizes into insoluble dianthracene $(C_{14}H_{10})_2$ on exposure to sunlight. A saturated solution of anthracene was made and placed in screw-cap vials with foil-lined bakelite caps.

The anthracene are then placed out in the habitat, on the ground or supported in a horizontal position at any particular level in the plant canopy. As exposure to light proceeds crystals of dianthracene will start to form, then increase in quantity. For purposes of measurement, the dianthracene was disregarded and the analysis was made on the amount of anthracene remaining in solution. To do this,

a spectrophotometer was used.

Dore (1958) found a logarithmic relationship existed between anthracene in solution (gm/lt) and exposure to light (foot candle-hours).

Subsequently, this technique has been used elsewhere (Friend 1959, Marquis and Yelanosky 1962, De Sloover and Marynen 1963, and Pierik 1965).

(b) Potassium iodide

Pearsall and Hewitt (1933) describe a method, in which the intensity of light is measured by estimating the amount of iodine liberated when a solution of potassium iodide mixed with sulphuric acid is exposed to the light. To do this, 20 cm^3 of 2% potassium iodide were mixed with an equal volume of 1.15% sulphuric acid (by weight) and were then exposed to light.

The solutions were exposed in conical flasks fastened by wire to a weighted line at fixed depths within a lake. The exposure period was six to eight hours. After exposure, the iodine liberated was titrated with freshly prepared and standardised potassium thiosulphate, N/100 or N/1000 depending on the amount of iodine liberated.

A rather complicated calibration procedure was followed to determine full daylight intensity and the results from the subaqueous intensities were expressed as percentages of the values for full daylight. In their results, they found that

the light intensities derived from the potassium-iodide technique were similar to those measured by a photo-electric cell behind a blue Wratten No.49 screen. This suggests, that the solution is sensitive to photosynthetically active radiation (400-700 nm). Unfortunately, this technique does not seem to have been tried subsequently.

(c) Uranyl oxalate

This method involves the photolysis of uranyl oxalate in aqueous solution in the presence of excess oxalic acid. The original method was developed by Heinicke (1963), based on the work by Atkins and Poole (1929), for measuring light in the canopy of a Canadian orchard where light intensity was about half full sunlight.

Smith and Scott (1970) used a modification of Heinicke's method for measuring light in a Miro *(Podocarpus ferrugineus)* forest in New Zealand. In the experiment, partially masked glass tubes of uranyl nitrate/oxalic acid solution were exposed to light for several days and the decomposition, shown to be linearly dependent on the amount of light received, was found by titration. Smith and Scott (1970) have stated, that tests in artificial light and natural forest show that the method is applicable to a wide range of light intensities.

(d) Potassium ferrioxalate

The techniques described previously, with the possible exception of Potassium Iodide, are sensitive to primarily shorter wavelengths (less than 450 nm) and because of this

photosynthetically active radiation (400-700 nm) is not measured directly.

Agnew and Causton (1982) propose a new photo-chemical technique using potassium ferrioxalate. The spectral sensitivity of the solution closely approximates the photosynthetically active wavelengths which gives it an obvious advantage over the other more spectrally selective techniques. The technique they describe still requires more experimentation but by and large, prospects appear promising. The main problems are, variations in response from meter to meter and a maximum integration total of only $25MJm^{-2}$.

3.1.2 Ammonia Diazo Paper

(a) Background

Friend (1961,p.577) reminds us, that while photo-electric light meters are capable of providing highly accurate measurements, the expense of having a number sufficient for adequate simultaneous sampling of various habitats is prohibitive.

Measurements of irradiance within forest communities is particularly difficult. The intensity and spectral quality of light received at one point within a stand may vary by several orders of magnitude as sunflecks move with position of the sun and as the branches sway in the wind. The light-climate of any forest system is therefore enormously complex. Spot measurements using photo-electrical sensors merely explain conditions at one time or at one place. An ideal approach

would be to sample irradiance at several sites and to do so over a much longer time period. The overall result would give a far better integrated picture of the light-climate of a particular plant community. As was previously stated, such an approach using photo-electric methods would be impossible because of the enormous expense involved.

A technique, first described by Friend (1961) making use of ammonia diazo paper, is inexpensive and does not require electronic data logging equipment. The preparation, calibration and development of diazo paper light sensors is described in greater detail in succeeding sections.

Diazo paper is used in the manufacture of blueprints and in certain types of copying machines. Light yellow in colour before exposure to light, this photo-sensitive compound forms a deep blue colour on exposure to ammonia vapour. When exposed to light the paper becomes bleached, the extent of which depends on the length of exposure and the intensity of the light source.

The technique used relies on counting the number of layers of the diazo paper which have been chemically changed during the exposure period. By placing the paper in square booklets (30 mm x 30 mm), each containing 15 sheets, Friend (1961) discovered that as the action of light is to bleach the paper, rather than darken it, a series of density filters is provided by the stack of paper itself. When calibrated with photo-electric integrated sensors it was found that a

logarithmic relationship exists between energy received by the photo-electric sensor and the number of papers changed in the diazo paper booklet.

(b) Preparation of booklets of diazo paper

The paper used was ammonium diazo A90/8, and B90/8, hereafter referred to as Type I and Type II respectively. The sensitivity of diazo paper varies considerably and for this reason it is important to calibrate any new batch. The paper also decays with age and re-calibration throughout its field use is recommended. When not being used the paper should be stored in a cool dark place. The preparation of the booklets is described in Friend (1961) and Young and Whitehead (1981). The same procedure was carried out in semi-dark conditions in the Geography Department, University of Canterbury. Fifteen sheets of A4 sized paper were stacked with the light sensitive side upmost (yellow colour) with plain paper top and bottom. A grid of 30 mm squares was ruled on the top sheet and one edge of each small square stapled, (figure 3.1). Cutting along the grid lines using a guillotine produced the individual booklets. Provided conditions are not too bright, a darkroom is not required for preparation. The prepared booklets are stored in a dark bag in a cool place.

(c) Light transmission through pyrex glass and plastic

Friend (1961) and Young and Whitehead (1981) both recommend the use of plastic petri dishes as containers for protecting the paper booklets whilst being exposed in the field. Purely out of curiosity an experiment was carried out

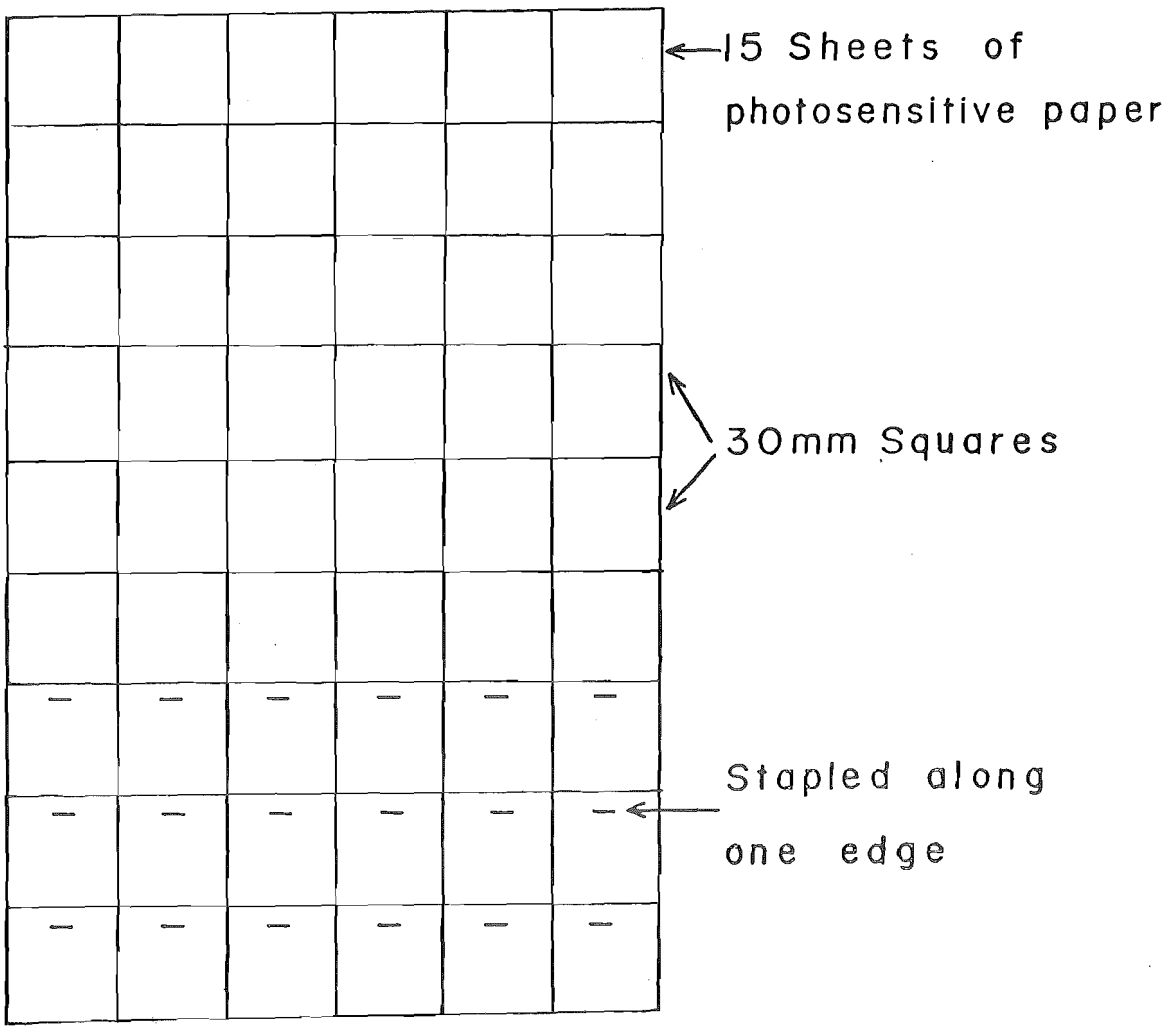

Figure 3.1: Arrangement for making booklets of photosensitive paper from large sheets.

in January, 1982 to compare the transmissivity of pyrex glass and plastic. Three plastic and three pyrex petri dishes were prepared in the manner described in section 3.1.2(d). The six dishes, containing booklets, were then exposed on the Geography Department roof over three time periods : one hour, six hours and 24 hours (excluding hours of darkness). The results of the experiment are shown in table 3.1.

Table 3.1: Transmissivity of pyrex Glass and plastic petri dishes containing diazo sensors in sunlight. (January, 1982)

exposure time (hours)	number of papers exposed: pyrex Glass	plastic
1.0	2.75	3.21
6.0	3.25	4.01
24.0	4.75	5.11

From the results in table 3.1 it does appear that the plastic petri dishes allowed a greater transmittance of light than the pyrex glass petri dishes. Pyrex glass is more spectrally selective in transmitting light but the specific wavelengths were not determined. One should also note, that upon becoming scratched, plastic becomes less permeable to light than pyrex glass. Great care should therefore be taken when handling the dishes in the field.

(d) Preparation of sensors in petri dishes

Plastic petri dishes, 90 mm in diameter, were used to keep the diazo paper booklets waterproof during the exposure period. The top of each petri dish was fitted with a circular

piece of black cardboard with a 20 mm diameter hole cut in the centre and a polystyrene disc in the bottom of the dish. The edges of the dishes were painted black to prevent any sidelight from entering. The booklet of diazo paper was placed beneath the 20 mm hole and the thickness of the polystyrene was arranged so that when the dish was closed the booklet was held tightly in position. Masking tape was used to hold the lid to the base and a piece of electrical tape was placed over the 20 mm window to prevent light entering before use (figure 3.2).

Several modifications to the design of Friend (1961) and Young and Whitehead (1981) were made. First, a larger 'light window' was used (20 mm in diameter, instead of 10 mm), because anything less would have made the use of the reflectometer more difficult (see section 3.1.2(e)(iii)). Second, because incident and reflected irradiance were being measured the sensor design for the latter had the light window on the base part of the petri dish (figure 3.2). And third, a strip of velcro tape was adhered to each sensor on the opposite side to the light window. The corresponding velcro strip was adhered to the transects (see section 3.1.2(h)(i)). This allowed for better servicing of dishes in the field and proved to be a strong enough bond, even during times of high wind.

Transport of the prepared dishes to the field sites was in a black plastic bag and when in position the exposure period was begun by removal of the black tape over the light window.

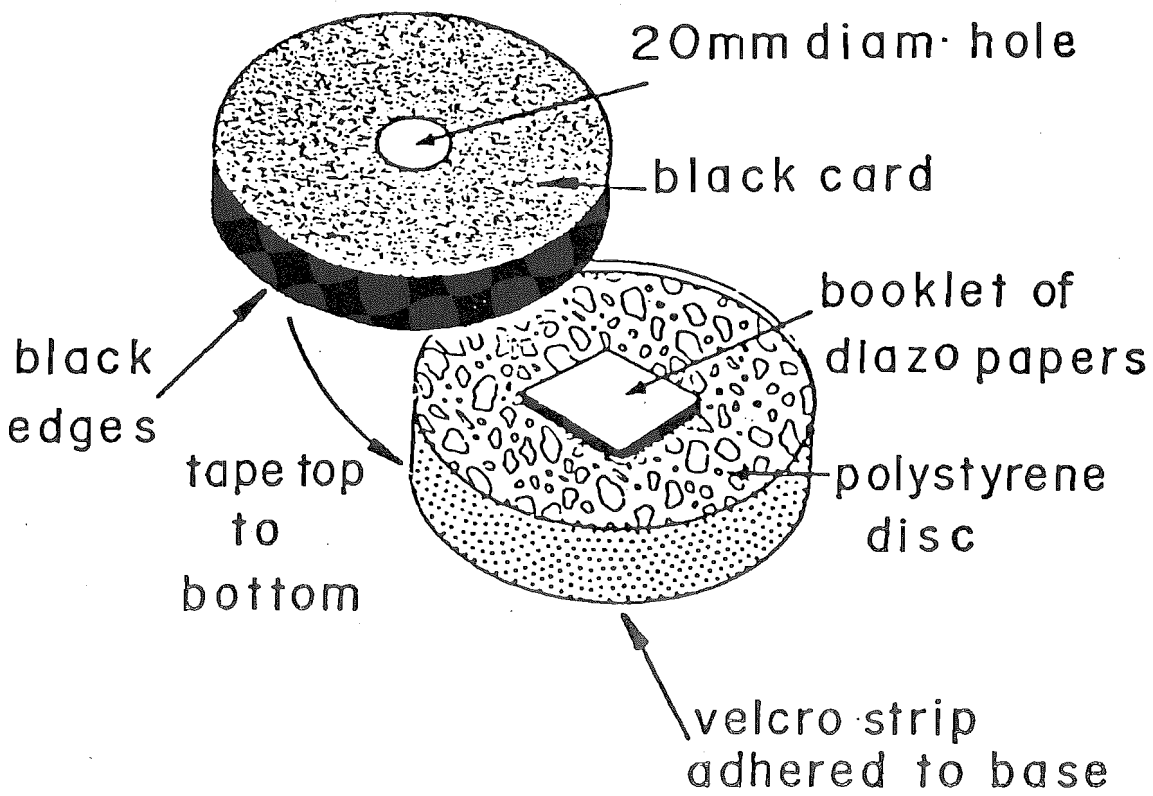

Figure 3.2: Preparation of sensors using plastic petri dishes.

(e) Development of diazo papers after exposure

(i) Ammonia vapour chamber

After one week's exposure in the field the dishes were taken back to the laboratory for development of the diazo papers in the ammonia vapour chamber (figure 3.3). In the laboratory the masking tape was removed and the booklets were prepared for developing.

25 mls of concentrated ammonia solution was placed in the bottom of a glass beaker in a fume hood, and the booklets were hung on rungs about 25 mm above the solution. During the developing process (5-15 minutes), the unexposed parts of the papers turned deep blue in colour while the fully exposed areas remained white. Partially exposed areas turned various shades from deep to pale blue.

(ii) Assessment of fully and partially exposed papers

The papers in the booklets which were neither white nor deep blue present some difficulty in interpretation. Young and Whitehead (1981) propose the use of a graded strip of developed diazo paper covering the range from white to deep blue. This method estimates values for the partially exposed papers down to one decimal point only, and relies on the judgment of the human eye when comparing the graded strip with the papers. Assessing the partially exposed papers is most important since the light intensity is reduced logarithmically as it passes through successive layers in the booklet.

To improve on the sensitivity of this technique the

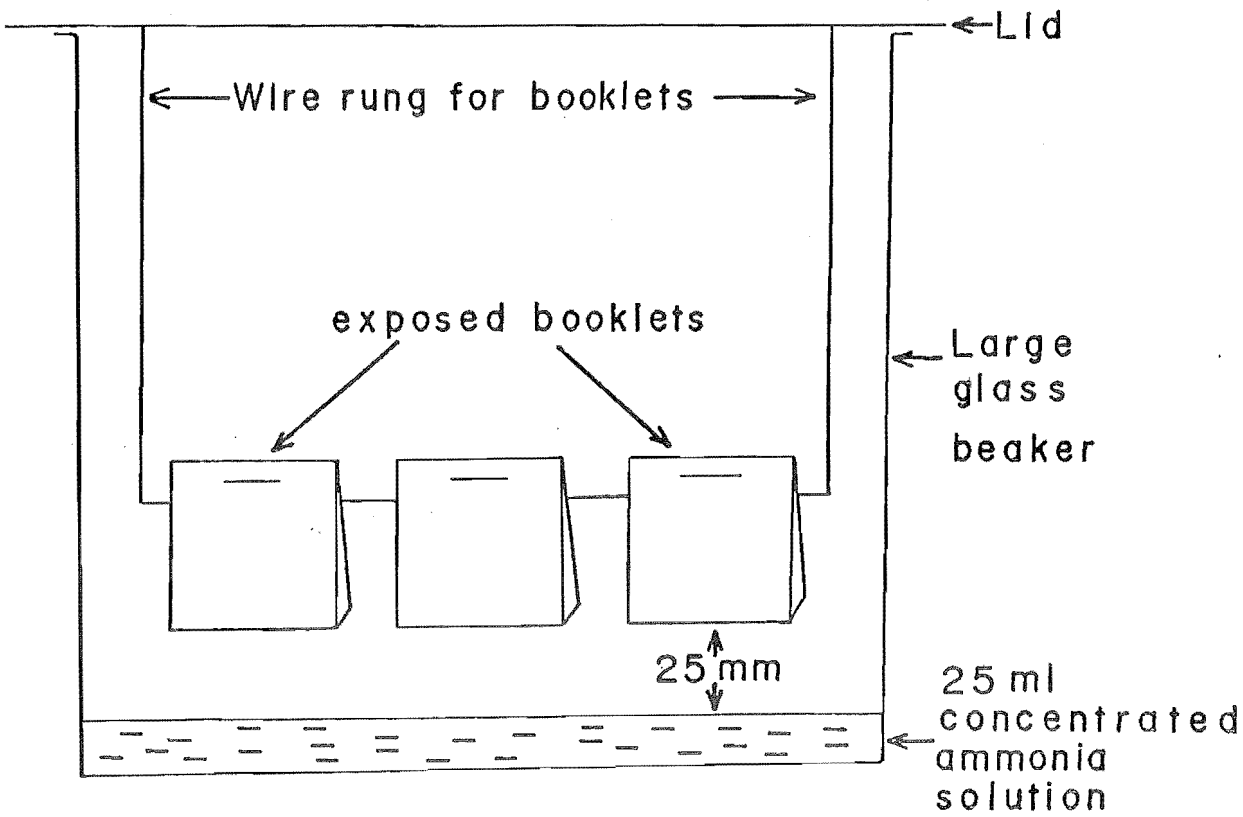

Figure 3.3: Ammonia vapour chamber for the development of exposed booklets.

partially exposed papers were analysed using a reflectometer (loaned by the National Radiation Laboratory, Christchurch). A reflectometer measures the albedo of a surface and because of this, it proved useful for obtaining accurate measurements for the partially exposed papers. The staples were removed from the developed booklets and the fully exposed papers were counted manually (depending on numbers fully exposed). It was then necessary to set the reflectometer scale on a fully exposed sheet (white) to 100, by turning a knob on the meter. A reading was then made on an unexposed sheet (deep blue) and was found to be 6.5 for type II paper. These two values represent the limits of the paper and any values in between can be determined to an accuracy of two decimal places (table 3.2).

Table 3.2: Reflectometer scale for partially exposed papers. (partially exposed fraction bracketed) 6.5 minimum; 100.0 maximum; 93.5 range.

6.5	(0.0)	- 11.17	(0.05)	- 15.85	(0.1)	
15.86	(0.11)	- 20.52	(0.15)	- 25.20	(0.2)	
25.21	(0.21)	- 29.87	(0.25)	- 34.55	(0.30)	
34.56	(0.31)	- 39.22	(0.35)	- 43.90	(0.40)	
43.91	(0.41)	- 48.57	(0.45)	- 53.25	(0.50)	
53.26	(0.51)	- 57.92	(0.55)	- 62.60	(0.60)	
62.61	(0.61)	- 67.27	(0.65)	- 71.95	(0.70)	
71.96	(0.71)	- 76.62	(0.75)	- 81.30	(0.80)	
81.31	(0.81)	- 85.97	(0.85)	- 90.65	(0.90)	
90.66	(0.91)	- 95.32	(0.95)	-100.00	(1.00)	fully exposed

Each booklet was analysed in this way and this proved an accurate method for assessing the developed diazo booklets.

For each booklet the number of papers fully exposed and the fractions given by the reflectometer were summed to give the total.

(f) Calibration of technique under Sunlight and Artificial Light

(i) Type I paper sensitivity test (January, 1982)

Over a period of seven days single diazo paper sensors were exposed for six different periods of time to full sunlight on the Geography Department roof. By the end of a week it was decided that type I paper was too insensitive (table 3.3). Given the high radiation values known for January, the small number of papers exposed in the booklets, and plans for autumn and early winter field-use when radiation levels are much lower, type I paper was therefore abandoned.

Table 3.3: Number of papers exposed over six time periods (type I paper) in sunlight, January, 1982.

time periods (hours)	number of papers exposed (n)
0.5	3.21
1.0	3.62
6.0	4.23
24.0	4.41
48.0	4.83
168.0	5.42

(ii) Type II paper sensitivity test (January, 1982)

Immediately following the experiment with type I paper an experiment using type II paper and seven time periods was conducted. The results from the experiment showed that type II paper was considerably more sensitive to sunlight than type I (table 3.4). Type II paper was therefore considered satisfactory for field-use.

Table 3.4: Number of papers exposed over seven time periods (type II paper) in sunlight, January, 1982.

time periods (hours)	number of papers exposed (n)
0.5	3.01
1.0	3.66
6.0	5.94
24.0	6.31
48.0	6.86
120.0	7.54
169.0	7.71

(iii) Type II paper calibrated with quantum sensor and integrator in sunlight, (March, 1982)

Having determined that type II paper was sensitive enough for field-use, an experiment was set up in March to calibrate the diazo paper with 400-700 nm irradiance received by a silicon photovoltaic quantum sensor and electronic integrator (both LAMBDA, Nebraska - for details, plate 3.1 and appendix 1). The data derived from the calibration is illustrated in table 3.5 and figure 3.4.

Plate 3.1: Silicon photovoltaic quantum sensor (on post) and integrator (both LAMBDA, Nebraska) : shown set up in the open near the Trig E forest stands.

Plate 3.2: Silicon photovoltaic sensor and portable recording meter (both LAMBDA, Nebraska) used for calibration of wavelengths and spot measurements.

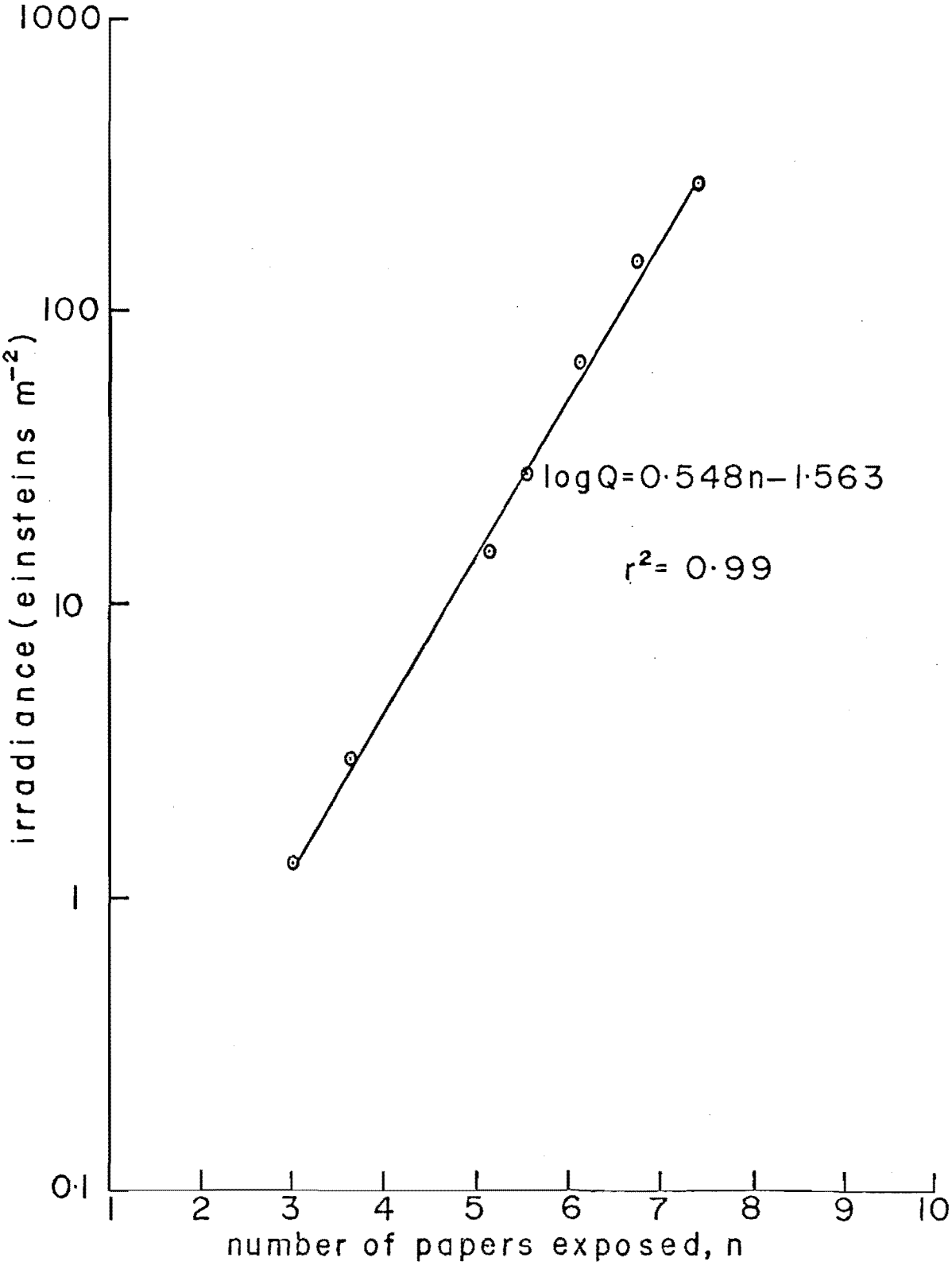

Figure 3.4: Relationship between number of papers exposed and log irradiance (Em^{-2}) received in sunlight in March : the points obtained by exposing the sensors for different times.

Table 3.5: Number of papers exposed (n) and irradiance received (einsteins m^{-2}) by quantum sensor (400-700 nm) over seven time periods (type II paper) in sunlight, March, 1982.

time periods (hours)	mean number of papers exposed (n)	(400-700 nm) irradiance received Em^{-2} (integrator)
0.5	3.01	1.30
1.0	3.66	2.99
6.0	5.11	15.54
24.0	5.57	27.76
48.0	6.18	67.72
96.0	6.78	148.90
168.0	7.23	278.34

(iv) Type II paper calibrated with quantum and pyrometric sensors under gro-lux fluorescent light bank

A similar experiment to that carried out by Young and Whitehead (1981) was simulated under gro-lux fluorescent tubes in the Biogeography Laboratory, University of Canterbury. The aim of the experiment was to measure the reaction of diazo paper under a constant light output. The output from the light bank was measured using silicon photovoltaic quantum and pyrometric sensors (LAMBDA, Nebraska, see plate 3.2 and appendix 1), and was found to be $59.13\mu Em^{-2}s^{-1}$ and $65.05Wm^{-2}$ respectively. The relationship between 400-700 nm and 300-3000 nm irradiance of $1Wm^{-2} \simeq 0.9\mu Em^{-2}s^{-1}$, is similar to that given by Young and Whitehead (1981), of $1Wm^{-2} \simeq 0.97\mu Em^{-2}s^{-1}$.

In the experiment, 14 petri dishes were exposed under the light bank (at the same level where the output was measured) over seven time periods. The integrated light output was interpolated for 400-700 nm and 300-3000 nm irradiance. The values derived assumed that the output from the light bank was constant at all times (table 3.6 and figures 3.5 and 3.6).

Table 3.6: Number of papers exposed (n) and irradiance received ($\mu Em^{-2}x10^{6}$) and (MJm^{-2}) over seven time periods (type II paper) at same level under GL fluorescent light bank.

time periods (hours)	irradiance (400-700 nm) Em^{-2}	irradiance (300-3000 nm) MJm^{-2}	mean number of papers exposed (n)
0.5	0.106	0.117	1.05
1.0	0.212	0.234	1.41
6.0	1.277	1.406	2.73
13.0	2.767	3.047	3.42
25.0	5.321	5.860	4.01
72.0	15.326	16.879	4.96
168.0	35.761	39.385	5.71

The correlation co-efficients for both graphs (figures 3.5 and 3.6) are lower than the one derived for sunlight (figure 3.4). One explanation could be, slight shifts in the voltage supply which would cause the output of light from the tubes to vary. To rectify the problem, a voltage regulator should have been used. Similarly, if an intergrator had been used in conjunction with the photovoltaic sensors then peaks and troughs in the light output would have been detected and allowed for in the regression.

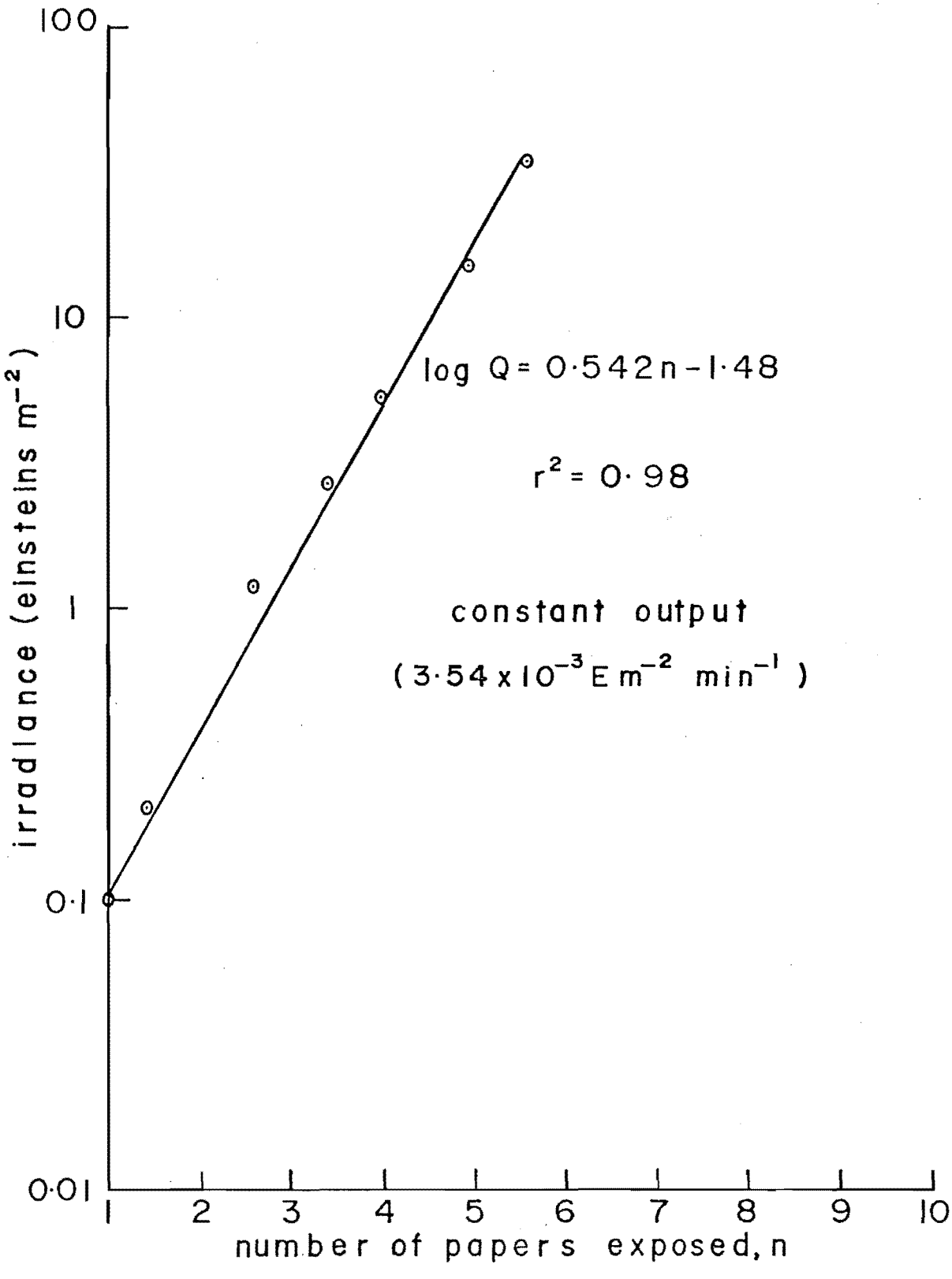

Figure 3.5: Relationship between number of papers exposed and log irradiance (Em^{-2}) received under GL fluorescent tubes : the points obtained by exposing the sensors for different times.

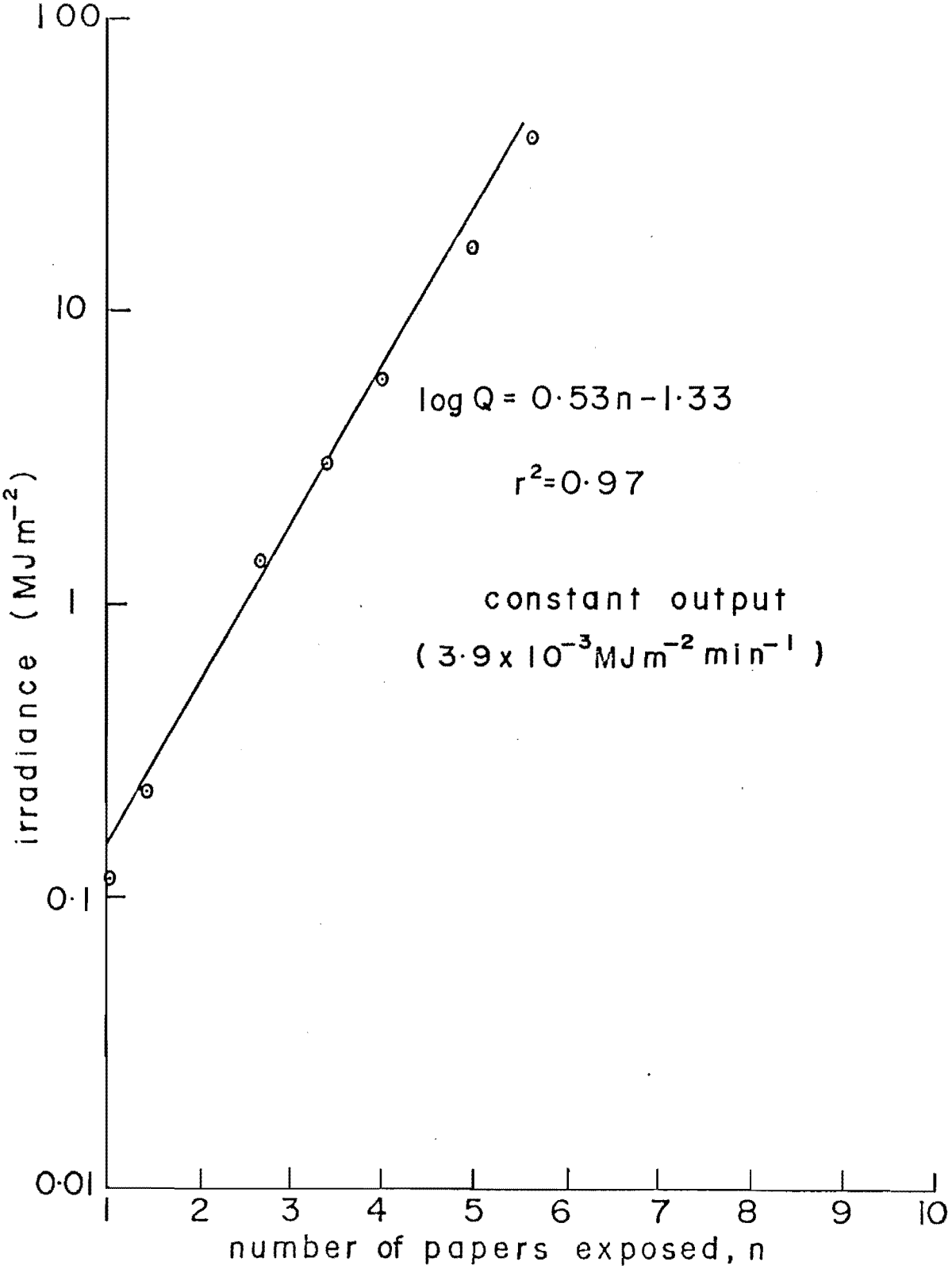

Figure 3.6: Relationship between number of papers exposed and log irradiance (MJm^{-2}) received under GL fluorescent tubes : the points obtained by exposing the sensors for different times.

The regression equation derived for 400-700 nm irradiance received (figure 3.5) is similar to that derived in sunlight in March (figure 3.4). This similarity is expected, because GL fluorescent tubes are designed to simulate the wavelengths that plants use in photosynthesis (400-700 nm).

(v) Type II paper calibrated with quantum and pyrometric sensors and integrator in sunlight, (May/June, 1982)

During late May, an experiment was initiated to re-calibrate type II paper in an attempt to detect any changes in the chemical response of diazo paper to light since the March calibration (section 3.1.2(f)(iii)).

Incident 300-3000 nm irradiance was measured with a Kipp solarimeter (Kipp-Zonen, Delft) attached to an integrator (TECHEN, Christchurch - for details on calibration, appendix 1). At the same time, 400-700 nm irradiance was measured with a silicon photovoltaic quantum sensor and integrator (both LAMBDA, Nebraska - for details, plate 3.1 and appendix 1). The aim being to calibrate the diazo paper with 400-700 nm and 300-3000 nm irradiance, simultaneously.

As before, two replicate sensors and seven time periods were used and the results are illustrated in table 3.7 and figure 3.7 and 3.8.

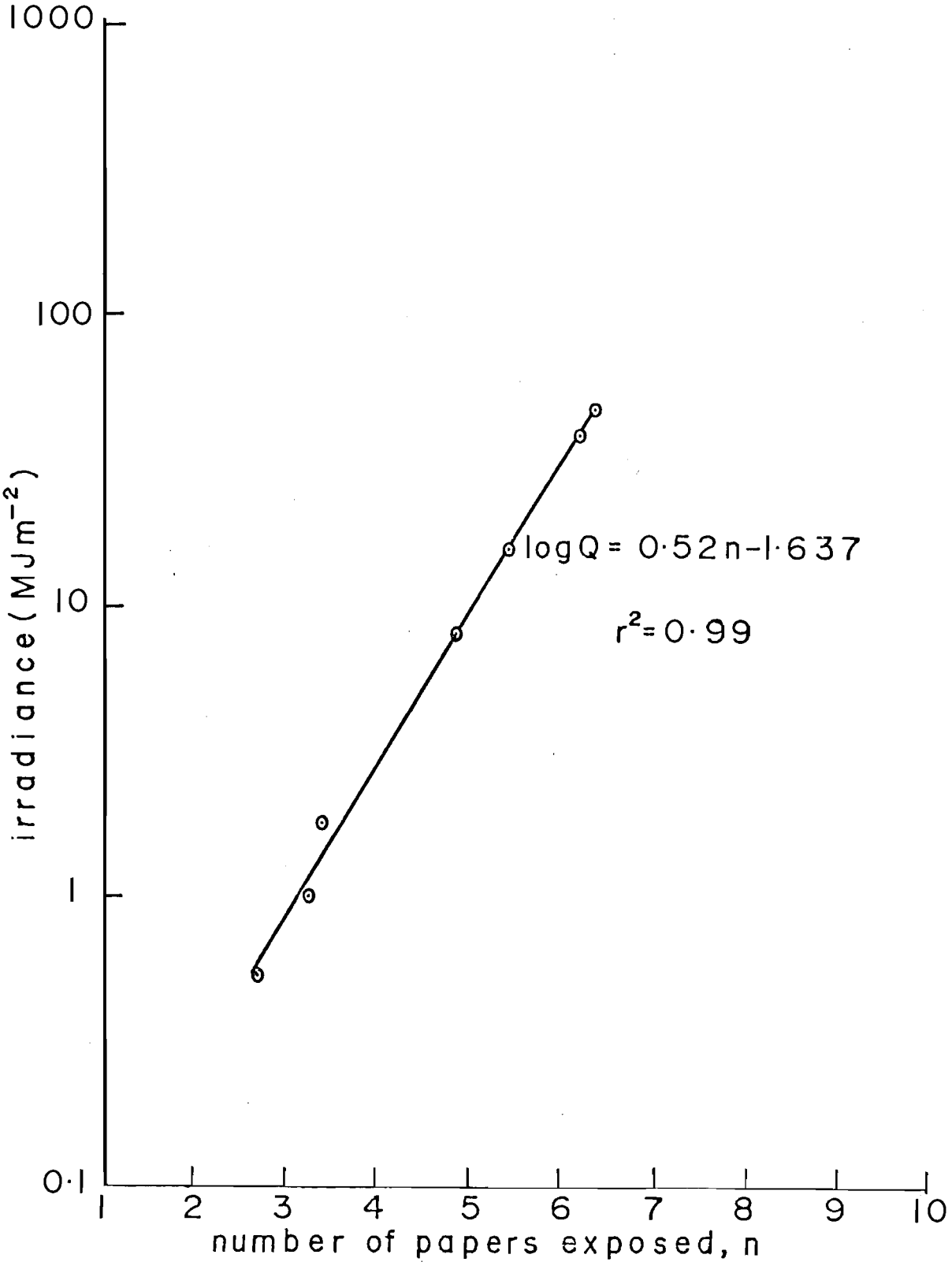

Figure 3.7: Relationship between number of papers exposed and log irradiance (MJm^{-2}) received in sunlight in May-June : the points obtained by exposing the sensors for different times.

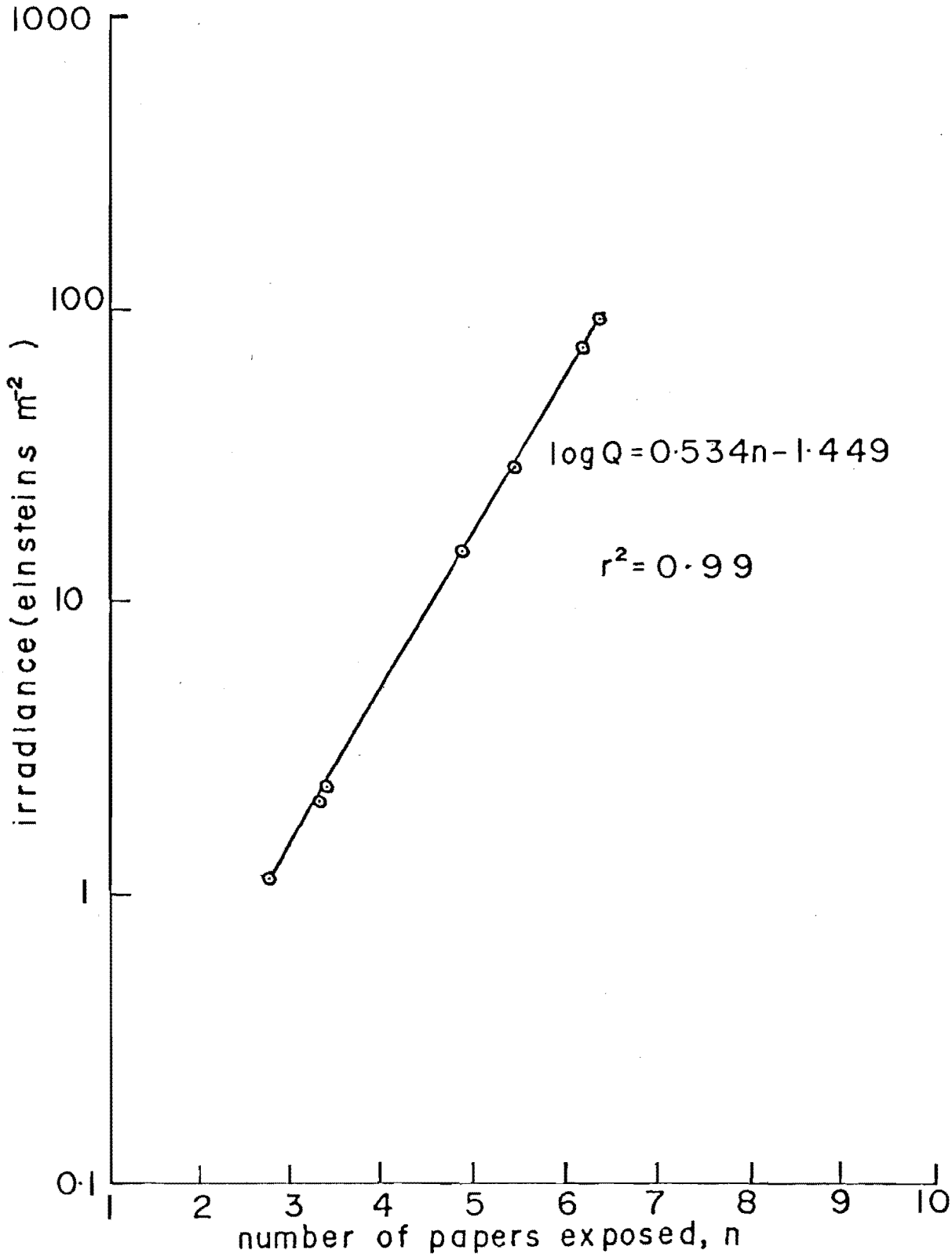

Figure 3.8: Relationship between number of papers exposed and log irradiance (Em^{-2}) received in sunlight in May-June : the points obtained by exposing the sensors for different times.

Table 3.7: Number of papers exposed (n) and irradiance received (einsteins m^{-2}) and (MJm^{-2}) over seven time periods (type II paper) in sunlight (May/June, 1982)

time periods (hours)	irradiance (400-700 nm) Em^{-2}	irradiance (300-3000 nm) MJm^{-2}	mean number of papers exposed (n)
0.5	1.101	0.545	2.75
1.0	2.024	1.014	3.26
6.0	2.304	1.800	3.39
24.0	14.704	8.125	4.87
48.0	28.81	15.522	5.46
121.0	75.32	38.852	6.21
168.0	90.20	46.367	6.38

From the results shown in table 3.7 and figure 3.8 it appears that the diazo paper has become less sensitive to light over time. The March calibration (figure 3.4) clearly shows that for a given amount of irradiance more papers were exposed than would be the case for the May/June recalibration. The shift in the lines for 400-700 nm irradiance in March (LogQ = 0.548n - 1.563) and May/June (Log Q = 0.534n - 1.449) illustrates this change.

The 300-3000 nm irradiance calibration for May/June provides a regression equation (Log Q = 0.52n - 1.637). By considering the relationship between the 400-700 nm irradiance in March (figure 3.4) and the new calibration (figure 3.8), a regression equation was derived for 300-3000 nm irradiance in March (Log Q = 0.507n - 1.71).

Table 3.8 provides a summary of the calibration functions derived for March and May/June and illustrates their applicability with respect to the field results (chapters five and six).

Table 3.8: Summary of calibration functions for irradiance (400-700 nm) and irradiance (300-3000 nm) (type II paper) in open sunlight

	REGRESSION EQUATIONS (LOG Q=)		
calibration period	irradiance (400-700 nm)	irradiance (300-3000 nm)	length of applicability
March	0.548n - 1.563	0.507n - 1.71	February/March
May/June	0.534n - 1.449	0.52n - 1.637	April/May/early June

(g) Spectral sensitivity of diazo paper

Diazo paper is sensitive mostly to blue, violet, and ultra-violet parts of the electromagnetic spectrum, and because of this, photosynthetically active wavelengths (400-700 nm) are only partly measured, (table 3.9).

Table 3.9: The light absorbed by the sensitive surface of diazo paper when sunlight is passed through layers of bleached paper (After Friend, 1961)

Wavelength (nm)		absorption as % of peak at 410 nm
440	*	12.4
430	blue	56.0
420		94.8
410		100.0
400	* violet	97.4
390		83.1
380	ultraviolet	66.1
370		25.1
360		34.9
350		12.7

Friend (1961) has shown, wavelengths around 410 nm are strongly absorbed by the sensitive layer on the diazo paper. Shorter wavelengths are active in bleaching the diazo compound, but are filtered out in the topmost sheet of the booklet. This implies that the sheets below the topmost layer are bleached by the wavelengths longer than 410 nm (blue).

(h) Applying diazo paper technique in the field

Having prepared the diazo booklets in the manner described and calibrated for 400-700 nm and 300-3000 nm irradiance (see section 3.1.2(b),(d), and (f)), the sensors were exposed in the field for periods of one week.

(i) Construction of transects in the forest stands

The main aim of the project as outlined in chapter one was to measure irradiance within the crown layer of several stands: *Larix decidua, Pinus contorta, Pseudotsuga menziesii, and Nothofagus solandri.* To do this, a method was developed which proved quite adequate for sampling incident and reflected irradiance at four fixed levels within the stands. Three planks (75 cm x 25 cm x 2 metres) were used as platforms for the petri dish sensors. An 80 mm strip of 'Velcro' tape was adhered at one metre intervals on both sides of the planks. This allowed the prepared diazo sensors, with a corresponding strip of 'Velcro' tape (see section 3.1.2(d)), to be attached to the planks, (figure 3.9).

The vertical spacing between the planks varied depending on the physical characteristics of the stands (chapters two and four). Horizontal spacing of the diazo sensors was a

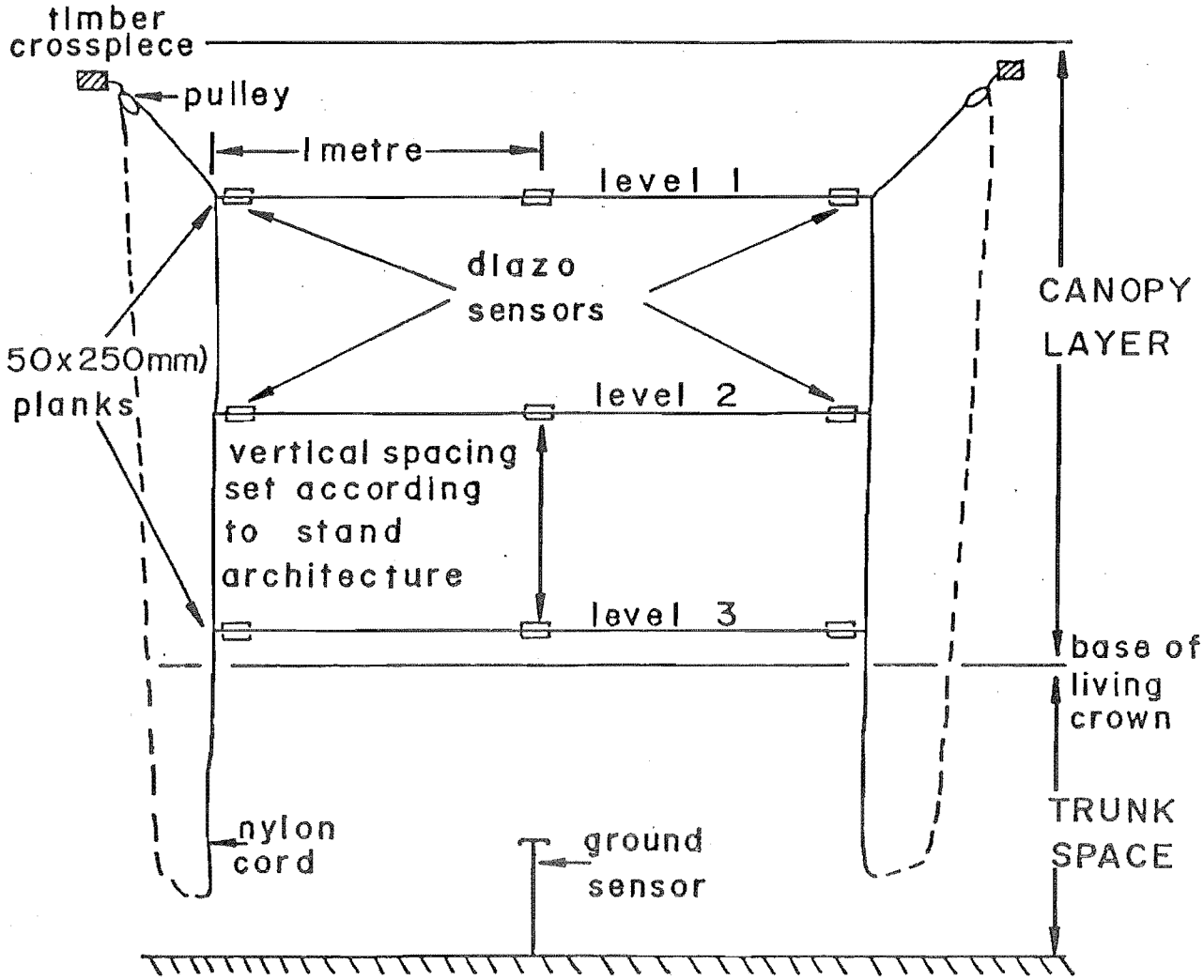

Figure 3.9: Technique used to measure incident and reflected irradiance at different levels within a forest stand.

standard one metre for all the stands.

Positioning the planks within the canopies was made possible using a simple rope and pulley system (figure 3.9). By tying a wooden crosspiece between two trees perpendicular to the planks it was possible to attach a pulley midway along the crosspiece. By doing the same between two trees further along, it was then possible to run the pulley system between the rows of the trees. All the planks were set up across the slope allowing measurement of irradiance on a horizontal surface. To ensure the correct positioning of the planks each week, a knot was placed in the rope above the top plank (figure 3.9) so that it caught in the pulley when the planks were hoisted into position.

Within each stand a fixed ground sensor was placed one metre above the ground. This gave some information of irradiance received within the trunk-space (figure 3.9). Similarly, an outside reference sensor was placed near the stands (see plate 3.3).

(ii) Ground transect under a forest opening

A fixed ground transect was constructed across a dense patch of mountain beech regeneration (chapter two); the regeneration being associated with a gap in the parent canopy (figure 3.10). Diazo sensors were placed at one metre intervals along the transect. The height of the sensors above the ground was made to correspond with the height of the regeneration. In an attempt to measure levels of irradiance

Figure 3.10: Mountain beech regeneration: transect across the floor beneath a canopy opening.

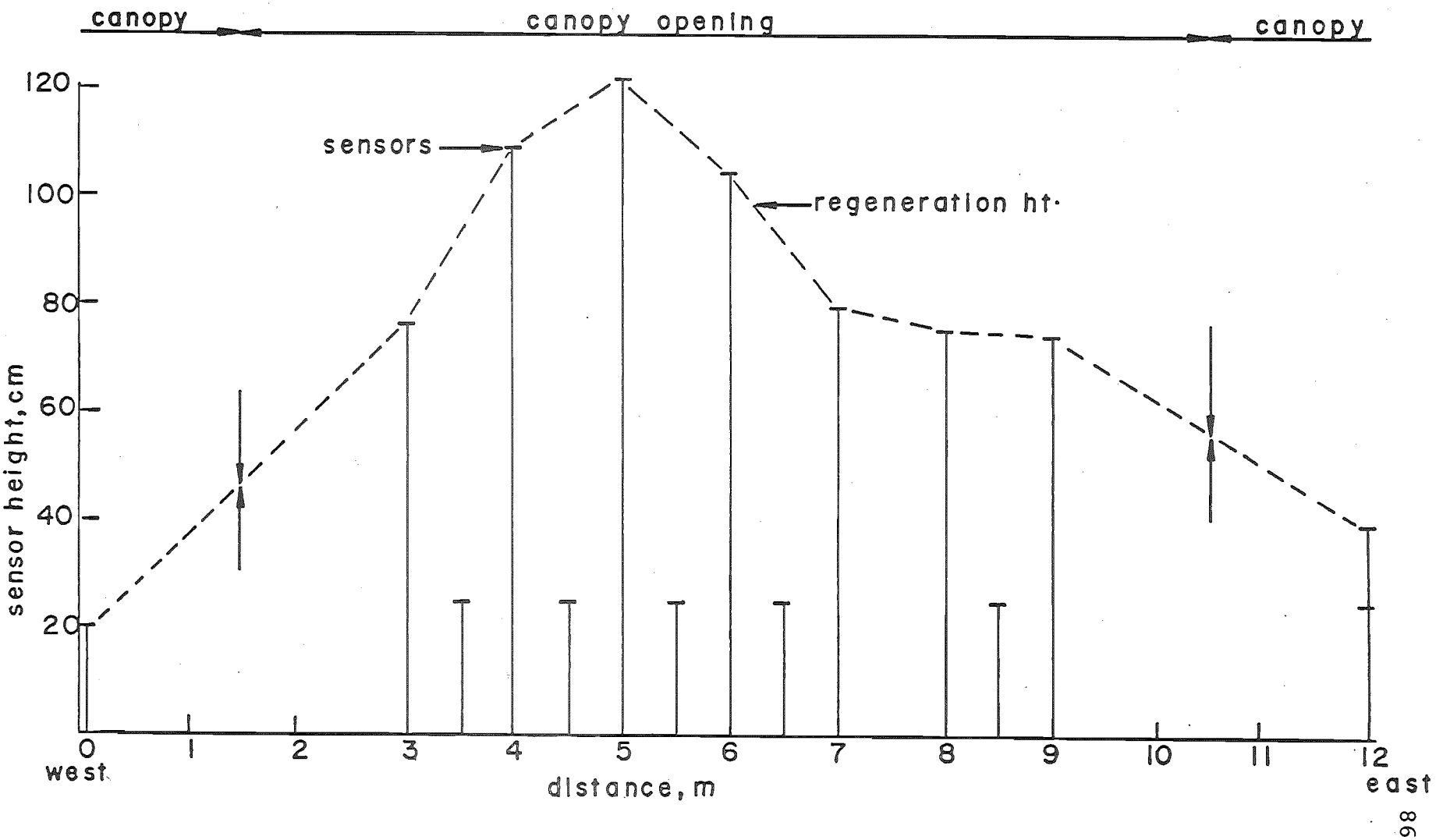

Plate 3.3: Ammonia diazo paper reference sensor (on post) : shown set up in the open near the Trig E forest stands.

Plate 3.4: Craigieburn Forest meteorological site (914 m a.s.l.). Illustrated : ammonia diazo paper sensor on post (front left), Fuess bimetallic actinograph (front right), and Stevenson screen (rear right).

beneath the regeneration, diazo sensors were placed at one metre intervals at a regular height of 25 cm along a lower transect (figure 3.10).

(iii) Calibration of diazo paper technique for different forest stands

Jarvis *et al* (1976) have shown that measurements of the spectral distribution of diffuse light on clear days under coniferous canopies show depletion in the violet and blue (400-450 nm), slight enrichment in the red (650-700 nm), and pronounced enrichment in the near-infra-red (700-750 nm). Federer and Tanner (1966a) found similar characteristics in the spectra measured under several canopy types.

The calibration procedure for the diazo paper and 400-700 nm and 300-3000 nm irradiance received provides a relationship for light conditions for open sunlight only (see table 3.8). As previously mentioned (section 3.1.2(g)), diazo paper is responsive mostly to ultraviolet, violet and blue irradiance (290-450 nm).

If the action of forest canopies is to deplete violet and blue light, then the calibration equations derived in the open, for 400-700 nm and 300-3000 nm irradiance require adjustment for use in the forest. The enrichment of near infra-red (710-4000 nm) beneath some canopies will also cause changes in the spectra beneath the canopy.

Provided the ratio of blue, violet and ultraviolet (290-450 nm) to the remaining wavelengths (450-3000 nm) is known for a particular stand, then it is possible to derive calibrations for specific species and for different heights within the stands.

In an attempt to derive calibration equations for 400-700 nm and 300-3000 nm irradiance received, for individual stands and for heights within the stands, measurements using silicon photovoltaic quantum and pyrometric sensors (both LAMBDA, Nebraska - for details, plate 3.2 and appendix 1), were made within the stands. Beneath each stand 20 measurements of 400-700 nm and 300-3000 nm irradiance were made using the quantum and pyrometric sensors respectively. Measurements of the same spectral wavelengths were made in the open at Craigieburn.

Mean values for the spectra were derived for each stand and the relationship, at ground level between 400-700 nm and 300-3000 nm irradiance was calculated, (see table 3.10).

Table 3.10: Relationships between irradiance received (400-700 nm, $\mu Em^{-2}s^{-1}$) and (300-3000 nm, Wm^{-2}) for the open (Trig E) and at ground level beneath four stands

site	relationship (300-3000 nm) ≃ (400-700 nm)
open (no canopy)	1 Wm^{-2} ≃ 2.7$\mu Em^{-2}s^{-1}$
Larix decidua	1 Wm^{-2} ≃ 2.43$\mu Em^{-2}s^{-1}$
Nothofagus solandri	1 Wm^{-2} ≃ 1.96$\mu Em^{-2}s^{-1}$
Pinus contorta	1 Wm^{-2} ≃ 1.66$\mu Em^{-2}s^{-1}$
Pseudotsuga menziesii	1 Wm^{-2} ≃ 1.45$\mu Em^{-2}s^{-1}$

Using these relationships, calibration equations were derived for the stands and for the four measured heights within the stands (tables 3.11 and 3.12).

The diazo paper sensors were collected after one week's exposure, and in each case 400-700 nm and 300-3000 nm irradiance received was calculated using the appropriate log function (see tables 3.11 and 3.12).

Table 3.11: Summary of calibrations for log irradiance (Q) received (400-700 nm, Em^{-2}) and (300-3000 nm, MJm^{-2}) and number of papers exposed, (n) for the four stands. (February and March)

Pseudotsuga menziesii

sensor position	height (metres)	irradiance (Em^{-2}) (λ400-700 nm)	irradiance (MJm^{-2}) (λ300-3000 nm)
above canopy	+7.5	Log Q = 0.548n-1.563	Log Q = 0.507n-1.71
top canopy	5.5	Log Q = 0.547n-1.49	Log Q = 0.511n-1.65
mid. canopy	4.5	Log Q = 0.547n-1.39	Log Q = 0.503n-1.54
bot. canopy	3.5	Log Q = 0.546n-1.27	Log Q = 0.507n-1.44
ground	1.0	Log Q = 0.546n-1.27	Log Q = 0.507n-1.44

Pinus contorta

sensor position	height (metres)	irradiance (Em^{-2}) (λ400-700 nm)	irradiance (MJm^{-2}) (λ300-3000 nm)
above canopy	+9.0	Log Q = 0.548n-1.563	Log Q = 0.507n-1.71
top canopy	7.2	Log Q = 0.545n-1.49	Log Q = 0.509n-1.64
mid. canopy	5.7	Log Q = 0.547n-1.42	Log Q = 0.503n-1.55
bot. canopy	4.2	Log Q = 0.549n-1.35	Log Q = 0.503n-1.47
ground	1.0	Log Q = 0.549n-1.35	Log Q = 0.503n-1.47

Nothofagus solandri

sensor position	height (metres)	irradiance (Em^{-2}) (λ400-700 nm)	irradiance (MJm^{-2}) (λ300-3000 nm)
above canopy	+6.5	Log Q = 0.548n-1.563	Log Q = 0.507n-1.71
top canopy	4.9	Log Q = 0.550n-1.53	Log Q = 0.510n-1.68
mid. canopy	4.4	Log Q = 0.551n-1.47	Log Q = 0.506n-1.61
bot. canopy	3.4	Log Q = 0.550n-1.43	Log Q = 0.503n-1.55
ground	1.0	Log Q = 0.550n-1.43	Log Q = 0.503n-1.55

Larix decidua

sensor position	height (metres)	irradiance (Em^{-2}) (λ400-700 nm)	irradiance (MJm^{-2}) (λ300-3000 nm)
above canopy	+7.0	Log Q = 0.548n-1.563	Log Q = 0.507n-1.71
top canopy	4.5	Log Q = 0.542n-1.52	Log Q = 0.510n-1.70
mid. canopy	3.5	Log Q = 0.550n-1.54	Log Q = 0.500n-1.64
bot. canopy	2.5	Log Q = 0.550n-1.53	Log Q = 0.500n-1.62
ground	1.0	Log Q = 0.550n-1.53	Log Q = 0.500n-1.62

Table 3.12: Summary of calibrations for log irradiance (Q) received (400-700 nm, Em^{-2}) and (300-3000 nm, MJm^{-2}) and numbers of papers exposed, (n) for the four stands. (April, May and June)

Pseudotsuga menziesii

sensor position	height (metres)	irradiance (Em^{-2}) (λ400-700 nm)	irradiance (MJm^{-2}) (λ300-3000 nm)
above canopy	+7.5	Log Q = 0.534n-1.449	Log Q = 0.520n-1.637
top canopy	5.5	Log Q = 0.532n-1.37	Log Q = 0.517n-1.55
mid. canopy	4.5	Log Q = 0.533n-1.27	Log Q = 0.521n-1.47
bot. canopy	3.5	Log Q = 0.532n-1.17	Log Q = 0.520n-1.36
ground	1.0	Log Q = 0.532n-1.19	Log Q = 0.520n-1.36

Pinus contorta

sensor position	height (metres)	irradiance (Em^{-2}) (λ400-700 nm)	irradiance (MJm^{-2}) (λ300-3000 nm)
above canopy	+9.0	Log Q = 0.534n-1.449	Log Q = 0.520n-1.637
top canopy	7.2	Log Q = 0.535n-1.39	Log Q = 0.517n-1.56
mid. canopy	5.7	Log Q = 0.522n-1.27	Log Q = 0.517n-1.49
bot. canopy	4.2	Log Q = 0.532n-1.22	Log Q = 0.518n-1.42
ground	1.0	Log Q = 0.532n-1.22	Log Q = 0.518n-1.42

Nothofagus solandri

sensor position	height (metres)	irradiance (Em^{-2}) (λ400-700 nm)	irradiance (MJm^{-2}) (λ300-3000 nm)
above canopy	+6.5	Log Q = 0.534n-1.449	Log Q = 0.520n-1.637
top canopy	4.9	Log Q = 0.527n-1.37	Log Q = 0.517n-1.58
mid. canopy	4.4	Log Q = 0.532n-1.35	Log Q = 0.518n-1.53
bot. canopy	3.4	Log Q = 0.532n-1.30	Log Q = 0.518n-1.49
ground	1.0	Log Q = 0.532n-1.30	Log Q = 0.518n-1.49

Larix decidua

sensor position	height (metres)	irradiance (Em^{-2}) (λ400-700 nm)	irradiance (MJm^{-2}) (λ300-3000 nm)
above canopy	+7.0	Log Q = 0.534n-1.449	Log Q = 0.520n-1.637
top canopy	4.5	Log Q = 0.515n-1.39	Log Q = 0.520n-1.62
mid. canopy	3.5	Log Q = 0.522n-1.37	Log Q = 0.522n-1.53
bot. canopy	2.5	Log Q = 0.527n-1.36	Log Q = 0.517n-1.48
ground	1.0	Log Q = 0.527n-1.36	Log Q = 0.517n-1.48

3.2 PHOTO-ELECTRICAL AND THERMO-MECHANICAL MEASUREMENT OF IRRADIANCE

3.2.1 Introduction

Reviews concerned with both the photo-electrical and thermo-mechanical measurement of irradiance are extensively covered in Poole and Atkins (1930), and Anderson (1964c, 1971). Details concerning the many instruments are explained in the Handbook of Meteorological Instruments (Anon, 1956), Anderson (1964c, 1971), Kubin (1971) and W.M.O. (W.M.O., No. 557, 1981). The following discussion will focus on the various instruments used in the field. Calibration procedures and technical aspects are covered in appendix 1.

3.2.2 Equipment used in the Field

A Fuess bimetallic actinograph (Robitzch, 1932) is located at the Craigieburn Forest meteorological site. This instrument measures total incident irradiance from 300-3000 nm (see appendix 1). The charts are changed daily and the observation record dates back to 1966. The current information obtainable from the actinograph is useful with respect to cross-checking the accuracy of the diazo sensors. To do this, a diazo sensor was placed adjacent to the actinograph for periods of one week. (Plate 3.4).

The actinograph data is also useful with respect to determining long-term radiation characteristics for the region. McCracken (1980) and more recently Cruden (1981) have written comprehensive summaries of the climatic characteristics of the Craigieburn Range. (Access to the record of past and current

radiation data was granted by the Forest Research Institute, Christchurch.)

A record of 400-700 nm irradiance received beneath the *Pinus contorta* stand (see chapter two) was obtained from a quantum sensor and integrator (both LAMBDA, Nebraska - for details, plate 3.1 and appendix 1). A diazo sensor was placed adjacent to the quantum sensor for periods of one week. This set up, provided a cross-check for the diazo sensors under a canopy and gave some hard data for variations in quantum flux at one point under the stand over time (see chapter five).

Spot measurements using a silicon photovoltaic quantum sensor and a meter (both LAMBDA, Nebraska - for details, plate 3.2 and appendix 1) were made on selected days over the five month study period. The measurements were made beneath the three stands on trig E : *Pinus contorta, Larix decidua,* and *Pseudotsuga menziesii* (see chapter two for details). In order to measure above canopy 400-700 nm irradiance, the quantum sensor and integrator (both LAMBDA, Nebraska - for details, appendix 1) were set up at the top of Trig E in the open (see plate 3.1). This provided some information on the penetration co-efficients of irradiance for the three stands, to be compared with the integrated values obtained from the diazo sensors.

3.3 INDIRECT ESTIMATES OF IRRADIANCE

Indirect estimates of light and stand structure are commonly derived from hemispherical (fish eye) canopy

photographs (Evans and Coombe 1959, and Anderson, 1964a, 1964c, 1971). These authors have used this technique for estimating light beneath a variety of canopy types (field crops to forest stands).

By superimposing solar tracks on the photographs, daily and seasonal variations in light were estimated. This technique also offers a method for estimating canopy closure. To do this, a grid is placed over the photograph and the area of foliage is calculated (see Anderson, 1971 pp.447-451). Apart from providing an estimate of radiation transmission, fish eye photographs provide a quick and convenient record of crop structure and are a useful check on the accuracy of point quadrat records (Wilson, 1965).

There are a number of inherent problems applying the fish eye photography technique in forest stands. The main problem concerns the distortion caused by the 180^{o} image. This often brings the stems into the sides of the image and squeezes the canopy itself into the centre of the image. This makes the estimation of light in terms of the canopy, particularly difficult.

It is suggested therefore, that a normal 55 mm lens should be used for photographing the canopy. The image obtained is undistorted and the stems are excluded. An attempt to interpret canopy photographs is made in chapter four of this thesis.

CHAPTER FOUR

CHARACTERISTICS OF THE FOREST SPECIES

4.1 BACKGROUND

In chapter two (section 2.3), the forest species chosen for this study were introduced. These species were chosen primarily because of differences in their architecture, similarities in their growth stage and siting, and because of their accessibility. A brief discussion of origins, ecology, and geographic distribution of the forest species will follow.

Pinus contorta (lodgepole pine) is a wide ranging tree of North America from lower California to Alaska and inland to the Rocky Mountains, at elevations ranging from 600-3500 m a.s.l. It is one of the most aggressive and hardy of western forest trees and under favourable conditions is capable of fully restocking cutover lands in a remarkably short time. This is largely because the trees are prolific seeders and often produce fertile seed before they are 10 years old. Fully grown, this species forms a medium-sized tree, ranging from 10-25 metres in height. *P. contorta* has proved useful as a pioneer species on poor soils.

Pseudotsuga menziesii (Douglas fir) is a widely distributed North American species, growing naturally throughout the Rockies from their eastern base to the Pacific Coast, and northern Mexico, southern New Mexico and Arizona to British Colombia.

This is a tall tree species (75-100 m), attaining its greatest height near sealevel in the coastal region of southern British Colombia. In favourable situations *P. menziesii* grows with extreme rapidity but requires adequate rainfall and moderately good soil.

Larix decidua (European larch) originates from the mountains of Central Europe from south-east France through the main chain of the Alps to Austria. When fully grown it reaches 30-40 metres in height. *L. decidua* is a deciduous species and has proved useful for reforestation work in many temperate regions of the world.

Nothofagus solandri (var.) *cliffortioides* (mountain beech) is indigenous to New Zealand, and is common at higher elevations. It is particularly important in the forests on the eastern side of the main divide in the South Island and in the central regions of the North Island (Wardle, 1970). It has been shown to grow on both wetter and drier sites at higher altitudes than most other New Zealand species. The height of *N. solandri* varies considerably; on good sites at lower altitudes it may attain 20 m or more.

4.2 STAND DIMENSIONS

4.2.1 Crown-Stem Configuration

Crown-stem dimensions for the four stands studied are shown in table 4.1, and general mensuration characteristics are in table 2.2 (chapter two). From the data presented in

table 4.1 it is evident that the stand of *Pinus contorta* has the greatest crown length (CL), 6.8 metres (75.5% of its total height). *Nothofagus solandri* has the smallest CL (3.3 m), being only 50.7% of its total height.

Table 4.1: Crown-stem dimensions for the four forest stands studied, 1982.

SPECIES	D (c.m.)	H (m)	HLC (m)	CL (m)
Pseudotsuga menziesii	*13.5	7.5	2.0 (26.6)	5.5 (73.3)
Larix decidua	*10.4	7.0	2.2 (31.4)	4.8 (68.5)
Pinus contorta	14.6	9.0	2.2 (24.4)	6.8 (75.5)
Nothofagus solandri	7.9	6.5	3.2 (49.2)	3.3 (50.7)

* 1980 data
D = diameter at breast height over bark
H = mean height
HLC = height to base of live crown
CL = crown length
( ) = percentage of total height, H

Pseudotsuga menziesii and *Larix decidua* have similar crown lengths, 5.5 m and 4.8 m respectively.

With the exception of *N. solandri*, the forest stands share similar height to live crown (HLC) measurements (ranging from 2.0-2.2 m). The distance between the ground and the base of the live crown is commonly called the trunk-space, where there is little or no living foliage (see figure 3.9).

Diameter at breast height over bark (D), was derived from the data presented in table 2.2. Current estimates for *L. decidua* and *P. menziesii* are not available, but one might expect the latter to be similar if not larger that the current figure for *P. contorta* of 14.6 cm. *N. solandri* has the smallest stem diameter at breast height (7.9 cm). The main reasons for this being its very high stocking density (19 000 ha^{-1}), and the fact that it uses more of its carbon increment for annual leaf and branch production (Benecke and Nordmeyer, 1982) than the conifers.

Stocking densities (stems ha^{-1}) vary considerably amongst the four stands studied (table 2.2). *P. contorta* has the highest stocking density (4430 ha^{-1}) for the exotic conifers (cf. *P. menziesii* 2700 ha^{-1}, and *L. decidua* 2400 ha^{-1}). *N. solandri* has a very high stocking density (19 000 ha^{-1}), and if the supressed living understorey is included the figure reaches 40 000 stems ha^{-1}. According to Wardle (in prep.) initial high stocking is normal in regeneration of *N. solandri* which frequently re-establishes after 'natural disturbance' mortality.

The crown and stem dimensions provided in table 4.1 provide the framework for further analysis of stand architecture. The sections to follow will attempt to illustrate specific architectural differences between the four forest species. As was outlined in chapter one, stand architecture has a great influence upon the processes of action and reaction between plants and their environment through the modification and interception of fluxes of radiation, heat, carbon dioxide, and so on.

THE LIBRARY
UNIVERSITY OF CANTERBURY
CHRISTCHURCH, N.Z.

4.2.2 Foliage Biomass and its Spatial Distribution

The surface area of leaves or of other photosynthetic organs ('foliage' in general) is an essential parameter determining the stand productive physiology, the micrometeorology and the optics of plant cover (Anderson, 1981). In this section foliage biomass and its spatial distribution throughout the crown is quantified.

(a) Foliage biomass

Table 4.2 illustrates foliage biomass for the four stands in late summer. By late summer it is assumed that foliage weight would be at or close to maximum for the growing season. Foliage biomass (t DM ha^{-1}) is given for the upper and lower crown, and in the case of *P. contorta* three crown positions are given (table 4.2).

In *N. solandri* there is a marked concentration of foliage in the upper sun crown, representing some 78% of the total foliage biomass. The remaining 22% in the lower crown is small and significantly different to the relative distributions measured in the conifers (table 4.2). Total foliage biomass (t DM ha^{-1}) is low compared to *P. contorta* and *P. menziesii*. However, of its total biomass (310.3 t DM ha^{-1}) *N. solandri* has more sizeable portions in its stem and branch biomass, 209 t DM ha^{-1} and 51.5 t DM ha^{-1} respectively (Benecke and Nordmeyer, 1982).

The distribution of foliage biomass in *L. decidua*, in contrast to *N. solandri*, is more even in the upper and lower crown, 51.4% and 48.5% respectively. Total foliage weight

Table 4.2: Total foliage biomass (t DM ha^{-1}) and its approximate distribution in the crown in late summer for the four forest stands (height measurements in metres)

Nothofagus solandri

foliage biomass t DM ha^{-1}			Reference
upper crown 4.85-6.5 m	lower crown 3.2-4.85 m	total crown 3.2-6.5 m	
10.0	2.8	12.8	Benecke and Nordmeyer, (1982)

Larix decidua

foliage biomass t DM ha^{-1}			Reference
upper crown 4.6-7.0 m	lower crown 2.2-4.6 m	total crown 2.2-7.0 m	
2.15	2.03	4.18	Ledgard (pers.comm.)

*Pseudotsuga menziesii**

foliage biomass t DM ha^{-1}			Reference
upper crown 4.95-7.5 m	lower crown 2.0-4.95 m	total crown 2.0-7.5 m	
7.6	11.6	19.2	Ledgard (pers.comm.)

Pinus contorta

foliage biomass t DM ha^{-1}				Reference
upper crown 6.8-9.0 m	middle crown 4.6-6.8 m	lower crown 2.2-4.6 m	total crown 2.2-9.0 m	
7.91	14.35	7.03	29.3	Benecke and Nordmeyer, (1982)

* estimated from a value of 16.4 t DM ha^{-1} in winter (1980) and by adding on a current annual production of 2.8 t DM $ha^{-1}a^{-1}$.

(4.18 t DM ha^{-1}) is much lower than the other species (table 4.2). The deciduous nature of *L. decidua* and its high demand for light at all levels within the crown are principal reasons for its low foliage weight. New foliage is produced each season and to be successful at trapping irradiance the foliage has to be light and evenly distributed.

The distribution of foliage biomass in *P. menziesii* is fairly typical of most evergreen conifers. There is a greater amount of foliage contained in the lower crown (60%), but the asymmetry is not as marked as for *N. solandri* (table 4.2). Total foliage weight (19.2 t DM ha^{-1}) is high but some 10 tonnes ha^{-1} less than that for *P. contorta*.

P. contorta has the greatest amount of foliage biomass among the four species (table 4.2). The total weight (29.3 t DM ha^{-1}) is high by world standards and reflects the suitable environment for tree growth. The distribution of foliage biomass shows a mid-crown dominance (48.9%), with a similar distribution in the upper and lower crown, 26.9% and 24.0% respectively. This distribution is similar to *P. menziesii*, and also contrasts *N. solandri*. The ability of this species to maintain large amounts of foliage biomass (hence leaf area) is related to its evergreen habit and its ability to absorb and utilise irradiance. In chapter six of this thesis canopy architecture and irradiance are discussed in detail.

(b) Leaf area index

In chapter one, section 1.2.2(d), the term leaf area index

was introduced. Watson (1958) defined leaf area index (L) as a dimensionless term, the one-sided area of photosynthetic tissue, irrespective of its inclination to the horizontal, per unit ground area (often referred to as projected leaf area). Consideration of the projected leaf area index (L) forms the basis of most models of canopy light interception (see section 1.2.2(d). It is perhaps more realistic to consider total surface leaf area (L_t) when the interest extends to evaluating such factors as canopy photosynthesis, respiration and transpiration. It is the aim of this chapter to illustrate the importance of using total photosynthetic leaf surface to ground surface ratios. However, the simplicity and utility of projected surface leaf area (L), especially for modelling purposes (see chapter six), is not rejected. The geometry of the various leaf types and their L/L_t ratios are explained in detail in section 4.3.2 of this chapter.

Total surface leaf area (L_t) for the four stands was derived using the surface area to weight ratios summarised in table 4.3. The figures given refer to the mean ratio between

Table 4.3: Mean surface area : weight ratios for the four forest stands.

Forest species	mean surface area : weight (cm^2/g)	Reference
Nothofagus solandri	139.0	Benecke and Nordmeyer (1982)
Larix decidua	298.5	Benecke (pers.comm.)
Pseudotsuga menziesii	173.4	Gholz *et al* (1976)
Pinus contorta	121.8	Benecke and Nordmeyer (1982)

surface area and foliage weight (table 4.2). The high surface area to weight ratio (e.g. *Larix decidua*) implies that this species has relatively light foliage for a given total surface leaf area. For *Larix* spp. it is common to find high surface area to weight ratios (e.g. Richards, 1981). In his study with *Larix lyallii* Richards concludes, that another result of the deciduous habit is the need to make rapid carbon gains for the duration of the short growing season ... larch produces leaves with high leaf area to weight ratios that are advantageous because low carbon investment is necessary for high subsequent carbon gain (Richards, 1981, p.193).

The remaining species which are all evergreen share relatively similar surface area to weight ratios (table 4.3). *Pinus contorta* has the lowest surface area to weight ratio suggesting heavier foliage for a given surface area.

Unlike deciduous species such as *Larix*, evergreen species such as *P. contorta* and *P. menziesii* are capable of assimilating greater amounts of carbon through their foliage because the needles survive on the trees for up to seven or more years. This is the main reason why high foliage weights (table 4.2) are observed for these two species.

Table 4.4 shows total surface and projected surface leaf area and its approximate distribution in the crown for the four stands. The figures presented were derived from the foliage biomass data (table 4.2) using the surface area to weight conversions given in table 4.3.

Table 4.4: Total surface and projected leaf area (m^2/m^2) and its approximate distribution in the crown in late summer for the four forest stands (estimated from foliage biomass weight : leaf area ratios). Project leaf area L in brackets.

Nothofagus solandri

total surface leaf area L_t (m^2/m^2)			ratio* L/L_t
upper crown	lower crown	total	
13.9 (6.9)	3.9 (1.9)	17.8 (8.9)	0.5

Larix decidua

total surface leaf area L_t (m^2/m^2)			ratio* L/L_t
upper crown	lower crown	total	
5.89 (2.45)	6.59 (2.75)	12.7 (5.2)	0.416

Pseudotsuga menziesii

total surface leaf area L_t (m^2/m^2)			ratio* L/L_t
upper crown	lower crown	total	
13.2 (5.5)	20.1 (8.3)	33.3 (13.8)	0.416

Pinus contorta

total surface leaf area L_t (m^2/m^2)				ratio* L/L_t
upper crown	middle crown	lower crown	total	
9.64 (3.75)	17.5 (6.8)	8.56 (3.3)	35.7 (13.9)	0.389

* see section 4.3.2

Distribution of foliage throughout the crown has already been discussed for the four stands (see section 4.2.2(a)). The leaf area indices (all surfaces, L_t, and projected surface, L) for the four species can be compared with others elsewhere (table 4.5).

The figure derived for *N. solandri* (L_t = 17.8) is comparable with those for *Fagus crenata* (L_t = 15.6) and *Fagus sylvatica* (L_t = 15.0). Likewise, Moir and Francis (1972) present a L_t = 35.9 for *P. contorta* which is comparable to that used in this study for the same species (L_t = 35.7). The figure for *P. menziesii* (L_t = 33.3) is higher than that reported by Ungs (1981) and Zobel *et al* (1976). However, Gholz *et al* (1976) suggest L_t values ranging from 20-42 m^2/m^2 for *P. menziesii* and other evergreen coniferous species in Oregon. The figure of L_t = 8.65 for *Larix leptolepis* is slightly lower than the value of L_t = 12.5 used in this study for *Larix decidua*.

In summary, the leaf area indices for the forest stands used in this study (table 4.4) are for the most part greater than those given elsewhere (table 4.5) for identical or similar species. There are a number of reasons for these differences. For example, table 4.5 merely provides a list of leaf area indices for a number of forest species. We know nothing about the site characteristics where these indices were derived. A low leaf area index could be merely related to a low stocking density in the forest where the measurements were made, or to a particularly dry climate (see Anderson, 1981). Great care therefore, should be taken when comparing leaf area index

Table 4.5: Leaf area indices for coniferous and broad-leaved species

SPECIES	L projected leaf area	L_t total surface leaf area	REFERENCE
a) Coniferous			
Pinus resinosa/strobus	3.1	7.96	Mukammal (1971)
Pinus radiata	8.3	21.3	Whitehead (unpub)
Pinus sylvestris	2.8	7.2	Whitehead & Jarvis(unpub)
Picea sitchensis	9.8	22.5	Norman & Jarvis (1974)
Picea abies	8.3	19.9	Baumgartner (unpub)
Pseudotsuga menziesii	11.0	26.4	Ungs (1981)
Pinus contorta	14.0	35.9	Moir and Francis (1972)
Larix leptolepis	3.6	8.65	Jarvis *et al* (1976)
Pseudotsuga menziesii	10.3	24.7	Zobel *et al* (1976)
Abies veitchii	5.5-10.6	13.2-25.5	Kira (1975)
b) Broad-leaved			
Fagus crenata	5.7-7.8	11.4-15.6	Kira (1975)
Castanopsis cuspidata	7.0	14.0	Kira *et al* (1969)
Fagus sylvatica	7.5	15.0	Moller (1946)
Populus tremula	7.1	14.2	Rauner (1976)
Castanopsis cuspidata	8.0-8.9	16-17.8	Kira (1975)
Eucalyptus maculata	2.8	5.6	Dunin & Reyenga (unpub)

between species growing in different areas. Differences may be a response to climate, edaphic conditions, or the physical characteristics of the forest where the measurements were made.

The high leaf areas reported for the forest species studied are likely to be related to the favourable climate in the Study Area. In a study by Gholz *et al* (1976) in the Western Oregon Cascades it was shown that the largest total surface leaf areas developed in communities at mid-altitude where growing season temperatures were cool. According to their study, temperature is the variable which permits large accumulations of foliage, but neither the warmest sites nor those with the longest growing season support the largest amount of foliage. They hypothesize that it is a special balance of temperatures that favours modest respiration rates but yet permits, even during the dormant season, considerable net photosynthesis (Gholz *et al*, 1976, p.55).

Mean monthly temperatures at montane altitude in the Craigieburn Region are mild (table 2.1), with an annual average temperature of 7.9^{o}C. It is not unreasonable to assume therefore, that the same balance of temperatures that favours the development of high leaf areas in Western Oregon are also operating at mid-altitude in the Craigieburn Range.

4.3 STAND GEOMETRY

4.3.1 Stem-Branch Orientation

The orientation of the branches with respect to the main stem or bole is an important architectural characteristic.

Knowledge of leaf area and its spatial distribution, as previously discussed, is of prime importance. The branches are the main support system for the canopy's foliage and the penetration of light into a stand is closely related to the inclination of its receiving surfaces. Two stands may share similar leaf area and leaf distribution, but their light regimes may differ purely because of their stem-branch geometry. Simplified descriptions of stem-branch geometry for the four forest species will follow.

(a) *Pinus contorta*

Branching in *P. contorta* crowns, as in most conifers, is excurrent : an undivided main stem or bole supports whorls of branches radiating outwards (figure 4.1, plate 4.1). In dense stands tall, clean, gradually tapering shafts with short, rounded, small branched crowns are developed.

One of the most notable characteristics of the stem-branching geometry of *P. contorta* is the upward inclination of the branches at all levels within the canopy (figure 4.1). This vertical branch system requires less space than a horizontal branch system, which explains in part why it can support a greater amount of foliage than the other forest species (table 4.2).

(b) *Pseudotsuga menziesii*

In *P. menziesii* the branches tend to be arranged in false whorls, with branchlets in between (figure 4.2, plate 4.2). Grown in full light, the young tree often shows a loose, pyramidal crown reaching nearly to the ground; but in stand form

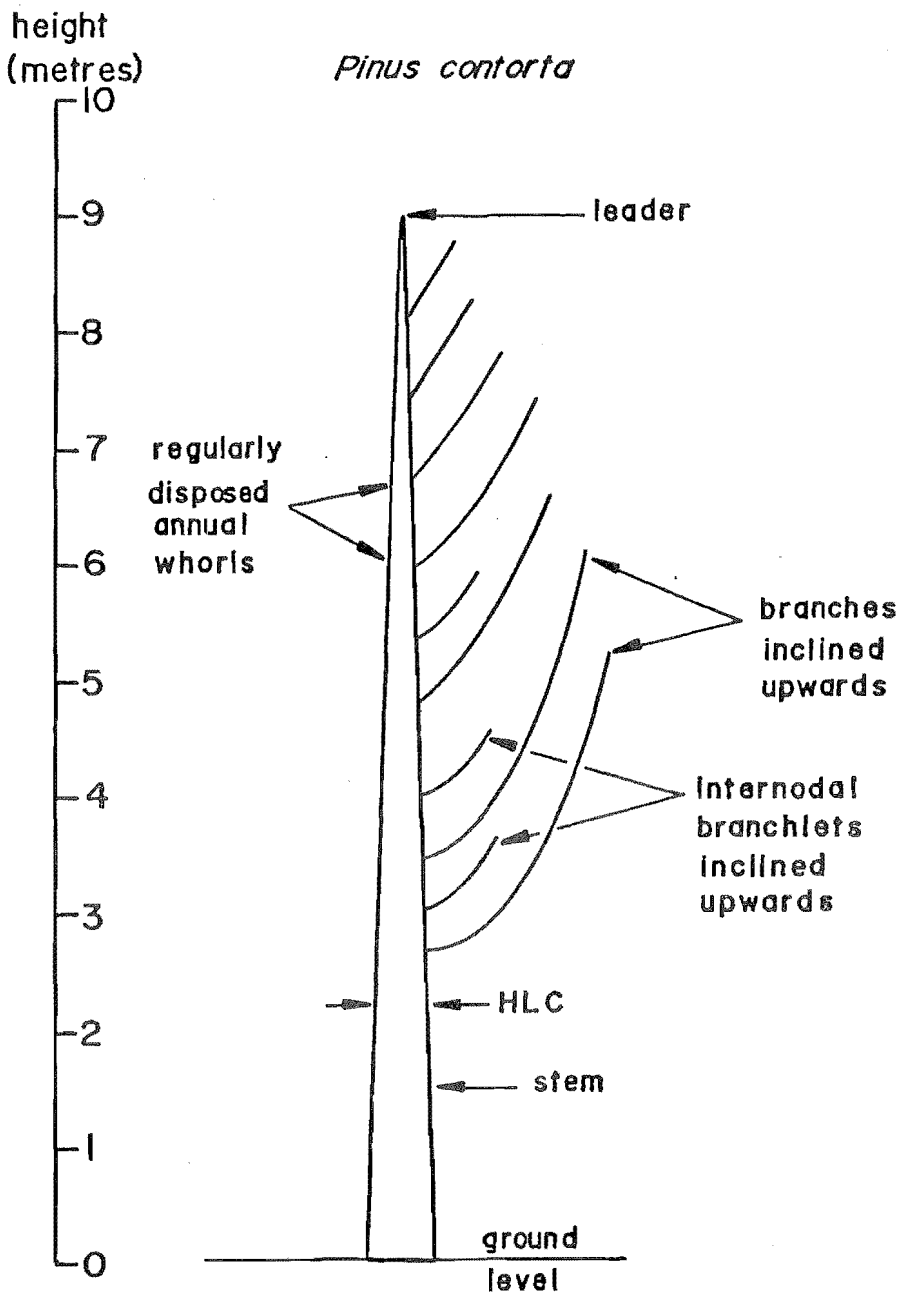

Figure 4.1: Stem-branch geometry for the *Pinus contorta* stand. HLC = height to the base of the living crown.

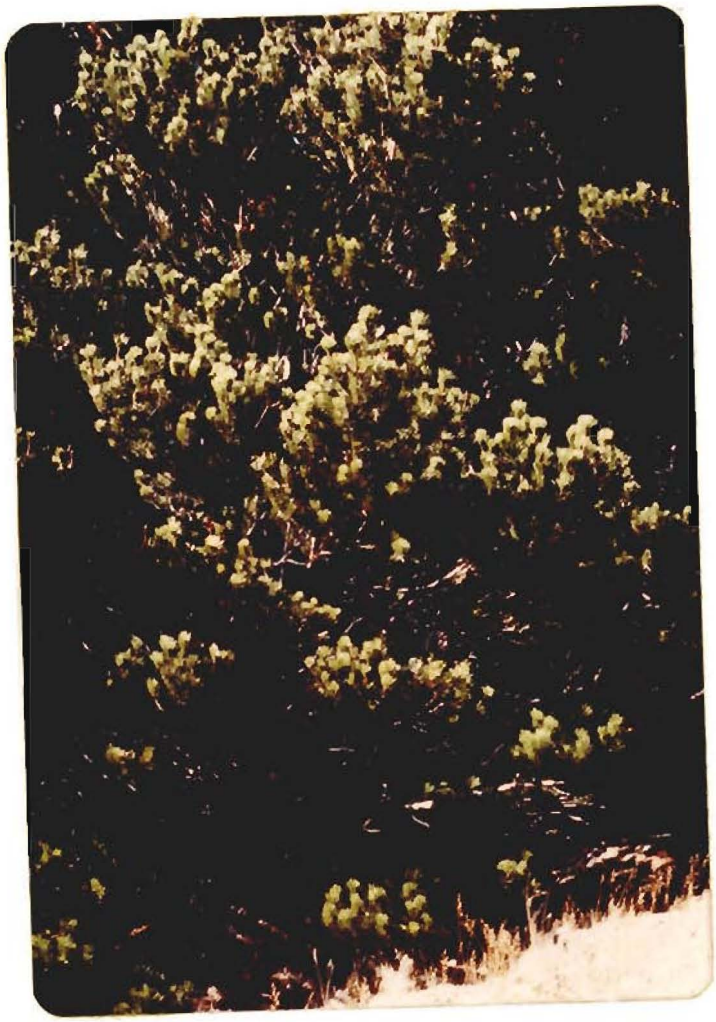

Plate 4.1: Side view of the *Pinus contorta* stand.

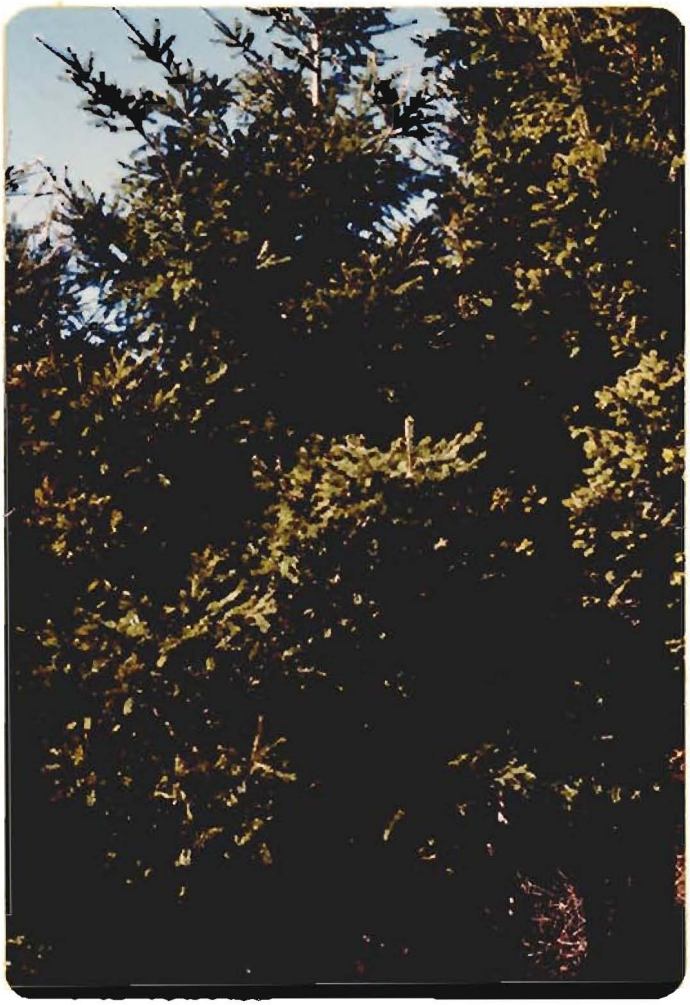

Plate 4.2: Side view of the *Pseudotsuga menziesii* stand.

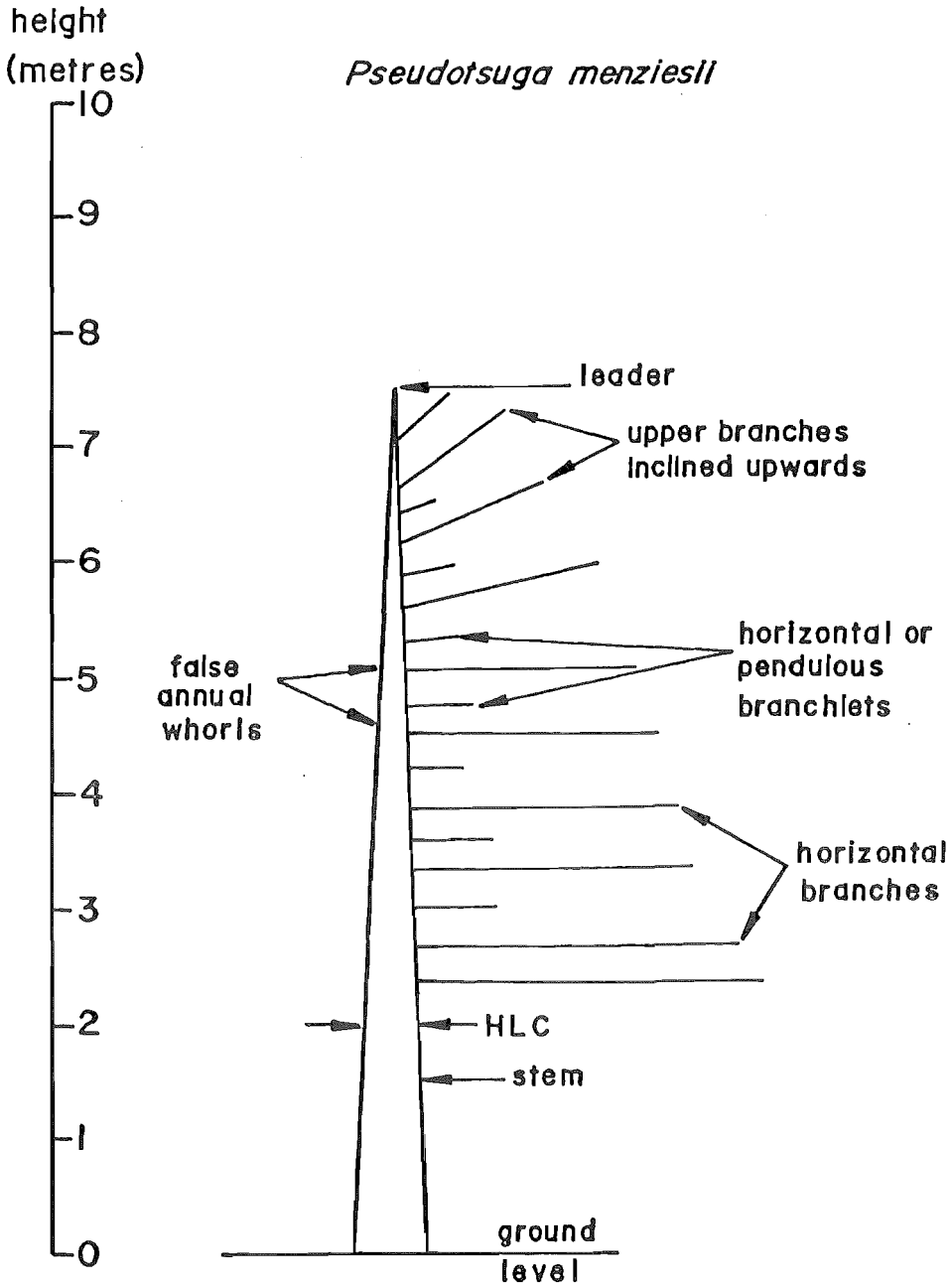

Figure 4.2: Stem-branch geometry for the *Pseudotsuga menziesii* stand. HLC = height to the base of the living crown.

the tall tree usually has a long, bare stem capped by a relatively narrow crown.

With the exception of the upmost branches, the main branches and branchlets tend to be largely perpendicular to the main stem (figure 4.2). From this flat horizontal branch system branchlets and young twigs incline or hang downwards.

(c) *Larix decidua*

In its general form *L. decidua* is a coniferous tree, but the main branches are not disposed in regular or false whorls (figure 4.3, plate 4.3). The tapering stem is usually straight and the main branches extend horizontally or incline downwards, while the branchlets mostly hang downwards (figure 4.3). Only the uppermost branches incline upwards.

The lightness of the crown and the early death of the lower branches illustrate the intense demands for light made by this species.

(d) *Nothofagus solandri*

Branching in *N. solandri*, unlike most of the conifers, is totally irregular (figure 4.4, plate 4.4). The upper branches tend to incline upwards but the main branches and branchlets are mostly horizontally oriented (figure 4.4). Unlike the conifers, the main branch system is concentrated in the top half of the stand (table 4.1). This suggests a possible reason why *N. solandri* has a limited ability to maintain large amounts of foliage compared with *Pinus contorta* and *Pseudotsuga menziesii*.

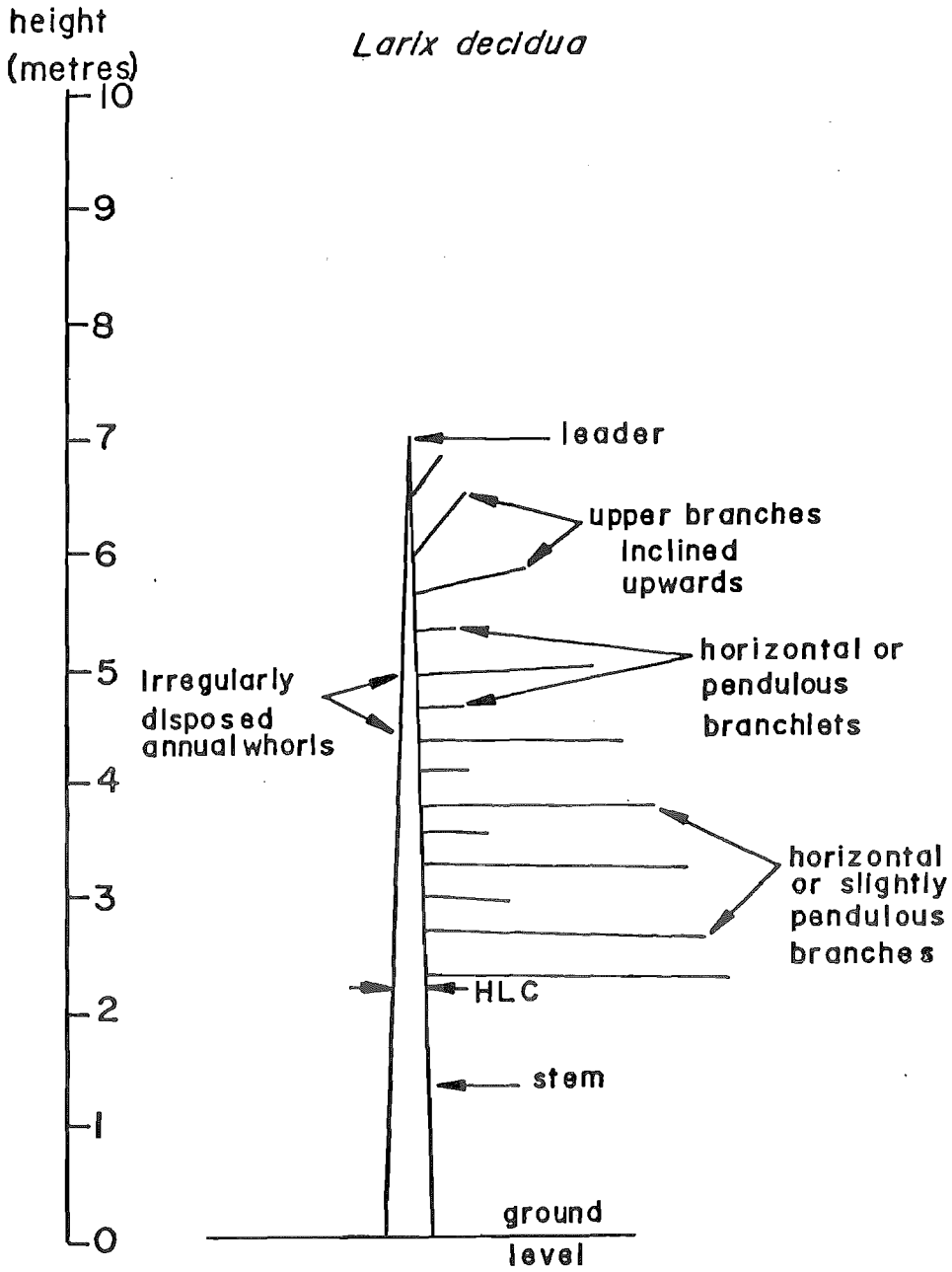

Figure 4.3: Stem-branch geometry for the *Larix decidua* stand. HLC = height to the base of the living crown.

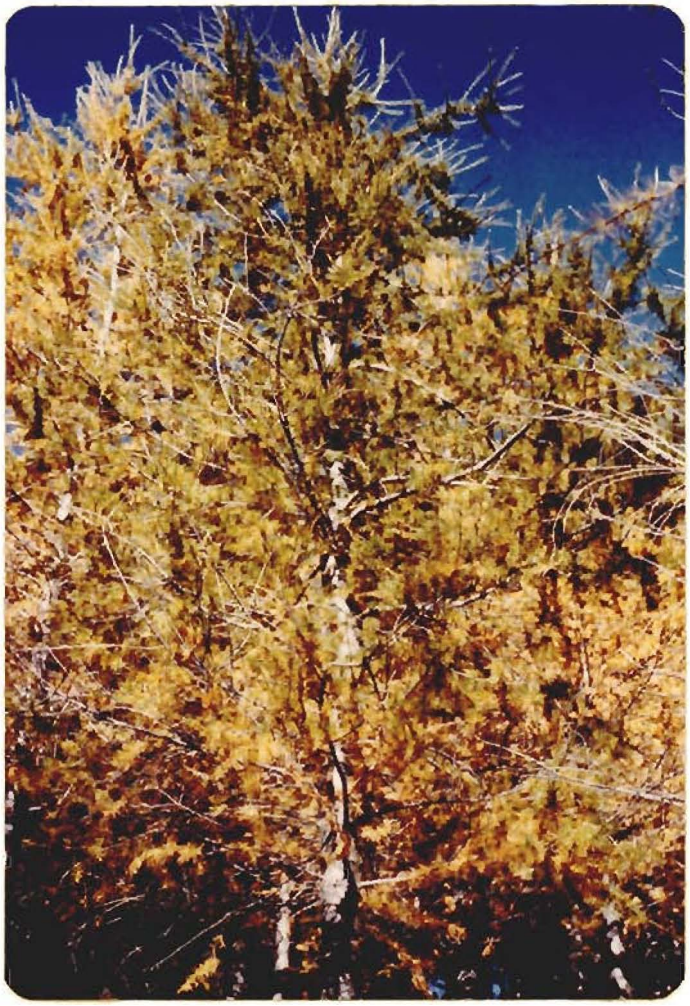

Plate 4.3: Side view of the *Larix decidua* stand.

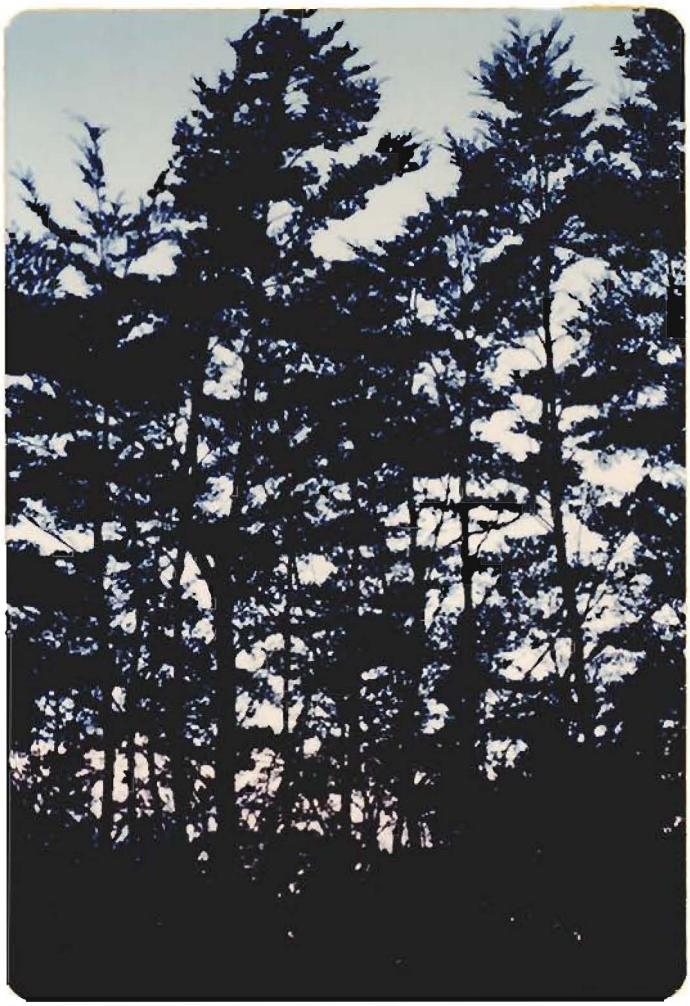

Plate 4.4: Side view of the *Nothofagus solandri* stand.

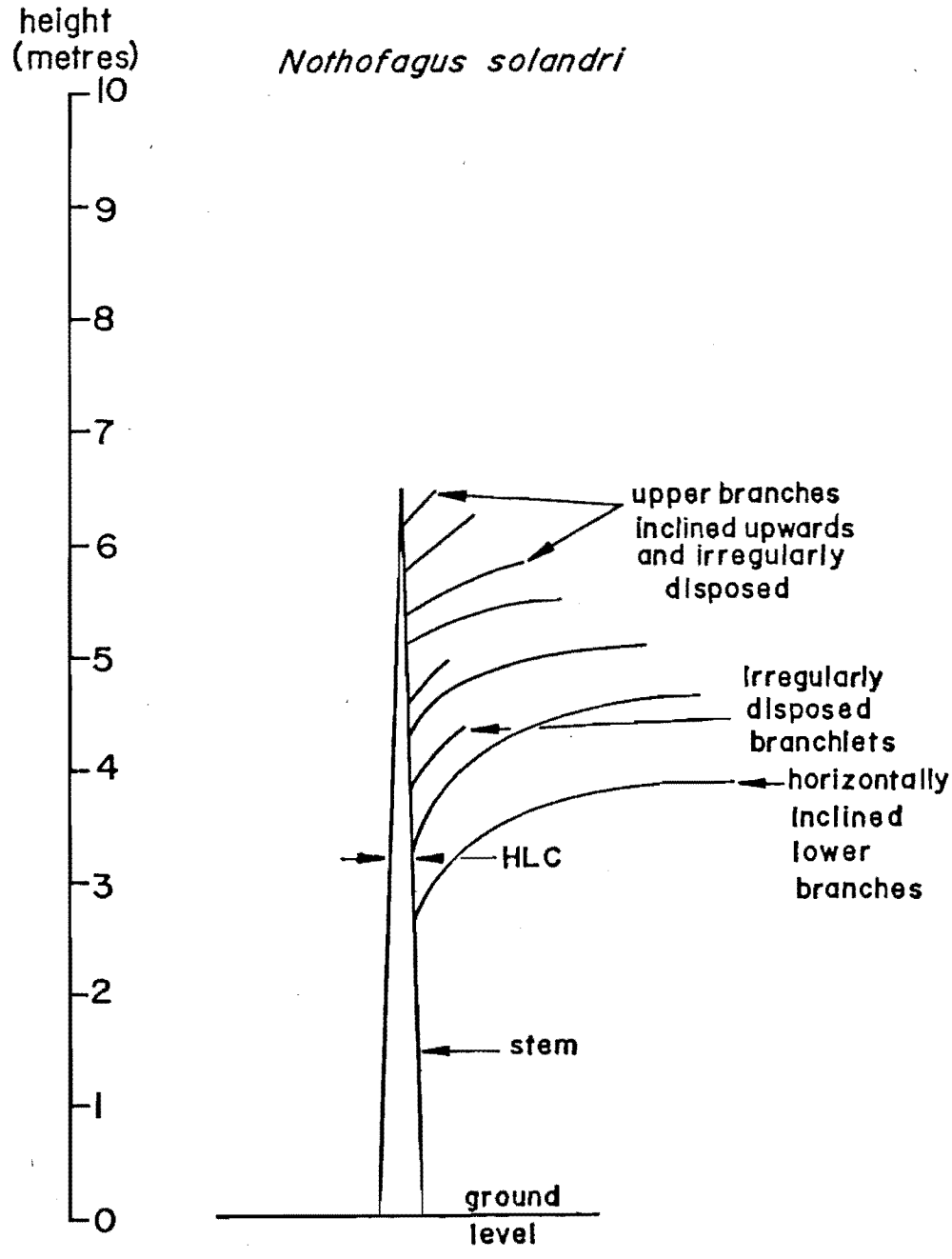

Figure 4.4: Stem-branch geometry for the *Nothofagus solandri* stand. HLC = height to the base of the living crown.

4.3.2 Foliage Orientation and Structure

In the preceding section simplified stem-branch geometry for the four stands was discussed. It was strongly evident that differences and similarities occurred between species. If the branches are the support systems for foliage then an understanding of the foliage orientation and structure on these support systems is necessary.

(a) *Pinus contorta*

P. contorta belongs to the group of two-needled pines. The needles are dark green in colour, arranged in pairs, range from 25-75 mm in length, and are rigid but often twisted.

Plate 4.5 illustrates the upward inclination of the foliage on the twigs. This is a notable characteristic of this species which facilitates an efficient use of penetrating irradiance.

In cross-section a *P. contorta* needle is hemispherically shaped (figure 4.5). The chloroplasts are contained within the mesophyll tissue in the centre. The needle shape and the central position of the chloroplasts allow irradiance to be absorbed from any direction. Therefore, applying projected leaf area indices (one side only) to needles under estimates total photosynthetic leaf surface.

Total surface leaf area (L_t) can be derived using simple geometry. Using equation 4.0,

Plate 4.5: Structure and orientation of *Pinus contorta* foliage.

Plate 4.6: Structure and orientation of *Pseudotsuga menziesii* foliage.

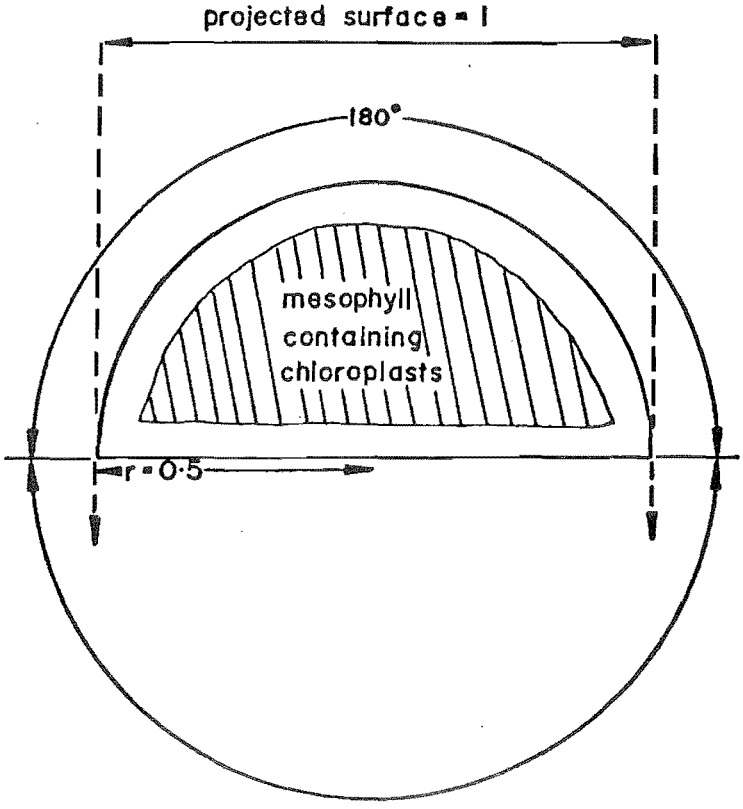

Figure 4.5: Cross-sectional geometry of a typical *Pinus contorta* needle : total surface area = 2.57 (see text)

$$L_t = \pi D/2 + D \qquad (4.0)$$
$$= 2.57$$

where L_t = circumference of a semi-circle (or a *P. contorta* needle), and D = 1.

To convert total surface leaf area (L_t) to projected surface leaf area L, equation 4.1 is used

$$L = L_t/2.57 \qquad (4.1)$$

(b) *Pseudotsuga menziesii*

In this species the spirally arranged needles are dark green in colour, solitary, and from 20-30 mm in length (plate 4.6). On shade branches they twist and arrange themselves in a double comb-like manner with the stomata facing the ground, and the needles springing from the upper face of the twig are shorter than the others. On erect shoots the needles are arranged all round the stem (plate 4.6), while on well-lit inclined branches (plate 4.2) they approximate to this disposition.

The horizontal branch system associated with this species and the tendency for the needles to spread out along the stems results in a rather over crowded and dense canopy.

In cross-section a *P. menziesii* needle has a slightly flattened top with a central rib, and a keeled bottom (figure 4.6). The chloroplasts are contained in the mesophyll, and in a similar way to *P. contorta* irradiance can be readily absorbed from any direction, but over a smaller surface.

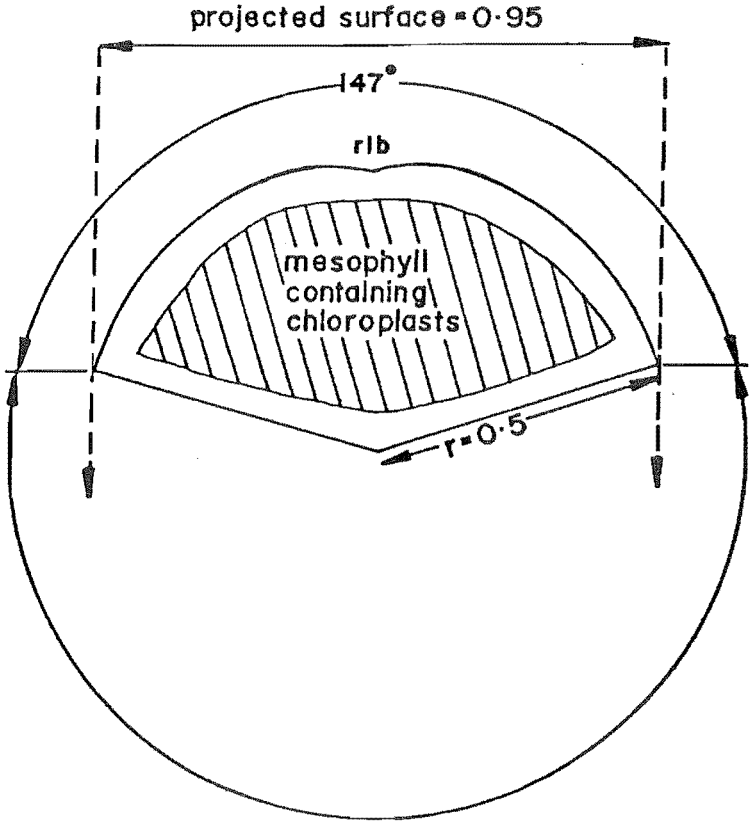

Figure 4.6: Cross-sectional geometry of a typical *Pseudotsuga menziesii* and *Larix decidua* needle : total surface area = 2.28 (see text)

Calculation of total surface leaf area (L_t) was slightly more complicated than for *P. contorta*. Given the angle of the arc for the *P. menziesii* cross-section 147°, then by using equation 4.2,

$$L_t = \pi D \times \frac{147}{360} + 1 \qquad (4.2)$$

$$= 2.28$$

where L_t = circumference of the *P. menziesii* needle.
To convert total surface leaf area L_t to projected surface leaf area L, equation 4.3 is used

$$L = (L_t/2.28) \times 0.95 \qquad (4.3)$$

(c) *Larix decidua*

This species is characterised by its yellow-green foliage and straw coloured twigs. The needles are deciduous, solitary, 20-37.5 mm in length, and spirally arranged on new growth (long-shoots), but on the short-shoots they are longer and form tufts, including from 25-60 needles (figure 4.7).

As plate 4.3 illustrates, the crown is loosely arranged with the foliage extending horizontally or downwards in the lower crown. *L. decidua* canopies are characterised by their open nature and because of this a well developed ground flora is often present.

In cross-section a *L. decidua* needle is more or less flattened on the top with a keeled bottom (figure 4.6). The chloroplasts are contained within the mesophyll tissue in the

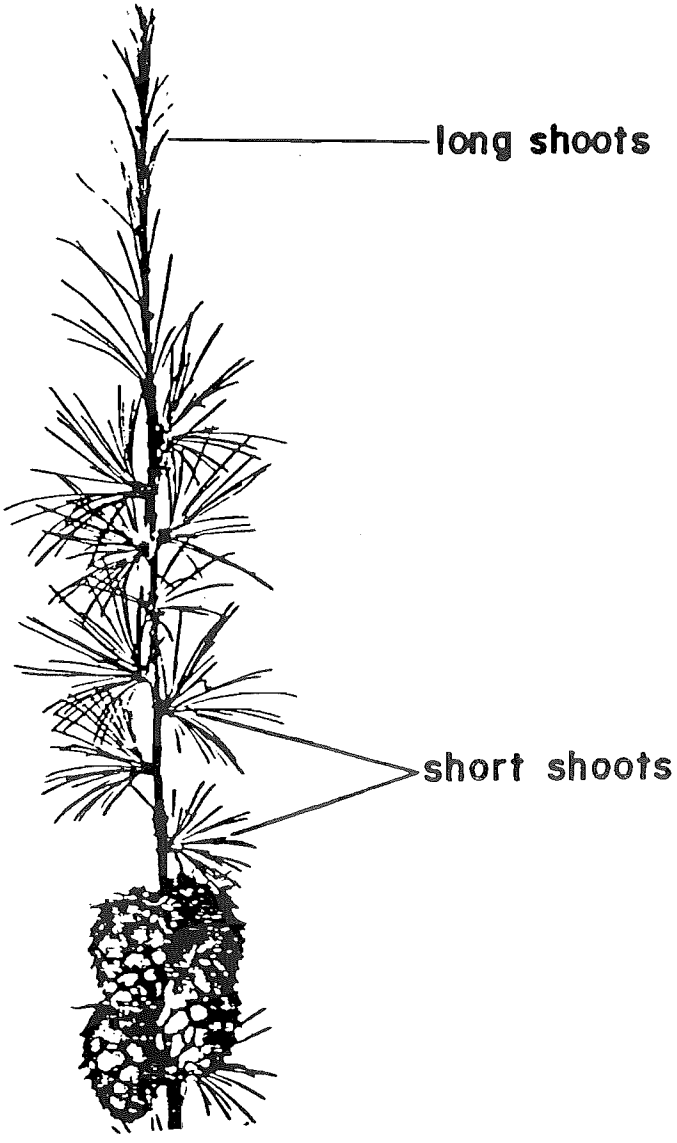

Figure 4.7: Structure and orientation of *Larix decidua* foliage.

centre, and as for the other two conifers, irradiance can be absorbed from any direction.

Geometrically, the cross-section for *L. decidua* was found to be very similar to *P. menziesii* (figure 4.6) so the same conversion ratios were used. (see equations 4.2, and 4.3)

(d) *Nothofagus solandri*

In *N. solandri* the leaves are light to dark green in colour and slightly glossy. They are ovate-triangular to elliptic ovate in shape (plate 4.7). Although not deciduous, the leaves are generally shed during the growing season after the one in which they are produced. Therefore, this species has affinities with deciduous broad-leaved genera such as *Fagus*. (Benecke and Nordmeyer, 1982).

Plate 4.7 shows the more or less horizontal inclination of the foliage on the twigs. The horizontal branch system (figure 4.4) and the tendency for the leaves to incline the same way is a notable characteristic of this species.

In cross-section a *N. solandri* leaf is more or less flat (figure 4.8). The chloroplasts are contained within the mesophyll in the centre of the leaf. Unlike the coniferous needles, *N. solandri* has a smaller effective light receiving surface.

Calculation of total surface leaf area (L_t) is very straight forward. Because the leaves are more or less flat their effective receiving area is equal to two. Converting total surface

Plate 4.7: Structure and orientation of *Nothofagus solandri* foliage.

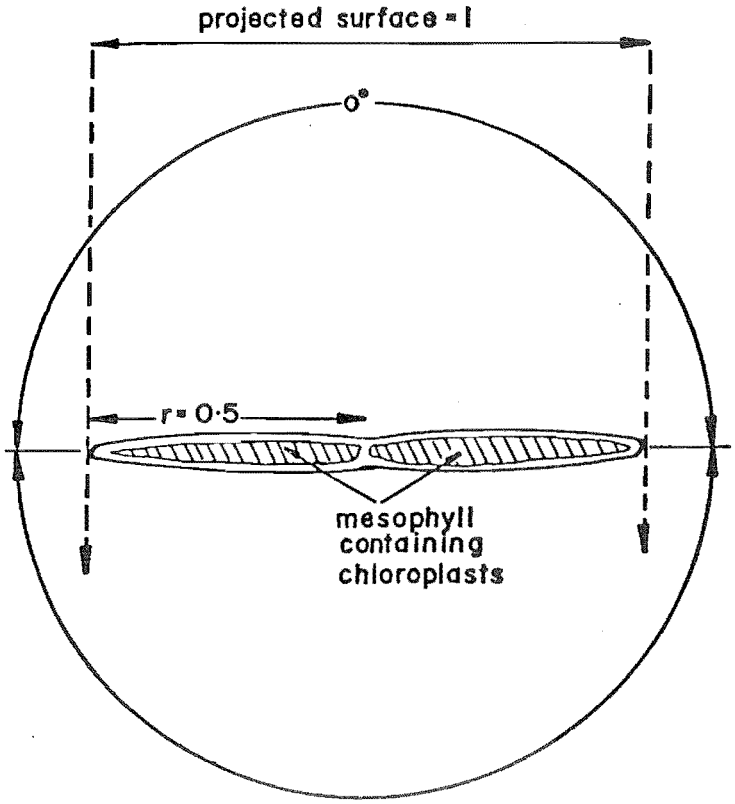

Figure 4.8: Cross-sectional geometry of a typical *Nothofagus solandri* leaf : total surface area = 2.0 (see text)

leaf area L_t to projected surface leaf area L is derived by using equation 4.4,

$$L = L_t/2 \qquad (4.4)$$

4.3.3 Canopy Closure

The discussion thus far has tended to focus on the vertical distribution of foliage within the canopy and its orientation in terms of the stem-branch geometry. In this section a brief analysis of canopy density for the four species will be made. Photographs of the canopy will form the basis of this analysis.

Plate 4.8 shows a view looking up into the *Pinus contorta* canopy. The canopy is not particularly dense and the upward branch-stem and foliage orientation, discussed previously (4.3.1(a), 4.3.2(a)), can be clearly seen. This particular canopy appears to allow adequate penetration of light through to the lower crown.

In apparent contrast to *P. contorta* is *Pseudotsuga menziesii* (plate 4.9). The view clearly shows a canopy opening with a dense canopy covering all round. The denseness of the foliage is related to its tendency to incline horizontally in a series of layers throughout the crown (see 4.3.1(b), 4.3.2(b)). One might expect therefore, that the penetration of light into this particular canopy would be severely impaired by its apparent denseness.

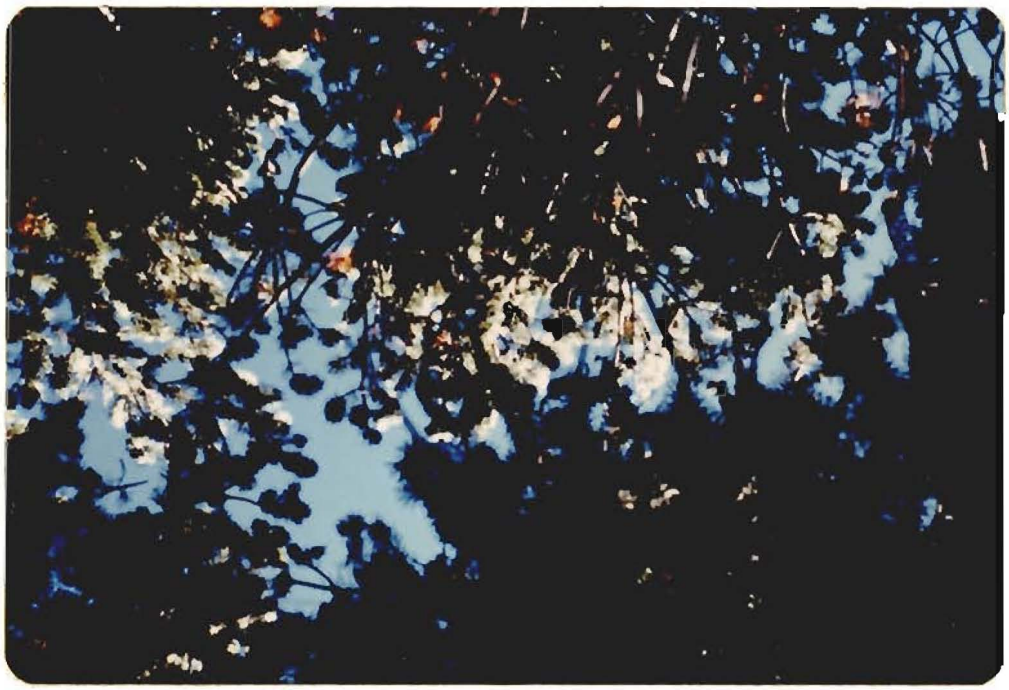

Plate 4.8: A view of the *Pinus contorta* canopy from within the trunk-space.

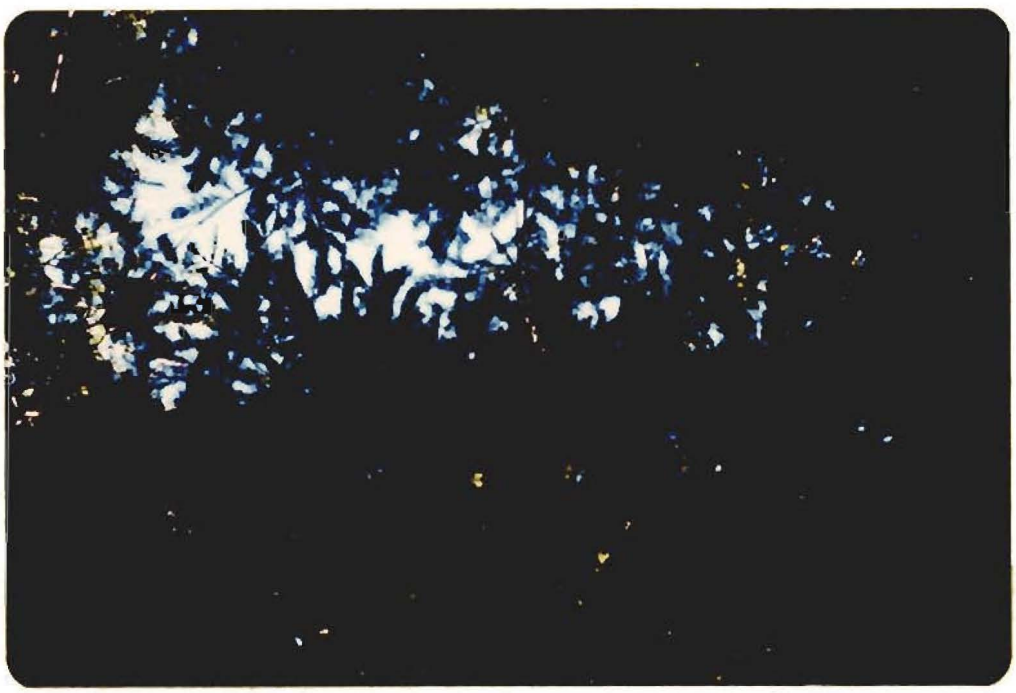

Plate 4.9: A view of the *Pseudotsuga menziesii* canopy from within the trunk-space.

The *Larix decidua* canopy (plate 4.10) is the most open of the four studied. This is a response to the intense light demands made by this species. Nonetheless, as the photograph shows the horizontal branch and foliage orientation (see 4.3.1(c), 4.3.2(c)) has some effect on penetrating light, especially considering the small leaf area given for this species (table 4.4).

The canopy image for *Nothofagus solandri* (plate 4.11) shows certain similarities to that for *P. menziesii*. In general, the canopy is quite dense because the foliage is also arranged in horizontal layers (see 4.3.1(d), 4.3.2(d)). One might therefore expect a similar light absorption curve for this canopy to that for *P. menziesii*.

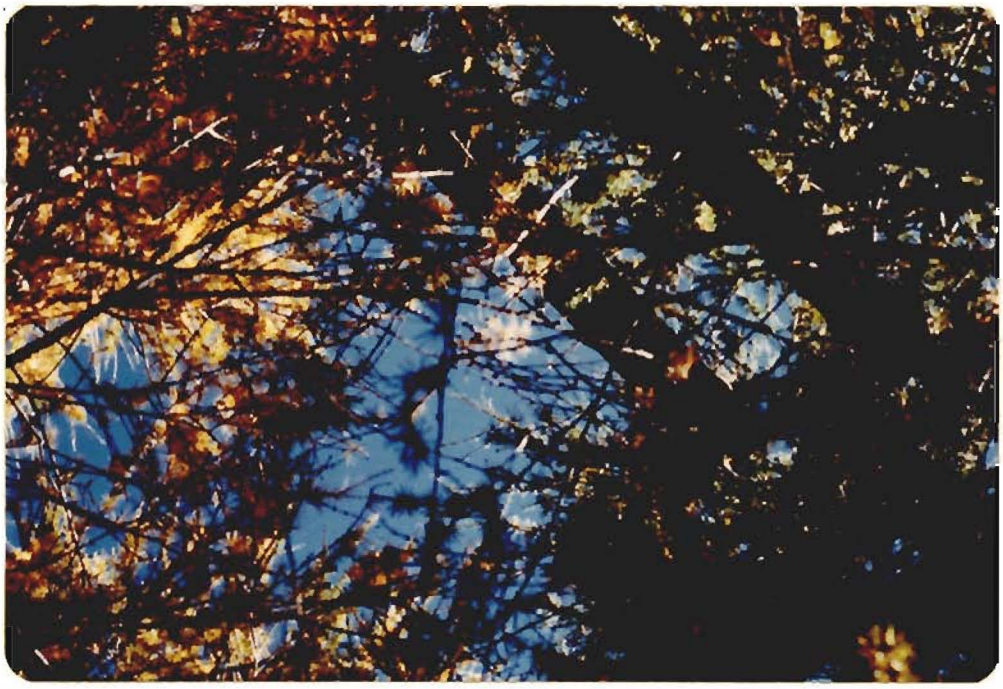

Plate 4.10: A view of the *Larix decidua* canopy from within the trunk-space.

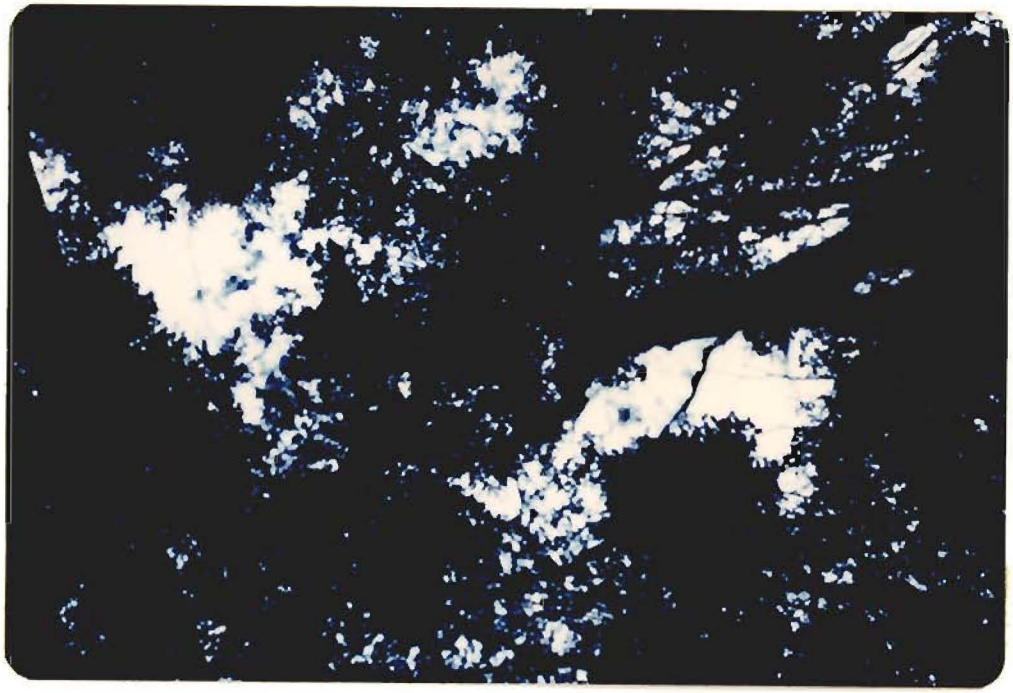

Plate 4.11: A view of the *Nothofagus solandri* canopy from within the trunk-space.

CHAPTER FIVE

RESULTS

5.1 ACTINOGRAPH RECORD AT CRAIGIEBURN FOREST METEOROLOGICAL SITE

Radiation was measured continuously over the entire study period (February-June) by the Fuess bimetallic actinograph, located at the Craigieburn Forest meteorological site (see section 2.1.3, 3.2.2, and plate 3.4). Details on the instrument and calibration procedures are covered in appendix 1.

Mean daily radiation totals for each month (January-June, 1982) are listed in table 5.1, together with the long-term daily averages (after McCracken, 1980).

Table 5.1: Mean daily radiation (MJm^{-2}) for January-June (1982) and the long term daily average (1965-80).

Radiation (MJm^{-2})	J	F	M	A	M	J
mean daily (1982)	20.2	18.4	13.1	8.2	5.3	4.6
long-term daily average (1965-80)	20.7	18.6	13.3	9.5	6.0	4.7

With the exception of April and May, the remaining months shown mean daily radiation totals similar to the long-term daily averages. The period of more intensive field investigation was February-March, and the figures for these months are very similar to the long-term mean. For radiation modelling purposes

February and March, 1982, may be regarded as representative of the long-term average.

5.2 MEASUREMENTS USING THE AMMONIA DIAZO PAPER TECHNIQUE

In chapter three, section 3.1.2, the ammonia diazo paper technique is discussed in detail. The method was used extensively in the field because of its simplicity and low cost. Considerable attention was given to calibration of the paper with particular wavelengths (see tables 3.11 and 3.12).

5.2.1 Cross-Checks With Other Radiation Measurements

(a) Actinograph record at Craigieburn Forest meteorological site.

As previously discussed (section 3.2.2), a diazo paper sensor was placed adjacent to the Fuess bimetallic actinograph. The objective of the exercise was to compare the radiation total from the actinograph with that derived from the diazo paper sensor. As previously discussed (section 3.2.1 and appendix 1) the Fuess bimetallic actinograph is a thermo-mechanical device and is responsive to 300-3000 nm irradiance. In comparison, the diazo paper is chemically changed by wavelengths primarily shorter than 410 nm (see section 3.1.2(g)). Although the diazo paper has been calibrated with a pyrometric sensor, which measures 300-3000 nm irradiance, one might expect small differences between weekly totals in irradiance for the actinograph and the diazo sensor because of the differences in their frequency responses.

Each week, the number of papers exposed in the diazo booklet was converted into energy units (MJm^{-2}) using the appropriate log function (see table 3.8 : λ300-3000 nm). The total from the actinograph was obtained by digitizing the daily charts and then converted to MJm^{-2} using the procedure outlined in appendix 1.

Table 5.2 provides a summary of the weekly radiation tables for the actinograph and the diazo paper sensor.

Table 5.2: Weekly radiation totals for the actinograph and the diazo paper sensors (λ300-3000 nm, MJm^{-2}): at the Craigieburn Forest meteorological site.

week	actinograph Q (MJm^{-2})	diazo sensor Q (MJm^{-2})	absolute difference (MJm^{-2})
03/2-10/2	152.5	159.0	+ 6.5
10/2-17/2	151.2	156.2	+ 5.0
17/2-24/2	123.1	132.1	+ 9.0
03/3-10/3	123.5	129.3	+ 5.8
10/3-17/3	91.0	85.2	- 5.8
24/3-31/3	75.5	83.1	+ 7.6
28/4-05/5	43.8	47.3	+ 3.5
12/5-19/5	38.0	43.0	+ 5.0
09/6-16/6	35.5	36.4	+ 0.9
16/6-23/6	31.9	32.6	+ 0.7

For each week, except 10-17 March, the radiation totals for the diazo paper sensors have exceeded those for the actinograph. One explanation for the difference, already mentioned, is that the two types of sensor have different frequency responses. As discussed in section 1.2.2(a), the spectral distribution of irradiance in the open is strongly influenced by cloud type and the transparency of the atmosphere. Both

these factors would affect the intensity of irradiance incident at the ground surface and its spectral distribution.

Another explanation for the difference could be that the actinograph gives a continuous trace of radiation levels, whereas the diazo paper sensor integrates to provide only one total. The actinograph pen trace often appears on a series of 'spikes', because of the higher variable radiation input associated with cloud conditions (see section 1.2.2(a)). It is very difficult to digitize the area under the curve for these charts with any reliable degree of precision. It is suggested therefore, that the actinograph radiation totals for days when the pen trace is highly variable, could be under estimating actual radiation totals, merely because valuable information is lost by the confusion of the pen trace.

Despite the differences in the weekly radiation totals for the two sensors, the two sets of data correlate highly ($r^2 = 0.99$) as shown by figure 5.1. This suggests that the ammonia diazo paper technique is very satisfactory as a method for measuring irradiance in the open over periods of one week.

(b) Quantum sensor record beneath the *Pinus contorta* canopy

As previously discussed (section 3.2.2), a diazo paper sensor was placed adjacent to an integrating quantum sensor beneath the *P. contorta* canopy each week. The objective of the exercise was to compare the radiation total from the quantum sensor with that derived from the diazo paper sensor beneath a forest canopy. This was necessary as a cross-check on the

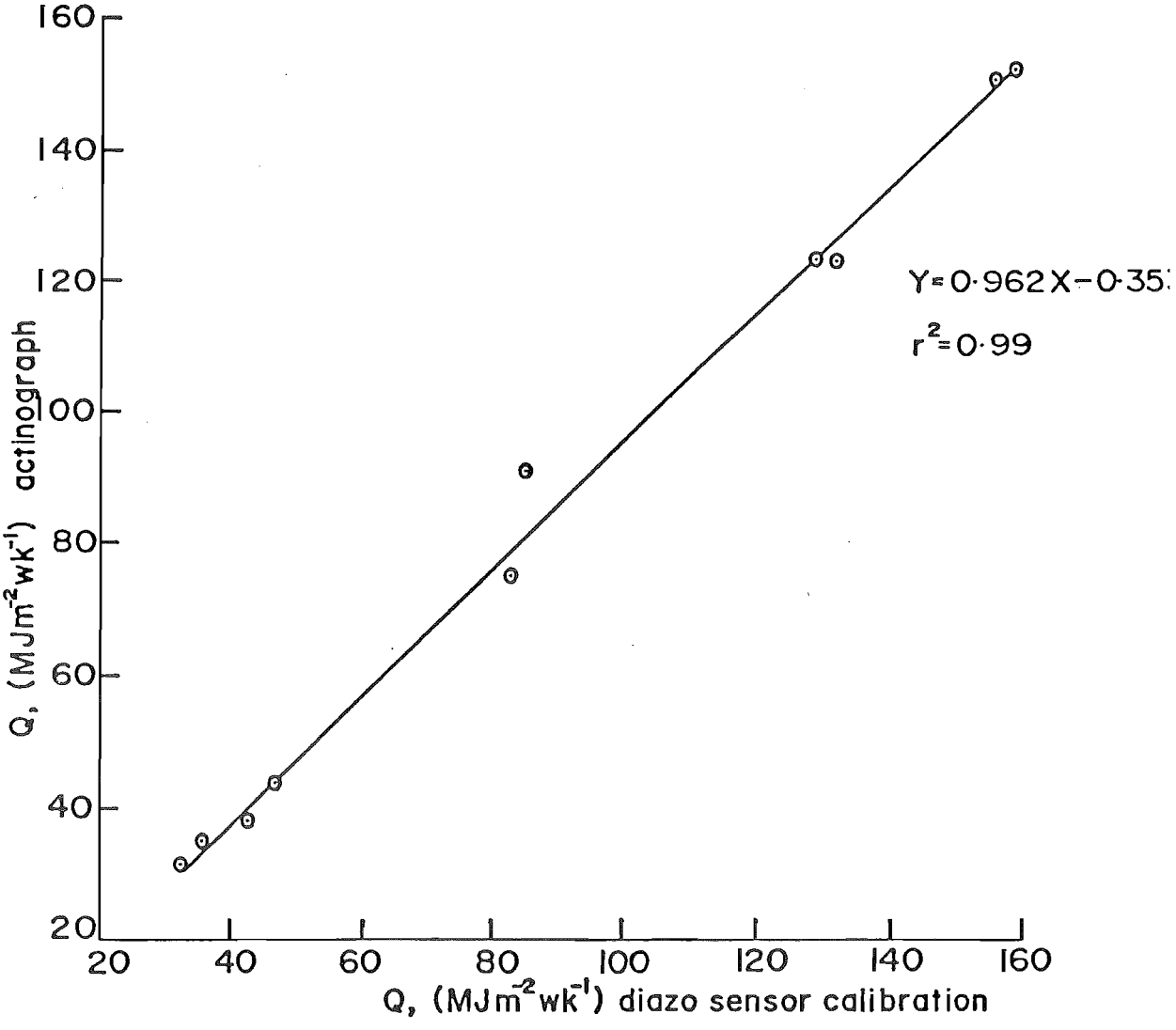

Figure 5.1: Relationship between 300-3000 nm irradiance ($MJm^{-2}wk^{-1}$) received by diazo paper sensors and the actinograph at the Craigieburn Forest meteorological site : the points represent different weeks.

sensitivity of the diazo paper to spectrally depleted irradiance known to occur beneath forest canopies (see sections 1.3.2(a) and 3.1.2(h)(iii)). Each week, the numbers of papers exposed in the diazo booklet was converted into energy units (Einsteins m^{-2}) using the appropriate log function (see tables 3.11 and 3.12 : λ400-700 nm at ground level). The total for the quantum sensor was obtained by summing hourly totals given by the integrator and converting into Em^{-2} using the procedure described in appendix 1.

The weekly radiation totals for the quantum sensor and the diazo paper sensors are listed in table 5.3.

Table 5.3: Weekly radiation totals for the quantum sensor and the diazo paper sensors (λ400-700 nm, Em^{-2}): located beneath the *Pinus contorta* canopy on Trig E.

week	quantum sensor Q (Em^{-2})	diazo sensor Q (Em^{-2})	absolute difference (Em^{-2})
03/2-10/2	8.9	10.4	+ 1.5
10/2-17/2	8.8	8.7	- 0.1
17/2-24/2	6.6	6.9	+ 0.3
24/3-31/3	8.9	8.6	- 0.3
07/4-14/4	3.6	4.8	+ 1.2
28/4-05/5	2.28	2.29	+ 0.01
12/5-19/5	2.02	2.1	+ 0.08

As table 5.3 shows the absolute differences between the two sets of data are not great. However, the percentage errors are greater than those for the actinograph and diazo paper (table 5.2). Nonetheless, the two sets of data still correlate to a significant level ($r^2 = 0.95$) as is shown by figure 5.2.

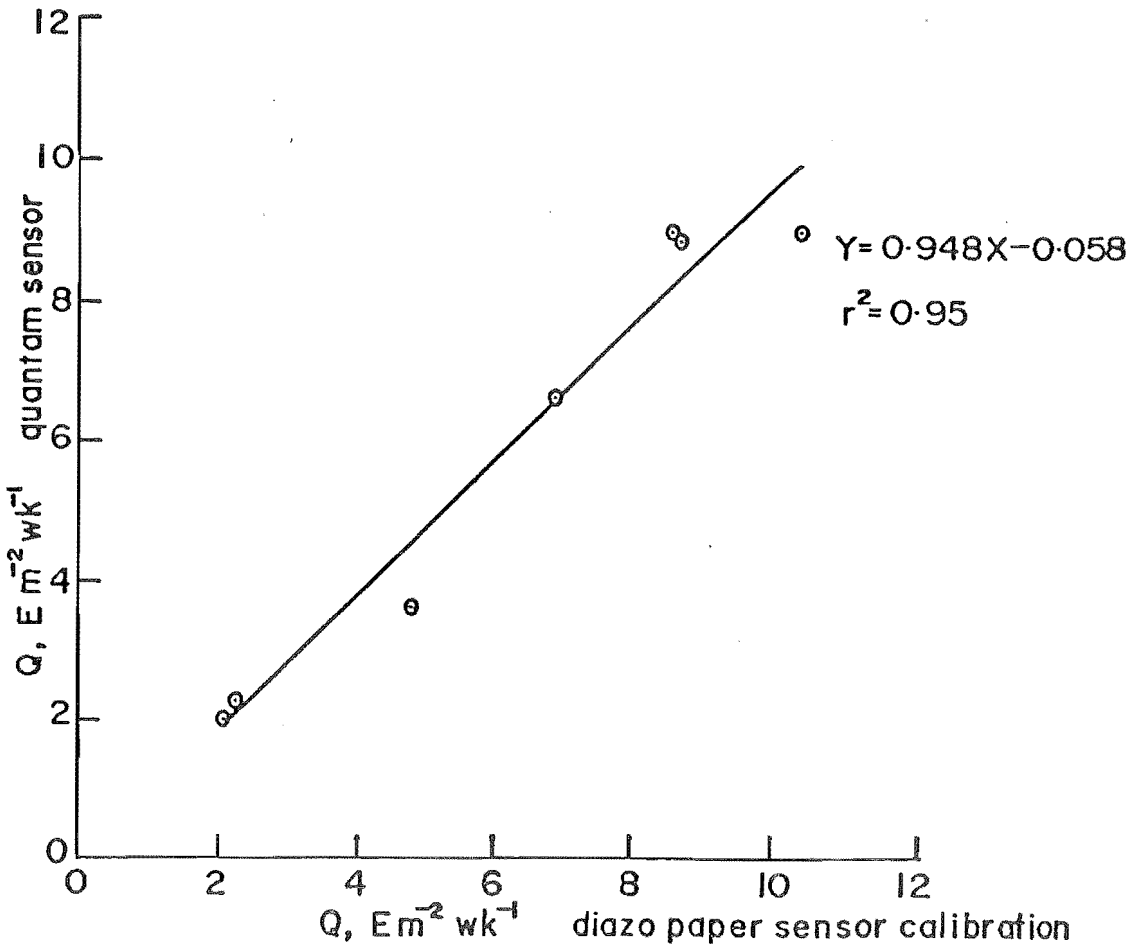

Figure 5.2: Relationship between 400-700 nm irradiance ($Em^{-2}wk^{-1}$) received by diazo paper sensors and the quantum sensor beneath the *Pinus contorta* canopy on Trig E : the points represent different weeks.

The variance shown between the two sets of data is largely attributable to the highly variable nature of the radiation climate beneath the canopy (see section 1.3.2), and to differences in the frequency response of the two types of sensor used. Even though the diazo paper sensor was placed immediately adjacent to the quantum sensor, it is highly unlikely that both sensors received identical incident irradiance.

In summary, the relatively high correlation between the two measurements of irradiance (figure 5.2) illustrates the utility of the diazo paper technique for work within forest stands, and emphasises the need to calibrate the paper in the light environment in which it is intended to be used.

5.2.2 Irradiance Within the Forest Stands

(a) Background

A generalised description of the forest stands used in this study is given in section 2.3, and their architectural characteristics are discussed in detail throughout chapter four. In the discussion to follow, the characteristics of the stands should be kept in mind. In this section results from the diazo paper sensors which were exposed at different levels within the different stands are presented. Details of the method used is discussed in section 3.1.2.

The vertical positioning of the wooden planks (transects) within the four forest stands is shown in table 5.4. It is mentioned previously (section 3.1.2(h)(i)) that the vertical distance between the transects varied among the four stands,

Table 5.4: Vertical positioning of transects within the four forest stands

FOREST SPECIES	H (m)	trunk-space		lower canopy			upper canopy			canopy top		HCL (m)	HCL/H
		z_{1} (m)	z_{1}/H	z_{2} (m)	z_{2}/H	z_{3} (m)	z_{3}/H	z_{4} (m)	z_{4}/H	z_{5} (m)	z_{5}/H		
Pinus contorta	9.0	1.0	0.11	4.2	0.46	5.7	0.63	7.2	0.80	9.0	1.00	2.2	0.24
Pseudotsuga menziesii	7.5	1.0	0.13	3.5	0.46	4.5	0.60	5.5	0.73	7.5	1.00	2.0	0.26
Larix decidua	7.0	1.0	0.14	2.5	0.35	3.5	0.50	4.5	0.64	7.0	1.00	2.2	0.31
Nothofagus solandri	6.5	1.0	0.15	3.4	0.52	4.4	0.67	4.9	0.75	6.5	1.00	3.2	0.49

$z_{1,2}$ etc = transect height

H = mean height (metres) of stand

HCL = height to base of live crown (metres)

being dependent on their architecture, in particular, the depth of canopy or crown length (see table 4.1).

From table 5.4 it should be noted that the height of the ground sensor is a constant one metre for all the stands. In the *Pinus contorta* canopy the vertical spacing between the transects was 1.5 metres at all levels, and for *Pseudotsuga menziesii* and *Larix decidua* a one metre spacing was used. For the *Nothofagus solandri* stand a one metre spacing between the bottom and middle transect and a half metre spacing between the middle and top transect was used.

Each week up to 36 diazo paper sensors were prepared (see section 3.1.2(b), (d)) and placed within each of the forest stands. After a weeks' exposure within the stands the sensors were brought back to Christchurch for developing and analysis (see section 3.1.2(e) for details). Conversion of the number of papers exposed in the diazo booklets into energy units was carried out using the appropriate log function for species, transect position, and time of year (see tables 3.11 and 3.12).

The data are available as 400-700 nm irradiance (Einsteins $m^{-2}wk^{-1}$) and as 300-3000 nm irradiance (Mega-joules $m^{-2}wk^{-1}$), and are summarised in appendix 2. The tables in appendix 2 illustrate the 'mean' irradiance received for the four levels within the stands (see table 5.4 for details).

From the absolute data shown in appendix 2, percentage

figures were derived, and these are discussed in this chapter. The figures are presented as irradiance received (Q) relative to that incident above the canopy (Q_o), by using equation 5.0.

$$Q(z) = 100\ Q/Q_o \qquad (5.0)$$

where $Q(z)$ = percentage irradiance at level (z);

Q = irradiance at level z (MJm^{-2} or EM^{-2}); and

Q_o = irradiance incident above the canopy (MJm^{-2} or EM^{-2}

The figure used for Q_o was taken from the reference sensor (plate 3.3) for the Trig E stands and from a sensor extended above the canopy for the *Nothofagus solandri* stand at Cheeseman. Cross-checks were also made with the actinograph record at the Craigieburn Forest meteorological site (plate 3.4) to ensure that the values for Q_o each week were within an acceptable range, after allowing for horizon differences between the sites (see section 2.1.3).

(b) Seasonal patterns of irradiance within the forest stands

(i) Introduction

One might expect seasonal patterns in the light regime of the forest stands because of changes in earth-sun geometry and phenological changes in forest structure. The measurements commenced in early February, when foliage biomass was nearing maximum for the season, and ceased in mid-June when it would be nearing its minimum for the season. The fieldwork covered a wide range of solar elevations progressing from the late summer position (February) through to winter solstice (21 June). The angle of direct beam radiation (Q_s) would have become

steadily lower as the fieldwork commenced.

In table 2.2 the characteristics of the four forest stands are shown and the horizons at the two main sites, Trig E and Cheeseman are illustrated in figures 2.3 and 2.4 respectively. It was previously stated that identical siting of all the forest stands was not possible, but provided details are known about horizon effects, and slope-aspect characteritics, then it is possible to compare the sites.

The Trig E stands (*Pinus contorta*, *Pseudotsuga menziesii*, and *Larix decidua*) share identical site chracteristics (table 2.2, and figure 2.3). The northerly aspect and the 30 degree slope angle allow this site to experience high levels of insolation throughout most of the year. The *Nothofagus solandri* stand at Cheeseman has a more easterly aspect but shares a similar slope angle (25^{o}). As the horizon diagram shows (figure 2.4) the site loses the direct beam of the sun at about 1600 hours at summer solstice (21 December) and at 1345 hours at winter solstice (21 June). There is little or no effect on the morning and midday direct beam irradiance at the site. Compared to the Trig E site, this site receives lower levels of irradiance throughout the year.

Table 5.5 contains a summary of the percentage irradiance received within the four stands for the months February-June, dervied from the data in appendix 2. Figures are given for 400-700 nm and 300-3000 nm incident and reflected irradiance for each of the levels. The transect positions, z_1, z_2 etc. refer to the heights given in table 5.4 for the forest stands.

Table 5.5: The percentage irradiance (P.A.R. and S.W.) received within the four stands (February-June, 1982), derived from the diazo paper sensor data in appendix 2.

Table 5.5(a) : February average n = 3 weeks

forest species	transect position	Q received relative to that above canopy Q_o (%)	
		λ400-700 nm (P.A.R.)	λ300-3000 nm (S.W.)
(incident irradiance)			
Pinus contorta	z_5	100.0	100.0
	z_4	22.7	25.4
	z_3	7.0	8.6
	z_2	1.9	2.6
	z_1	1.6	2.1
Pseudotsuga menziesii	z_5	100.0	100.0
	z_4	3.3	4.3
	z_3	1.9	2.7
	z_2	1.1	1.6
	z_1	0.26	0.43
Larix decidua	z_5	100.0	100.0
	z_4	23.0	25.7
	z_3	10.0	11.8
	z_2	5.2	6.5
	z_1	4.4	5.6
Nothofagus solandri	z_5	100.0	100.0
	z_4	4.5	5.6
	z_3	3.0	3.9
	z_2	1.7	2.4
	z_1	1.5	2.0
(reflected irradiance)			
Pinus contorta	z_4	0.13	0.22
	z_3	0.08	0.15
	z_2	0.05	0.10
Pseudotsuga menziesii	z_4	0.08	0.14
	z_3	0.07	0.13
	z_2	0.07	0.13
Larix decidua	z_4	0.27	0.42
	z_3	0.22	0.36
	z_2	0.15	0.26
Nothofagus solandri	z_4	0.11	0.19
	z_3	0.08	0.14
	z_2	0.05	0.10

Table 5.5(b) : March average n = 3 weeks

forest species	transect position	Q received relative to that above canopy Q_o (%)	
		λ400-700 nm (P.A.R.)	λ300-3000 nm (S.W.)
(incident irradiance)			
Pinus contorta	z_5	100.0	100.0
	z_4	18.3	20.7
	z_3	5.3	6.5
	z_2	2.0	2.7
	z_1	1.6	2.2
Pseudotsuga menziesii	z_5	100.0	100.0
	z_4	2.9	3.8
	z_3	1.8	2.5
	z_2	1.0	1.5
	z_1	0.6	0.9
Larix decidua	z_5	100.0	100.0
	z_4	19.1	21.7
	z_3	10.1	12.0
	z_2	5.9	7.3
	z_1	5.0	6.4
Nothofagus solandri	z_5	100.0	100.0
	z_4	4.4	5.6
	z_3	4.1	5.2
	z_2	3.6	4.7
	z_1	2.8	3.6
(reflected irradiance)			
Pinus contorta	z_4	0.15	0.25
	z_3	0.09	0.14
	z_2	0.07	0.12
Pseudotsuga menziesii	z_4	0.08	0.12
	z_3	0.07	0.10
	z_2	0.07	0.10
Larix decidua	z_4	0.46	0.70
	z_3	0.32	0.55
	z_2	0.20	0.33
Nothofagus solandri	z_4	0.18	0.3
	z_3	0.14	0.23
	z_2	0.09	0.15

Table 5.5(c) : April average n = 2 weeks

forest species	transect position	Q received relative to that above canopy Q_o (%)	
		λ400-700 nm (P.A.R)	λ300-3000 nm (S.W.)
(incident irradiance)			
Pinus contorta	z_5	100.0	100.0
	z_4	24.9	25.8
	z_3	6.0	6.5
	z_2	2.4	2.6
	z_1	2.2	2.4
Pseudotsuga menziesii	z_5	100.0	100.0
	z_4	3.4	3.8
	z_3	2.4	2.7
	z_2	1.3	1.5
	z_1	1.0	1.2
Larix decidua	z_5	100.0	100.0
	z_4	31.3	32.3
	z_3	19.0	19.8
	z_2	11.1	11.7
	z_1	11.0	11.6
Nothofagus solandri	z_5	100.0	100.0
	z_4	4.6	4.9
	z_3	3.6	3.9
	z_2	3.5	3.8
	z_1	3.0	3.3
(reflected irradiance)			
Pinus contorta	z_4	0.36	0.41
	z_3	0.16	0.18
	z_2	0.15	0.17
Pseudotsuga menziesii	z_4	0.12	0.15
	z_3	0.11	0.14
	z_2	0.11	0.14
Larix decidua	z_4	1.4	1.6
	z_3	0.74	0.85
	z_2	0.53	0.62
Nothofagus solandri	z_4	0.24	0.29
	z_3	0.23	0.27
	z_2	0.22	0.26

Table 5.5(d) : May average n = 1 week

forest species	transect position	Q received relative to that above canopy Q_o (%)	
		λ400-700 nm (P.A.R.)	λ300-3000 nm (S.W.)
(incident irradiance)			
Pinus contorta	z_5	100.0	100.0
	z_4	24.3	25.3
	z_3	4.8	5.2
	z_2	2.3	2.6
	z_1	2.0	2.3
Pseudotsuga menziesii	z_5	100.0	100.0
	z_4	ca. 3.8	ca. 4.2
	z_3	2.6	2.9
	z_2	1.8	2.0
	z_1	1.1	1.3
*Larix decidua**	z_5	100.0	100.0
	z_4	42.8	44.0
	z_3	24.0	25.0
	z_2	21.6	22.6
	z_1	21.2	22.1
Nothofagus solandri	z_5	100.0	100.0
	z_4	4.7	5.1
	z_3	3.7	4.0
	z_2	3.6	3.9
	z_1	3.3	3.6
(reflected irradiance)			
Pinus contorta	z_4	0.32	0.38
	z_3	0.17	0.20
	z_2	0.15	0.18
Pseudotsuga menziesii	z_4	0.17	0.20
	z_3	0.15	0.17
	z_2	0.14	0.16
*Larix decidua**	z_4	2.1	2.4
	z_3	1.7	1.9
	z_2	1.5	1.7
Nothofagus solandri	z_4	0.22	0.26
	z_3	0.21	0.25
	z_2	0.20	0.24

* little or no foliage present at time of measurement.

ca. interpolated from best-fit curve.

Table 5.5(e) : June average n = 1 week

forest species	transect position	Q received relative to that above canopy Q_o (%)	
		λ400-700 nm (P.A.R.)	λ300-3000 nm (S.W.)
(incident irradiance)			
Pinus contorta	z_5	100.0	100.0
	z_4	44.9	45.9
	z_3	3.66	4.0
	z_2	2.32	2.5
	z_1	1.8	2.0
Pseudotsuga menziesii	z_5	100.0	100.0
	z_4	6.2	6.6
	z_3	1.7	2.0
	z_2	1.6	1.8
	z_1	1.2	1.4
(reflected irradiance)			
Pinus contorta	z_4	0.39	0.45
	z_3	0.25	0.29
	z_2	0.23	0.27
Pseudotsuga menziesii	z_4	0.24	0.27
	z_3	0.21	0.25
	z_2	0.21	0.25

no data available for *Larix decidua* and *Nothofagus solandri*.

The transmission and reflection of 300-3000 nm irradiance (S.W.) exceeds that for 400-700 nm irradiance (P.A.R.) in all the examples given. The reason for this, already discussed in section 1.2.2(b), is because P.A.R. (400-700 nm) is absorbed more readily than S.W. radiation (300-3000 nm), because the latter has a greater coefficient of scattering (ω).

The ratio between 400-700 nm irradiance (Em^{-2}) and 300-3000 nm irradiance (MJm^{-2}) in the tables in appendix 2, clearly shows how irradiance becomes photosynthetically less active as it penetrates through the canopy to the floor. For example: week one, species one (*Larix decidua*) has ratios of 2.9 for above the canopy, 2.6 for the top transect, 2.4 for the middle transect, 2.35 for the bottom transect, and 2.3 for the ground sensor. In contrast, species two (*Pseudotsuga menziesii*) has the following ratios: above canopy 2.9, top transect 2.2, middle transect 2.1, bottom transect 1.9, and ground sensor 1.8. In other words, the *P. menziesii* canopy has a greater effect on the transmitting photosynthetically active radiation than the *L. decidua* canopy. The ratios of 400-700 nm irradiance and 300-3000 nm irradiance for the four stands compare well with those given in table 3.10, which were based on measurements made with photo-electric sensors.

(ii) Incident irradiance

The summary of data in table 5.5 clearly shows the marked differences in the percentage transmission of irradiance for the four stands. Figures 5.3 and 5.4 illustrate these differences more clearly by comparing February and May, for the

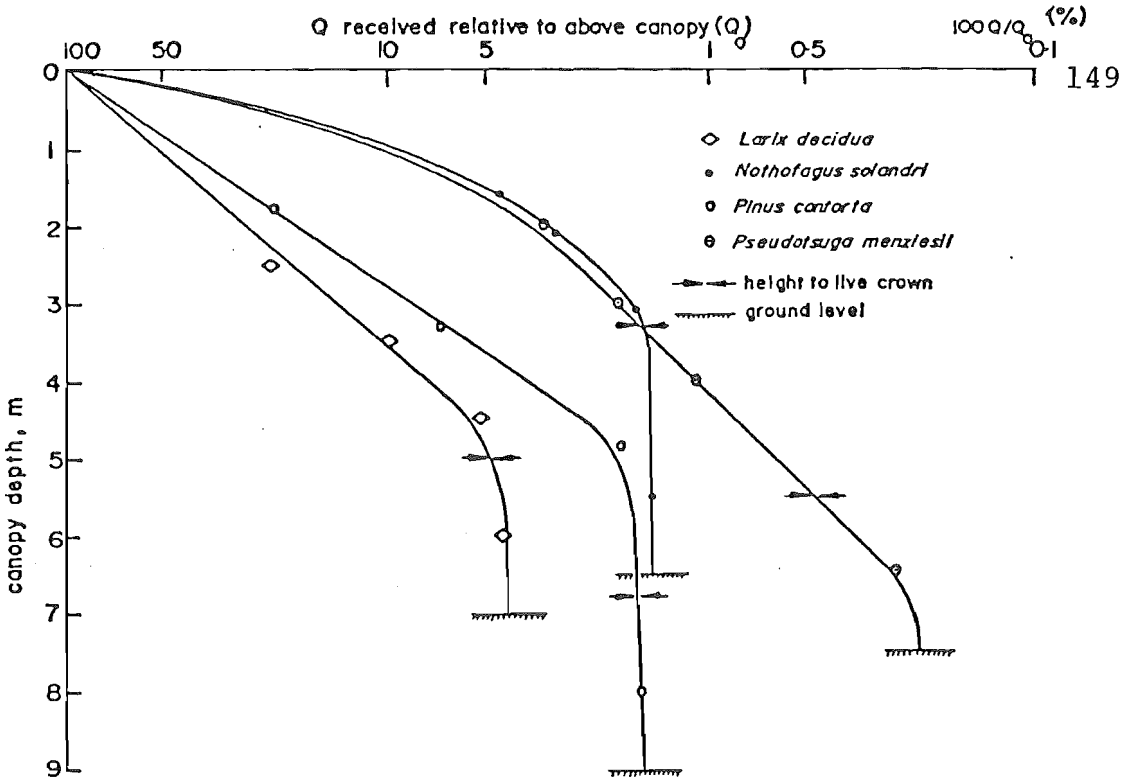

Figure 5.3: Absorbance of 400-700 nm irradiance (P.A.R.) as measured by the diazo paper sensors in the four forest stands in February, 1982.

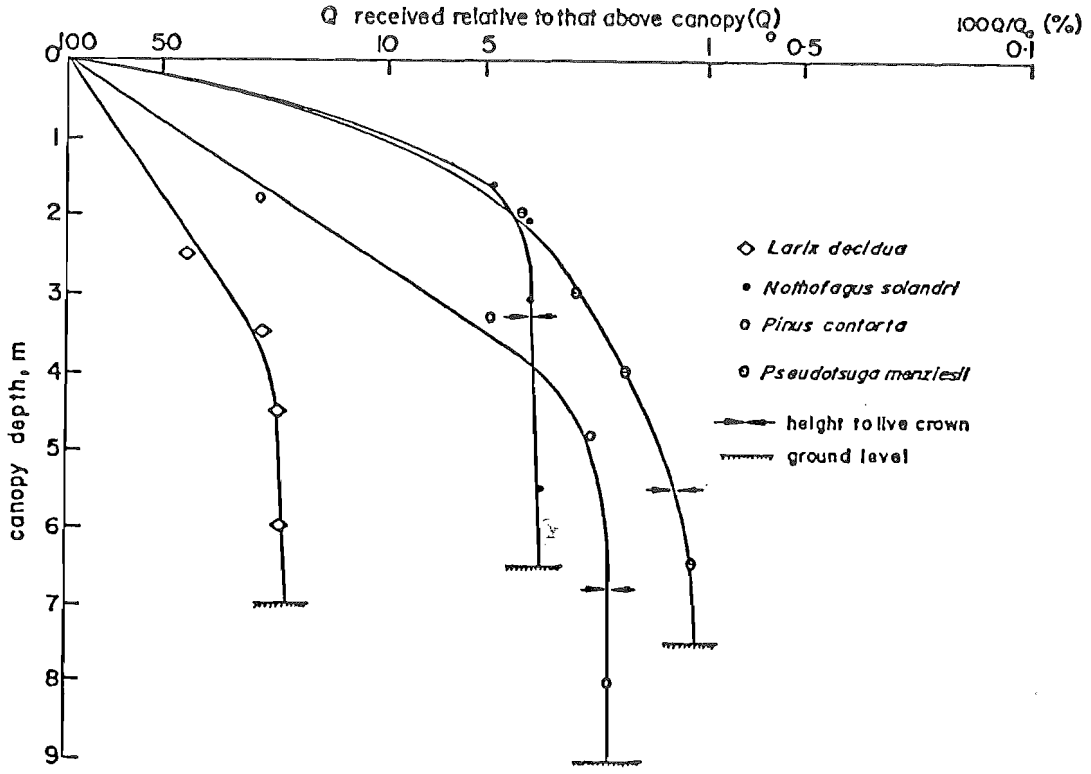

Figure 5.4: Absorbance of 400-700 nm irradiance (P.A.R.) as measured by the diazo paper sensors in the four forest stands in May, 1982.

transmission of 400-700 nm irradiance (P.A.R.). The reasons for these differences are largely due to architectural differences between the stands, and in chapter six these reasons are discussed in detail.

In February it appears that the *Larix decidua* stand allowed the greatest penetration of irradiance through the canopy to the ground, followed by the *Pinus contorta* stand. Both these stands share a similar light extinction curve (figure 5.3), which is more or less a straight line through to the base of the living crown (HLC). Beneath the HLC position there is little or no attenuation of light because there is little interference apart from the main stems.

The *Pseudotsuga menziesii* and *Nothofagus solandri* stands share very similar light extinction curves, especially in the upper crown. The curves are more or less parabolic in form which suggests a rather rapid absorption of irradiance in the upper crown. In *N. solandri* the extinction of light more or less ceases from the mid-crown region to the ground (figure 5.3). Whereas, in *P. menziesii* the light extinction curve straightens out at the mid-crown level and continues throughout the entire canopy, and in consequence very low light levels are found beneath the canopy (figure 5.3, table 5.5(a)).

The light extinction curves for May (figure 5.4) show the same basic differences between the forest stands. However, these curves show a number of differences compared with February (figure 5.3). It is suggested that the differences relate to

changes in earth-sun geometry and stand phenology.

The changes in the light extinction curves for the four stands between February and May are most marked in the lower crown and trunk-space, except in *L. decidua* where the change is dramatic throughout the entire crown; this is attributed to its deciduous habit (figure 5.3 and 5.4). The main period of needle fall, as shown by the field results was between 7-28 April (see appendix 2). The light extinction curve for *L. decidua* in May (figure 5.4) therefore, illustrates the transmission of irradiance through a crown without foliage.

The evergreen forest species studied also experienced changes in their phenology over the study period. Leaf death occurs throughout the growing season but is compensated for by new growth; the result is net leaf gain. From early April onwards, the summer expansion of new growth, predominantly in the upper crown, is likely to have caused increased leaf death in the lower crown because of reduced light levels there. From this period onwards net leaf loss in the lower crown is likely to have occurred.

In the *N. solandri* stand considerable leaf fall was observed from late March onwards. According to Wardle (1970, p 642) leaf fall reaches a maximum between March-May in *N. solandri*.

Out of all stands studied, the *P. contorta* stand has shown the smallest seasonal variation in its light regime (figures

5.3 and 5.4). Apart from a slight increase in the percentage of light being received in the lower crown and trunk-space, the light extinction curve is very similar for all the months studied (table 5.5). It is suggested, that because of the architecture of its canopy, it is able to absorb irradiance effectively at all times of the year. The small increase in irradiance in the lower crown is undoubtedly due to the fall of needles in that region, and the increase in the trunk-space is more likely to be associated with the lower solar elevation and light passing through the sides of the stand.

The problem of side-light entering through the sides of the stand were especially marked in the *P. menziesii* stand. The greater amount of light received within the trunk-space in May compared with February is mostly attributed to side light. Problems of this nature are undoubtedly severe when working in stands of limited size. However, there is an interesting change in the amount of light received in the lower crown between February and May. The percentage increase in May and June is likely to be associated with needle-fall in the lower-crown and lower solar elevation. The more horizontal foliage orientation associated with *P. menziesii* in the middle and lower crown (chapter four) has a greater effect on penetrating irradiance when solar elevation is higher. At times of lower solar elevation, the rays are able to pass more freely into the lower levels of the crown. This effect is exemplified largely because of the northward inclination of the slope. The change in the upper crown for *P. menziesii*, as in all the stands except *L. decidua*, is minimal. The main reasons

being: for all the species there is a more vertical inclination of foliage in this region of the crown (see chapter four), and there is little or no phenological change because the foliage is much younger than that in the lower crown.

N. solandri illustrates rather well, the effects of leaf fall on the percentage penetration of irradiance. Net leaf loss in the lower and middle crown from early April onwards has resulted in a relative increase in the amount of light penetrating through to the ground (figures 5.3 and 5.4). The effec of lower solar elevation would contribute to a lesser extent because there are no side-light problems associated with this stand. The change in light penetration in the upper crown is minimal, and this is most likely a result of little or no leaf fall in that region because the foliage is primarily new seasons' growth.

In summary, the data presented in table 5.5 for incident irradiance in the four stands, illustrates the effects of changes in earth-sun geometry and phenological changes in canopy structure on the radiation regimes within the canopies. With the exception of *L. decidua* which is deciduous, the forest stands share similar changes in their light extinction curves between February and May. The most marked changes occurred in the lower-crown and trunk-space and this was shown to be largely related to net leaf loss and lower solar elevation in the autumn, and, with the exception of *P. contorta*, to the horizontally orientated foliage. Changes in the upper-crown were less marked because the foliage is younger and more

vertically orientated. The results suggest, that changes in solar elevation will have little effect on penetrating irradiance in canopies with more vertically orientated foliage (c.f. *P. contorta*).

(iii) Reflected irradiance

Reflected irradiance plays a minor role in the radiation regime of forest canopies. From the data in table 5.5 it is evident that 400-700 nm irradiance (P.A.R.) has a lower reflection coefficient (ρ) than 300-3000 nm irradiance (S.W.). The reason for this, already discussed in section 1.2.2(b), is because P.A.R. is more readily absorbed by the vegetation than short-wave radiation.

The amounts of reflected irradiance within the four stands are by and large small, and related to the intensity of incident irradiance. For example, *L. decidua* has the highest reflection values and in turn it allows the greatest amount of irradiance to pass through the canopy (table 5.5). Reflected irradiance is therefore directly related to the intensity of the incident irradiance. This relationship is clearly shown from the data in table 5.5. As the measurements commenced from February to June, the proportion of irradiance reflected from the ground beneath the canopies (measured by bottom transect) and within the canopies (measured by middle and top transects) increased. It has already been shown in the preceding section, that relative levels of incident irradiance received in the lower crown and trunk-space increased as the field work progressed into the early winter.

Above canopy reflected irradiance was not measured for the four stands with the diazo paper technique. However, in an attempt to estimate total reflection coefficients (ρ) for the four stands, measurements were made using pyrometric and quantum sensors on individual trees in the open under different sky conditions. The average values for the four stands are summarised in table 5.6.

Table 5.6: Mean reflection coefficients (ρ) for the four stands studied : expressed in terms of the irradiance received above the canopy Q_o (Q_o = 100%) for P.A.R. and S.W. radiation.

forest species	total irradiance Q reflected from the stands (%)	
	λ400-700 nm (P.A.R.)	λ300-3000 nm (S.W.)
Larix decidua	8.0	22.0
Pseudotsuga menziesii	6.0	20.0
Pinus contorta	5.0	19.0
Nothofagus solandri	9.0	24.0

300-3000 nm irradiance (S.W.) has the greatest reflection coefficient for reasons already discussed in section 1.2.2(b). The reflection coefficient for 400-700 nm irradiance is low in comparison because P.A.R. is less scattered by the vegetation.

Compared with irradiance reflected from the ground and from within the stands, the total reflection coefficients for the four stands suggest that most of the reflection occurs within the immediate upper crown. This is because the amount of irradiance reflected is directly proportional to the intensity of the incident irradiance. The incident irradiance is most intense in the immediate upper crown.

N. solandri shows the greatest reflection of irradiance and this is largely because of the flat glossy nature of its leaves. *L. decidua* is close behind, and its high reflection coefficient can be attributed to the open nature of its canopy. Because more irradiance reaches the floor than in the other stands, reflection off the ground is greater. *P. menziesii* and *P. contorta* show relatively low reflectance values, this being related to their needle structure and to the density of their canopies. The values for P.A.R. of 6.0% and 5.0% for *P. menziesi* and *P. contorta* respectively, compare well with those given by Jarvis *et al* (1976, p174).

From the data shown in tables 5.5 and 5.6 it is strongly evident that reflected irradiance decreases motonically with the depth of the stand and thus differs from the downward profile of incident irradiance (figure 5.3 and 5.4).

5.2.3 Irradiance Across the *Nothofagus solandri* Regeneration Transect

(a) Background

Irradiance was measured across a dense patch of *N. solandr* regeneration beneath a canopy opening (for details see sections 2.3.2 and 3.1.2(h)(ii)). Ammonia diazo paper sensors were plac on top of posts which were set at regular one metre intervals along the transect (see figure 3.10).

Sensors were exposed from 7-14 May, 1982. Unfortunately an early snowfall and very damp conditions completely ruined the paper booklets towards the end of the week. Sensors were

then exposed from 21-28 May and the results proved satisfactory because drier weather prevailed over the exposure period.

This study comprises of only one weeks' data and is therefore of only limited application. Nonetheless, the result emphasises the usefulness of the diazo paper technique for the long-term measurement of irradiance across the forest floor in the presence of regeneration.

(b) Results

Figure 5.5. illustrates the variability of irradiance received ($MJm^{-2}wk^{-1}$) along the transect. Irradiance was measured at the height of the regeneration and at a constant height of 25 cm within the regeneration itself. From the diagram, it is strongly evident that the highest levels of irradiance were measured beneath the canopy opening and the lowest levels were recorded beneath the main canopy. This pattern is primarily a result of the shading effect provided by the main canopy above.

Irradiance received along the lower transect beneath the regeneration is relatively even as shown by the lower line (figure 5.5). The slight decrease observed between the six and seven metre positions can be attributed to the stronger shading effect provided by the taller regeneration above these points (figure 5.5).

In an attempt to determine whether there is any relationship between irradiance received and the height of the regeneration

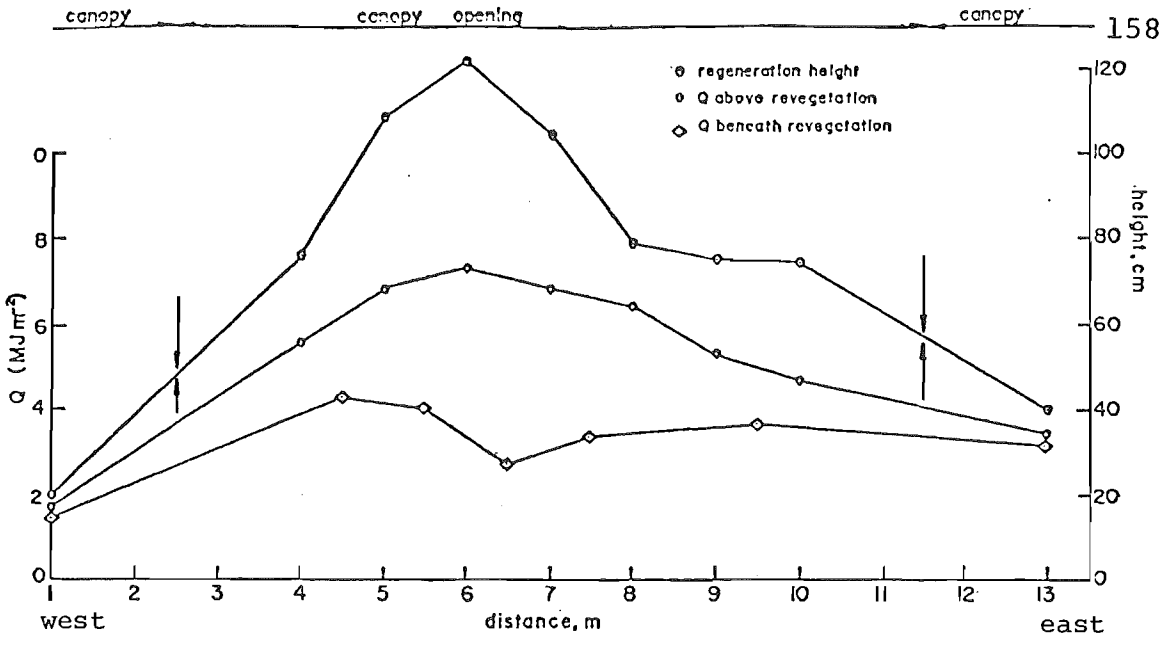

Figure 5.5: 300-3000 nm irradiance received ($MJm^{-2}wk^{-1}$) across a 13 metre transect on the forest floor beneath a canopy opening in a *Nothofagus solandri* forest. Irradiance measured by diazo paper sensors at one metre intervals at the height of the vegetation and at a constant height of 25 cm within the revegetation.

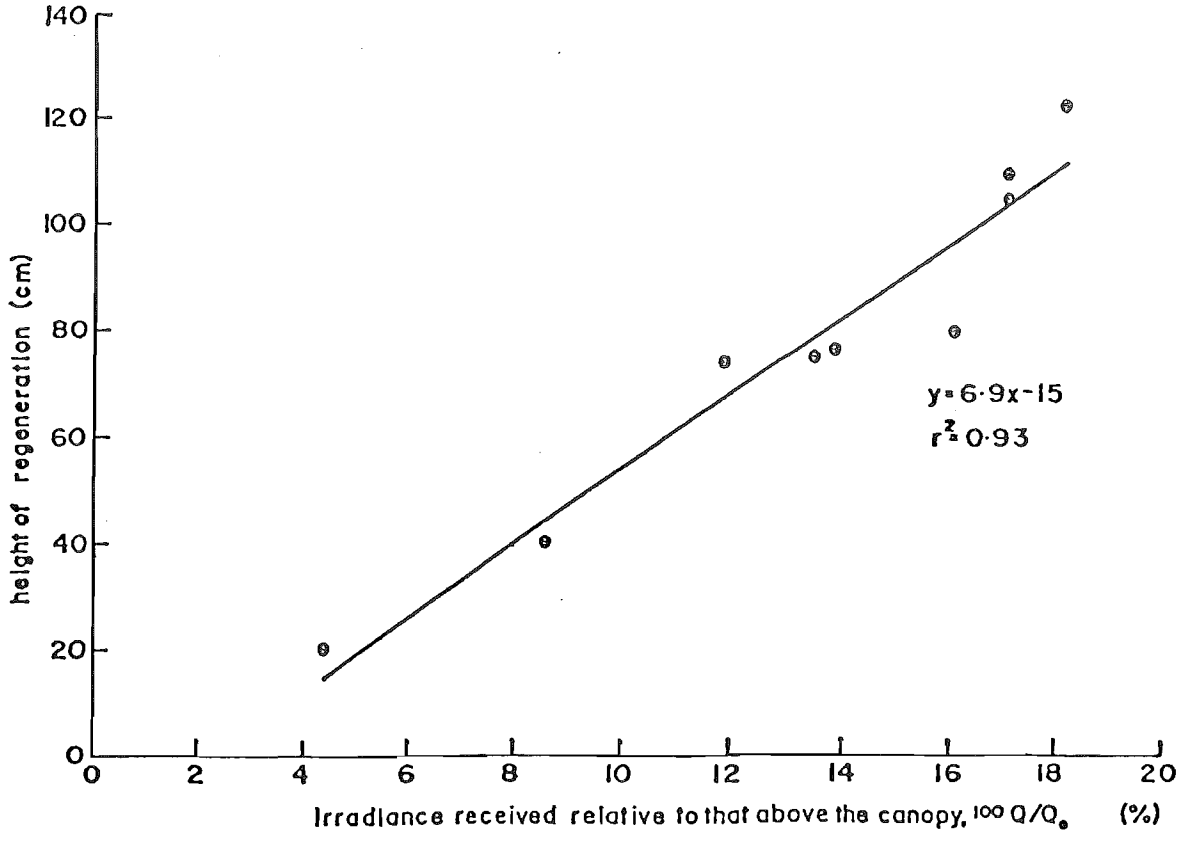

Figure 5.6: Relationship between 300-3000 nm irradiance (S.W.) received relative to that above the canopy and the height of regenerating *Nothofagus solandri* trees (cm).

regression analysis was made comparing the two variables. Above canopy irradiance Q_o was derived from the actinograph record at the Craigieburn Forest meteorological site, which has a similar horizon to the study site (see section 2.1.3). Total irradiance received for the week ending 28 May was 41 MJm^{-2}.

Using equation 5.0, irradiance received Q relative to that above the canopy Q_o was derived for each of the diazo sensors above the regeneration (figure 5.5). The relationship between irradiance received relative to that above the canopy (%) and the height of the regeneration (cm) is shown by figure 5.6. For the week studied (21-28 May, 1982), there appears to be a strong positive relationship ($r^2 = 0.93$) between the two variables, suggesting that the height of the regeneration is strongly dependent on the amount of light received. However, due to the limited data base such factors as : optimal light intensity, and compensating light intensity for the *N. solandri* seedlings cannot be determined with any degree of certainty.

5.3 PHOTO-ELECTRICAL MEASUREMENTS BENEATH THE EXOTIC FOREST STANDS

5.3.1 Background

Spot measurements were made beneath the three exotic forest stands on Trig E (*Pinus contorta, Larix decidua,* and *Pseudotsuga menziesii*) with the portable quantum sensor and meter (both LAMBDA, Nebraska - for details, plate 3.2 and appendix 1). Above canopy incident irradiance was measured with the quantum sensor and integrator set up in the open near the forest

stands (both LAMBDA, Nebraska - for details, plate 3.1 and appendix 1). All measurements described in this section were made during clear sky conditions. Attempts to make measurements during overcast sky conditions were made, but the sensitivity of the electronic recording meter was insufficient for the very low levels of irradiance beneath the canopies.

5.3.2 Results

Table 5.7 provides a summary of observations for 400-700 nm irradiance incident above canopy (Q_o) and beneath canopy (Q) for the three exotic stands on Trig E. The data presented is the mean of twenty measurements made beneath each of the canopies. Using equation 5.0, irradiance received (Q) relative to that above the canopy (Q_o) was derived for each of the stands. These percentage values can be compared with the monthly averages shown in table 5.5 for the ground level diazo paper sensor (z_1). Table 5.8 compares the spot measurements from the quantum sensor with the monthly averages derived from the integrating diazo paper technique. The absolute percentage difference provides an indication of the variability of irradiance beneath the canopies. With the exception of *L. decidua* in May, there is comparatively little difference between the two sets of data. The large differences between the spot measurements and the integrated diazo paper sensor value for *L. decidua* are largely due to sampling errors. At the time of measurement the stand was more or less devoid of foliage and hence the major part of the irradiance sampled by the quantum sensor was direct beam. The difficulties of sampling direct beam irradiance beneath forest canopies are

Table 5.7: Summary of observations for 400-700 nm irradiance (P.A.R.) incident above canopy (Q_o) and beneath canopy (Q) for the three exotic stands on Trig E. All measurements made with quantum sensors (LAMBDA, Nebraska) during clear sky conditions.

date	time of day (hrs)	forest species	mean irradiance n = 20 readings		
			Q_o ($\mu Em^{-2}s^{-1}$)	Q ($\mu Em^{-2}s^{-1}$)	100 Q/Q_o (%)
24/3/82	1200	*P.contorta*	1584.7	24.0	1.51
		P.menziesii	1588.3	6.9	0.434
		L.decidua	1592.3	87.5	5.5
	1300	*P.contorta*	1577.3	18.37	1.16
		P.menziesii	1571.6	8.5	0.54
		L.decidua	1563.5	66.75	4.27
	1500	*P.contorta*	1154.7	13.8	1.19
		P.menziesii	1156.9	7.37	0.637
		L.decidua	1157.8	44.5	3.84
06/5/82	1500	*P.contorta*	561.5	5.83	1.03
		P.menziesii	564.8	4.3	0.761
		L.decidua	566.9	35.1	6.19
25/5/82	1200	*P.contorta*	840.9	13.22	1.58
		P.menziesii	906.37	4.82	0.531
		*L.decidua**	904.1	426.25	47.19
	1400	*P.contorta*	758.4	15.25	2.01
		P.menziesii	741.6	4.9	0.663
		*L.decidua**	715.1	275.0	38.44

*no foilage present at time of measurement

Table 5.8: Comparing 400-700 nm irradiance received (Q) relative to that above the canopy (Q_o) for the spot measurements with the quantum sensors (LAMBDA, Nebraska) and the monthly average derived from the ammonia diazo paper sensors (see table 5.5).

date	time of day (hrs)	forest species	100 Q/Q_o quantum sensor (%)	100 Q/Q_o monthly average from diazo sensors (%)	absolute difference (%)
24/3/82	1200	*P.contorta*	1.51	1.6	- 0.09
		P.menziesii	0.434	0.6	- 1.66
		L.decidua	5.5	5.0	- 0.5
	1300	*P.contorta*	1.16	1.6	- 0.44
		P.menziesii	0.54	0.6	- 0.06
		L.decidua	4.27	5.0	- 0.73
	1500	*P.contorta*	1.19	1.6	- 0.41
		P.menziesii	0.637	0.6	- 0.037
		L.decidua	3.84	5.0	- 1.16
06/5/82	1500	*P.contorta*	1.03	2.0	- 0.97
		P.menziesii	0.761	1.1	- 0.339
		L.decidua	6.19	11.0	- 4.81
25/5/82	1200	*P.contorta*	1.58	2.0	- 0.42
		P.menziesii	0.531	1.1	- 0.569
		L.decidua	47.19	21.2	+25.9
	1400	*P.contorta*	2.01	2.0	+ 0.01
		P.menziesii	0.663	1.1	- 0.437
		L.decidua	38.44	21.2	+17.24

immense, as discussed in section 1.3.2.

In summary, the photo-electrical measurement of quantum flux made above and beneath the canopies, are of limited use apart from providing a comparison with the diazo paper method. Little is known about the variability of irradiance within the canopies because measurements were only made above and below canopy.

CHAPTER SIX

IRRADIANCE AND STAND ARCHITECTURE

6.1 INTRODUCTION

From the discussion of stand architecture (chapter four) and stand light interception (chapter five), it was determined that differences and similarities occurred between the four forest species studied.

The analysis of stand architecture made reference to such factors as : foliage biomass (leaf area) and its spatial distribution; stem-branch configuration; foliage orientation and structure; and canopy closure as interpreted from photographs of the canopy from beneath.

In the analysis of light interception, it was determined that the penetration of irradiance into a canopy depends on many factors, including the source distribution and intensity of irradiance above the canopy, and the conditions within the canopy, as well as on the wavelength of the irradiance. Seasonal variations in light interception were shown to be related to changes in earth-sun geometry and forest structure (phenology).

Knowledge of leaf area, its spatial distribution within the crown, and its geometry can be useful in many ways, including estimation of plant productivity, and in the study of gas exchange. Furthermore, to predict the photosynthesis of leaves

at a certain position in the crown requires a knowledge of the irradiance reaching the leaves and of the corresponding physiological responses of the leaves (Norman and Jarvis, 1974).

In this chapter, the relationships between irradiance interception, as derived from the diazo paper sensors (chapter five), and vertical canopy architecture (chapter four) are considered in detail. The discussion is combined with details of the physiological characteristics of the leaves, for example : light saturation (Q_{sat}) and compensation (Q_c) levels, and photosynthetic rates (P). The analysis concentrates on the observations made in late summer (February/March); at this time foliage biomass would have been nearing its maximum for the season.

6.2 LIGHT INTERCEPTION AND CROWN ARCHITECTURE IN LATE SUMMER (FEBRUARY/MARCH)

6.2.1 General Characteristics

Figures 6.1 - 6.4 illustrate the interception of 400-700 nm irradiance (P.A.R.) within the four stands in late summer. The curves are drawn from the mean values derived from the diazo paper sensors for February and March (see table 5.5 and appendix 2). Combined with the light absorbance curves are details of total surface leaf area and its approximate spatial distribution within the crown (taken from the data in table 4.4).

(a) *Pinus contorta*

The absorption of 400-700 nm irradiance (P.A.R.) within the *P. contorta* stand is gradual throughout the entire crown,

especially considering the large total surface leaf area (figure 6.1). The reasons for this particular pattern relate to the architecture of the canopy. The main architectural characteristics which explain the light absorbance curve are as follows:

(i) a large crown length (6.8 metres) and therefore a well-spread layer of foliage in the vertical;

(ii) a stem-branch configuration (figure 4.1) which is orientated towards the vertical at all depths within the crown; and

(iii) in combination with the upward branch configuration, a foliage orientation which is also towards the vertical (plate 4.5).

As a result of the above characteristics, the *P. contorta* stand is able to absorb significant amounts of irradiance throughout the entire crown over a large total surface leaf area (figure 6.1).

(b) *Pseudotsuga menziesii*

The absorption of 400-700 nm irradiance (P.A.R.) within the *P. menziesii* stand is rapid throughout the entire crown (figure 6.2). As for *P. contorta*, the reasons for this particular pattern are related to the architectural characteristics of the canopy. In summary the main characteristics are as follows:

(i) a stem-branch configuration (figure 4.2) which is orientated towards the horizontal through most of the crown, except for the immediate top branches; and

(ii) in combination with the horizontal branch configuration, a foliage orientation which is also towards the horizontal (plate 4.6).

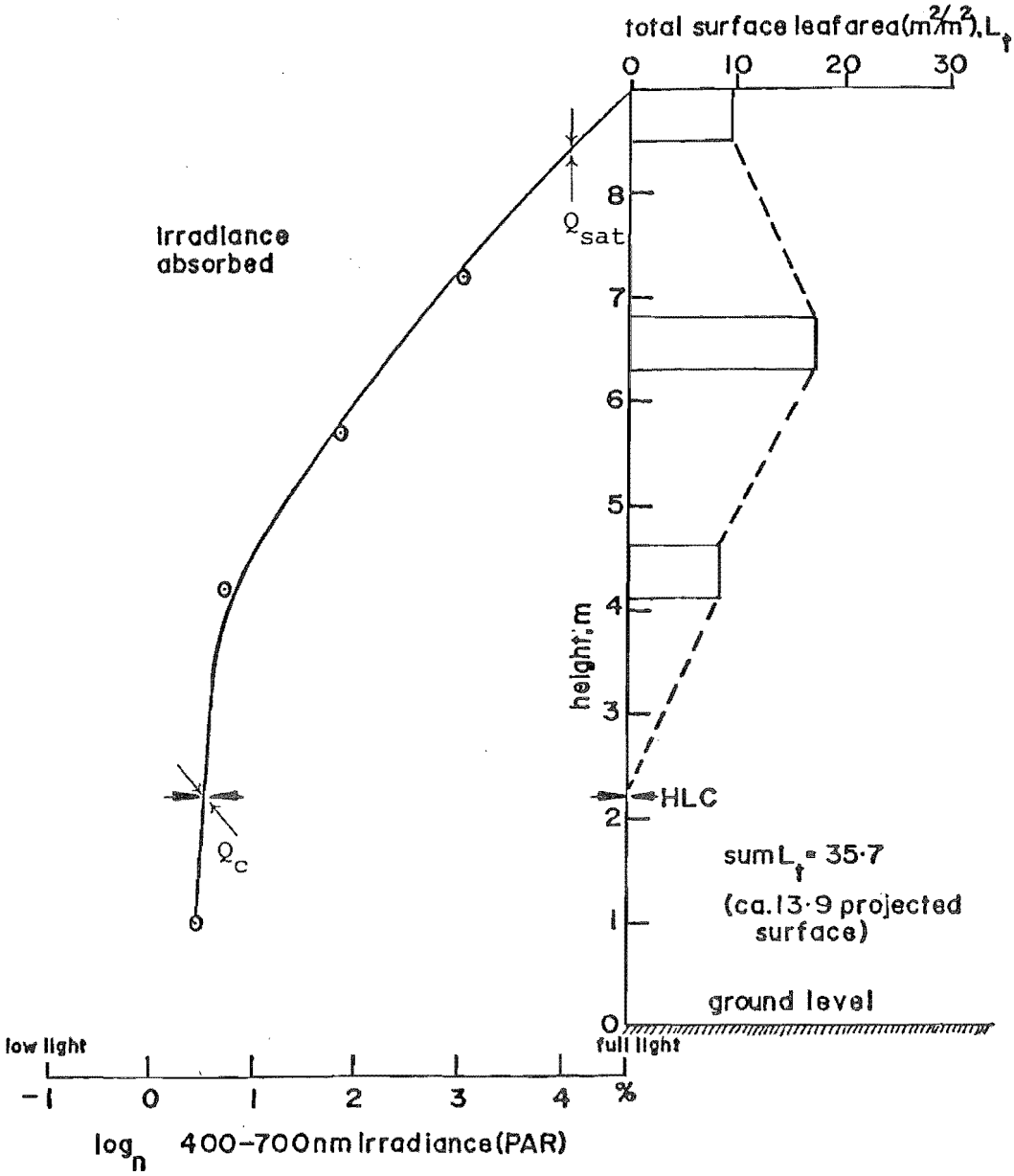

Figure 6.1: Total surface leaf area, L_t (m^2/m^2) and its approximate distribution in the crown of the *Pinus contorta* stand in late summer (biomass data after Bénecke and Nordmeyer, 1982). Absorbance of 400–700 nm irradiance (P.A.R.) as measured by ammonia diazo paper technique : mean of February and March data shown by curve.

HLC = height to base of living crown
Q_{sat} = light saturation point
Q_c = light compensation point (see text for details)

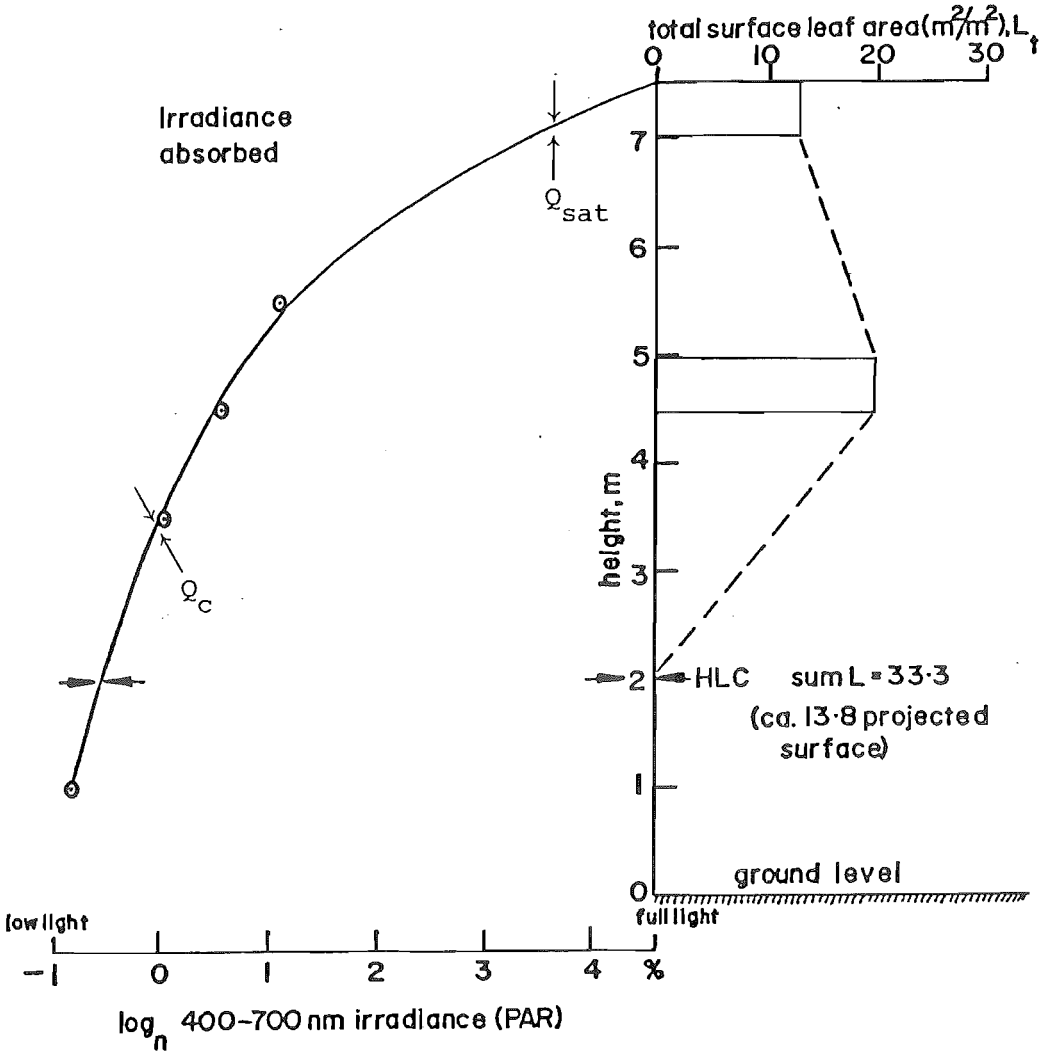

Figure 6.2: Total surface leaf area, L_t (m^2/m^2) and its approximate distribution in the crown of the *Pseudotsuga menziesii* stand in late summer (biomass data after Ledgard, pers.comm.) Absorbance of 400-700 nm irradiance (P.A.R.) as measured by ammonia diazo paper technique : mean of February and March data shown by curve.

HLC = height to base of living crown
Q_{sat} = light saturation point
Q_c = light compensation point (see text for details)

The *P. menziesii* canopy gives the appearance of being very dense (plate 4.9) in comparison with the *P. contorta* canopy (plate 4.8), even though it has a slightly smaller total surface leaf area. It is undoubtedly the vertical structure of the canopy which explains these differences. A horizontal orientation, as shown by *P. menziesii* has a greater effect on penetrating irradiance than a more vertical orientation, as shown by *P. contorta*. It is because of their similar total surface leaf areas and their markedly different light absorption curves that *P. contorta* and *P. menziesii* make for an interesting comparison.

(c) *Larix decidua*

The absorption of 400-700 nm irradiance (P.A.R.) in the *L. decidua* stand (figure 6.3) is similar to that for *P. contorta* (figure 6.1) except that it is more gradual. However, *P. contorta* has nearly three times the leaf area of *L. decidua*, yet its canopy has only slightly more effect on penetrating irradiance. The main architectural characteristics which explain the light absorbance curve in *L. decidua* are as follows:

(i) a stem-branch configuration (figure 4.3) which is orientated towards the horizontal through most of the crown, except for the immediate upper branches;

(ii) a relatively large crown length (4.8 metres) over which the foliage is evenly distributed; and

(iii) a small total surface leaf area index (12.5 m^2/m^2), in comparison with the other stands.

The horizontal stem-branch configuration for *L. decidua* is similar to that found for *P. menziesii* (figure 6.2) and *N. solandri*

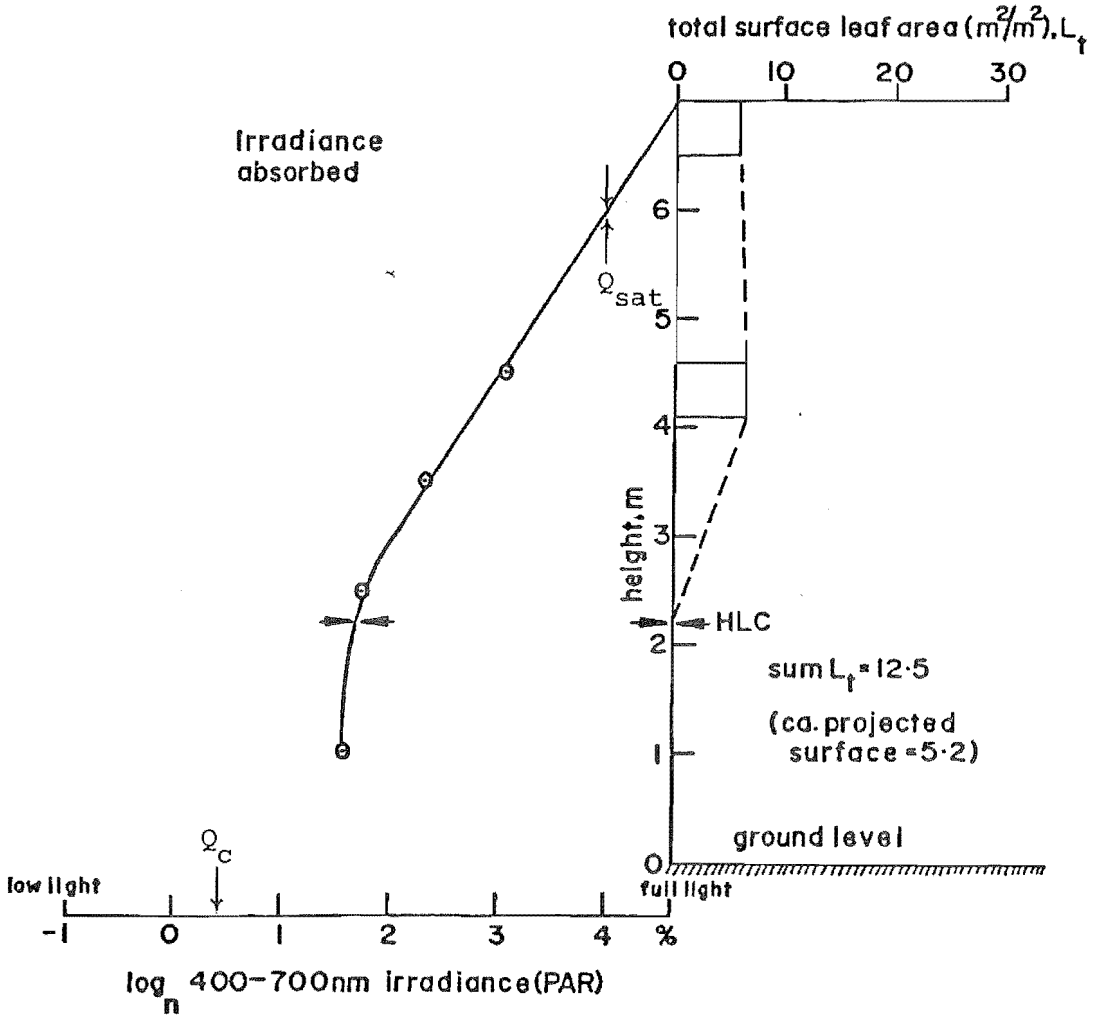

Figure 6.3: Total surface leaf area, L_t (m^2/m^2) and its approximate distribution in the crown of the *Larix decidua* stand in late summer (biomass data after Ledgard, pers.comm.). Absorbance of 400-700 nm irradiance (P.A.R.) as measured by ammonia diazo paper technique : mean of February and March data shown by curve.

HLC = height to base of living crown
Q_{sat} = light saturation point
Q_c = light compensation point (see text for details)

(figure 6.4). However, the main reason why the *L. decidua* canopy is so well illuminated is because of the small total surface area of foliage, and the reasonably large crown-length over which this foliage is evenly distributed.

(d) *Nothofagus solandri*

The absorption of 400-700 nm irradiance (P.A.R.) within the upper crown of the *N. solandri* stand (figure 6.4) is similar to that for *P. menziesii* (figure 6.3). The absorption of irradiance is rapid in the upper crown and more gradual in the middle and lower crown. The main factors affecting the light absorbance in the *N. solandri* stand are:

(i) a narrow crown length (3.3. metres) and therefore a concentrated layer of foliage in the upper-crown (figure 6.4);

(ii) a stem-branch configuration (figure 4.4) which is orientated towards the horizontal through most of the crown, except for the immediate upper branches; and

(iii) in combination with the horizontal branch configuration, a foliage orientation which is also towards the horizontal (plate 4.7).

In terms of foliage distribution, the *N. solandri* stand has an asymmetrical pattern with a marked concentration in the upper crown. This, in combination with the factors listed above, explains why most of the penetrating irradiance is absorbed in the immediate upper crown.

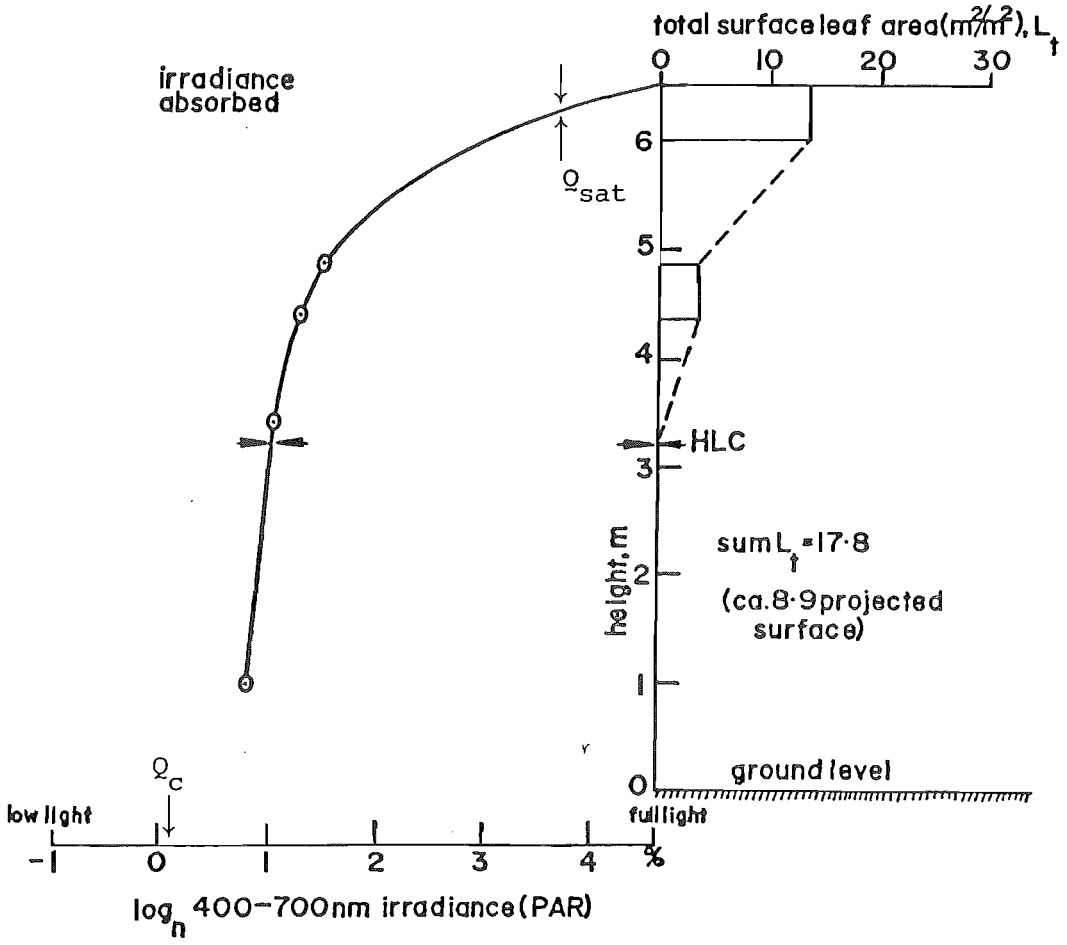

Figure 6.4: Total surface leaf area, L_t (m^2/m^2) and its approximate distribution in the crown of the *Nothofagus solandri* stand in late summer (biomass data after Benecke and Nordmeyer, 1982). Absorbance of 400-700 nm irradiance (P.A.R.) as measured by ammonia diazo paper technique : mean of February and March data shown by curve.

HLC = height to base of living crown
Q_{sat} = light saturation point
Q_c = light compenstion point (see text for details)

6.2.2 Light Saturation and Compensation Levels

(a) Background

In section 1.2.3(b) the relationship between net photosynthesis (P) and light intensity (Q) is shown by a saturating curve (figure 1.5). The curve has two important characteristics light saturation point (Q_{sat}) and light compensation point (Q_c). At Q_{sat} net-photosynthesis reaches its maximum rate (P_{max}), and at Q_c net-photosynthesis is balanced by respiration (R).

Q_{sat} and Q_c are strongly influenced by temperature. At lower temperatures (not below 0^oC) Q_{sat} and Q_c levels (μmol photons $m^{-2}s^{-1}$) are generally lower than at higher temperatures, because the rate of respiration (or CO_2 loss) increase with temperature. Figure 4 in Benecke and Havranek (1980b) illustrates the relationship between irradiance, temperature and net-photosynthesis. The diagram clearly shows how net-photosynthesis reaches a maximum rate when the temperature is at or near 19^oC. This is the optimum temperature for net CO_2 uptake for most temperate tree species. For the purposes of this study, the optimal temperature range for photosynthesis is given as $16-22^oC$.

As briefly discussed in section 1.2.2(b), sun and shade foliage have morphological and physiological differences. Sun leaves are generally thicker and the chloroplasts are more loosely distributed through several layers of palisade cells. In contrast, shade leaves are generally thinner and the chloroplasts are concentrated into a thin layer near the upper surface of the leaf. A paper by Lewandowska *et al* (1977), illustrates

the important differences between sun and shade foliage in a *Picea sitchensis* (Sitka Spruce) forest. They conclude, that the larger specific leaf area and smaller dry weight fraction of the needles at the bottom of the canopy than at the top, indicate morphological changes during needle development which have resulted in larger but thinner needles with thinner cell walls and less dense cells (Lewandowska *et al* 1977, p 127). Thus, needles in different parts of the canopy emerge and grow in very different light regimes and are, as a result, morphologically and anatomically different.

Because of their differing morphology and physiology, sun and shade foliage will show differing responses to light. Light saturation and compensation levels will vary depending on where the foliage has developed within the crown. Sun foliage receives diffuse irradiance from the whole sky and direct irradiance from a large section of the sky, and in any plant canopy most light reaching the lower levels comes from angles near the vertical, and one would therefore expect shade foliage to be structually and physiologically acclimatized to make the most effective use of this light in photosynthesis. (Leverenz and Jarvis, 1980, p 67).

(b) Light saturation within the four stands

Using mean daily maximum temperatures from the long-term record for Craigieburn Forest meteorological site (table 2.1), the months December-March were chosen because they have values within the optimal range for photosynthesis (16-22^{o}C). Radiation levels are also at their highest over the summer months.

Table 6.1 provides a summary of saturating irradiance levels (μmol photons $m^{-2}s^{-1}$) for sun foliage, when the temperature is within the optimal range.

Table 6.1: Saturating irradiance (Q_{sat}) when the temperature is within the optimal range (16-22°C) for sun foliage (μmol photons $m^{-2}s^{-1}$)

forest species	Q_{sat} (16-22°C) (μmol photons $m^{-2}s^{-1}$)*	reference
Larix decidua	1000	Benecke *et al* (1981)
Pinus contorta	1100	Benecke and Nordmeyer (1982)
Pseudotsuga menziesii	800	Leverenz (1981a, b)
Nothofagus solandri	850	Benecke and Nordmeyer (1982)

*μmol photons $m^{-2}s^{-1}$ = μEm$^{-2}s^{-1}$

As discussed in the previous section, sun and shade foliage have different light saturation levels. For purposes of illustration Q_{sat} values are given for sun foliage, because sun foliage dominates the upper-crown, which is likewise affected by higher levels of irradiance than the more shaded lower-crown.

Under conditions of optimum temperature *L. decidua* and *P. contorta* have similar light saturation levels, and in contrast, the levels for *N. solandri* and *P. menziesii* are lower (table 6.1).

The light saturation levels (Q_{sat}) for the four species appear to be valid in terms of the light absorbance curves for the stands (figures 6.1 - 6.4). The *P. contorta* and *L. decidua* stands both exhibit a gradual absorption of irradiance through their crowns (figures 6.1 and 6.3). As shown in table 6.1, both

these species require fairly high levels of irradiance to reach saturation point. In contrast, the *P. menziesii* and *N. solandri* stands experience a more rapid absorption of irradiance through their crowns (figures 6.2 and 6.4). As shown in table 6.1, both these species have lower Q_{sat} levels and are therefore more tolerant to lower light conditions than *P.contorta* and *L. decidua*.

(c) Light compensation within the four stands

Light compensation point (Q_c) in a similar way to light saturation point (Q_{sat}) is temperature dependent. As for Q_{sat}, the Q_c values presented in this section are for the optimal temperature range (16-22°C). Table 6.2 provides a summary of compensating irradiance levels (µmol photons $m^{-2}s^{-1}$) for shade foliage, when the temperature is within the optimal range.

Table 6.2: Compensating irradiance (Q_c) when the temperature is within the optimal range (16-22°C) for shade foliage (µmol photons $m^{-2}s^{-1}$)

forest species	Q_c (16-22°C) (µmol photons $m^{-2}s^{-1}$)*	reference
Larix decidua	29	Mattyssek (1981)
Pinus contorta	30	Benecke (pers. comm.)
Pseudotsuga menziesii	18**	
Nothofagus solandri	20	Benecke (pers. comm.)

*µmol photons $m^{-2}s^{-1}$ = µEm $^{-2}s^{-1}$

**estimated using the ratio of Q_{sat}(sun) : Q_c(shade) = 42.5 observed for *N. solandri*, as Q_{sat} value for *N. solandri* is similar to *P. menziesii* (table 6.1). Reliable data for *P. menziesii* was not available in the literature.

For purposes of illustration Q_c values are given for shade foliage, because shade foliage dominates the lower crown, and because light levels are generally lower in this region of the crown.

As found for light saturation (Q_{sat}) levels, light compensation (Q_c) levels for *P. contorta* and *L. decidua* are similar, and as expected the Q_c levels for *P. menziesii* and *N. solandri* are lower (table 6.2).

The Q_c levels for the four species, as with the Q_{sat} levels, relate well with their light absorbance curves (figures 6.1 - 6.4). *P. contorta* and *L. decidua*, which share similar light absorbance curves, have higher Q_c levels in comparison with *P. menziesii* and *N. solandri* which appear to be more tolerant to lower light levels (table 6.2).

(d) Photosynthetic rates for the forest species

The maximum rate of net-photosynthesis (P_{max}), when temperature, CO_2 concentration, and water level are non-limiting, occurs when irradiance reaches saturation point (Q_{sat}). As irradiance declines, net-photosynthesis (P) also declines until irradiance compensation point (Q_c) is reached. At light levels below Q_c, light respiration (R) exceeds photosynthesis (P).

Maximum photosynthetic rates, given the optimal conditions described above, for the four forest species are presented in table 6.3. The rate of CO_2 uptake is given on a total surface area basis ($\mu mol\ m^{-2}s^{-1}$). Separate rates are given for sun

Table 6.3: Maximum rate of net-photosynthesis (P_{max}, µmol CO_2 $m^{-2}s^{-1}$) obtained near optimum temperature (19°C) with light non-limiting (Q_{sat}) for the four forest species. (Total surface areas given, except where indicated.)

(a) Sun-foliage

forest species	P_{max} (µmol $m^{-2}s^{-1}$)*	reference
Larix decidua	4.9	Benecke and Havranek (1980b)
Pinus contorta	5.0	Benecke and Nordmeyer (1982)
Nothofagus solandri	5.1	Benecke and Nordmeyer (1982)

(b) Shade-foliage

forest species	P_{max} (µmol $m^{-2}s^{-1}$)	reference
Larix decidua	3.5	Matyssek (1981)
Pinus contorta	4.1	Benecke and Nordmeyer (1982)
Nothofagus solandri	3.5	Benecke and Nordmeyer (1982)

(c) mean for all foliage

forest species	P_{max} (µmol $m^{-2}s^{-1}$) (all surfaces)	P_{max} (mol $m^{-2}s^{-1}$) (projected surface)
Larix decidua	4.2	9.5
Pinus contorta	4.5	11.5
Nothofagus solandri	4.3	8.6
Pseudotsuga menziesii	2.1	4.8**

*µmol $m^{-2}s^{-1}$ = 0.63 mg $dm^{-2}h^{-1}$
**from Leverenz (1981a).

and shade foliage, except for *P. menziesii* where only a mean rate for all foliage is given, because separate values for sun and shade foliage were not available.

With the exception of *P. menziesii*, the mean maximum photosynthetic rates (P_{max}) are relatively similar (4.2 - 4.5 μmol $m^{-2}s^{-1}$). Several authors (e.g. Larcher 1969, Sestak *et al* 1971, Schulze *et al* 1977a, b, c, and Fry and Phillips 1976, 1977) claim that evergreen trees appear to have lower rates of photosynthesis than those shown by deciduous species. This suggests that the potentially longer period for photosynthesis in evergreen species compensates for their lower photosynthetic capacity. However, the above authors have generally given photosynthetic rates on a foliage weight rather than a total area basis. In table 6.3, it is shown that the mean maximum rate of P_{max} for *L. decidua* is slightly less than that for *P. contorta*. Using the mean surface area to weight ratios from table 4.3, the rate for *L. decidua* becomes 19.7 mg CO_2 $g^{-1}hr^{-1}$, and *P. contorta* becomes 8.7 mg CO_2 $g^{-1}hr^{-1}$. On a weight basis, the photosynthetic rate for *L. decidua* is almost double that for *P. contorta*. This is because *L. decidua* has a higher surface area to weight ratio (cm^2/g) than the other species (see section 4.2.2(b)).

The mean P_{max} for all surfaces given for *P. menziesii* is very low compared with the other species (table 6.3). The amount of literature on the subject of gas-exchange in the field for *P. menziesii* is small. The value given in table 6.3 of 4.8 μmol $m^{-2}s^{-1}$ on a projected area basis was taken from

Leverenz (1981a) who was working with excised shoots. It should be noted however, that *P. menziesii* is hypostomatous (stomata on the underside of the needle only). With the exception of *N. solandri*, the other species are amphistomatous (stomata on all surfaces of the needle). If one compares the projected surface value (one-side only) for *P. menziesii* with the values for all surfaces for the remaining species, then the difference is considerably less (table 6.3). Without any other reliable reference for photosynthetic rates for *P. menziesii* it is difficult to determine whether the value given by Leverenz (1981a) for excised foliage is of any use. The fact that *P. menziesii* is hypostamatous may serve to explain why its maximum photosynthetic rates (for total surface area) are lower than the other species. However, *N. solandri* is also hypostamatous and its maximum photosynthetic rate for a projected leaf area is still significantly higher than *P. menziesii* (table 6.3).

(e) A simple model of canopy photosynthesis

Using the data for light saturation (Q_{sat}) and compensation (Q_c) levels (tables 6.1 and 6.2), an optimum temperature range of 16-22°C, and the light absorbance curves for the four stands (figures 6.1 - 6.4) a simple empirical model for canopy photosynthesis is presented. The model uses the mean daily maximum temperatures for December-March (table 2.1) and holds the assumption that at the time of maximum temperature irradiance would be at or near its maximum, and that CO_2 concentration and water availability are non-limiting. For irradiance in the open a mean flux density of 1800 μmol photons $m^{-2}s^{-1}$ is suggested. The Q_{sat} values from table 6.1 and Q_c values from

table 6.2 are applied to the model. Details are illustrated in table 6.4.

Table 6.4: Light saturation (Q_{sat}) and compensation (Q_c) for the four species expressed as a percentage of 1800 µmol photons $m^{-2}s^{-1}$ (Q_o) at a temperature at or near optimum (19°C)

forest species	irradiance within the crown (µmol photons $m^{-2}s^{-1}$) Q_{sat}	Q_c	100 Q_{sat}/Q_o (%)	100 Q_c/Q_o (%)
Larix decidua	1000	29	55.5 (4.0)	1.6 (0.47)
Pinus contorta	1100	30	61.1 (4.1)	1.6 (0.5)
Pseudotsuga menziesii	800	18	44.4 (3.7)	1.0 (0)
Nothofagus solandri	850	20	47.2 (3.8)	1.1 (0.1)

( ) = Log_n %

If irradiance incident upon the top of the canopy (Q_o) is taken to be 1800 µmol photons $m^{-2}s^{-1}$ and temperature is within the optimal range (16-22°C), then by using the Log_n % values from table 6.4 and applying these to the light absorbance curves (figures 6.1 - 6.4), a simple model of canopy photosynthesis is proposed.

In the *L. decidua* canopy, given the conditions set out in the model, it appears that all the foliage in the crown would have been experiencing light levels above compensation point. From figure 6.3 it is clearly evident that Q_c would occur at a much lower level than that given by the general light absorbance curve. Light levels are relatively high beneath

the canopy and this may explain why there is a considerable ground flora present beneath the stand.

In the *P. contorta* canopy Q_c occurs at almost the same position as the base of living crown (figure 6.1). This suggests, that all the foliage above the HLC position is illuminated above compensation point, when the conditions of the model are met.

In the *P. menziesii* canopy Q_c occurs just below the height of the bottom sensor, some one and a half metres above the base of the living crown. However, as figure 6.2 illustrates, the greatest amount of foliage in the crown occurs above this point.

The *N. solandri* canopy, like the *L. decidua* canopy, experiences levels of irradiance above compensation point throughout its entire crown (figure 6.4). Although no ground flora is present beneath this stand there is some living foliage present beneath the main crown. It is possible that *N. solandri* seedlings could grow in some sites beneath this canopy, but conditions would be very marginal for growth.

A tentative estimate of net-photosynthesis (P) for the four stands is given in table 6.5. Values are given as μmol CO_2 ~~evolved~~ produced s^{-1}/m^2 ground area. The values presented are merely estimates and should not be taken as absolute because of the crude methods used to derive them. It is the relative differences between the species that are important.

Table 6.5: A tentative estimate of net-photosynthesis (μmol CO_2 s^{-1}/m^2 ground area) for the four forest stands, at a temperature within the optimal range (16-22°C) and an above canopy irradiance flux of 1800 μmol photons $m^{-2}s^{-1}$.

forest species	total surface leaf area (L_t) illuminated at or above compensation points (Q_c) (m^2/m^2)	mean photosynthetic rate ($\bar{P}$)* (μmol $m^{-2}s^{-1}$)	net-photosynthesis (P) (μmol s^{-1}/m^2 ground area)
Larix decidua	12.5	2.45	30.6
Pinus contorta	35.0	2.5	87.5
Pseudotsuga menziesii	26.0	2.1	54.6
Nothofagus solandri	17.8	2.55	45.4

*derived by taking the mean of P_{max} (sun foliage) and P = 0 (compensation point), except for *P. menziesii* where mean P_{max} was used.

From the data presented in table 6.5 it appears that the *P. contorta* canopy has the greatest rate of photosynthesis per unit area of ground. This relates primarily to its ability to absorb irradiance over a large total surface leaf area.

For *P. mensiesii* the estimate of net-photosynthesis per unit ground area falls somewhat short of that for *P. contorta*, but is very similar to that for *N. solandri* (table 6.5). It is interesting to note that both these canopies share similar light absorbance curves and generally horizontally orientated foliage. However, *P. menziesii* has a greater leaf area than *N. solandri*, but as is shown in table 6.5, out of a total surface area of 33.3 m^2/m^2 only 26 m^2/m^2 is illuminated at or above Q_c, whereas all the *N. solandri* canopy is illuminated above Q_c.

The *L. decidua* canopy has the lowest estimate of net photosynthesis per unit ground area, and this is most likely because of its low total surface leaf area (table 6.5). As is shown by its light absorbance curve (figure 6.3), the open nature of the crown allows high levels of irradiance to penetrate through to the ground. Because of this, the mean photosynthetic rate ($\bar{P}$) in table 6.5 is perhaps a little low and could be weighted to fit in with the light absorbance curve. However, if $\bar{P}$ is increased to 3.0 μmol $m^{-2}s^{-1}$, net-photosynthesis is only 37 μmol s^{-1}/m^2 ground, some 8.4 less than that for *N. solandri*.

6.3 EXTINCTION COEFFICIENTS (K) FOR THE STANDS

In section 1.2.2(d) the discussion focused on the theoretical relationships between irradiance and stand architecture. According to the Monsi and Saeki (1953) simple negative exponential formula, the relative light intensity incident above a plant stand (Q_o) decreases exponentially as the downward cumulative projected leaf area index (L) increases through the canopy (equation 1.6). The Monsi and Saeki (1953) model assumes that the distribution of foliage is random throughout the canopy.

In this section extinction coefficients (K) are presented for the four stands using light data from the diazo paper sensors and projected leaf areas from table 4.4. The light data is the mean of the observations for February and March (see table 5.5 and appendix 2). Table 6.6 provides a summary of observations

for the four stands, and K was calculated by using equation 1.7. A high K value (e.g. K = 1.0) suggests that for a given leaf area (L) a small amount of irradiance passes through the canopy. In contrast, a low K value (e.g. K = 0.2) suggests that for a given leaf area (L), a large amount of irradiance passes through the canopy (for details see section 1.2.2(d)).

Table 6.6: Extinction coefficients (K) for the four stands (February/March average). Values given for the total canopy. Irradiance above canopy Q_o = 100%.

forest species	irradiance (Q) received below the canopy (%)	projected leaf area index L (m^2/m^2)	extinction coefficient (K)
Pinus contorta	1.62	13.9	0.30
Pseudotsuga menziesii	0.42	13.8	0.40
Larix decidua	4.76	5.2	0.58
Nothofagus solandri	2.28	8.9	0.42

Table 6.6 and figure 6.5 illustrate total-crown extinction coefficients (K) for the four stands. Figure 6.5 shows how the K values range from 0.3 - 0.58. The extinction coefficient for *P. contorta* is the lowest, which suggests that for its given leaf area the canopy allows a greater transmission of irradiance than the other stands. *P. menziesii* has a similar leaf area, but its extinction coefficient is higher, implying that the canopy has a greater effect on transmitting irradiance. *N. solandri* has a similar extinction coefficient to *P. menziesii*, but it has a smaller leaf area. In consequence, the K value is

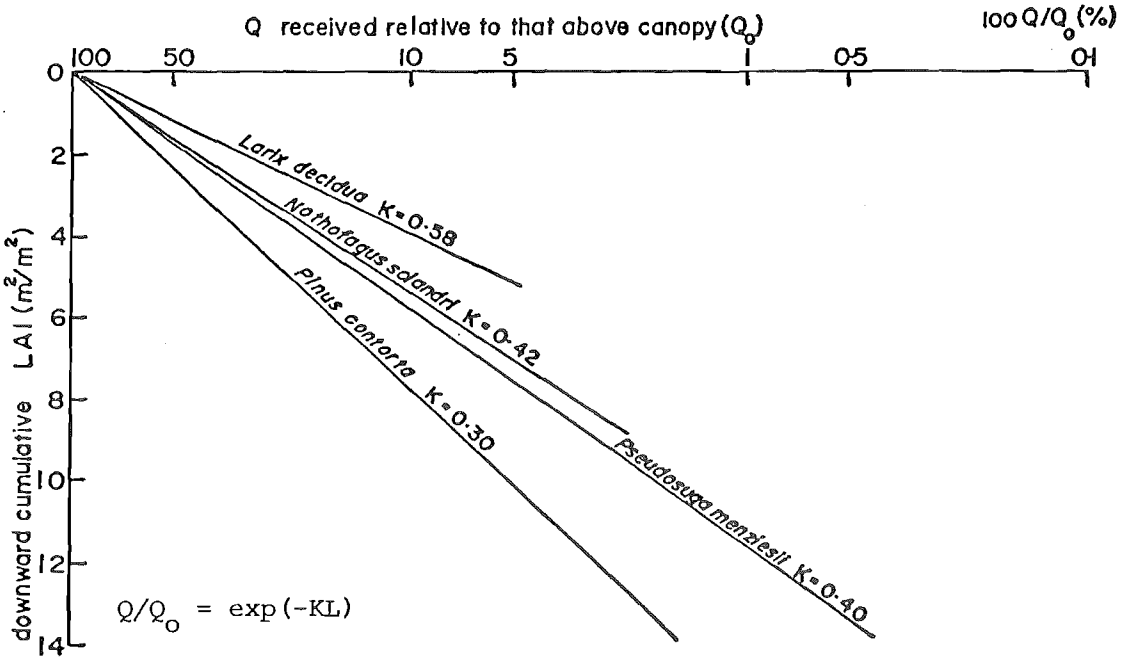

Figure 6.5: The exponential decrease of 400-700 nm irradiance (P.A.R.) in the different forest stands as a function of projected leaf area index (L).

K = extinction coefficient

a little higher. The extinction coefficient for *L. decidua* is a response to its small leaf area and its attenuation of light.

The relationship between the extinction coefficients for the stands (figure 6.5) are very similar to those given in the simple model of canopy photosynthesis (table 6.5). The *P.contorta* canopy allows the greatest transmittance of irradiance through its canopy over the largest leaf area (figure 6.5). In table 6.5, its estimate for net-photosynthesis was the highest for the four stands.

P. menziesii and *N. solandri*, which share similar extinction coefficients (figure 6.5), likewise share similar estimates for net-photosynthesis (P). *P. menziesii* has a slightly greater estimate for P, and in turn has a slightly smaller K value.

The *L. decidua* canopy has the highest extinction coefficient (figure 6.5), and from table 6.5 its estimate for net-photosynthesis is the lowest for the four stands.

In summary, from the extinction coefficients shown in figure 6.5, the *P. contorta* stand makes undoubtedly the most efficient use of light within its crown over the largest leaf area. The low K value is likely to be related to the architecture of its canopy - more especially the more vertical geometry of its light receiving surfaces. The *P. menziesii* stand falls someway behind *P. contorta* as the most efficient user of light. The intermediate position of this stand, which is also shared by *N. solandri* (figure 6.5 and table 6.5) can be related to the

more horizontal geometry of their light receiving surfaces. The *L. decidua* stand has a high K value because it is a light demanding species. Large accumulations of foliage are not possible because of its deciduous habit and its need for high light levels.

CHAPTER SEVEN

CONCLUSION

7.1 SUMMARY

7.1.1 The Objectives

With reference to the main aim of this thesis, stated in chapter one, it is evident that a better understanding of the radiation regime within the crown of different forest stands has been achieved.

In respect to the specific objectives proposed, it can be said, that a simple, inexpensive method was developed which proved useful for measuring irradiance in forests. It is also evident, that by choosing stands with different architecture that the light climate measured within the stands is undoubtedly a function of their architecture. A further objective, to assess the effects of changes in earth-sun geometry and forest structure on the radiation regimes in the stands, has been demonstrated through field measurements from February to June. The final objective called for tentative estimates of carbon uptake in the crown of the forest stands. In an attempt to assess the ability of the various stands to absorb carbon, a simple model of canopy photosynthesis was developed, using light absorbance and canopy architectural characteristics.

7.1.2 The Methods

Most of the results presented in this thesis were derived from the relatively new ammonia diazo paper technique, with

photo-electrical and thermo-mechanical measurements being made with various instruments, mainly for cross-reference purposes. Considerable attention was given to the calibration of the diazo paper with the wavelengths used (P.A.R. and S.W.). From the calibration procedures discussed in chapter three, it is clearly evident that the relationship between number of papers exposed and irradiance received is logarithmic and the high correlation coefficient illustrates the utility of the method.

In using this technique it is essential, however, to ensure that the diazo paper is carefully calibrated in the light environment in which it is intended for use. In this study, separate calibration functions have been derived for each stand, and for different positions within the crown. The diazo paper was calibrated in March and later in May and June so as to allow for the chemical change in the paper that occurs over time. An improvement was made over the previous method of comparing the partially exposed papers with a graded strip. In this study the analysis of these papers was more objective because a reflectometer was used.

The method of placing diazo paper sensors within the canopies was simple and inexpensive. There were no problems with sensors being removed during high winds and the utility of the Velcro tape allowed the sensors to be changed quickly each week. Similarly, because of the fairly dry conditions in the field area there were little problems with moisture affecting the diazo paper, which can be a problem in some areas.

As a method for the long-term measurement of irradiance within forests the ammonia diazo paper technique is of considerable use. The diazo paper sensors are simple and inexpensive to manufacture, and provided the paper is calibrated in the light environment in which it is intended for use, there appears to be no major disadvantages. It is possible to overcome the problem of spatial variability in irradiance within forests by exposing replicate sensors, and because the diazo paper integrates over the long-term the problem of temporal variability in irradiance is also overcome to a large extent.

7.1.3 The Results

The results from the diazo paper measurements have shown that differences and similarities in the light absorbance curves for the four stands are related to their architectural characteristics. *P. menziesii* and *N. solandri* shared similar light extinction curves in their upper crowns because they both had horizontal receiving surfaces and similar leaf areas and distributions in the upper crown. The horizontal system of branches and foliage caused the absorption of irradiance to be rapid in the upper crown. The light extinction curve for *L. decidua* showed a very gradual absorption throughout the entire crown because it is a light demanding species and it therefore requires a well lit crown. The crown length was relatively large and the leaf area small and evenly distributed throughout the canopy. The *P. contorta* stand was found to be well adapted to absorbing significant amounts of irradiance throughout its entire crown over a large total leaf area. This ability is largely related to the more vertical orientation of its light

receiving surfaces. The upward inclination of its branches and foliage allows irradiance to filter through to greater crown depth than would otherwise occur if the inclination was horizontal. The greater crown length and hence the more spread out nature of its receiving surfaces are other key reasons why this species is able to absorb irradiance over a large leaf area.

Seasonal variations in the light regime of the forest stands were related to changes in earth-sun geometry and forest phenology. The *L. decidua* canopy showed the greatest seasonal change in its light regime because of its deciduous habit. In the remaining evergreen species it was discovered that the greatest changes occurred in the lower crown and trunk-space. The changes in the lower crown were related to net leaf loss in that region from early April onwards and also to lower solar elevation in the autumn. Changes in the upper crown were minimal because leaf loss would have been small and the effect of lower solar elevation less marked because of the more vertical orientation of the foliage in this region. As a result of its vertically orientated light receiving surfaces at all crown depths the light regime in the *P. contorta* canopy showed little seasonal variation. Some of the stands were affected by sidelight entering into the trunk-space and this was accepted as a problem associated with working in stands of limited size.

The simple model of canopy photosynthesis illustrates the relative differences between the four stands in terms of their ability to absorb irradiance over their leaf surfaces.

From the model, tentative estimates of net-photosynthesis per unit ground area were made for the four stands. *P. contorta* had the greatest net-photosynthesis per unit ground area among the four stands. It is suggested that this is a function of its crown architecture which enables it to absorb irradiance over a large leaf area. *P. menziesii* and *N. solandri* share similar estimates for net-photosynthesis, which are lower than *P. contorta*. The lowest estimate for net-photosynthesis per unit ground area was given for *L. decidua*, and it is suggested that the main reason for this low figure is because of its small leaf area.

Extinction coefficients (K) were given for the four stands using projected leaf area (L) and light absorbance data for February and March. The high extinction coefficients given for *L. decidua* (0.58) is a function of its small leaf area (L), and the low extinction coefficient given for *P. contorta* (0.30) is a function of its architecture, more specifically, its vertically orientated receiving surfaces. The remaining stands, *P. menziesii* and *N. solandri*, have extinction coefficients, which fall mid-way between *P. contorta* and *L. decidua*.

7.2 SUGGESTIONS FOR FURTHER RESEARCH

In this study, the ammonia diazo paper technique was used to measure irradiance within the canopy of several single-aged stands. Similarly, the technique was also used in a separate study to measure irradiance across the forest floor beneath a main canopy in the presence of regenerating trees. The method can be used by ecologists, botanists, foresters, and geographers for any research the requires the long-term

measurement of irradiance (i.e. longer than one week). Its use is not necessarily restricted to work in forests, as the technique has scope for use in herbaceous canopies, crops and grasslands.

The technique can be used in most situations, but in wetter areas there should be some action taken to prevent moisture from getting into the dishes and ruining the diazo paper. Some protection can be provided by placing a small quantity of silicon crystals in a cavity in the polystyrene beneath the diazo booklet in the petri dish (figure 3.2). In more extreme cases, a silicon seal should be used to prevent moisture from entering through the sides of the petri dish.

REFERENCES

AGNEW, A.D.G., and CAUSTON, D.R. (1982) A photochemical light meter suitable for ecological survey, Acta Oecologica Oecol. Plant., 3(17) no.1: 101-111.

ALLEN, L.H., and LEMON, J.R. (1976) Tropical rain forest. In: Monteith, J.L. (ed.). Vegetation and the Atmosphere, vol.2. Academic Press, London: 265-308.

ANDERSON, M.C. (1964a) Studies of the woodland light climate I : the photographic computation of light conditions. Journal of Ecology, 52: 27-41.

——————— (1964b) Studies of the woodland light climate II : seasonal variation in the light climate. Journal of Ecology, 52: 643-663.

——————— (1964c) Light relationships of terrestrial plant communities and their measurement. Biological Reviews, 39: 425-486.

——————— (1966a) Some problems of simple characterisation of the light climate in plant communities. In: Bainbridge, R., Evans, G.C., and Rackman, O. (eds.). Light as an Ecological Factor. Blackwell Scientific Publications: 77-90.

——————— (1966b) Stand structure and light penetration II : a theoretical analysis. Journal of Applied Ecology, 3: 41-54.

——————— (1970) Radiation climate, crop architecture and photosynthesis. In: Setlik, I. (ed.). Prediction and Measurement of Photosynthetic Productivity. Proceedings of the IBP/PP Technical Meeting, Trebon, 14-21 September 1969: 71-89.

——————— (1971) Radiation and crop structure. In: Sestak, Z., Catsky, J., and Jarvis, P.G. (eds.). Plant Photosynthetic Production: Manual of Methods. Dr. W. Junk n.v., The Hague: 412-467.

——————— (1981) The geometry of leaf distribution in some south-eastern Australian forests. Agricultural Meteorology, 25: 195-205.

ANON. (1956) Handbook of Meteorological Instruments, Part 1. H.M.S.O., London.

ATKINS, W.R.G., and POOLE, H.H. (1929) The uranyl oxolate method of daylight photometry and its photo-electric standardisation. Scientific Proceedings Royal Dublin Society, 19: 321-339.

BARRY, R.G., and CHORLEY, R.J. (1976) Atmosphere, Weather, and Climate. (third ed.). Methuen and Co. Ltd.

BENECKE, U., and MORRIS, J.Y. (1978) Tree provenance trials. In: Orwin, J. (ed.). Revegetation in the Rehabilitation of Mountain Lands. N.Z.F.S., F.R.I. Symposium no.16: 99-138.

BENECKE, U., BAKER, G., and MCCRACKEN, I.J. (1978) Tree growth in the Craigieburn Range. In: Orwin, J. (ed.). Revegetation in the Rehabilitation of Mountain Lands. N.Z.F.S., F.R.I. Symposium no.16: 77-98.

BENECKE, U., and HAVRANEK, W.M. (1980a) Phenological growth characteristics of trees with increasing altitude, Craigieburn Range, New Zealand. In: Benecke, U., and Davis, M.R. (eds.). Mountain Environments and Subalpine Tree Growth. N.Z.F.S., F.R.I. Technical Paper no.70: 155-174.

———————(1980b) Gas-exchange of trees at altitudes up to timberline, Craigieburn Range, New Zealand. In: Benecke, U., and Davis, M.R. (eds.). Mountain Environments and Subalpine Tree Growth. N.Z.F.S., F.R.I. Technical Paper no.70: 195-210.

BENECKE, U., SCHULZE, E.D., MATYSSEK, R., and HAVRANEK, W.M. (1981) Environment control of CO_2 - assimilation and leaf conductance in *Larix decidua* Mill., I: a comparison of contrasting natural environments. Oecologia, 50: 54-61.

BENECKE, U., and NORDMEYER, A.H. (1982) Carbon uptake and allocation by *Nothofagus solandri* var *cliffortioides*, (Hook.f.) Poole and *Pinus contorta* Douglas ex. Loudon ssp. *contorta* at montane and subalpine altitudes. In: Waring, R.H.(ed. Carbon Uptake and Allocation in Subalpine Ecosystems as a Key to Management. Proceedings I.U.F.R.O. Workshop. Oregon State University, Corvallis, Oregon, U.S.A.: (in press).

BRANDT, A.B., and TAGEYEVA, S.V. (1967) Optical Parameters of Plant Organisms. Nauka, Moscow (in Russian).

COOMBE, D.E. (1957) The spectral composition of shade light in woodlands. Journal of Ecology, 45: 823-30.

———— (1966) The seasonal light climate and plant growth in a Cambridgeshire wood. In: Bainbridge, R., Evans, G.C., and Rackman, O. (eds.). Light as an Ecological factor. Blackwell Scientific Publications: 148-166.

COULSON, K.L. (1975) Solar and Terrestrial Radiation. Academic Press, New York.

COULTER, J.D. (1973) Ecological aspects of climate. In: Williams, G.R. (ed.). The Natural History of New Zealand. A.H. and A.W. Reed, Wellington.

COWAN, I.R. (1968) The interception and absorption of radiation in plant stands. Journal of Applied Ecology, 5: 367-379.

CRUDEN, J. (1981) Climate Observations in the Craigieburn Range for the Season July 1979 to June 1980. N.Z.F.S., F.R.I. Protection Forestry Report no.184, (unpublished).

DAVIS, M.R. (1978) Phosphate responses of grasses and legumes growing on subsoil. In: Orwin, J. (ed.). Revegetation in the Rehabilitation of Mountain Lands. N.Z.F.S., F.R.I. Symposium no.16: 21-38.

———— (1981) Growth and nutrition of legumes on a high country yellow-brown earth subsoil, I: phosphate response of *Lotus, Trifolium, Lupinus, Astragalus,* and *Coronilla* species and cultivars. New Zealand Journal of Agricultural Research, 24: 321-332.

DE SLOOVER, J., and MARYNEN, T. (1963) Une mesure écologique de la quantité d'éclairement et de l'irradiation. C.R. Acad. Sci. Paris, 257: 2707-2710.

DORE, W.G. (1958) A simple chemical light meter. Ecology, 39: 151-152.

EBER, W. (1971) The characterisation of the woodland light climate. In: Ellenberg, H. (ed.). Integrated Experimental Ecology. Chapman and Hall Ltd, London: 143-152.

EVANS, G.C. (1956) An area survey method of investigating the distribution of light intensity in woodlands with particular reference to sunflecks. Journal of Ecology, 44: 391-428.

————————(1959) Hemispherical and woodland canopy photography and the light climate. Journal of Ecology, 47: 103-113.

————————(1966) Model and measurement in the study of woodland light climates. In: Bainbridge, R., Evans, G.C., and Rackman, O. (eds.). Light as an Ecological Factor. Blackwell Scientific Publications: 53-76.

EVANS, G.R. (1980) Phytomass, litter and nutrients in montane and alpine grasslands, Craigieburn Range, New Zealand. In: Benecke, U., and Davis, M.R. (eds.). Mountain Environments and Subalpine Tree Growth. N.Z.F.S., F.R.I. Technical Paper no.70: 95-109.

FEDERER, C.A., and TANNER, C.B. (1966a) Spectral distribution of light in the forest. Ecology, 47: 555-560.

————————(1966b) Sensors for measuring light available for photosynthesis. Ecology, 47: 654-657.

FREYMAN, S. (1968) Canadian Journal of Plant Science, 48: 326-328.

FRIEND, D.T.C. (1961) A simple method of measuring integrated light values in the field. Ecology, 42: 577-580.

FRIEND, M.T. (1959) Shade measurements by a chemical radiation meter. East African Agricultural Journal, 25: 110-112.

FRY, D.J., and PHILLIPS, I.D.J. (1976) Photosynthesis of conifers in relation to annual growth cycles and dry matter production, I: some C_4 characteristics in photosynthesis of Japanese larch (*Larix leptolepis*). Physiologia Plantarum, 37: 185-190.

————————(1977) Photosynthesis of conifers in relation to annual growth cycles and dry matter production, II: seasonal photosynthetic capacity and mesophyll ultrastructure in *Abies grandis, Picea sitchensis, Tsuga heterophylla* and *Larix leptolepis* growing in S.W. England. Physiologia Plantarum, 40: 300-306.

GARNIER, B.J., and OHMURA, A. (1968) A method of calculating direct shortwave radiation income of slopes. Journal of Applied Meteorology, 7 (5): 796-800.

GATES, D.M., KEEGAN, H.J., SCHLETER, J.L., and WEIDNER, V.R. (1965) Spectral properties of plants. Applied Optics, 4: 11-20.

GAY, L.W., KNOERR, K.R., and BRAATEN, M.O. (1971) Solar radiation variability on the floor of a pine plantation. Agricultural Meteorology, 8: 39-50.

GHOLZ, H.L., FRANKLIN, K.F., and WARING, R.H. (1976) Leaf area differences associated with old-growth forest communitie in the western Oregon Cascades. Canadian Journal of Forest Research, 6: 49-57.

HARRISON, J.B.L. (1982) Soil periodicity in a formerly glaciated basin, Ryton Valley, Craigieburn Range, Canterbury, New Zealand. M. Agric. Sci. Thesis, Lincoln College, University of Canterbury, New Zealand.

HAY, J.E. (1978) Calculation of monthly mean solar radiation for horizontal and inclined surfaces. Solar Energy, 23 (4): 301-307.

HEINICKE, D.R. (1963) The micro-climate of fruit trees, I: light measurements with uranyl actinometers. Canadian Journal of Plant Science, 43: 561-568.

HORN, H.S. (1971) The Adaptive Geometry of Trees. Princeton Uni. Press, Princeton, New Jersey.

HUTCHISON, B.A., and MATT, D.R. (1977) The distribution of solar radiation within a deciduous forest. Ecological Monographs, 47: 185-207.

JARVIS, P.G., JAMES, G.B., and LANDSBERG, J.J. (1976) Conifer forest. In: Monteith, J.L. (ed.). Vegetation and the Atmosphere, vol.2. Academic Press, London: 171-240.

JUPP, D.L.B., ANDERSON, M.C., ADOMEIL, E.M., and WITTS, S.J. (1980) PISCES - a computer program for analysing hemispherical canopy photographs. C.S.I.R.O., Div. Land Use Res., Canberra, Tech. Mem. 80/23.

KELLAND, C.M. (1978) Chemical analysis of some soils from the Craigieburn Range. In: Orwin, J. (ed.). Revegetation in the Rehabilitation of Mountain Lands. N.Z.F.S., F.R.I. Symposium no.16: 51-59.

KIRA, T., SHINOZAKI, K., and HOZUMI, K. (1969) Structure of forest canopies as related to their primary productivity. Plant and Cell Physiology, 10: 129-142.

KIRA, T. (1975) Primary production of forests. In: Cooper, J.P. (ed.). Photosynthesis and Productivity in Different Environments. International Biological Programme, vol.3. Cambridge Uni. Press, London: 5-40.

KOK, B. (1967) Photosynthesis - physical aspects. In: San Pietro, A., Greer, F.A., and Thomas, J.A. (eds.). Harvesting the Sun : Photosynthesis in Plant Life. Academic Press, New York: 29-48.

KONDRAT'YEV, K.Y. (1965) Radiative Heat Exchange in the Atmosphere. Pergamon Press, New York and London.

————————(1969) Radiation in the Atmosphere, Academic Press, New York.

————————(1977) Radiation Regime of Inclined Surfaces. W.M.O. (Geneva) Tech. Note, 152 (467).

KUBIN, S. (1971) Measurement of radiant energy. In: Sestak, Z., Catsky, J., and Jarvis, P.G. (eds.). Plant Photosynthetic Production : Manual of Methods. Dr. W. Junk n.v., The Hague: 702-763.

KUROIWA, S., and MONSI, M. (1963) Theoretical analysis of light factor and photosynthesis in plant communities, I: relationships between foliage structure and direct, diffuse and total solar radiation. Journal of Agricultural Meteorology (Tokyo), 18: 143-151.

KUROIWA, S. Total photosynthesis of foliage in relation to inclination of leaves. In: Setlik, I. (ed.). Prediction and Measurement of Photosynthetic Productivity. Proceedings of the IBP/PP Technical Meeting, Trebon, 14-21 September 1969: 79-102.

LARCHER, W. (1969) The effect of environmental and physiological variables on the carbon dioxide exchange of trees. Photosynthetica, 3: 167-198.

LARCHER, W. (1975) Physiological Plant Ecology. Springer-Verlag, Berlin, Heidelberg, New York.

LEDGARD, N.J. (1980) Specific and intraspecific growth differences in tree trials up to timberline in the Craigieburn Range, New Zealand. In: Benecke, U., and Davis, M.R. (eds.). Mountain Environments and Subalpine Tree Growth. N.Z.F.S., F.R.I. Technical Paper no.70: 137-153.

LEVERENZ, J.W., and JARVIS, P.G. (1980) Photosynthesis in Sitka spruce (*Picea sitchensis* (Bong.) Carr.), IX: the relative contribution made by needles at various positions on the shoot. Journal of Applied Ecology, 17: 59-68.

LEVERENZ, J.W. (1981a) Photosynthesis and transpiration in a large forest-grown Douglas-fir : diurnal trends. Canadian Journal of Botany, 59: 349-356.

————————(1981b) Photosynthesis and transpiration in a large forest-grown Douglas-fir : interactions with apical control. Canadian Journal of Botany, 59: 2568-2576.

LEWANDOWSKA, M., HART, J.W., and JARVIS, P.G. (1977) Photosynthetic electron transport in shoots of Sitka spruce from different levels in a forest canopy. Physiologia Plantarum, 41: 124-128.

MARQUIS, D.A., and YELANOSKY, G. (1962) A Chemical Light Meter for Forest Research. Stn. Pop. N.west Forest Exp. Stn., no.165.

MATYSSEK, R. (1981) Die abhängigbeit der CO_2 - assimilation, transpiration, und stomatären leitfähigkeit der lärch von den standärtlichen klimafaktoren in jahresgang. Diplomarbeit Vorgelegt.

MAYER, H. (1981) The vertical distribution of the net radiation budget within a spruce forest in summer. Archives for Meteorology, Geophysics, and Bioclimatology, ser. B., 29: 381-392.

MOIR, W.H., and FRANCIS, R. (1972) Foliage biomass and surface area in three *Pinus contorta* plots in Colorado. Forest Science, 18 (1): 41-45.

MOLDAU, H. (1965) In: Phytoactinometric Investigations of Plant Canopies. Valgus, Tallinn (in Russian): 89-109.

MØLLER, C.M. (1946) Untersuchungen über laubmenge, stoffverlust and stoffproduktion des waldes. Det Forstlige Forsøgsvosen i Danmark, 17: 1-287.

MOLLOY, B.P.J. (1969) Recent history of the vegetation. In: Knox, G.A. (ed.). The Natural History of Canterbury. A.H. and A.W. Reed, Wellington: 340-360.

MONSI, M., and SAEKI, T. (1953) Über den lichtfaktor in den pflanzengesellschaften und seine bedeutung für die stoffproduktion. Japanese Journal of Botany, 14: 22-52.

MONTEITH, J.L. (1973) Principles of Environmental Physics. Edward Arnold, London.

MORRIS, J.Y. (1965) Climate investigations in the Craigieburn Range, New Zealand. New Zealand Journal of Science, 8: 556-582.

MUKAMMAL, E.I. (1971) Some aspects of radiant energy in a red pine forest. Archives for Meteorology, Geophysics and Bioclimatology, ser. B., 19: 29-52.

MCCRACKEN, I.J. (1980) Mountain climate in the Craigieburn Range, New Zealand. In: Benecke, U., and Davis, M.R. (eds.). Mountain Environments and Subalpine Tree Growth. N.Z.F.S., F.R.I. Technical Paper no.70: 41-59.

NIILISK, H., NILSON, T., and ROSS, J. (1970) Radiation in plant canopies and its measurement. In: Setlik, I. (ed.). Prediction and Measurement of Photosynthetic Productivity. Proceedings of the IBP/PP Technical Meeting, Trebon, 14-21 September 1969: 165-177.

NORDMEYER, A.H. (1978a) Effects of P, S, Ca, Mg, K, N, and lime on white clover seedlings in subsoil. In: Orwin, J. (ed.). Revegetation in the Rehabilitation of Mountain Lands. N.Z.F.S., F.R.I. Symposium no.16: 39-50.

———————(1978b) Bacteria in some mountain soils. In: Orwin, J. (ed.). Revegetation in the Rehabilitation of Mountain Lands. N.Z.F.S., F.R.I. Symposium no.16: 60-76.

———————(1980a) Tree nutrient concentrations near timberline, Craigieburn Range, New Zealand. In: Benecke, U., and Davis, M.R. (eds.). Mountain Environments and Subalpine Tree Growth. N.Z.F.S., F.R.I. Technical Paper no.70: 83-94.

———————(1980b) Phytomass in different tree stands near timberline. In: Benecke, U., and Davis, M.R. (eds.). Mountain Environment and Subalpine Tree Growth. N.Z.F.S., F.R.I. Technical Paper no.70: 111-124.

NORMAN, J.M., and JARVIS, P.G. (1974) Photosynthesis in Sitka spruce (*Picea sitchensis* (Bong.) Carr.), III: measurements of canopy structure and interception of radiation. Journal of Applied Ecology, 11: 375-398.

NORMAN, J.M., and JARVIS, P.G. (1975) Photosynthesis in Sitka spruce (*Picea sitchensis* (Bong.) Carr.), V: radiation penetration theory and test case. Journal of Applied Ecology, 12: 839-878.

OHMURA, A. (1968) The computation of direct insolation on a slope. Climatological Bulletin, (McGill Uni.): 42-53.

OKE, T.R. (1978) Boundary Layer Climates. Methuen and Co. Ltd., New York.

OKER-BLOM, P., and KELLOMÄKI, S. (1981) Light regime and photosynthetic production in the canopy of a Scots pine stand during a prolonged period. Agricultural Meteorology, 24: 185-199.

———————(1982) Effect of angular distribution of foliage on light absorption and photosynthesis in the plant canopy : theoretical computations. Agricultural Meteorology, 26: 105-116.

ORWIN, J. (comp., and ed.)(1978) Revegetation in the Rehabitation of Mountain Lands. N.Z.F.S., F.R.I. Symposium no.16.

PEARSALL, W.H., and HEWITT, T. (1933) Light penetration and fresh water II: light penetration and changes in vegetation limits in Windermere. Journal of Experimental Biology, 10: 306-312.

PIERIK, R.L.M. (1965) Integrating photochemical light measurements : an ecological study in the Middachten woodland in the Netherlands. Meded. Landb. Hoogesch. Wageningen, 65: 1-16.

POOLE, H.H., and ATKINS, W.R.G. (1930) Methods for the photo-electric and photo-chemical measurement of daylight. Biological Reviews, 5: 91-113.

RAESIDE, C.G. *et al* (1968) Soils of South Island. In: Soils of New Zealand, part 1. Soil Bureau Bulletin 26 (1). New Zealand D.S.I.R.

RAUNER, J.L. (1976) Deciduous forests. In: Monteith, J.L. (ed.). Vegetation and the Atmosphere, vol.2. Academic Press, London: 241-264.

REIFSNYDER, W.E., and LULL, H.W. (1965) Radiant Energy in Relation to Forests. Technical Bulletin no.1344, U.S.D.A. Forest Service, U.S. Govt. Printing Office, Washington D.C.

REIFSNYDER, W.E. (1967) Forest meteorology : the forest energy balance. International Reviews of Forest Research, 2: 127-179.

REIFSNYDER, W.E., FURNIVAL, G.M., and HOROWITZ, J.L. (1971) Spatial and temporal distribution of solar radiation beneath forest canopies. Agricultural Meteorology, 9 (1): 21-37.

RICHARDS, J.H. (1981) Ecophysiology of a deciduous timberline tree *Larix lyallii* Parl.. Ph.D. Thesis, Uni. of Alberta, Edmonton, Alberta, Canada.

ROBINSON, N. (ed.)(1966) Solar Radiation. Elsevier, Amsterdam.

ROSS, J., and NILSON, T. (1965) The extinction of direct radiation in crops. In: Vaprosy radiatsionnogo rezhima rastitelnogo pokrova. I.P.A., Tartu: 25-64.

ROSS, J. (1970) Mathematical models of photosynthesis in a plant stand. In: Setlik, I. (ed.). Prediction and Measurement of Photosynthetic Productivity. Proceedings of the IBP/PP Technical Meeting, Trebon, 14-21 September 1969: 29-45.

————(1975) Radiative transfer in plant communities. In: Monteith, J.L. (ed.). Vegetation and the Atmosphere, vol.1. Academic Press, London: 13-55.

SAEKI, T., and KUROIWA, S. (1959) On the establishment of the vertical distribution of photosynthetic system in a plant community. Botanical Magazine (Tokyo), 72: 27-35.

SAEKI, T. (1960) Interrelationships between leaf amount, light distribution, and total photosynthesis in a plant community. Botanical Magazine (Tokyo), 73: 55-63.

SAN PIETRO, A. (1967) Electron transport in chloroplasts. In: San Pietro, A., Greer, F.A., and Thomas, J.A. (eds.). Harvesting the Sun : Photosynthesis in Plant Life. Academic Press, New York: 49-68.

SCHULGIN, I.A. (1963) Morphophysiological Adaptations of Plants to Light. Moscow Uni. Press, Moscow (in Russian).

SCHULZE, E.D., FUCHS, M.I., and FUCHS, M. (1977a) Spatial distribution of photosynthetic capacity and performance in a mountain spruce forest of Northern Germany, I: biomass distribution and daily CO_2 uptake in different crown layers. Oecologia, 29: 43-61.

————(1977b) Spatial distribution of photosynthetic capacity and performance in a mountain spruce forest of Northern Germany, II: Climatic control of carbon dioxide uptake. Oecologia, 29: 329-340.

————(1977c) Spatial distribution of photosynthetic capacity and performance in a mountain spruce forest of Northern Germany, III: the significance of the evergreen habit. Oecologia, 30: 239-248.

SESTAK, Z., CATSKY, J., and JARVIS, P.G. (1971) Plant Photosynthetic Production : A Manual of Methods. Dr.W. Junk n.v., The Hague.

SMITH, P.M.F., and SCOTT, G.A.M. (1970) A simple chemical light-meter for use in forests. Proceedings of the New Zealand Ecological Society, 17: 139-142.

UNGS, M.J. (1981) Distribution of light within the crowns of an open-grown Douglas-fir. Ph.D Thesis, Oregon State Uni., Corvallis, Oregon, U.S.A.

VERNON, L.P. (1967) The Photosynthetic Apparatus of Bacteria. In: San Pietro, A., Greer, F.A., and Thomas, J.A. (eds.). Harvesting the Sun : Photosynthesis in Plant Life. Academic Press, New York: 15-28.

VÉZINA, P.E. (1961) Variations in total solar radiation in three Norway Spruce plantations. Forest Science, 7: 257-264.

VÉZINA, P.E., and PÉCH, G. (1964) Solar radiation beneath conifer canopies in relation to crown closure. Forest Science, 10: 443-450.

WALSH, J.W.T. (1961) The Science of Daylight. MacDonald, London.

WARDLE, J. (1970) The ecology of *Nothofagus solandri*. New Zealand Journal of Botany, 8: 494-646.

————(1980) Distribution and dynamics of the indigenous forests in New Zealand with major emphasis on the beeches. In: Benecke, U., and Davis, M.R. (eds.). Mountain Environments and Subalpine Tree Growth. N.Z.F.S., F.R.I. Technical Paper no.70: 13-19.

————(1982) The Ecology, Utilisation and Management of the New Zealand Beech Forests. (in prep.).

WATSON, D.J. (1958) The dependence of net assimilation rate upon leaf area index. Annals of Botany, London, New Series, 22: 37-54.

WILSON, J. (1959) Analysis of spatial distribution of foliage by two-dimensional point quadrats. New Phytologist, 58: 92-101.

————(1960) Inclined point quadrats. New Phytologist, 59: 1-8.

————————(1963) Estimation of foliage denseness and foliage angle by inclined point quadrats. Australian Journal of Botany, 11: 95-105.

————————(1965) Stand structure and light penetration, I: analysis by point quadrats. Journal of Applied Ecology, 2: 383-390.

————————(1967) Stand structure and light penetration, III: sunlit foliage area. Journal of Applied Ecology, 4: 159-166.

WORLD METEOROLOGICAL ORGANISATION (1981) Meteorological Aspects of the Utilisation of Solar Radiation as an Energy Source. Technical Note no.172, W.M.O. 557, (Geneva).

YELLOT, J.I., CHAMNES, L., and SELCUK, K. (1962) Measurement of direct, diffuse and total solar radiation with silicon photovoltaic cells. Solar Energy, 6: 155-163.

YOUNG, S.C., and WHITEHEAD, D. (1981) A Technique for the Long-term Measurement of Irradiance on the Forest Floor. N.Z.F.S., F.R.I. Tree Physiology Report no.36 (unpublished).

ZOBEL, D.B.A., MCKEE, G.M., HAWK, G.M., and DYRNESS, C.T. (1976) Relationships of environment to composition, structure and diversity of forest communities of the central western Cascades of Oregon. Ecological Monographs, 46: 135-156.

APPENDIX 1

INSTRUMENTATION AND CALIBRATION

1.1 Radiometric Instruments

These instruments are normally used to measure the heat produced when a black surface, usually a thermocouple, absorbs radiation. Robinson (1966), Anderson (1971), Kubin (1971), and W.M.O. (W.M.O., No. 557, 1981) cover the principles of these instruments in considerable detail.

(a) Kipp solarimeters

These radiometric instruments are used to measure total shortwave solar energy (300-3000 nm) incident on a horizontal surface, though they may be covered by coloured glass filters to reduce the waveband range, and be fitted with shade rings, to measure diffuse sky radiation. Kipp solarimeters (after Kipp and Zonen, Delft, Holland) require much attention to keep thoroughly dry, but if properly used, make very suitable reference instruments. Kubin (1971, pp.754-756) describes in great detail the construction of these instruments and their optical properties, and Anderson (1971, pp.422-423) makes comparisons with other short wave pyranometers.

In general, these instruments are precise, expensive and require an external recording circuit and a good deal of maintenance. Data obtained from this instrument is generally given in Wm^{-2}, or MJm^{-2} over time.

(i) Calibration procedure for Kipp Solarimeter

The Kipp solarimeter (CM5,ser.no.721340) used for the calibration of 300-3000 nm irradiance received and number of papers exposed had the following characteristics:

$1 Wcm^{-2}$ produces an E.M.F. of 105mV

Using, $\left(\frac{1 Wcm^{-2}}{1}\right)\left(\frac{10^4 cm^{-2}}{m^2}\right) = 1 Wm^{-2}$

Taking E.M.F. factor, $\frac{1 \times 10^4 Wcm^{-2}}{105mV} = 95.23 Jm^{-2}s^{-1}/mV$

Therefore $mV.\ 95.23 \rightarrow Wm^{-2}$

$mVs\ 95.23 \rightarrow Jm^{-2}s^{-1}$

(ii) Integration

The Kipp solarimeter (CM5,ser.no.721340) was attached to a millivolt integrator (TECHEN, Christchurch, I.M.S. system 601, ser.no.01). The normal integration rate is one count per second when the meter scale reads full (i.e. one count represents 1mV second, 3, 10, etc depending on the range). During the calibration of 300-3000 nm irradiance received by the Kipp solarimeter and number of papers exposed, the integrator was set up as follows:

Scale	30mV
Offset	0%
Print interval	15 mins

Use calibration constant to convert to required units (Wm^{-2})

example:-

154 counts over 15 minutes gives 0.17 counts per second.

0.17 x 30 = 5.13Mv = integrated value

5.13 x 94.23 = 483.9Wm^{-2}

(Calibration constant for Kipp Solarimeter = 94.23 x mV → Wm^{-2})

1.2 Thermo-mechanical Instruments

Unlike radiometric and photometric instruments, these intruments do not require an external recording circuit. For details, Anderson (1971) and Kubin (1971) should be consulted.

(a) Fuess bimetallic actinograph

This instrument (plate 3.4) has the advantage of providing a record independently of a power supply. However, it cannot provide accurate instantaneous readings, and requires careful maintenance, and its sensitivity varies appreciably with solar altitude and azimuth, casing temperature and incident flux. Corrections can be made for solar altitude and azimuth and provided the instrument is regularly serviced, then useful data at the daily level or greater can be obtained. The data is commonly expressed in MJm^{-2}.

(i) Correction for sun's elevation angle

To obtain daily totals of solar radiation (300-3000 nm, MJm^{-2}) the following table is used to correct for changes in solar elevation.

Station: Craigieburn Forest

Elevation: 914 m a.s.l.

Instrument: Ser.no.9789

Dates to apply	this	factor
23 November - 22 January		1.20
23 January - 05 February	07 November - 22 November	1.19
06 February - 16 February	26 October - 06 November	1.18
17 February - 27 February	14 October - 25 October	1.17
28 February - 09 March	04 October - 13 October	1.16
10 March - 18 March	26 September - 03 October	1.15
19 March - 28 March	18 September - 25 September	1.14
27 March - 06 April	11 September - 17 September	1.13
07 April - 15 April	05 September - 10 September	1.12
16 April - 22 April	27 August - 04 September	1.11
23 April - 01 May	21 August - 26 August	1.10
02 May - 07 May	13 August - 20 August	1.09
08 May - 15 May	05 August - 12 August	1.08
16 May - 25 May	28 July - 04 August	1.07
26 May - 08 June	19 July - 27 July	1.06
09 June - 18 June	03 July - 18 July	1.05
19 June - 02 July		1.04

PROCEDURE:

1.43 (correction factor) x sun's L (factor from table) x area under curve reading (from chart) x 0.041868 (to convert from Langleys to MJm^{-2}) = MJm^{-2}

1.3 Photometric Instruments

Unlike radiometric instruments, photometric instruments are usually much more highly spectrally selective and include such devices as photoemissive and photoconductive cells. Walsh (1961), Federer and Tanner (1966b), and Kubin (1971) describe their structure and optical characteristics.

(a) Silicon photovoltaic sensors

The silicon photovoltaic cell is perhaps the most common light sensor for plant work. Yellot *et al* (1962) describe these cells in considerable detail. There are two main types used for ecological work, quantum and pyrometric.

Quantum sensors are designed to measure light in the 400-700 nm range, which is the approximate spectral response of plants during photosynthesis (as outlined in chapter one). According to Federer and Tanner (1966b), in the 400-700 nm range absorptivities are between 60% and 90% due to chlorophylls and carotenoids. The quantum sensor is designed to give measurement of the number of photons in the 400-700 nm range. Since one Einstein is defined as Avogadro's number of photons (6.02×10^{23}), microeinsteins $m^{-2}s^{-1}$ ($\mu Em^{-2}s^{-1}$) in the 400-700 nm range is a convenient photosynthesis light unit (Brooks, 1964).

Pyrometric sensors are designed to measure light in the 300-3000 nm range, and therefore cover a similar range to other pyranometers such as Kipp (Kipp-Zonen, Delft). Readings are likewise given in Wm^{-2}, and MJm^{-2} over time.

Silicon photovoltaic sensors are often cosine-corrected, which gives them an advantage in the field compared with the poorly cosine-corrected radiometric and thermo-mechanical instruments.

As for radiometric instruments, photometric sensors have to be connected to an external recording circuit, but require considerably less maintenance.

(i) Calibration procedure for silicon photovoltaic sensors

Spot measurements were made in the field using the following equipment (all LAMBDA, Nebraska):

Quantum sensor, ser.no.Q427-7400

Pyrometric sensor, ser.no.Py304-7407

Portable recording meter, LI-170,ser.no.PRQ185-7406 (see plate 3.2)

No calibration procedure is necessary because the LI-170 meter has been adjusted for the particular sensor used.

(ii) Calibration procedure for quantum sensor and integrator

A quantum sensor (ser.no.Q2317-7709) was attached to a portable field integrator (ser.no.Pl-250-7709), (both LAMBDA, Nebraska, see plate 3.1).

The integrator unit contained a 190M Module which was designed for integrating 400-700 nm irradiance.

Calibration procedure

LAMBDA, LI-550 integrator containing 190 Module with LI-190S Quantum sensor.

to find (a) total μEm^{-2} over the print interval

(b) average $\mu Em^{-2}sec^{-1}$ during the print interval.

quantum sensor Q2317-7709 calibration constant as for 5/5/78 = $8.47\mu A/1000\mu Em^{-2}s^{-1}$

Table

Divider Switch	190M Module counts/hr μA/Quantum
0	7168
1	3584
2	1792
3	896
4	448
5	224
6	112
7	56

example:-

to calculate (a), total μEm^{-2}, with divider switch at 0 and print interval at 1 min.

Using table,

$$\frac{7168 \text{ counts/hr}}{1\mu A} \cdot \frac{8.47 \text{ A}}{1000\mu Em^{-2}s^{-1}} \cdot \frac{1 \text{ Hr}}{3600 \text{ secs}}$$

$$= \frac{60712.96 \text{ counts}}{3600000\mu Em^{-2}} = \frac{1 \text{ count}}{59.29\mu Em^{-2}}$$

if 1000 counts are made then,

$$1000 \text{ counts} \cdot \frac{59.29\mu Em^{-2}}{1 \text{ count}} = 59290.0\mu Em^{-2}$$

to calculate (b), average $\mu Em^{-2}s^{-1}$ during the print interval, divide by print interval (secs)

$$\frac{59290.0\mu Em^{-2}}{60 \text{ secs}} = 988.2\mu Em^{-2}sec^{-1}$$

example:-

to calculate (a), total μEm^{-2} with divider switch at 2 and print interval at 10 mins.

Using table,

$$\frac{1792 \text{ counts/hr}}{1\mu A} \cdot \frac{8.47\mu A}{1000\mu Em^{-2}s^{-1}} \cdot \frac{1 \text{ Hr}}{3600 \text{ secs}}$$

$$= \frac{15178.24 \text{ counts}}{3600000\mu Em^{-2}} = \frac{1 \text{ count}}{237.18\mu Em^{-2}}$$

if 1000 counts are made then,

$$1000 \text{ counts} \cdot \frac{237.18\mu Em^{-2}}{1 \text{ count}} = 237180.0\mu Em^{-2}$$

to calculate (b), average $\mu Em^{-2}sec^{-1}$ during the print interval, divide by print interval (secs)

$$\frac{237180.0\mu Em^{-2}}{600 \text{ secs}} = 395.3\mu Em^{-2}sec^{-1}$$

example:-

to calculate (a), total μEm^{-2}, with divider switch at 4 and print interval at 1 Hr.

Using table,

$$\frac{448 \text{ counts/hr}}{1\mu A} \cdot \frac{8.47\mu A}{1000\mu Em^{-2}s^{-1}} \cdot \frac{1 \text{ Hr}}{3600 \text{ secs}}$$

$$= \frac{3794.56 \text{ counts}}{3600000 \mu Em^{-2}} = \frac{1 \text{ count}}{948.72 \mu Em^{-2}}$$

if 1000 counts are made then,

$$1000 \text{ counts} \cdot \frac{948.72 \mu Em^{-2}}{1 \text{ count}} = 948720.0 \mu Em^{-2}$$

to calculate (b), average $\mu Em^{-2}sec^{-1}$ during the print interval, divide by print interval (secs)

$$\frac{94870.0 \mu Em^{-2}}{3600 \text{ secs}} = 263.53 \mu Em^{-2}sec^{-1}$$

APPENDIX 2 : AMMONIA DIAZO PAPER TECHNIQUE DATA SUMMARY (February-June)

SPECIES KEY

1=LARIX DECIDUA
2=PSEUDOTSUGA MENZIESII
3=PINUS CONTORTA
4=NOTHOFAGUS SOLANDRI

WEEKLY DATA KEY

1= 03/2 TO 10/2
2= 10/2 TO 17/2
3= 17/2 TO 24/2
4= 24/2 TO 03/3
5= 03/3 TO 10/3
6= 24/3 TO 31/3

400-700 nm irradiance (P.A.R.) data summary. The number of papers exposed is transformed into energy units (Einsteins $m^{-2}wk^{-1}$) using the appropriate log functions from tables 3.11 and 3.12.

WEEK NUMBER 1

SPECIES NUMBER 1

SENSOR POSITION	NUMBER OF PAPERS	EINSTEINS/M^2
ABV CANOPY INCIDENT IRRADIANCE	7.83	534.367455
TOP CANOPY INCIDENT IRRADIANCE	6.71	130.04091
MID CANOPY INCIDENT IRRADIANCE	5.96	50.4754268
BOT CANOPY INCIDENT IRRADIANCE	5.43	25.8606836
GROUND INCIDENT IRRADIANCE	5.41	25.2162209
TOP CANOPY REFLECTED IRRADIANCE	3.08	1.33303023
MID CANOPY REFLECTED IRRADIANCE	2.98	1.17500577
BOT CANOPY REFLECTED IRRADIANCE	2.66	.784657264

WEEK NUMBER 2

SPECIES NUMBER 1

SENSOR POSITION	NUMBER OF PAPERS	EINSTEINS/M^2
ABV CANOPY INCIDENT IRRADIANCE	7.82	527.667079
TOP CANOPY INCIDENT IRRADIANCE	6.55	106.267387
MID CANOPY INCIDENT IRRADIANCE	6.07	57.9909202
BOT CANOPY INCIDENT IRRADIANCE	5.59	31.6460857
GROUND INCIDENT IRRADIANCE	5.21	19.5920554
TOP CANOPY REFLECTED IRRADIANCE	3.27	1.69418175
MID CANOPY REFLECTED IRRADIANCE	3.06	1.29981038
BOT CANOPY REFLECTED IRRADIANCE	2.86	1.00990379

WEEK NUMBER 3

SPECIES NUMBER 1

SENSOR POSITION	NUMBER OF PAPERS	EINSTEINS/M^2
ABV CANOPY INCIDENT IRRADIANCE	7.63	415.183418
TOP CANOPY INCIDENT IRRADIANCE	6.52	102.319875
MID CANOPY INCIDENT IRRADIANCE	5.77	39.7154968
BOT CANOPY INCIDENT IRRADIANCE	5.24	20.347919
GROUND INCIDENT IRRADIANCE	5.24	20.347919
TOP CANOPY REFLECTED IRRADIANCE	2.87	1.02272766
MID CANOPY REFLECTED IRRADIANCE	2.81	.948156442
BOT CANOPY REFLECTED IRRADIANCE	2.47	.617390582

WEEK NUMBER 4

SPECIES NUMBER 1

SENSOR POSITION	NUMBER OF PAPERS	EINSTEINS/M^2
ABV CANOPY INCIDENT IRRADIANCE	7.29	270.346033
TOP CANOPY INCIDENT IRRADIANCE	6.01	53.7625674
MID CANOPY INCIDENT IRRADIANCE	5.41	25.2162209
BOT CANOPY INCIDENT IRRADIANCE	4.89	13.0833814
GROUND INCIDENT IRRADIANCE	4.85	12.4394162
TOP CANOPY REFLECTED IRRADIANCE	2.78	.912935299
MID CANOPY REFLECTED IRRADIANCE	2.48	.625230275
BOT CANOPY REFLECTED IRRADIANCE	2.18	.42819343

WEEK NUMBER 5

SPECIES NUMBER 1

SENSOR POSITION	NUMBER OF PAPERS	EINSTEINS/M^2
ABV CANOPY INCIDENT IRRADIANCE	7.61	404.836816
TOP CANOPY INCIDENT IRRADIANCE	6.38	85.7511592
MID CANOPY INCIDENT IRRADIANCE	5.57	30.8574476
BOT CANOPY INCIDENT IRRADIANCE	5.21	19.5920554
GROUND INCIDENT IRRADIANCE	5.21	19.5920554
TOP CANOPY REFLECTED IRRADIANCE	3.28	1.71569466
MID CANOPY REFLECTED IRRADIANCE	3.04	1.26741838
BOT CANOPY REFLECTED IRRADIANCE	2.78	.912935299

WEEK NUMBER 6

SPECIES NUMBER 1

SENSOR POSITION	NUMBER OF PAPERS	EINSTEINS/M^2
ABV CANOPY INCIDENT IRRADIANCE	7.21	244.388069
TOP CANOPY INCIDENT IRRADIANCE	5.78	40.2198086
MID CANOPY INCIDENT IRRADIANCE	5.63	33.2843438
BOT CANOPY INCIDENT IRRADIANCE	5.23	20.0927787
GROUND INCIDENT IRRADIANCE	4.96	14.2915719
TOP CANOPY REFLECTED IRRADIANCE	3.21	1.5706521
MID CANOPY REFLECTED IRRADIANCE	2.91	1.07567234
BOT CANOPY REFLECTED IRRADIANCE	2.46	.609649185

WEEK NUMBER 1

SPECIES NUMBER 2

SENSOR POSITION	NUMBER OF PAPERS	EINSTEINS/M^2
ABV CANOPY INCIDENT IRRADIANCE	7.83	534.367455
TOP CANOPY INCIDENT IRRADIANCE	4.91	16.1659752
MID CANOPY INCIDENT IRRADIANCE	4.32	9.51229252
BOT CANOPY INCIDENT IRRADIANCE	3.68	5.3624608
GROUND INCIDENT IRRADIANCE	2.61	1.38996585
TOP CANOPY REFLECTED IRRADIANCE	2.13	.484352903
MID CANOPY REFLECTED IRRADIANCE	2.09	.57048627
BOT CANOPY REFLECTED IRRADIANCE	2.11	.739612309

WEEK NUMBER 2

SPECIES NUMBER 2

SENSOR POSITION	NUMBER OF PAPERS	EINSTEINS/M^2
ABV CANOPY INCIDENT IRRADIANCE	7.82	527.667079
TOP CANOPY INCIDENT IRRADIANCE	5.03	18.8088355
MID CANOPY INCIDENT IRRADIANCE	4.44	11.0673896
BOT CANOPY INCIDENT IRRADIANCE	3.79	6.16089958
GROUND INCIDENT IRRADIANCE	2.41	1.0799512
TOP CANOPY REFLECTED IRRADIANCE	2.21	.53579901
MID CANOPY REFLECTED IRRADIANCE	2.19	.647209967
BOT CANOPY REFLECTED IRRADIANCE	2.21	.839081469

WEEK NUMBER 3

SPECIES NUMBER 2

SENSOR POSITION	NUMBER OF PAPERS	EINSTEINS/M^2
ABV CANOPY INCIDENT IRRADIANCE	7.63	415.183418
TOP CANOPY INCIDENT IRRADIANCE	4.81	14.2495748
MID CANOPY INCIDENT IRRADIANCE	4.22	8.384655
BOT CANOPY INCIDENT IRRADIANCE	3.61	4.90912544
GROUND INCIDENT IRRADIANCE	2.59	1.35532713
TOP CANOPY REFLECTED IRRADIANCE	2.03	.426935145
MID CANOPY REFLECTED IRRADIANCE	1.99	.502857807
BOT CANOPY REFLECTED IRRADIANCE	2.02	.660213089

WEEK NUMBER 4

SPECIES NUMBER 2

SENSOR POSITION	NUMBER OF PAPERS	EINSTEINS/M^2
ABV CANOPY INCIDENT IRRADIANCE	7.29	270.346033
TOP CANOPY INCIDENT IRRADIANCE	4.51	9.75892336
MID CANOPY INCIDENT IRRADIANCE	3.92	5.74229099
BOT CANOPY INCIDENT IRRADIANCE	3.27	3.19656935
GROUND INCIDENT IRRADIANCE	2.34	.988653549
TOP CANOPY REFLECTED IRRADIANCE	1.69	.277998151
MID CANOPY REFLECTED IRRADIANCE	1.67	.335803483
BOT CANOPY REFLECTED IRRADIANCE	1.65	.413927356

WEEK NUMBER 5

SPECIES NUMBER 2

SENSOR POSITION	NUMBER OF PAPERS	EINSTEINS/M^2
ABV CANOPY INCIDENT IRRADIANCE	7.61	404.836816
TOP CANOPY INCIDENT IRRADIANCE	4.51	9.75892336
MID CANOPY INCIDENT IRRADIANCE	4.04	6.68105731
BOT CANOPY INCIDENT IRRADIANCE	3.58	4.7267663
GROUND INCIDENT IRRADIANCE	3.21	2.96349453
TOP CANOPY REFLECTED IRRADIANCE	2.02	.421581852
MID CANOPY REFLECTED IRRADIANCE	2.97	1.73175
BOT CANOPY REFLECTED IRRADIANCE	2.01	.651934749

WEEK NUMBER 6

SPECIES NUMBER 2

SENSOR POSITION	NUMBER OF PAPERS	EINSTEINS/M^2
ABV CANOPY INCIDENT IRRADIANCE	7.21	244.388069
TOP CANOPY INCIDENT IRRADIANCE	4.21	6.68346853
MID CANOPY INCIDENT IRRADIANCE	3.63	3.98258631
BOT CANOPY INCIDENT IRRADIANCE	2.86	1.90547884
GROUND INCIDENT IRRADIANCE	2.77	1.70092095
TOP CANOPY REFLECTED IRRADIANCE	1.18	.146070295
MID CANOPY REFLECTED IRRADIANCE	1.06	.155526786
BOT CANOPY REFLECTED IRRADIANCE	1.14	.217492422

WEEK NUMBER 1

SPECIES NUMBER 3

SENSOR POSITION	NUMBER OF PAPERS	EINSTEINS/M^2
ABV CANOPY INCIDENT IRRADIANCE	7.83	534.367455
TOP CANOPY INCIDENT IRRADIANCE	6.66	122.089974
MID CANOPY INCIDENT IRRADIANCE	5.78	40.2198086
BOT CANOPY INCIDENT IRRADIANCE	4.76	11.104014
GROUND INCIDENT IRRADIANCE	4.71	10.4250945
TOP CANOPY REFLECTED IRRADIANCE	2.65	.774818533
MID CANOPY REFLECTED IRRADIANCE	2.21	.444713179
BOT CANOPY REFLECTED IRRADIANCE	1.86	.285943349

WEEK NUMBER 2

SPECIES NUMBER 3

SENSOR POSITION	NUMBER OF PAPERS	EINSTEINS/M^2
ABV CANOPY INCIDENT IRRADIANCE	7.82	527.667079
TOP CANOPY INCIDENT IRRADIANCE	6.63	117.554701
MID CANOPY INCIDENT IRRADIANCE	5.61	32.4548794
BOT CANOPY INCIDENT IRRADIANCE	4.57	8.736953
GROUND INCIDENT IRRADIANCE	4.32	6.37323598
TOP CANOPY REFLECTED IRRADIANCE	2.51	.649351727
MID CANOPY REFLECTED IRRADIANCE	2.29	.491948906
BOT CANOPY REFLECTED IRRADIANCE	2.08	.377433114

WEEK NUMBER 3

SPECIES NUMBER 3

SENSOR POSITION	NUMBER OF PAPERS	EINSTEINS/M^2
ABV CANOPY INCIDENT IRRADIANCE	7.63	415.183418
TOP CANOPY INCIDENT IRRADIANCE	6.47	96.0638523
MID CANOPY INCIDENT IRRADIANCE	5.58	31.2492789
BOT CANOPY INCIDENT IRRADIANCE	4.57	8.736953
GROUND INCIDENT IRRADIANCE	4.39	6.96177528
TOP CANOPY REFLECTED IRRADIANCE	2.37	.544201833
MID CANOPY REFLECTED IRRADIANCE	2.02	.349912937
BOT CANOPY REFLECTED IRRADIANCE	1.68	.227845261

WEEK NUMBER 4

SPECIES NUMBER 3

SENSOR POSITION	NUMBER OF PAPERS	EINSTEINS/M^2
ABV CANOPY INCIDENT IRRADIANCE	7.29	270.346033
TOP CANOPY INCIDENT IRRADIANCE	5.92	47.9910221
MID CANOPY INCIDENT IRRADIANCE	5.04	15.8095679
BOT CANOPY INCIDENT IRRADIANCE	4.43	7.32217323
GROUND INCIDENT IRRADIANCE	4.11	4.88967506
TOP CANOPY REFLECTED IRRADIANCE	1.85	.282357937
MID CANOPY REFLECTED IRRADIANCE	1.56	.19583035
BOT CANOPY REFLECTED IRRADIANCE	1.44	.168313906

WEEK NUMBER 5

SPECIES NUMBER 3

SENSOR POSITION	NUMBER OF PAPERS	EINSTEINS/M^2
ABV CANOPY INCIDENT IRRADIANCE	7.61	404.836816
TOP CANOPY INCIDENT IRRADIANCE	6.38	85.7511592
MID CANOPY INCIDENT IRRADIANCE	5.23	20.0927787
BOT CANOPY INCIDENT IRRADIANCE	4.36	6.70316639
GROUND INCIDENT IRRADIANCE	4.27	5.98356481
TOP CANOPY REFLECTED IRRADIANCE	2.57	.700422357
MID CANOPY REFLECTED IRRADIANCE	1.98	.332690193
BOT CANOPY REFLECTED IRRADIANCE	1.71	.236635555

WEEK NUMBER 6

SPECIES NUMBER 3

SENSOR POSITION	NUMBER OF PAPERS	EINSTEINS/M^2
ABV CANOPY INCIDENT IRRADIANCE	7.21	244.388069
TOP CANOPY INCIDENT IRRADIANCE	5.75	38.7257645
MID CANOPY INCIDENT IRRADIANCE	4.83	12.129419
BOT CANOPY INCIDENT IRRADIANCE	3.95	3.99576557
GROUND INCIDENT IRRADIANCE	4.56	8.62740129
TOP CANOPY REFLECTED IRRADIANCE	2.24	.461870261
MID CANOPY REFLECTED IRRADIANCE	1.66	.22216723
BOT CANOPY REFLECTED IRRADIANCE	1.63	.21391439

WEEK NUMBER 2

SPECIES NUMBER 4

SENSOR POSITION	NUMBER OF PAPERS	EINSTEINS/M^2
ABV CANOPY INCIDENT IRRADIANCE	7.44	326.678085
TOP CANOPY INCIDENT IRRADIANCE	4.97	14.4730479
MID CANOPY INCIDENT IRRADIANCE	4.55	8.51922327
BOT CANOPY INCIDENT IRRADIANCE	4.11	4.88967506
GROUND INCIDENT IRRADIANCE	4.05	4.53314906
TOP CANOPY REFLECTED IRRADIANCE	2.03	.35435617
MID CANOPY REFLECTED IRRADIANCE	1.79	.261770076
BOT CANOPY REFLECTED IRRADIANCE	1.48	.1770272

WEEK NUMBER 3

SPECIES NUMBER 4

SENSOR POSITION	NUMBER OF PAPERS	EINSTEINS/M^2
ABV CANOPY INCIDENT IRRADIANCE	7.39	306.704396
TOP CANOPY INCIDENT IRRADIANCE	4.92	13.5881396
MID CANOPY INCIDENT IRRADIANCE	4.71	10.4250945
BOT CANOPY INCIDENT IRRADIANCE	4.31	6.29332266
GROUND INCIDENT IRRADIANCE	4.12	4.95176471
TOP CANOPY REFLECTED IRRADIANCE	2.09	.382225801
MID CANOPY REFLECTED IRRADIANCE	1.84	.278817481
BOT CANOPY REFLECTED IRRADIANCE	1.53	.188555845

WEEK NUMBER 4

SPECIES NUMBER 4

SENSOR POSITION	NUMBER OF PAPERS	EINSTEINS/M^2
ABV CANOPY INCIDENT IRRADIANCE	6.92	169.496213
TOP CANOPY INCIDENT IRRADIANCE	4.45	7.50930941
MID CANOPY INCIDENT IRRADIANCE	4.41	7.13970059
BOT CANOPY INCIDENT IRRADIANCE	4.31	6.29332266
GROUND INCIDENT IRRADIANCE	4.08	4.70803844
TOP CANOPY REFLECTED IRRADIANCE	1.73	.24268336
MID CANOPY REFLECTED IRRADIANCE	1.48	.1770272
BOT CANOPY REFLECTED IRRADIANCE	1.18	.121238345

WEEK NUMBER 5

SPECIES NUMBER 4

SENSOR POSITION	NUMBER OF PAPERS	EINSTEINS/M^2
ABV CANOPY INCIDENT IRRADIANCE	6.77	140.268451
TOP CANOPY INCIDENT IRRADIANCE	4.31	6.29332266
MID CANOPY INCIDENT IRRADIANCE	4.26	5.90853755
BOT CANOPY INCIDENT IRRADIANCE	4.23	5.68905327
GROUND INCIDENT IRRADIANCE	3.92	3.84733497
TOP CANOPY REFLECTED IRRADIANCE	1.95	.32033176
MID CANOPY REFLECTED IRRADIANCE	1.78	.25848777
BOT CANOPY REFLECTED IRRADIANCE	1.39	.15802289

WEEK NUMBER 6

SPECIES NUMBER 4

SENSOR POSITION	NUMBER OF PAPERS	EINSTEINS/M^2
ABV CANOPY INCIDENT IRRADIANCE	7.04	197.205944
TOP CANOPY INCIDENT IRRADIANCE	4.56	8.62740129
MID CANOPY INCIDENT IRRADIANCE	4.47	7.70122835
BOT CANOPY INCIDENT IRRADIANCE	4.32	6.37323598
GROUND INCIDENT IRRADIANCE	4.24	5.7612935
TOP CANOPY REFLECTED IRRADIANCE	2.06	.36802727
MID CANOPY REFLECTED IRRADIANCE	1.81	.268460256
BOT CANOPY REFLECTED IRRADIANCE	1.47	.174807475

SPECIES KEY

1=LARIX DECIDUA
2=PSEUDOTSUGA MENZIESII
3=PINUS CONTORTA
4=NOTHOFAGUS SOLANDRI

WEEKLY DATA KEY

7= 07/4 TO 14/4
8= 28/4 TO 05/5
9= 12/5 TO 19/5
10= 16/6 TO 23/6

WEEK NUMBER 7

SPECIES NUMBER 1

SENSOR POSITION	NUMBER OF PAPERS	EINSTEINS/M^2
ABV CANOPY INCIDENT IRRADIANCE	6.72	137.873246
TOP CANOPY INCIDENT IRRADIANCE	5.87	48.4819412
MID CANOPY INCIDENT IRRADIANCE	5.25	22.6203854
BOT CANOPY INCIDENT IRRADIANCE	4.93	15.2623005
GROUND INCIDENT IRRADIANCE	4.93	15.2623005
TOP CANOPY REFLECTED IRRADIANCE	2.99	1.40494719
MID CANOPY REFLECTED IRRADIANCE	2.56	.828018425
BOT CANOPY REFLECTED IRRADIANCE	2.25	.565587757

WEEK NUMBER 8

SPECIES NUMBER 1

SENSOR POSITION	NUMBER OF PAPERS	EINSTEINS/M^2
ABV CANOPY INCIDENT IRRADIANCE	6.42	95.3410651
TOP CANOPY INCIDENT IRRADIANCE	5.37	26.2168193
MID CANOPY INCIDENT IRRADIANCE	5.17	20.5012339
BOT CANOPY INCIDENT IRRADIANCE	4.63	10.5540707
GROUND INCIDENT IRRADIANCE	4.63	10.5540707
TOP CANOPY REFLECTED IRRADIANCE	3.18	1.77467978
MID CANOPY REFLECTED IRRADIANCE	2.58	.848633165
BOT CANOPY REFLECTED IRRADIANCE	2.34	.631771456

WEEK NUMBER 9

SPECIES NUMBER 1

SENSOR POSITION	NUMBER OF PAPERS	EINSTEINS/M^2
ABV CANOPY INCIDENT IRRADIANCE	6.37	89.6561325
TOP CANOPY INCIDENT IRRADIANCE	5.68	38.3813283
MID CANOPY INCIDENT IRRADIANCE	5.13	19.5173118
BOT CANOPY INCIDENT IRRADIANCE	5.13	19.5173118
GROUND INCIDENT IRRADIANCE	5.11	19.0432031
TOP CANOPY REFLECTED IRRADIANCE	3.25	1.93419386
MID CANOPY REFLECTED IRRADIANCE	3.07	1.5501724
BOT CANOPY REFLECTED IRRADIANCE	2.97	1.37081864

WEEK NUMBER 7

SPECIES NUMBER 2

SENSOR POSITION	NUMBER OF PAPERS	EINSTEINS/M^2
ABV CANOPY INCIDENT IRRADIANCE	6.72	137.873246
TOP CANOPY INCIDENT IRRADIANCE	3.94	5.37874201
MID CANOPY INCIDENT IRRADIANCE	3.34	3.1772478
BOT CANOPY INCIDENT IRRADIANCE	2.68	1.81069011
GROUND INCIDENT IRRADIANCE	2.48	1.41593765
TOP CANOPY REFLECTED IRRADIANCE	1.13	.169879398
MID CANOPY REFLECTED IRRADIANCE	1.09	.199779576
BOT CANOPY REFLECTED IRRADIANCE	1.13	.26924282

WEEK NUMBER 8

SPECIES NUMBER 2

SENSOR POSITION	NUMBER OF PAPERS	EINSTEINS/M^2
ABV CANOPY INCIDENT IRRADIANCE	6.42	95.3410651
TOP CANOPY INCIDENT IRRADIANCE	3.43	2.87303366
MID CANOPY INCIDENT IRRADIANCE	3.11	2.39458958
BOT CANOPY INCIDENT IRRADIANCE	2.24	1.05410562
GROUND INCIDENT IRRADIANCE	2.42	1.31523734
TOP CANOPY REFLECTED IRRADIANCE	1.12	.167803384
MID CANOPY REFLECTED IRRADIANCE	1.03	.185571419
BOT CANOPY REFLECTED IRRADIANCE	1.05	.244019274

WEEK NUMBER 9

SPECIES NUMBER 2

SENSOR POSITION	NUMBER OF PAPERS	EINSTEINS/M^2
ABV CANOPY INCIDENT IRRADIANCE	6.37	89.6561325
TOP CANOPY INCIDENT IRRADIANCE	3.29	2.41869282
MID CANOPY INCIDENT IRRADIANCE	3.15	2.51530751
BOT CANOPY INCIDENT IRRADIANCE	2.61	1.66136146
GROUND INCIDENT IRRADIANCE	2.24	1.05410562
TOP CANOPY REFLECTED IRRADIANCE	1.21	.187439326
MID CANOPY REFLECTED IRRADIANCE	1.05	.190191493
BOT CANOPY REFLECTED IRRADIANCE	1.04	.241037232

WEEK NUMBER 10

SPECIES NUMBER 2

SENSOR POSITION	NUMBER OF PAPERS	EINSTEINS/M^2
ABV CANOPY INCIDENT IRRADIANCE	6.08	62.7653566
TOP CANOPY INCIDENT IRRADIANCE	3.67	3.85923046
MID CANOPY INCIDENT IRRADIANCE	2.48	1.10359846
BOT CANOPY INCIDENT IRRADIANCE	2.23	1.0412239
GROUND INCIDENT IRRADIANCE	1.99	.775147107
TOP CANOPY REFLECTED IRRADIANCE	1.17	.178443492
MID CANOPY REFLECTED IRRADIANCE	1.07	.194926591
BOT CANOPY REFLECTED IRRADIANCE	1.08	.25318959

WEEK NUMBER 7

SPECIES NUMBER 3

SENSOR POSITION	NUMBER OF PAPERS	EINSTEINS/M^2
ABV CANOPY INCIDENT IRRADIANCE	6.72	137.873246
TOP CANOPY INCIDENT IRRADIANCE	5.98	55.5034528
MID CANOPY INCIDENT IRRADIANCE	4.62	10.4250945
BOT CANOPY INCIDENT IRRADIANCE	3.56	2.83165279
GROUND INCIDENT IRRADIANCE	3.99	4.80463058
TOP CANOPY REFLECTED IRRADIANCE	2.13	.4880002
MID CANOPY REFLECTED IRRADIANCE	1.44	.208910371
BOT CANOPY REFLECTED IRRADIANCE	1.51	.227687926

WEEK NUMBER 8

SPECIES NUMBER 3

SENSOR POSITION	NUMBER OF PAPERS	EINSTEINS/M^2
ABV CANOPY INCIDENT IRRADIANCE	6.42	95.3410651
TOP CANOPY INCIDENT IRRADIANCE	5.29	23.7607421
MID CANOPY INCIDENT IRRADIANCE	4.14	5.77776669
BOT CANOPY INCIDENT IRRADIANCE	3.31	2.08228418
GROUND INCIDENT IRRADIANCE	3.39	2.2975237
TOP CANOPY REFLECTED IRRADIANCE	1.86	.350138608
MID CANOPY REFLECTED IRRADIANCE	1.14	.144464121
BOT CANOPY REFLECTED IRRADIANCE	1.18	.15174696

WEEK NUMBER 9

SPECIES NUMBER 3

SENSOR POSITION	NUMBER OF PAPERS	EINSTEINS/M^2
ABV CANOPY INCIDENT IRRADIANCE	6.37	89.6561325
TOP CANOPY INCIDENT IRRADIANCE	5.22	21.80118
MID CANOPY INCIDENT IRRADIANCE	3.91	4.35451709
BOT CANOPY INCIDENT IRRADIANCE	3.22	1.86414633
GROUND INCIDENT IRRADIANCE	3.32	2.1080456
TOP CANOPY REFLECTED IRRADIANCE	1.72	.294767773
MID CANOPY REFLECTED IRRADIANCE	1.11	.139232301
BOT CANOPY REFLECTED IRRADIANCE	1.19	.153624329

WEEK NUMBER 10

SPECIES NUMBER 3

SENSOR POSITION	NUMBER OF PAPERS	EINSTEINS/M^2
ABV CANOPY INCIDENT IRRADIANCE	6.08	62.7653566
TOP CANOPY INCIDENT IRRADIANCE	5.43	28.2240934
MID CANOPY INCIDENT IRRADIANCE	3.39	2.2975237
BOT CANOPY INCIDENT IRRADIANCE	3.02	1.45773976
GROUND INCIDENT IRRADIANCE	2.81	1.12600417
TOP CANOPY REFLECTED IRRADIANCE	1.57	.245120707
MID CANOPY REFLECTED IRRADIANCE	1.15	.146251389
BOT CANOPY REFLECTED IRRADIANCE	1.21	.157449034

WEEK NUMBER 8

SPECIES NUMBER 4

SENSOR POSITION	NUMBER OF PAPERS	EINSTEINS/M^2
ABV CANOPY INCIDENT IRRADIANCE	6.02	58.3015364
TOP CANOPY INCIDENT IRRADIANCE	3.51	2.6628089
MID CANOPY INCIDENT IRRADIANCE	3.31	2.08228418
BOT CANOPY INCIDENT IRRADIANCE	3.32	2.1080456
GROUND INCIDENT IRRADIANCE	3.17	1.75299227
TOP CANOPY REFLECTED IRRADIANCE	1.14	.144464121
MID CANOPY REFLECTED IRRADIANCE	1.09	.135850112
BOT CANOPY REFLECTED IRRADIANCE	1.06	.130930251

WEEK NUMBER 9

SPECIES NUMBER 4

SENSOR POSITION	NUMBER OF PAPERS	EINSTEINS/M^2
ABV CANOPY INCIDENT IRRADIANCE	6.09	63.5418713
TOP CANOPY INCIDENT IRRADIANCE	3.61	3.01120276
MID CANOPY INCIDENT IRRADIANCE	3.41	2.35472394
BOT CANOPY INCIDENT IRRADIANCE	3.39	2.2975237
GROUND INCIDENT IRRADIANCE	3.31	2.08228418
TOP CANOPY REFLECTED IRRADIANCE	1.11	.139232301
MID CANOPY REFLECTED IRRADIANCE	1.09	.135850112
BOT CANOPY REFLECTED IRRADIANCE	1.07	.132550082

300-3000 nm irradiance (S.W.) data summary.
The number of papers exposed is transformed into energy units (Mega-Joules $m^{-2}wk^{-1}$) using the appropriate log functions from tables 3.11 and 3.12.

SPECIES KEY

1=LARIX DECIDUA
2=PSEUDOTSUGA MENZIESII
3=PINUS CONTORTA
4=NOTHOFAGUS SOLANDRI

WEEKLY DATA KEY

1= 03/2 TO 10/2
2= 10/2 TO 17/2
3= 17/2 TO 24/2
4= 24/2 TO 03/3
5= 03/3 TO 10/3
6= 24/3 TO 31/3

WEEK NUMBER 1

SPECIES NUMBER 1

SENSOR POSITION	NUMBER OF PAPERS	MEGA-JOULES/M^2
ABV CANOPY INCIDENT IRRADIANCE	7.83	181.890493
TOP CANOPY INCIDENT IRRADIANCE	6.71	49.2005547
MID CANOPY INCIDENT IRRADIANCE	5.96	20.4984017
BOT CANOPY INCIDENT IRRADIANCE	5.43	11.0410404
GROUND INCIDENT IRRADIANCE	5.41	10.786238
TOP CANOPY REFLECTED IRRADIANCE	3.08	.710493321
MID CANOPY REFLECTED IRRADIANCE	2.98	.632208019
BOT CANOPY REFLECTED IRRADIANCE	2.66	.435130975

WEEK NUMBER 2

SPECIES NUMBER 1

SENSOR POSITION	NUMBER OF PAPERS	MEGA-JOULES/M^2
ABV CANOPY INCIDENT IRRADIANCE	7.82	179.77943
TOP CANOPY INCIDENT IRRADIANCE	6.55	40.8178383
MID CANOPY INCIDENT IRRADIANCE	6.07	23.3071945
BOT CANOPY INCIDENT IRRADIANCE	5.59	13.3085273
GROUND INCIDENT IRRADIANCE	5.21	8.5402385
TOP CANOPY REFLECTED IRRADIANCE	3.27	.886931339
MID CANOPY REFLECTED IRRADIANCE	3.06	.694096733
BOT CANOPY REFLECTED IRRADIANCE	2.86	.549566182

WEEK NUMBER 3

SPECIES NUMBER 1

SENSOR POSITION	NUMBER OF PAPERS	MEGA-JOULES/M^2
ABV CANOPY INCIDENT IRRADIANCE	7.63	144.015753
TOP CANOPY INCIDENT IRRADIANCE	6.52	39.413046
MID CANOPY INCIDENT IRRADIANCE	5.77	16.420637
BOT CANOPY INCIDENT IRRADIANCE	5.24	8.84463673
GROUND INCIDENT IRRADIANCE	5.24	8.84463673
TOP CANOPY REFLECTED IRRADIANCE	2.87	.556019471
MID CANOPY REFLECTED IRRADIANCE	2.81	.518405977
BOT CANOPY REFLECTED IRRADIANCE	2.47	.348569995

WEEK NUMBER 4

SPECIES NUMBER 1

SENSOR POSITION	NUMBER OF PAPERS	MEGA-JOULES/M^2
ABV CANOPY INCIDENT IRRADIANCE	7.29	96.8344746
TOP CANOPY INCIDENT IRRADIANCE	6.01	21.730514
MID CANOPY INCIDENT IRRADIANCE	5.41	10.786238
BOT CANOPY INCIDENT IRRADIANCE	4.89	5.87800567
GROUND INCIDENT IRRADIANCE	4.85	5.60983387
TOP CANOPY REFLECTED IRRADIANCE	2.78	.500564446
MID CANOPY REFLECTED IRRADIANCE	2.48	.352663083
BOT CANOPY REFLECTED IRRADIANCE	2.18	.248462013

WEEK NUMBER 5

SPECIES NUMBER 1

SENSOR POSITION	NUMBER OF PAPERS	MEGA-JOULES/M^2
ABV CANOPY INCIDENT IRRADIANCE	7.61	140.692193
TOP CANOPY INCIDENT IRRADIANCE	6.38	33.4703304
MID CANOPY INCIDENT IRRADIANCE	5.57	13.0013964
BOT CANOPY INCIDENT IRRADIANCE	5.21	8.5402385
GROUND INCIDENT IRRADIANCE	5.21	8.5402385
TOP CANOPY REFLECTED IRRADIANCE	3.28	.897346141
MID CANOPY REFLECTED IRRADIANCE	3.04	.67807854
BOT CANOPY REFLECTED IRRADIANCE	2.78	.500564446

WEEK NUMBER 6

SPECIES NUMBER 1

SENSOR POSITION	NUMBER OF PAPERS	MEGA-JOULES/M^2
ABV CANOPY INCIDENT IRRADIANCE	7.21	88.2002873
TOP CANOPY INCIDENT IRRADIANCE	5.78	16.6134565
MID CANOPY INCIDENT IRRADIANCE	5.63	13.9447264
BOT CANOPY INCIDENT IRRADIANCE	5.23	8.74198386
GROUND INCIDENT IRRADIANCE	4.96	6.37852115
TOP CANOPY REFLECTED IRRADIANCE	3.21	.826932383
MID CANOPY REFLECTED IRRADIANCE	2.91	.582599356
BOT CANOPY REFLECTED IRRADIANCE	2.46	.344524412

WEEK NUMBER 1

SPECIES NUMBER 2

SENSOR POSITION	NUMBER OF PAPERS	MEGA-JOULES/M^2
ABV CANOPY INCIDENT IRRADIANCE	7.83	181.890493
TOP CANOPY INCIDENT IRRADIANCE	4.91	7.16293011
MID CANOPY INCIDENT IRRADIANCE	4.32	4.4435604
BOT CANOPY INCIDENT IRRADIANCE	3.68	2.70074842
GROUND INCIDENT IRRADIANCE	2.61	.774451331
TOP CANOPY REFLECTED IRRADIANCE	2.13	.279017031
MID CANOPY REFLECTED IRRADIANCE	2.09	.328943332
BOT CANOPY REFLECTED IRRADIANCE	2.11	.432010329

WEEK NUMBER 2

SPECIES NUMBER 2

SENSOR POSITION	NUMBER OF PAPERS	MEGA-JOULES/M^2
ABV CANOPY INCIDENT IRRADIANCE	7.82	179.77943
TOP CANOPY INCIDENT IRRADIANCE	5.03	8.24006646
MID CANOPY INCIDENT IRRADIANCE	4.44	5.11176745
BOT CANOPY INCIDENT IRRADIANCE	3.79	3.07081838
GROUND INCIDENT IRRADIANCE	2.41	.613188682
TOP CANOPY REFLECTED IRRADIANCE	2.21	.306330835
MID CANOPY REFLECTED IRRADIANCE	2.19	.369675856
BOT CANOPY REFLECTED IRRADIANCE	2.21	.485505474

WEEK NUMBER 3

SPECIES NUMBER 2

SENSOR POSITION	NUMBER OF PAPERS	MEGA-JOULES/M^2
ABV CANOPY INCIDENT IRRADIANCE	7.63	144.015753
TOP CANOPY INCIDENT IRRADIANCE	4.81	6.37368672
MID CANOPY INCIDENT IRRADIANCE	4.22	3.95394922
BOT CANOPY INCIDENT IRRADIANCE	3.61	2.48882368
GROUND INCIDENT IRRADIANCE	2.59	.756578734
TOP CANOPY REFLECTED IRRADIANCE	2.03	.248273698
MID CANOPY REFLECTED IRRADIANCE	1.99	.292698898
BOT CANOPY REFLECTED IRRADIANCE	2.02	.388923451

WEEK NUMBER 4

SPECIES NUMBER 2

SENSOR POSITION	NUMBER OF PAPERS	MEGA-JOULES/M^2
ABV CANOPY INCIDENT IRRADIANCE	7.29	96.8344746
TOP CANOPY INCIDENT IRRADIANCE	4.51	4.49045877
MID CANOPY INCIDENT IRRADIANCE	3.92	2.78567911
BOT CANOPY INCIDENT IRRADIANCE	3.27	1.67345536
GROUND INCIDENT IRRADIANCE	2.34	.565072445
TOP CANOPY REFLECTED IRRADIANCE	1.69	.166936273
MID CANOPY REFLECTED IRRADIANCE	1.67	.201456409
BOT CANOPY REFLECTED IRRADIANCE	1.65	.252507412

WEEK NUMBER 5

SPECIES NUMBER 2

SENSOR POSITION	NUMBER OF PAPERS	MEGA-JOULES/M^2
ABV CANOPY INCIDENT IRRADIANCE	7.61	140.692193
TOP CANOPY INCIDENT IRRADIANCE	4.51	4.49045877
MID CANOPY INCIDENT IRRADIANCE	4.04	3.20457978
BOT CANOPY INCIDENT IRRADIANCE	3.58	2.40316799
GROUND INCIDENT IRRADIANCE	3.21	1.56024978
TOP CANOPY REFLECTED IRRADIANCE	2.02	.245392177
MID CANOPY REFLECTED IRRADIANCE	2.97	.91892716
BOT CANOPY REFLECTED IRRADIANCE	2.01	.384409516

WEEK NUMBER 6

SPECIES NUMBER 2

SENSOR POSITION	NUMBER OF PAPERS	MEGA-JOULES/M^2
ABV CANOPY INCIDENT IRRADIANCE	7.21	88.2002873
TOP CANOPY INCIDENT IRRADIANCE	4.21	3.16366663
MID CANOPY INCIDENT IRRADIANCE	3.63	1.98564262
BOT CANOPY INCIDENT IRRADIANCE	2.86	1.03691733
GROUND INCIDENT IRRADIANCE	2.77	.933499588
TOP CANOPY REFLECTED IRRADIANCE	1.18	.0920408698
MID CANOPY REFLECTED IRRADIANCE	1.06	.0988350729
BOT CANOPY REFLECTED IRRADIANCE	1.14	.139220802

WEEK NUMBER 1

SPECIES NUMBER 3

SENSOR POSITION	NUMBER OF PAPERS	MEGA-JOULES/M^2
ABV CANOPY INCIDENT IRRADIANCE	7.83	181.890493
TOP CANOPY INCIDENT IRRADIANCE	6.66	46.4109011
MID CANOPY INCIDENT IRRADIANCE	5.78	16.6134565
BOT CANOPY INCIDENT IRRADIANCE	4.76	5.05033282
GROUND INCIDENT IRRADIANCE	4.71	4.76398077
TOP CANOPY REFLECTED IRRADIANCE	2.65	.430080746
MID CANOPY REFLECTED IRRADIANCE	2.21	.257317901
BOT CANOPY REFLECTED IRRADIANCE	1.86	.171009407

WEEK NUMBER 2

SPECIES NUMBER 3

SENSOR POSITION	NUMBER OF PAPERS	MEGA-JOULES/M^2
ABV CANOPY INCIDENT IRRADIANCE	7.82	179.77943
TOP CANOPY INCIDENT IRRADIANCE	6.63	44.8136173
MID CANOPY INCIDENT IRRADIANCE	5.61	13.6229135
BOT CANOPY INCIDENT IRRADIANCE	4.57	4.04566576
GROUND INCIDENT IRRADIANCE	4.32	3.02162107
TOP CANOPY REFLECTED IRRADIANCE	2.51	.365232991
MID CANOPY REFLECTED IRRADIANCE	2.29	.282507512
BOT CANOPY REFLECTED IRRADIANCE	2.08	.221085368

WEEK NUMBER 3

SPECIES NUMBER 3

SENSOR POSITION	NUMBER OF PAPERS	MEGA-JOULES/M^2
ABV CANOPY INCIDENT IRRADIANCE	7.63	144.015753
TOP CANOPY INCIDENT IRRADIANCE	6.47	37.1783404
MID CANOPY INCIDENT IRRADIANCE	5.58	13.1540655
BOT CANOPY INCIDENT IRRADIANCE	4.57	4.04566576
GROUND INCIDENT IRRADIANCE	4.39	3.27891381
TOP CANOPY REFLECTED IRRADIANCE	2.37	.310163008
MID CANOPY REFLECTED IRRADIANCE	2.02	.206129429
BOT CANOPY REFLECTED IRRADIANCE	1.68	.138598969

WEEK NUMBER 4

SPECIES NUMBER 3

SENSOR POSITION	NUMBER OF PAPERS	MEGA-JOULES/M^2
ABV CANOPY INCIDENT IRRADIANCE	7.29	96.8344746
TOP CANOPY INCIDENT IRRADIANCE	5.92	19.5632047
MID CANOPY INCIDENT IRRADIANCE	5.04	7.00293347
BOT CANOPY INCIDENT IRRADIANCE	4.43	3.43565859
GROUND INCIDENT IRRADIANCE	4.11	2.36466705
TOP CANOPY REFLECTED IRRADIANCE	1.85	.169024632
MID CANOPY REFLECTED IRRADIANCE	1.56	.120481399
BOT CANOPY REFLECTED IRRADIANCE	1.44	.104732145

WEEK NUMBER 5

SPECIES NUMBER 3

SENSOR POSITION	NUMBER OF PAPERS	MEGA-JOULES/M^2
ABV CANOPY INCIDENT IRRADIANCE	7.61	140.692193
TOP CANOPY INCIDENT IRRADIANCE	6.38	33.4703304
MID CANOPY INCIDENT IRRADIANCE	5.23	8.74198386
BOT CANOPY INCIDENT IRRADIANCE	4.36	3.16606626
GROUND INCIDENT IRRADIANCE	4.27	2.85029624
TOP CANOPY REFLECTED IRRADIANCE	2.57	.391732857
MID CANOPY REFLECTED IRRADIANCE	1.98	.196725202
BOT CANOPY REFLECTED IRRADIANCE	1.71	.143539028

WEEK NUMBER 6

SPECIES NUMBER 3

SENSOR POSITION	NUMBER OF PAPERS	MEGA-JOULES/M^2
ABV CANOPY INCIDENT IRRADIANCE	7.21	88.2002873
TOP CANOPY INCIDENT IRRADIANCE	5.75	16.0416856
MID CANOPY INCIDENT IRRADIANCE	4.83	5.48037151
BOT CANOPY INCIDENT IRRADIANCE	3.95	1.96177863
GROUND INCIDENT IRRADIANCE	4.56	3.99871083
TOP CANOPY REFLECTED IRRADIANCE	2.24	.266489438
MID CANOPY REFLECTED IRRADIANCE	1.66	.135400416
BOT CANOPY REFLECTED IRRADIANCE	1.63	.130740457

WEEK NUMBER 2

SPECIES NUMBER 4

SENSOR POSITION	NUMBER OF PAPERS	MEGA-JOULES/M^2
ABV CANOPY INCIDENT IRRADIANCE	7.44	115.366575
TOP CANOPY INCIDENT IRRADIANCE	4.97	6.45342104
MID CANOPY INCIDENT IRRADIANCE	4.55	3.95230089
BOT CANOPY INCIDENT IRRADIANCE	4.11	2.36466705
GROUND INCIDENT IRRADIANCE	4.05	2.20470253
TOP CANOPY REFLECTED IRRADIANCE	2.03	.208549907
MID CANOPY REFLECTED IRRADIANCE	1.79	.157590488
BOT CANOPY REFLECTED IRRADIANCE	1.48	.109738748

WEEK NUMBER 3

SPECIES NUMBER 4

SENSOR POSITION	NUMBER OF PAPERS	MEGA-JOULES/M^2
ABV CANOPY INCIDENT IRRADIANCE	7.39	108.825332
TOP CANOPY INCIDENT IRRADIANCE	4.92	6.08751438
MID CANOPY INCIDENT IRRADIANCE	4.71	4.76398077
BOT CANOPY INCIDENT IRRADIANCE	4.31	2.98655144
GROUND INCIDENT IRRADIANCE	4.12	2.39243419
TOP CANOPY REFLECTED IRRADIANCE	2.09	.223681466
MID CANOPY REFLECTED IRRADIANCE	1.84	.167062894
BOT CANOPY REFLECTED IRRADIANCE	1.53	.116334894

WEEK NUMBER 4

SPECIES NUMBER 4

SENSOR POSITION	NUMBER OF PAPERS	MEGA-JOULES/M^2
ABV CANOPY INCIDENT IRRADIANCE	6.92	62.869499
TOP CANOPY INCIDENT IRRADIANCE	4.45	3.51681886
MID CANOPY INCIDENT IRRADIANCE	4.41	3.35637131
BOT CANOPY INCIDENT IRRADIANCE	4.31	2.98655144
GROUND INCIDENT IRRADIANCE	4.08	2.28328435
TOP CANOPY REFLECTED IRRADIANCE	1.73	.146929838
MID CANOPY REFLECTED IRRADIANCE	1.48	.109738748
BOT CANOPY REFLECTED IRRADIANCE	1.18	.0773143306

WEEK NUMBER 5

SPECIES NUMBER 4

SENSOR POSITION	NUMBER OF PAPERS	MEGA-JOULES/M^2
ABV CANOPY INCIDENT IRRADIANCE	6.77	52.770353
TOP CANOPY INCIDENT IRRADIANCE	4.31	2.98655144
MID CANOPY INCIDENT IRRADIANCE	4.26	2.81721505
BOT CANOPY INCIDENT IRRADIANCE	4.23	2.7202574
GROUND INCIDENT IRRADIANCE	3.92	1.89426179
TOP CANOPY REFLECTED IRRADIANCE	1.95	.189954681
MID CANOPY REFLECTED IRRADIANCE	1.78	.155761457
BOT CANOPY REFLECTED IRRADIANCE	1.39	.0987938704

WEEK NUMBER 6

SPECIES NUMBER 4

SENSOR POSITION	NUMBER OF PAPERS	MEGA-JOULES/M^2
ABV CANOPY INCIDENT IRRADIANCE	7.04	72.3235942
TOP CANOPY INCIDENT IRRADIANCE	4.56	3.99871083
MID CANOPY INCIDENT IRRADIANCE	4.47	3.59989638
BOT CANOPY INCIDENT IRRADIANCE	4.32	3.02162107
GROUND INCIDENT IRRADIANCE	4.24	2.75220006
TOP CANOPY REFLECTED IRRADIANCE	2.06	.215983214
MID CANOPY REFLECTED IRRADIANCE	1.81	.161313235
BOT CANOPY REFLECTED IRRADIANCE	1.47	.108465095

SPECIES KEY

1=LARIX DECIDUA
2=PSEUDOTSUGA MENZIESII
3=PINUS CONTORTA
4=NOTHOFAGUS SOLANDRI

WEEKLY DATA KEY

7= 07/4 TO 14/4
8= 28/4 TO 05/5
9= 12/5 TO 19/5
10= 16/6 TO 23/6

WEEK NUMBER 7

SPECIES NUMBER 1

SENSOR POSITION	NUMBER OF PAPERS	MEGA-JOULES/M^2
ABV CANOPY INCIDENT IRRADIANCE	6.72	72.011192
TOP CANOPY INCIDENT IRRADIANCE	5.87	26.0255551
MID CANOPY INCIDENT IRRADIANCE	5.25	12.3879659
BOT CANOPY INCIDENT IRRADIANCE	4.93	8.44500674
GROUND INCIDENT IRRADIANCE	4.93	8.44500674
TOP CANOPY REFLECTED IRRADIANCE	2.99	.827560971
MID CANOPY REFLECTED IRRADIANCE	2.56	.494538379
BOT CANOPY REFLECTED IRRADIANCE	2.25	.341192912

WEEK NUMBER 8

SPECIES NUMBER 1

SENSOR POSITION	NUMBER OF PAPERS	MEGA-JOULES/M^2
ABV CANOPY INCIDENT IRRADIANCE	6.42	50.2805477
TOP CANOPY INCIDENT IRRADIANCE	5.37	14.3021063
MID CANOPY INCIDENT IRRADIANCE	5.17	11.2564125
BOT CANOPY INCIDENT IRRADIANCE	4.63	5.89657735
GROUND INCIDENT IRRADIANCE	4.63	5.89657735
TOP CANOPY REFLECTED IRRADIANCE	3.18	1.03896281
MID CANOPY REFLECTED IRRADIANCE	2.58	.506523968
BOT CANOPY REFLECTED IRRADIANCE	2.34	.380014353

WEEK NUMBER 9

SPECIES NUMBER 1

SENSOR POSITION	NUMBER OF PAPERS	MEGA-JOULES/M^2
ABV CANOPY INCIDENT IRRADIANCE	6.37	47.358725
TOP CANOPY INCIDENT IRRADIANCE	5.68	20.7300333
MID CANOPY INCIDENT IRRADIANCE	5.13	10.7300069
BOT CANOPY INCIDENT IRRADIANCE	5.13	10.7300069
GROUND INCIDENT IRRADIANCE	5.11	10.4761088
TOP CANOPY REFLECTED IRRADIANCE	3.25	1.12979592
MID CANOPY REFLECTED IRRADIANCE	3.07	.910751721
BOT CANOPY REFLECTED IRRADIANCE	2.97	.807978865

WEEK NUMBER 7

SPECIES NUMBER 2

SENSOR POSITION	NUMBER OF PAPERS	MEGA-JOULES/M^2
ABV CANOPY INCIDENT IRRADIANCE	6.72	72.011192
TOP CANOPY INCIDENT IRRADIANCE	3.94	3.07270392
MID CANOPY INCIDENT IRRADIANCE	3.34	1.85050852
BOT CANOPY INCIDENT IRRADIANCE	2.68	1.07726892
GROUND INCIDENT IRRADIANCE	2.48	.847859968
TOP CANOPY REFLECTED IRRADIANCE	1.13	.106247988
MID CANOPY REFLECTED IRRADIANCE	1.09	.12510973
BOT CANOPY REFLECTED IRRADIANCE	1.13	.168393037

WEEK NUMBER 8

SPECIES NUMBER 2

SENSOR POSITION	NUMBER OF PAPERS	MEGA-JOULES/M^2
ABV CANOPY INCIDENT IRRADIANCE	6.42	50.2805477
TOP CANOPY INCIDENT IRRADIANCE	3.43	1.66847888
MID CANOPY INCIDENT IRRADIANCE	3.11	1.40504776
BOT CANOPY INCIDENT IRRADIANCE	2.24	.636098148
GROUND INCIDENT IRRADIANCE	2.42	.789085624
TOP CANOPY REFLECTED IRRADIANCE	1.12	.10498342
MID CANOPY REFLECTED IRRADIANCE	1.03	.116437022
BOT CANOPY REFLECTED IRRADIANCE	1.05	.15301152

WEEK NUMBER 9

SPECIES NUMBER 2

SENSOR POSITION	NUMBER OF PAPERS	MEGA-JOULES/M^2
ABV CANOPY INCIDENT IRRADIANCE	6.37	47.358725
TOP CANOPY INCIDENT IRRADIANCE	3.29	1.41097954
MID CANOPY INCIDENT IRRADIANCE	3.15	1.47397829
BOT CANOPY INCIDENT IRRADIANCE	2.61	.990658867
GROUND INCIDENT IRRADIANCE	2.24	.636098148
TOP CANOPY REFLECTED IRRADIANCE	1.21	.11692859
MID CANOPY REFLECTED IRRADIANCE	1.05	.119258979
BOT CANOPY REFLECTED IRRADIANCE	1.04	.15119037

WEEK NUMBER 10

SPECIES NUMBER 2

SENSOR POSITION	NUMBER OF PAPERS	MEGA-JOULES/M^2
ABV CANOPY INCIDENT IRRADIANCE	6.08	33.4657067
TOP CANOPY INCIDENT IRRADIANCE	3.67	2.22392796
MID CANOPY INCIDENT IRRADIANCE	2.48	.660832034
BOT CANOPY INCIDENT IRRADIANCE	2.23	.628527278
GROUND INCIDENT IRRADIANCE	1.99	.471546071
TOP CANOPY REFLECTED IRRADIANCE	1.17	.11146043
MID CANOPY REFLECTED IRRADIANCE	1.07	.122149329
BOT CANOPY REFLECTED IRRADIANCE	1.08	.15860765

WEEK NUMBER 7

SPECIES NUMBER 3

SENSOR POSITION	NUMBER OF PAPERS	MEGA-JOULES/M^2
ABV CANOPY INCIDENT IRRADIANCE	6.72	72.011192
TOP CANOPY INCIDENT IRRADIANCE	5.98	29.6893029
MID CANOPY INCIDENT IRRADIANCE	4.62	5.82639604
BOT CANOPY INCIDENT IRRADIANCE	3.56	1.63757048
GROUND INCIDENT IRRADIANCE	3.99	2.74031193
TOP CANOPY REFLECTED IRRADIANCE	2.13	.295528929
MID CANOPY REFLECTED IRRADIANCE	1.44	.129359998
BOT CANOPY REFLECTED IRRADIANCE	1.51	.140669518

WEEK NUMBER 8

SPECIES NUMBER 3

SENSOR POSITION	NUMBER OF PAPERS	MEGA-JOULES/M^2
ABV CANOPY INCIDENT IRRADIANCE	6.42	50.2805477
TOP CANOPY INCIDENT IRRADIANCE	5.29	12.9957097
MID CANOPY INCIDENT IRRADIANCE	4.14	3.27944235
BOT CANOPY INCIDENT IRRADIANCE	3.31	1.21394777
GROUND INCIDENT IRRADIANCE	3.39	1.33598014
TOP CANOPY REFLECTED IRRADIANCE	1.86	.213894689
MID CANOPY REFLECTED IRRADIANCE	1.14	.0903233424
BOT CANOPY REFLECTED IRRADIANCE	1.18	.094754534

WEEK NUMBER 9

SPECIES NUMBER 3

SENSOR POSITION	NUMBER OF PAPERS	MEGA-JOULES/M^2
ABV CANOPY INCIDENT IRRADIANCE	6.37	47.358725
TOP CANOPY INCIDENT IRRADIANCE	5.22	11.9508832
MID CANOPY INCIDENT IRRADIANCE	3.91	2.49000374
BOT CANOPY INCIDENT IRRADIANCE	3.22	1.0899335
GROUND INCIDENT IRRADIANCE	3.32	1.22857027
TOP CANOPY REFLECTED IRRADIANCE	1.72	.180883936
MID CANOPY REFLECTED IRRADIANCE	1.11	.0871364777
BOT CANOPY REFLECTED IRRADIANCE	1.19	.0958958913

WEEK NUMBER 10

SPECIES NUMBER 3

SENSOR POSITION	NUMBER OF PAPERS	MEGA-JOULES/M^2
ABV CANOPY INCIDENT IRRADIANCE	6.08	33.4657067
TOP CANOPY INCIDENT IRRADIANCE	5.43	15.367386
MID CANOPY INCIDENT IRRADIANCE	3.39	1.33598014
BOT CANOPY INCIDENT IRRADIANCE	3.02	.857827571
GROUND INCIDENT IRRADIANCE	2.81	.667113917
TOP CANOPY REFLECTED IRRADIANCE	1.57	.151147163
MID CANOPY REFLECTED IRRADIANCE	1.15	.0914113242
BOT CANOPY REFLECTED IRRADIANCE	1.21	.0982200159

WEEK NUMBER 8

SPECIES NUMBER 4

SENSOR POSITION	NUMBER OF PAPERS	MEGA-JOULES/M^2
ABV CANOPY INCIDENT IRRADIANCE	6.02	31.1458366
TOP CANOPY INCIDENT IRRADIANCE	3.51	1.5424106
MID CANOPY INCIDENT IRRADIANCE	3.31	1.21394777
BOT CANOPY INCIDENT IRRADIANCE	3.32	1.22857027
GROUND INCIDENT IRRADIANCE	3.17	1.02659702
TOP CANOPY REFLECTED IRRADIANCE	1.14	.0903233424
MID CANOPY REFLECTED IRRADIANCE	1.09	.0850746165
BOT CANOPY REFLECTED IRRADIANCE	1.06	.0820729418

WEEK NUMBER 9

SPECIES NUMBER 4

SENSOR POSITION	NUMBER OF PAPERS	MEGA-JOULES/M^2
ABV CANOPY INCIDENT IRRADIANCE	6.09	33.8688149
TOP CANOPY INCIDENT IRRADIANCE	3.61	1.7386013
MID CANOPY INCIDENT IRRADIANCE	3.41	1.36835883
BOT CANOPY INCIDENT IRRADIANCE	3.39	1.33598014
GROUND INCIDENT IRRADIANCE	3.31	1.21394777
TOP CANOPY REFLECTED IRRADIANCE	1.11	.0871364777
MID CANOPY REFLECTED IRRADIANCE	1.09	.0850746165
BOT CANOPY REFLECTED IRRADIANCE	1.07	.0830615441